# TRENDS IN THE EXCHANGE OF $CO_2$ AND $CH_4$ BETWEEN THE ATMOSPHERE AND EASTERN CANADIAN SUBARCTIC AND ARCTIC ECOSYSTEMS

**MARTIN PILOTE**

Thesis submitted to the
Faculty of Graduate and Postdoctoral Studies
in partial fulfillment of the requirementsfor the
PhD degree in Earth and Environmental Sciences

Ottawa – Carleton Geoscience Centre
Department of Earth and Environmental Sciences
Faculty of Science
University of Ottawa

Thèse soumise à la
Faculté des études supérieures et postdoctorales
en vue de l'obtention d'un
Doctorat en Sciences de la Terre et de l'Environnement

Centre Géoscientifique d'Ottawa – Carleton
Département des Sciences de la Terre et de l'Environnement
Faculté des sciences
Université d'Ottawa

***Abstract***

Significant warming of Arctic and northern regions is ongoing and may greatly alter the carbon cycle of these regions. During the International Polar Year, an extensive study was carried out in the Eastern Canadian subarctic and Arctic in order to characterize $CO_2$ and $CH_4$ exchanges from these potentially sensitive ecosystems. The main objectives of this study were to identify the land cover and environmental factors leading to greatest $CO_2$ and $CH_4$ emissions in a highly heterogeneous subarctic landscape, to quantify interannual variability in the net ecosystem exchange of $CO_2$ (NEE) in subarctic forest tundra and investigate the weather conditions that increase net uptake of $CO_2$, and finally, to evaluate the general trends of mid-summer NEE along a latitudinal gradient spanning from 55° to the 72° north. At the landscape level, $CO_2$ and $CH_4$ exchanges showed large variability. Although $CH_4$ emissions were greatest in wetlands, their areal coverage is small in the Kuujuarapik area and limited the influence of these $CH_4$ sources. At the ecosystem level, large-scale atmospheric processes controlled growing season length and cumulative growing degree days which greatly influenced annual and seasonal NEE trends. The subarctic forest tundra near Kuujuarapik was a net source of $CO_2$ in all 3 study years but the source strength was least with the greatest growing degree days while the length of the snow-free period appeared to be less important. Across a latitudinal gradient covering subarctic forest tundra to Arctic tundra, variations in summer NEE could be linked to surface organic carbon content with higher net $CO_2$ uptake at sites with greater soil organic carbon. Warmer days tended to correlate with smaller daily net $CO_2$ uptake (or greater net $CO_2$ losses) but overall, warmer growing seasons reduced the net losses of $CO_2$ on an annual basis. Carbon fluxes in Eastern Canadian subarctic and Arctic regions are highly variable in space and time but these observations help establish a baseline for future examinations of how these carbon exchanges may change with further warming.

***Résumé***

Un réchauffement significatif de l'Arctique est présentement observé, pouvant affecter le cycle du carbone. Au cours de l'Année Polaire International, une étude écosystémique sur les échanges de carbone s'est déroulée dans les régions subarctiques et arctiques de l'Est du Canada afin de caractériser les échanges de $CO_2$ et $CH_4$. Les principaux objectifs de l'étude étaient d'identifier les substrats et les facteurs environnementaux conduisant aux sources supérieures de $CO_2$ et $CH_4$ dans une région subarctique hétérogène, de quantifier la variabilité interannuelle des échanges écosystémiques nets de $CO_2$ dans une toundra forestière subarctique et d'évaluer les conditions météorologiques favorables à l'augmentation de l'absorption nette de $CO_2$, ainsi que d'évaluer les tendances estivales de NEE le long d'un gradient latitudinal de 55° à 72° nord. Au niveau du substrat, les émissions de $CH_4$ sont plus importantes dans les milieux humides, mais leur faible superficie dans la région de Kuujjuarapik limite l'influence de ces sources. À l'échelle écosystémique, les processus atmosphériques contrôlent la longueur de la saison de croissance et le nombre cumulatif de degrés-jours qui influencent les tendances saisonnière et annuelle de NEE. La toundra forestière subarctique s'est avérée être une source nette de $CO_2$, mais avec une intensité moindre lors d'un nombre cumulatif de degrés-jours de croissance supérieure, alors que la longueur de la période libre de neige semble être un facteur moins déterminant. Le long d'un gradient latitudinal, les variations estivales de NEE sont étroitement liées aux teneurs de carbone organique de surface, avec une absorption nette de $CO_2$ plus élevé dans les milieux enrichis en carbone. Les températures plus chaudes ont tendance à se corréler avec un plus faible taux d'absorption de $CO_2$ (ou une plus grande perte de $CO_2$) sur une base journalière, mais dans l'ensemble une saison de croissance plus chaude réduit les pertes nettes de $CO_2$ sur une base annuelle. Les flux de carbone dans les régions subarctiques et Arctiques de l'Est du Canada varient largement au niveau spatial et temporel, et contribuent à établir les niveaux de référence pour les études subséquentes sur la façon dont ces échanges de carbone peuvent évoluer avec les changements climatiques.

“ *On peut se demander si l'humanité a avantage à connaître les secrets de la nature, si elle est mure pour en profiter ou si cette connaissance ne sera pas nuisible.* ”

**Pierre Curie (1859-1906)**

" *A man can be as great as he wants to be. If you believe in yourself and have the courage, the determination, the dedication, the competitive drive and if you are willing to sacrifice the little things in life and pay the price for the things that are worthwhile, it can be done.* "

**Vincent "Vince" Lombardi (1913 - 1970)**

***Acknowledgements***

First and foremost, I would like to thank my first thesis supervisor Dr. Laurier Poissant, a Senior Researcher at Environment Canada and adjunct professor at the Earth Sciences department of the University of Ottawa. Particularly, for his support, integrity and passion for environmental chemistry that he shared with me during our more than 15 years of time working together at Environment Canada. I want to thank him for the encouragement to pursue a PhD degree in environmental geosciences. I would also like to thank my second thesis supervisor Dr. Elyn Humphreys, Associate Professor in the Department of Geography and Environmental Studies at Carleton University, for taking on the lead of my supervision after the early retirement of Dr. Laurier Poissant, particularly for her support, ideas, passion and knowledge on greenhouse gas exchange and the Arctic ecosystems. I would like to also sincerely thank my thesis committee Dr. Danielle Fortin and Dr. Konrad Gajewski, the members of the Earth Sciences Department and the Ottawa – Carleton Geoscience Centre, and especially Dr. Bill Arnott for his support during my entire PhD thesis program.

Grateful thanks go to Environment Canada and the International Polar Year (IPY) Climate Change Impacts on Canadian Arctic Tundra Ecosystems project (CiCAT) for funding support. I also thank the Centre for Northern Studies of the University Laval for support and logistics at Kuujjuarapik, Umiujaq and Bylot Island, most particularly Claude Tremblay, Christine Barnard and Dr. Warwick Vincent. I am grateful to Parks Canada for welcoming us on Bylot Island, and the indispensable logistic support of the Polar Continental Shelf Program (PCSP). Finally, special thanks to the G.G. Hatch Stable Isotope Laboratory at the University of Ottawa including Paul Middlestead, Wendy Albi and Patricia Wickham.

I also like to thank some friends, Dr. Marc-André Coté, Dr. Lilly Lessard, Dr. Francis Pelletier and Martin Pelletier, for their support, company and philosophical discussion along the entire process of this research. I should also thank Patrice Turcotte for his scientific curiosity and especially longtime friends Martin Durocher and Eric Gervais for their determination and moral support.

Lastly, but not least, I thank Florent and Félix-Antoine Pilote, my two teens, whom I hope will also pursue their dreams, persevere in life and never give up, and my wife Suzanne, for her patience over the course of my thesis.

***Remerciements***

En tout premier lieu, je tiens à remercier mon premier superviseur de thèse, le Dr Laurier Poissant, chercheur senior au sein d'Environnement Canada et professeur associé au département des Sciences de la terre à l'Université d'Ottawa, pour son support, son intégrité et sa passion de la chimie environnementale pendant plus de 15 ans à ses côtés, et plus spécialement pour son ouverture et m'avoir donné l'opportunité de poursuivre des études doctorales en géochimie de l'environnement et ses encouragements tout au long de mon projet de recherche sur le terrain. Je tiens également à remercier mon second superviseur de thèse, le Dr Elyn Humphreys, professeure agrégée au département de géographie et des études environnementales à l'Université de Carleton, pour avoir pris la relève de ma supervision après un départ prématuré à la retraite du Dr Laurier Poissant, ainsi que pour son support, ses idées et son expertise sur les échanges de gaz à effet de serre et l'Arctique. Je tiens également à remercier les membres de mon comité de thèse, le Dr Danielle Fortin et le Dr Konrad Gajewski, les membres du département des Sciences de la terre et le centre géoscientifique d'Ottawa-Carleton, et plus spécialement le Dr Bill Arnott pour son support durant la durée de mon programme de doctorat.

Une reconnaissance particulière à Environnement Canada et l'Année Polaire Internationale (API) via le programme sur les impacts des changements climatiques sur la toundra Arctique Canadienne (CiCAT) pour le financement, au centre d'Études Nordiques (CEN) de l'Université Laval pour son support et pour la logistique à Kuujjuarapik, Umiujaq et l'île Bylot. Plus particulièrement, j'aimerais remercier Claude Tremblay, Christine Barnard et le Dr Warwick Vincent du CEN, Parc Canada pour son accueil sur l'île Bylot, et le support indispensable du Programme du plateau continental polaire (PPCP), Finalement, des remerciements vont également au laboratoire d'analyses des isotopes stables G.G. Hatch de l'Université d'Ottawa et de son équipe Paul Middlestead, Wendy Albi et Patricia Wickham.

Je tiens également à remercier certain ami, Dr Marc-André Coté, Dr Lilly Lessard, Dr Francis Pelletier et Martin Pelletier, pour leur support, compagnie et les nombreuses discussions philosophiques au cours de cette recherche. Je tiens également à remercier Patrice Turcotte pour

sa curiosité en science et plus particulièrement deux amis de longue date Martin Durocher et Éric Gervais pour leur détermination et leur support moral.

Dernièrement et non les moindres, mes deux adolescents Florent et Félix-Antoine, à qui je me fais un devoir quotidien de leur montrer de foncer dans la vie, de poursuivre leurs rêves et de ne jamais laisser tomber, ainsi qu'à mon épouse Suzanne pour sa patience et sa compréhension tout au long de ma thèse.

***Statement of contribution***

The basis for this research thesis and the main objectives were initialy established between the author and Dr. Laurier Poissant (original thesis advisor, Environment Canada (ECan)). Funding support was provided by ECan and the International Polar Year (IPY) Climate Change Impacts on Canadian Arctic Tundra Ecosystems project (CiCAT) to Dr. Laurier Poissant. The author was responsible for all statistical and graphical data analysis, interpretation and writing in this thesis. Assistance with editing was provided by Keltie Purcell (ECan) (Chapter 2), Len Goldberg (Ecan) (Chapter 3) and Dr. Elyn Humphreys (current thesis advisor, Carleton University). All maps (MapInfo®), graphics (SigmaPlot®), and tables (Microsoft Excel®) were drafted by the author or source cited. The reproduction of copyright material (figures in Chapter 2) is approved by ACIA, NRCan and the NOAA for educational and non-commercial uses. The results and text from this thesis do not appear in print elsewhere, while some of the material has been presented at conferences.

The first research chapter on spatial variability and landscape-scale estimates of $CO_2$ and $CH_4$ emissions in the Eastern Canadian subarctic (Chapter 3) included data collected over two consecutive years (2006 and 2007). Preliminary flux measurements at Kuujjuarapik in July 2006 and subsequent gas analysis were performed by Philippe Constant (INRS) and assisted by Ripon Banik (UOttawa). The extended gas exchange measurements at the same location in July 2007 were carried out by the author along with all soil and water sampling. Soil characterization (texture, density, pH and GWC) were done by the author. Other supporting soil and water parameters were analysed by G.G. Hatch Stable Isotope Laboratory at the University of Ottawa (C, N and isotopes) and by Environment Canada Quebec Laboratory for Environmental Testing (C, N, P, major ions and chlorophyll).

The second research chapter on annual and seasonal trend in ecosystem-scale $CO_2$ exchange of forest tundra in Eastern Canada (Chapter 4) included data collected over a period of three years (2008 to 2010) in Kuujjuarapik. The author was responsible for the assembly, programming and calibration of instruments associated with the eddy covariance flux tower and was assisted by Conrad Beauvais (ECan) in 2008. SAS® programming for QA/QC of the weather and flux

variables and data analysis was carried out by the author with programming tips provided by Pierre Gagnon (ECan). Data gap-filling was carried out in matlab using a Matlab routine created by Dr. Elyn Humphreys. Additional supporting meteorological parameters and climate normals were provided by the Centre for Northern Studies (ULaval) and the Meteorological Service of Canada, respectively.

The third and last research chapter on general trends of $CO_2$ exchange between ecosystems and the atmosphere along a latitudinal gradient from 55° to the 72° north in the Eastern Canadian Arctic (Chapter 5) included data collected over a period of four consecutive years (2006 – 2009). Field work including assembly, programming and calibration of instruments associated with the eddy covariance flux towers and bowen ratio towers was carried out by the author between 2007 and 2009 with assistance from Conrad Beauvais (ECan) as described above for the second research chapter. In addition, micrometeorological towers at Kuujjuarapik were installed and operated by Philippe Constant (INRS) and assisted by Ripon Banik (UOttawa) in 2006.

***Table of content***

***List of tables***

***List of figures***

***Acronyms and abbreviations***

| | |
|---|---|
| ACIA | Arctic Climate Impact Assessment |
| $\alpha$ | Effective Quantum Yield |
| AMAP | Arctic Monitoring and Assessment Programme |
| $A_{max}$ | Maximum Photosynthetic Uptake |
| AO | Arctic Oscillation index |
| API | Année Polaire Internationale |
| ASL | Above Sea Level |
| Berkeley | University of California, Berkeley earth group model |
| C | Carbon |
| Ca | Calcium |
| CALA | Canadian Association for Laboratory Accreditation |
| CEN | Centre for Northern Studies / Centre d'Études Nordiques |
| CFCs | Chlorofluorocarbons |
| Chla | Chlorophyll a |
| CiCAT | Climate Change Impacts on Canadian Arctic Tundra / Incidences des Changements Climatiques sur la Toundra de l'Arctique Canadien |
| $CO_2$ | Carbon Dioxide / Dioxyde de Carbone |
| $CH_4$ | Methane / Méthane |
| CMIP | Coupled Model Intercomparison Project Phase 5 |
| CRUTEM | Climatic Research Unit Temperature model |
| CRU TS | Climatic Research Unit Time Series |
| DOY | Day Of Year |
| EC | Eddy covariance |
| ECHAM | European Centre Hamburg Atmospheric general circulation Model |
| $E_h$ | Reduction Potential |
| ENSO | El Niño Southern Oscillation |
| ECan | Environment Canada |
| ER | Ecosystem Respiration / Respiration Écosystémique |
| ERSST | Extended Reconstructed Sea Surface Temperature |
| $Fe^{+2}$ | Iron |
| GDD | Growing number of Degree-Days |
| GES | Gas à Effet de Serre |
| GEP | Gross Ecosystem Production |
| GHCN | Global Historical Climate Network model |
| GHG | Greenhouse Gas |
| GISS | Goddard Institute for Space Studies model |
| GPCC | Global Precipitation Climatology Center |
| GPP | Gross Primary Production / Productivité Primaire Brute |

| | |
|---|---|
| HadSST | Hadley Center Sea Surface Temperature model |
| HCl | Hydrochloric Acid |
| $H_2O$ | Water |
| $H_2S$ | Hydrogen Sulfide |
| IPCC | Intergovernmental Panel on Climate Change |
| IPY | International Polar Year |
| IRGA | Infra-Red Gas Analyzer |
| ISO | International Organization for Standardization |
| LAI | Leaf Area Index |
| LOSU | Level Of Scientific Understanding |
| Mg | Magnesium |
| $Mn^{+2}$ | Manganese |
| N | Nitrogen |
| N | North |
| Na | Sodium |
| NAO | North Atlantic Oscillation |
| NEE | Net Ecosystem Exchange / Échange Écosystémique Net |
| $NH_3$ | Ammonia |
| NIST | National Institute of Standards and Technology |
| NOAA | National Oceanic and Atmospheric Administration |
| NRCan | Natural Resources Canada / Ressources Naturelles Canada |
| NSIDC | National Snow and Ice Data Center |
| $O_2$ | Oxygen |
| P | Phosphorus |
| p | Probability |
| PAR | Photosynthetically Active Radiation |
| *p*CH4 | Partial pressure of Methane |
| $pCO_2$ | Partial pressure of Carbon Dioxide |
| pH | Potential of Hydrogen |
| PCSP | Polar Continental Shelf Program |
| PPCP | Programme du plateau continental polaire |
| $Q_{10}$ | Exponential Relationship of Ecosystem Respiration and Temperature |
| QA | Quality Assurance |
| QC | Quality Control |
| QLET | Environment Canada Quebec Laboratory for Environmental Testing |
| r | Correlation Coefficient |
| $r^2$ | Coefficient of Determination |
| $R_{10}$ | Ecosystem Respiration at reference soil temperature of 10 °C |
| RF | Radiative Forcing |
| RH | Relative Humidity |

| | |
|---|---|
| $S^{-2}$ | Sulfide |
| SFC | Static Flux Chamber |
| TDS | Total Dissolved Solid |
| TDG | Total Dissolved Gas |
| TOC | Total Organic Carbon |
| USDOE | United State Department Of Energy |
| UV-B | Ultraviolet B |
| VAC | Voltage Alternating Current |
| VWC | Volumetric Water Content |
| W | West |

## *Chapter 1: Introduction*

Direct measurement and remote sensing (Galbraith and Larouche 2011) observations have shown that temperatures at the Earth's surface have been rising globally (IPCC 2013), but with significant regional variations (Overpeck et al. 1997). Warming may impact the surrounding environment either positively or negatively and in unpredictable ways. The increase in temperature over the last century (1911-2012) has been significant, representing a rise of as much as 1.01 °C (0.95 to 1.07 °C) worldwide (Hansen et al. 2010; Lawrimore et al. 2011; Jones et al. 2012; Rohde et al. 2013). Different models predict that the mean global surface temperature will increase a further 0.47–1.0 °C by 2035 (Meehl et al. 2007; Kirtman et al. 2013). The most pessimistic scenarios predict an increase of 0.7–2.0 °C by mid century and 1.0–3.7 °C by the end of 2100 (Kirtman et al. 2013; Collins et al. 2013). Both the rate and the impact of warming is expected to be greatest at high latitudes, where temperature has an undeniable influence on Arctic and in subarctic ecosystems (Rodionow et al. 2006; Collins et al. 2013).

Increasing temperature is expected to have a great effect on subarctic and tree-line ecosystems along the 0 °C mean annual isotherm (Christensen et al. 2004; Stottlemyer et al. 2001). In these ecosystems, a small temperature change should significantly affect soil thermal and moisture regimes close to the freezing point and consequently impact major ecosystem functions such as hydrological cycling, vegetation dynamics, and carbon (C) cycling. Degradation of the permafrost at these latitudes is particularly important when considering how C cycling is currently—and will continue to be—impacted by climate warming (Payette et al. 2004). Recent estimates suggest that permafrost regions contain more than 50% of the global soil organic carbon (Tarnocai et al. 2009), thus the impact of climate change on these ecosystems has important implications for the global C cycle and global climate. Many studies have also pointed out that Arctic and subarctic regions are among the first environments to show the effects of climate change through significant impacts on ecosystems and communities (Hinzman et al. 2005; Prowse et al. 2006; Schindler and Smol 2006). However, the C cycle in Arctic and subarctic ecosystems is complex and although a growing body of literature on this topic is emerging, few ecosystem scale studies have been carried out in the Eastern Canadian arctic with its unique physiography and huge variety of ecosystems.

In order to improve models for predicting the influence of warming and permafrost degradation on climate change, it is essential to increase our understanding of the environmental factors involved in controlling C gas exchange processes in northern regions. The main objective of this research is to quantify contemporary $CO_2$ and $CH_4$ exchanges in Canada's Eastern subarctic and Arctic ecosystems and determine the factors that currently influence spatial and temporal variations in these exchanges. The main hypothesis is that spatial and temporal variations in surface-atmosphere exchanges of $CO_2$ and $CH_4$ will be substantial at both small and large scales but factors that promote productivity and result in greater above ground biomass and greater soil organic C stocks will be associated with the greatest rates of C exchange with a balance towards net uptake of C in summer. To meet this objective and address this hypothesis, this research uses small- and large-scale techniques to measure $CO_2$ and $CH_4$ fluxes in various aquatic and terrestrial ecosystems along a latitudinal gradient over a number of years to provide data on a range of climate and weather conditions.

This thesis will first present background context for this PhD research (Chapter 2). The subsequent chapters of the thesis will present three research studies that address the following objectives:

Chapter 3: At a landscape level, evaluate the impact of environmental variables on $CO_2$ and $CH_4$ exchanges in both aquatic and terrestrial subarctic ecosystems, and attempt to correlate the magnitude of these fluxes to C stocks and biogeochemical characteristics/processes. In 2006 and 2007, $CO_2$ and $CH_4$ exchanges measurements were made using opaque chamber methods in various aquatic systems (bog, lake, marsh and thermokarst pond) and terrestrial vegetation communities (forb, lichen, non-sphagnum moss, small shrub and bare soil) in summer within a 10 km radius of Kuujjuarapik on the east coast of Hudson Bay in the Eastern Canadian subarctic. Emissions of $CO_2$ and exchanges of $CH_4$ are then scaled to the landscape level to evaluate the importance of 'hotspots' on landscape-scale C emissions to the atmosphere.

Chapter 4: At the ecosystem level, evaluate the annual and growing season net ecosystem exchange (NEE) interannual variability in subarctic forest tundra and attempt to correlate

NEE trends to variations in temperature and precipitation. The data set includes three continuous years (2008–2010) of annual eddy covariance measurements of NEE near Kuujjuarapik.

Chapter 5: Evaluate the general trends in summer NEE along a gradient spanning from 55° N to 72° N in the Canadian Eastern subarctic and Arctic tundra and attempt to associate these with spatial trends in vegetation communities and soil organic content. The data set includes July NEE measurements (2006-2010) at one forest tundra site and three subarctic and Arctic tundra sites.

The final chapter will summarize how this research has improved our understanding of C cycling in these subarctic and Arctic ecosystems.

## *Chapter 2: Background*

### *1.1. Introduction*

Life on Earth depends on carbon (C). The C cycle involves complex exchanges among many pools including the atmosphere, the biosphere, oceans and freshwater bodies, the soil, and the geosphere. The global climate system is impacted by changes in the C cycle that lead to changes in atmospheric concentrations of $CO_2$, $CH_4$ and CFCs. These compounds are some of the major GHGs present in the atmosphere that contribute directly to global warming by regulating the amount of infrared radiation absorbed and re-emitted. By this action, they control the temperature and global climate of Earth's surface and thereby influence biogeochemical activities.

The exchange of these GHGs in northern wetlands and tundra regions has attracted much attention in recent years due to the large stores of organic C, accumulated slowly over centuries, in these soils and permafrost (Tarnocai et al. 2009; Hugelius et al. 2013). It remains uncertain how these subarctic and Arctic C pools will respond to climate change. Positive climate feedback scenarios suggest $CO_2$ emissions may be enhanced, since warming and drying in the soil along with permafrost degradation and lowering of the water table enhances aerobic decomposition and respiration (Smith et al. 2004). Similarly, warming may enhance $CH_4$ emissions, as warming and permafrost degradation lead to wetland expansion/formation and enhance anaerobic decomposition and $CH_4$ export, particularly in ice-rich soil (Corradi et al. 2005). Negative feedback scenarios suggest warming can promote $CO_2$ uptake by vegetation as a result of longer growing seasons, higher biomass and greater photosynthetic activity as well as over longer time scales a succession to more productive plant communities (Grant et al. 2011; Elberling et al. 2004; Kaplan and New 2006). Winter C cycle processes may be impacted by the length and severity of the cold season (Venäläinen et al. 2001), as well as by the extent and duration of snow cover (Aurela et al. 2004; Öquist and Laudon 2008).

### *1.2. Overview of climate change*

Climatic change is part of history on a geological time scale. Analysis of proxy data such as sediments and glaciers in paleoclimate records has revealed major temperature and precipitation variations throughout the last hundreds of thousands of years (Petit et al. 1999; Miller et al. 2010). Over the last 450 000 years, five glacial–interglacial transitions have been observed successively over the Earth's surface (Cortese et al. 2007). Earth's internal dynamics such as thermohaline circulation and the impact of external natural forcing factors such as volcanic eruptions and solar radiation, have been identified as elements regulating past climate (Degens et al. 1981). The ocean's thermohaline circulation controls heat convection worldwide and has been recognized as an important factor influencing atmospheric temperature (Marotzke 2000). Volcanism releases huge amounts of particles and $CO_2$, but the haze effect created by the eruption-generated particles offsets the warming impact of GHGs emission and produces a net cooling effect by influencing the solar radiation budget (Crowley 2000; Robock 2000). The three fundamental processes involved in the control of the solar radiation budget at the earth's surface are direct variations in incoming solar radiation, changes in albedo, and changing GHG concentrations (IPCC 2013). Incoming solar radiation is mainly regulated by solar intensity, distance between sun and earth and orbital effects (Maxwell 1987). Land cover type and ice sheets largely influence albedo and the relative amount of heat absorbed by the Earth's surface and the amount re-emitted to the atmosphere. While solar radiation and albedo have fluctuated somewhat in the last centuries, the factor that has changed most significantly is the chemical composition of the atmosphere (AMAP 2010). Contemporary observation has shown that normal temperature variations have been accentuated in the last centuries, particularly after 1850 (Crowley 2000; Turner and Gyakum 2010). Anthropogenic factors that may induce changes in climate are increased production of GHGs such as $CO_2$ and $CH_4$, the use of aerosols, and significant changes in land use (Houghton et al. 2001).

Radiative forcing (RF) refers to the impact of climate change drivers on the net radiation at the top of the troposphere as a function of the solar radiation absorbed in the atmosphere and at the earth's surface and the energy reflected or emitted to the stratosphere. Positive RF represent a net surface warming, while negative RF lead to net surface cooling (Ramaswamy et al. 2001). This

concept is used for quantitative comparisons of the impact of anthropic and natural drivers of climate change including GHGs. Among the two main GHGs, $CO_2$ has a smaller warming effect than $CH_4$ (Forster et al. 2013). Within a 20 years horizon, $CH_4$ has a global-warming potential 86 times greater than $CO_2$ (Myhre et al. 2013). $CH_4$ has high capacity to absorb infrared radiation and strong ability to link with atmospheric aerosols, altering $O_3$ and stratospheric water vapour concentrations (IPCC 2013). Since the start of the industrial era around 1750, concentrations of GHGs, mainly dominated by $CO_2$, $CH_4$, tropospheric ozone and halocarbons, have increased significantly as a result of fossil fuel combustion and other anthropogenic activities (IPCC 2013). $CO_2$ concentrations have increased by 139 % (280 to 390 ppm) from 1750 to 2011 (Stocker et al. 2013), while $CH_4$ concentrations have exponentially increase by 217 % (830 to 1800 ppb) from 1750 to 2010 (Kirschke et al. 2013).

Based on various trend analyses, mean surface temperature increased by 0.092 °C per decade (0.086 to 0.095 °C per decade depending on the model scenario) since the start of the industrial era (1880-2012) (CRUTEM4.1.1.0; GHCNv3.2.0; GISS; Berkeley). The warming trend was weaker at the beginning of the last century (1901-1950) at 0.102 °C per decade (0.097 to 0.111), increased to 0.184 °C per decade (0.175 to 0.197) (1951-2012) and then rised to 0.262 °C per decade (0.254 to 0.273) in the last decades (1979-2012) (Hartmann et al. 2013). For the period 1979–2005, temperature trends were greater in the Northern Hemisphere (0.328 °C per decade) than in the Southern Hemisphere (0.134 °C per decade) and this same pattern has also been observed in longer records (Brohan et al. 2006). Arctic amplification is the framework used to explain the processes responsible for this south–north difference (Screen and Simmonds 2010); this process will be explained in more detail below.

Mean sea surface temperature based on data from moving ships and buoy measurements (HadSST2 & HadSST3) increased by 0.053 °C per decade (0.051 to 0.054) from pre-industrial era to present (1880-2012), with the greatest rate of warming in the last decades (1979-2012) at 0.123 °C per decade (0.121 to 0.124) (Hartmann et al. 2013). Ocean temperature trends are also more accentuated in the Northern Hemisphere than in the Southern Hemisphere but to a lesser degree than the atmosphere: 0.190 and 0.089 °C per decade, respectively, in 1979–2005 (Rayner et al. 2006). The same pattern is also observed in longer temperature records (IPCC 2013).

Precipitation trends are more difficult to analyze and interpret than temperature changes in terms of their contribution to a regional or a global view of change. Instrument networks and precipitation measurements are scarce and are not distributed uniformly around the globe. They are mainly concentrated in urban areas and developed countries, with only a very small percentage over the ocean and Arctic region (Prowse et al. 2009a). The IPCC 2013 showed from various trend studies (CRU TS 3.10.01; GHCN V2; GPCC V6; ERSST) that global mean annual precipitation increased significantly by 1.835 mm/yr per decade (1.01 to 2.77) over the last century (1901-2008) although over the last half century, the trend was -1.438 mm/yr per decade (-2.77 to 0.68) (1951-2008) (Hartmann et al. 2013). At high latitudes (60 to 90° N), precipitation increased at a greater rate of 3.415 mm/yr per decade (0.63 to 5.82) over the last decades (1951-2008) when compared to temperate regions (30 to 60° N) at a rate of 1.248 mm/yr per decade (0.97 to 1.50) (Hartmann et al. 2013).

### *1.3. Climate change in the Arctic*

A number of studies suggest that the increase in the Arctic's average temperature is more than two times the increase in the global average temperature (Graversen et al. 2008; Overland et al. 2011). This trend is expected to continue and increase in the near future because of Arctic amplification (Collins et al. 2013). Temperature trends varied between studies and model scenarios as a function of time scale and geography used to define the Arctic (Groendahl et al. 2007). In this thesis, the northern circumpolar region known as the Arctic includes the circumpolar region located north of the Arctic Circle (66°32' N) or where average July temperature is ~10 °C or at the limit of the treeline (ACIA 2004). The subarctic is a transition zone between the boreal forest and the treeline and combines both characteristics of the boreal forest and Arctic tundra (AMAP 2010). More details on the features used to determine these regional limits are discussed below and shown in Figure 1.1.

A compilation of paleoclimatic and proxy data over the past 400 years has shown that Arctic warming reached a peak between 1840 and the mid-20th century (Overpeck et al. 1997). The Arctic experienced a slight cooling, -0.20 °C per decade, between the mid-1940s and mid-1960s, and tremendous warming thereafter to present (McBean 2004). Mean annual warming in Alaska

reached 0.4°C per decade for this period, and even more in winter at 0.7 °C per decade (USGCRP 2009). Since the early nineteenth century, the mean annual temperature in the circumpolar Arctic increased by 0.12 °C per decade (0.6 to 2.4), with an accentuated warming during winter (mean January) at 0.23 °C per decade (0.3 to 5.1) relative to summer (mean July) at 0.05 °C per decade (0.4 to 1.1) (van Wijngaarden 2014).

Canadian Arctic mean annual temperatures display some of the largest intra- and interannual variance and regional disparity in the world (Turner and Gyakum 2010). Between 1950 and 1998, daily maximum and minimum annual temperatures increased by 1.5 to 2.0 °C in the western Canadian Arctic while they decreased by -1.0 to -1.5 °C in the Eastern Canadian Arctic regions. These spatial variations are mainly related to large-scale hemispheric phenomena, such as ocean and atmospheric circulation, the El Niño Southern Oscillation (ENSO) and the North Atlantic Oscillation (NAO) (Zhang et al. 2000b). When including the most recent decade, annual mean temperature in the Eastern Canadian Arctic slightly increased by 0.31°C per decade (1953-2012) particularly owing to accentuated recent warming, 0.78°C per decade (1980-2012) (Peterson and Pettipas 2013). The general warming trend in the Canadian Arctic is accentuated in winter and spring, although all seasons are also slighty impacted, which is similar to the whole circumpolar Arctic (Prowse et al. 2009b).

Arctic warming is also coupled with a significant increase in precipitation and changes in the nature of precipitation, leading to deeper snow in winter and early spring, as well as more rain in summer (McBean 2004; Kittel et al. 2011). However, due to the limited availability and uneven distribution of precipitation monitoring networks, precipitation changes are more complex to analyze and interpret than temperature trends (Prowse et al. 2009a). All data sets must therefore be adjusted to counteract this effect before an analysis of spatial and temporal trends over the polar regions can be made (Zhang et al. 2000b). Precipitation trends show an increase in precipitation, 0.5 to 1% per decade in the mid and high latitudes of the Northern Hemisphere (New et al. 2001). In the Arctic, increases in precipitation are slightly greater depending on the time scale and correspond to 1.4% per decade in the last century (1900 to 2003). During significant Arctic warming periods, 1900-1945 and 1966-2003, precipitation trends increase respectively by 2.3 and 2.2 % per decade. The rate of increase in precipitation, 1.3% per decade,

was lower during 1946-1965 and was associated with a slight cooling trend (McBean 2004). Some regional studies show a significant increase in precipitation from mid-1960s to early 2000s of up to 20% in Alaska, northern Canada and the Russian permafrost-free zone (McBean 2004). The largest increases in precipitation in the Canadian Arctic, from 1948 to 2005, were observed in the Arctic mountains and over the more northerly Canadian Arctic tundra where precipitation increased by 16 and 25 %, respectively (Prowse et al. 2009b). Precipitation increased in all seasons, mainly associated with large-scale processes in the ocean and atmospheric systems, but the largest increases were observed and measured in spring, fall and winter (New 2005). However, in another Arctic region (Norwegian Arctic), precipitation increases occurred mainly as rain, while snow decreased as a result of snow conversion to mixed precipitation and rain (Forland and Hanssen-Bauer 2000).

Based on climate normals for 1990–2000, various model scenarios predict global temperature increases of 0.3 to 1.3 °C for 2020–2030. However, the variability between different scenarios and predictions greatly increases over longer time periods with a minimum temperature increase variation of 2.3 to 3.3 °C, and a maximum variation of 4.5 to 6.3 °C for the next century (Stott and Kettleborough 2002). In the Arctic, model projections are similar, with a general warming of 2 °C from present to 2040, and between 4 to 7 °C by 2100 (Weller 2004). The IPCC report uses a prediction of Arctic warming between 2.2 ± 1.7 °C (RCP2.6) and 8.3 ± 1.9 °C (RCP8.5) by the end of this century (Collins et al. 2013).

### *1.4. General Arctic climatology*

As there is little historical and limited current surface meteorological data and despite recent advances in remote sensing techniques, it difficult to obtain a good portrait of the surface Arctic climate (Bromwich et al. 2007; Serreze and Barry 2011). The available information mostly originates from either airport weather stations or some research sites where the parameters and time scales are different, and where quality assurance and quality control are not certain. Ice core studies and other paleoclimate records have shown that at the beginning of the last glaciation, the Arctic climate was warmer, but with higher precipitation. However, during the last glaciation, the Arctic was covered by ice and the climate was much colder and drier. Temperature and

precipitation have increased during the last 5000 years (Maxwell, 1987). During the last part of the Holocene and prior to the industrial era, the Canadian Arctic climate has oscillated between warmer and cooler periods, such as the Holocene climatic optimum (~6000–8000 years BP), the Medieval Warm Period (~1000 years BP) and the Little Ice Age (~500 years BP) (Prowse et al. 2009b). Within the last centuries, the overall Northern Hemisphere climate has experienced a general warming at the beginning of the 1900s, followed by a cooling period between the 1940s and the 1960s, and now the warming that we know today (Maxwell 1987; IPCC 2013).

In the Canadian Arctic, mean annual temperatures range from about -5 °C in the southern regions to about -20 °C in the Arctic islands (climate normal 1971–2000) (Prowse et al. 2009a). Canadian Arctic temperatures are influenced by continental, maritime and coastal climatic regimes (Sechrist et al. 1989). Overall, winter seasons are cold, dry and associated with continental Arctic air masses from Siberia, the Arctic Ocean and Greenland (Prowse et al. 2009a). Average winter temperature averages from -15 to -20 °C at lower latitudes and -35 °C at higher latitudes (Prowse et al. 2009a). Summer temperature averages from near 0 °C at high latitudes to about 15 °C at southern latitudes (Prowse et al. 2009a)

The amount of precipitation received in polar regions is generally low relative to southern latitudes. The northern parts of the Arctic are comparable in precipitation to arid regions elsewhere with average annual precipitation of 100 mm or less (Huntington and Weller 2004). At lower latitudes, precipitation in the Arctic reaches about 400 mm (Prowse et al. 2009a). Most precipitation—30 to 50% in the North American Arctic and about 33% in the Eurasian Arctic—occurs as rain between June and August (Bliss 2000). Precipitation across the Canadian Arctic is controlled by atmospheric transport mechanisms, influences of Arctic air masses and major circulation systems, general land morphology, influences of significant water bodies such as the Arctic Ocean and Hudson Bay, sea-ice cover, and continental impacts. Throughout most of the Canadian Archipelago and the polar basin, about 90% of precipitation falls in summer, between May and October (Sechrist et al. 1989). In maritime regions, high evaporation rates create foggy conditions—about 100 days per year—when the large water bodies are open to the atmosphere (Sechrist et al. 1989). In winter, dry and cold conditions are not favourable to wet deposition, and the precipitation amounts received in the Arctic are quite low (Sechrist et al. 1989). A large part

of snow precipitation occurs in late summer and fall, when air moisture content is much higher and frontal storms may penetrate the dominant high-pressure systems (Bliss 2000).

Overall, in maritime climate conditions, winters are cold and stormy and summers are cloudy and mild. The Arctic Ocean and other large water bodies have a major effect in summer when they are not covered by ice; the warmer water helps regulate air temperature, producing warmer and wetter conditions. In non-coastal areas, however, the overall summer climate is warmer, drier and less stable (Sechrist et al. 1989). Once ice is reformed in coastal areas, less difference in continental and maritime region weather occurs since all exchanges between the ocean and the atmosphere are limited by sea ice, thus producing more uniformly cold and dry conditions (Ricard 1998). In the cold season, temperature inversions in the Arctic environment are common, regulated mainly by night-time surface conditions, wind speed, surface atmosphere characteristics and snow cover (Sechrist et al. 1989). These inversions in turn significantly affect surface wind conditions, producing winds that are considerably weaker than would be expected.

Surface weather is also a function of the position and strength of the circumpolar vortex in the middle and upper atmospheres, the main jet streams of these atmospheres (Sechrist et al. 1989) and their related cyclone and anticyclone distribution and strength (NSIDC 2011). In winter, anticyclonic circulation promotes cold and dry air advection southward (Overland et al. 2011). In summer, warmer surfaces in the Arctic allow cyclonic systems to move northward, coupled by an increase in Arctic precipitation (Bliss 2000). In winter, the Arctic front extends to lower latitudes and wind velocity increases significantly (AMAP 2006). The negative or positive Arctic Oscillation index (AO) and North Atlantic Oscillation (NAO) index may also significantly influence the Arctic circumpolar vortex (Overland et al. 2011). The AO refers to significant pressure variations between the Arctic (low pressure) and northern mid-latitude (high pressure), and impacts Arctic weather. In the positive phase, the high Arctic and Greenland has colder stratosphere and warmer and wetter weather at lower latitude. The NAO refers to the reverse pattern with high pressure in the Arctic and low pressure at northern mid-latitude and impacts Arctic weather. In the negative phase, the high Arctic has less cold stratosphere and temperate region weather turns cold and stormy.

The climate in all Arctic areas is also affected by the extreme variations in solar radiation that occur at high latitudes, from midnight sun to polar night (NSIDC 2011). Annual mean incoming solar radiation north of the Arctic Circle is 100 $W/m^2$, most of it being received between the spring and autumn equinoxes. In comparison, mid-latitude locations receive about 150 to 200 $W/m^2$ on average (Linacre and Geerts 1998), with less variation between the summer and winter months.

### *1.5. Arctic amplification*

In the 1990s, greater warming in Arctic regions and the processes that lead to this phenomenon were termed and popularized Arctic amplification, but the phenomenon of greater warming was observed long before (Serreze and Barry 2011). Arctic amplification is complex and involves a suite of causes that may act simultaneously on broad temporal and spatial scales (Serreze and Barry 2011). The main causes of Arctic amplification include, but are not limited to, the decline of sea ice, albedo feedbacks, increase in atmospheric heat flux, presence of a relatively shallow boundary layer, and changes in cloud cover and atmospheric water vapour (Screen and Simmonds 2010). Over the last century, Arctic amplification processes may have contributed to 33 to 66% of warming in polar regions and 66 to 90% of warming in the last 50 years (Weller 2004).

Both direct observations and numerical simulation by global climate model ECHAM show that variations in sea-ice cover in the Arctic Ocean is strongly correlated with present Arctic warming (Bengtsson et al. 2004; Screen and Simmonds 2010). Significant melting of snow and ice in polar regions largely impact surface albedo, with less solar energy reflected to the atmosphere and more solar energy absorbed by land and ocean surfaces (Weller 2004). Sea-ice and snow has a high albedo and reflects about 85-90% of sunlight while land (vegetation and dark soil) and ocean reflects about 20% and 10% of solar energy, respectively (McBean 2004). The reduction in sea-ice extent in spring and fall increases the transfer of ocean heat to the atmosphere and contributes to warming (Weller 2004). In summer months, less sea-ice extent and thus more open water leads to warming of the Arctic Ocean mixed layer (Ghatak et al. 2010). In addition, earlier melting of sea ice and delayed freeze-up reduces ice thickness and insulating properties, which

leads to further losses of heat to the atmosphere between the warm ocean and a cold atmosphere (Holland and Bitz 2003).

The feedback created by less ice and snow cover is also amplified by the presence of soot and dust particles on the top layer, which also reduce albedo and promote heat absorption (Serreze and Barry 2011). They lead to further reductions in sea ice and snow cover and thereby increase Arctic amplification mechanisms (Holland and Bitz 2003; IPCC 2013).

In the Arctic, the atmospheric boundary layer is thinner than in temperate and tropical regions, and consequently, less energy is required to warm the near-surface air (Weller 2004). Arctic warming however, leads to a significant increase in the thickness of this atmospheric layer, which may alter atmospheric circulation patterns (Cohen et al. 2014).

Direct observations and CMIP 5 model simulations clearly show that the increase in atmospheric heat flux from a warmer landscape is a major contributor to Arctic amplification (Lesins et al. 2012; Pithan and Mauritsen 2014). At higher latitudes, partitioning of energy at the surface is primarily to sensible heat flux. At lower latitudes, relatively more of the absorbed energy is partitioned into latent heat fluxes or evaporation, resulting in a large water feedback to the atmosphere in addition to sensible heat (Weller 2004). The nature of the landscape surface largely influences partitioning of latent and sensible heat flux with latent heat fluxes becoming more important with more vegetation cover and open water. Increasing water vapour and cloud cover in the lower atmosphere leads to a larger greenhouse effect in the Arctic than at lower latitudes (Pithan and Mauritsen 2014). Mainly in the cold season, direct observations show a net warming trend with cloud cover (particularly Arctic stratus), increasing downward longwave radiation because of low incoming solar radiation and high surface snow/ice albedo (Serreze and Barry 2011). This contrasts with southern latitudes and summer Arctic observations where cloud cover limits solar radiation input, resulting in a net cooling effect (Holland and Bitz 2003).

### *1.6. The interaction between global climate and the global and Arctic carbon cycle*

In the Earth's system, global climate is closely linked with major biogeochemical processes, the C cycle and human activities. It is sometimes difficult to determine whether climate is influenced

by changes in the C cycle or whether the C cycle responds to changing climate. The inorganic forms of C are involved in major biogeochemical processes such as photosynthesis, weathering and biomineralization (Bendel et al. 2000). Even though $CO_2$ and $CH_4$ do not constitute a large part of the mass fraction in the atmosphere, changes in atmospheric $CO_2$ and $CH_4$ efflux are closely linked with the C cycle and global climate because of the specific radiative forcing properties of these GHGs (Falkowski et al. 2000). Both well-mixed GHGs, $CO_2$ and $CH_4$, have high radiative forcing in the atmosphere, 1.68 and 0.97, respectively, that impact the earth's radiation balance and Arctic and global warming (IPCC 2013).

Atmospheric C concentrations depend on the balance between $CO_2$ emissions and the major reservoirs' ability to uptake $CO_2$ and $CH_4$ (Falkowski et al. 2000). Plant respiration and photosynthesis, as well as soil respiration and microbial oxidation are the main processes regulating $CO_2$ exchange in the biosphere (Trumbore 2006). When in balance, these very large fluxes are approximately 120 Pg C per year sequestered by the biosphere and roughly the same amount emitted to the atmosphere (Mahli 2002). The primary natural sources of $CH_4$ are anoxic fermentation in wetlands, followed by termites, ocean, vegetation and the degassing of underwater gas hydrate (Walter et al. 2001; Krey et al. 2009). Volcanic eruptions constitute a large natural source of $CO_2$, while silicate weathering, carbonate deposition and organic C burial in marine sediments are a large sink of $CO_2$ (Gerlach 2011). Silicate weathering consumes atmospheric $CO_2$ previously trapped in ocean carbonates. The oceans play a very important role in the control of atmospheric $CO_2$ concentrations through physical process such as $CO_2$ dissolution—the solubility pump—and through biological process such as photosynthesis by marine microorganisms—the biological pump (Sigman and Boyle 2000). About 50% of global photosynthesis is from algae and primary production in the ocean (Chisholm 2000). When in balance, these very large fluxes are approximately 90 Pg C per year sequestered by the ocean and roughly the same amount emitted to the atmosphere.

Since the industrial era, new sources of $CO_2$ to the atmosphere have resulted from the combustion of fossil fuels, coal mining, the burning of biomass and changes in land use (IPCC 2013). The fossil fuel sources of C effectively represent ancient C accumulated over years being brought back into the modern C cycle. The main drivers controlling anthropogenic $CH_4$

concentrations in the atmosphere have been an increase in agriculture involving grazing animals and crop production, particularly rice production, as well as landfills (Fowler et al. 2009). Currently, approximately 9 Pg C is released annually by anthropogenic activities; of this, about 3 Pg C is captured by plant processes and 2 Pg C by ocean processes leaving about 4 Pg C to contribute to the net atmospheric increase (USDOE 2008).

Ice core records over Antarctica show that temperature over the last ~ 650 000 years has changed significantly and that the $CO_2$ trend is closely related, but with some temporal leads and lags (Petit et al. 1999; Siegenthaler et al. 2005). During this period, the amount of $CO_2$ in the atmosphere never exceeded 180 ppm in glacial periods and 300 ppm in interglacial periods (Siegenthaler et al. 2005). However, ice core observations in Greenland show a weaker relationship between temperature and $CO_2$. This lower correlation might be explained by major biogeochemical processes in the Southern Hemisphere that influenced global $CO_2$ concentrations between glacial and interglacial periods (Fisher et al. 2010) and/or by the presence of large amounts of dust in the ice core as a result of colder, drier and windier conditions during the Younger Dryas (Alley 2000). The southern ocean surrounding Antarctica is very productive, and primary production may have changed $CO_2$ uptake via the biological pump process (Sigman and Boyle 2000). $CH_4$ observations in both Antarctica and Greenland ice core records show a strong correlation between temperature and gas concentrations (Blunier and Brook 2001). During this period, the amount of $CH_4$ in the atmosphere also remained between 320 and 790 ppb.

Since the beginning of the industrial age, atmospheric $CO_2$ has increased significantly, from around 280 ppm in 1750 to 400 ppm in 2014, due to strong anthropogenic influences (Blunden et al. 2011; GCP 2014). Atmospheric $CH_4$ concentrations have also increased significantly during the last centuries, from about 772 ppb in 1750 to around 1799 ppb in 2011 and 1803 ppb in 2013 (Fluckiger et al. 2002; Blunden et al. 2011; Kirschke et al. 2013; GPP 2014). The $CH_4$ trend is mainly controlled by the rate of surface emissions and photochemical activities within the atmosphere (Bousquet et al. 2006) although much uncertainty exists around interannual variability. Various model scenarios predict that atmospheric $CO_2$ concentrations will reach about 985 ppm (794 to 1142) by the end of the 21st century. $CH_4$ concentration predictions for the end of the 21$^{st}$ century are more variable ranging from a reduction of 230 ppb below present

levels to an increase in $CH_4$ abundance by an additional 520 ppb (Kirtman et al. 2013). Of the two gases, $CO_2$ is expected to represent about 80 to 90 % of the radiative forcing related to anthropogenic emission (Collins et al. 2013).

There are two main factors that explain the importance of boreal, subarctic and Arctic regions in the global Earth climate system. First, these regions cover a vast area (22%) of the Earth's land surface (Chapin et al. 2000). Second, at these latitudes, major biological and physical processes are highly sensitive to climate change. Internationally, the Arctic has been recognized as a harbinger of global warming due to its sensitivity to changes in climate. This is largely because its physical environment is dominated by cryospheric components—including both seasonal and multi-year forms of freshwater and sea ice, permafrost, snow, glaciers and small ice caps—that are particularly responsive to changes in the climate system (Prowse and Furgal 2009b).

One impact of global warming is that some vulnerable C pools will be subject to significant perturbations in the 21st century. In terrestrial ecosystems, C stored in permafrost and wetlands are often discussed as having the highest potential risk of loss to the atmosphere. Permafrost is soil or rock that remains below 0 °C for more than two consecutive years (Zhang et al. 2000a; Schuur et al. 2009). Permafrost-affected soils in subarctic and Arctic ecosystems around the world may contain 1300 Pg C of which 800 Pg is perennially frozen (Hugelius et al. 2014). Thawing permafrost under relatively modest warming in the 21st century may release about 20% of this previously accumulated C stock (Gruber et al. 2004). The worst warming scenario estimates that the top permafrost (0-3m) will degrade by 9 to 15 % in the next decades (2040) and by 47 to 61 % by the end of the century (2100) (Schuur et al. 2011).

Frozen soil contains deposits of both young and old organic matter that is easily decomposed (Canadell and Raupach 2009; Schuur et al. 2009). The decomposition of soil organic matter is site-specific and depends on various environmental conditions, such as the quality and abundance of organic matter, soil temperature, water content and microbial activity (Eberling et al. 2004; Waldrop et al. 2010). The amount and forms of C release also depends of the chemistry and the origin of C trapped in the permafrost, such as undecomposed roots, DOC, or organic matter bounded to mineral particles (Schuur et al. 2009).

The C pool in wetlands such as peatlands is also considerable, about 500 Pg C worldwide (Tarnocai 2006). About 400 Pg C is present in northern peatlands and is highly vulnerable to warming and climate change while 100 Pg C is present in tropical peatland and is vulnerable to climate change and land-use modification and drainage (IPCC 2013). Wetlands are highly sensitive to water table variations that control the level and nature of $CO_2$ and $CH_4$ efflux (Whiting and Chanton 2001; Comas et al. 2008).

Soil C is the largest terrestrial C pool worldwide, with about 3000 Pg C (Tarnocai et al. 2009). Carbon in non-permafrost soils and terrestrial biomass may be less impacted by warming but may also have a potentially important global effect due to the sheer amount and extended cover (Gruber et al. 2004). Land modifications and fire are currently the main factors that may alter surface soil organic matter (Tarnocai et al. 2009). Surface weather conditions may change significantly with climate change and may lead to increased wind velocity and more frequent extreme storms, drought, forest fires and insects ravaging, that can significantly impact terrestrial biosphere (NRCan 2013).

Terrestrial biomass contains about 500 Pg C in surface vegetation and is also highly vulnerable to climate change (Canadell and Raupach 2008). In the Arctic, $CO_2$ uptake by vegetation may significantly increase with warming. Warming may lengthen the growing season, promote the northward migration of plant species and the tree line, and result in higher biomass production, LAI and photosynthetic activity, which may all promote and enhance C uptake (Canadell and Raupach 2009). Vegetation changes might also decrease Arctic albedo and promote regional warming (ACIA 2004). However, warming in the boreal forest and in the subarctic region may enhance drought, insect devastation and fire. Forest fires are a significant source of $CO_2$ as C stored in vegetation is immediately released into the atmosphere during combustion (NRCan 2013). Soil nutrients and water and/or oxygen availability limits plant growth in many regions of the Arctic, especially in dry conditions and in polar deserts (Dormann and Woodin 2002). Warming may enhance nutrient mineralization and other cycling processes and lead to increased nutrient availability with benefits to plant biomass and productivity (Epstein et al. 2000). Despite these processes, it is suggested that C emissions may outpace C uptake as warming increases in the Arctic (Canadell and Raupach 2009).

About 1000 Pg C is estimated to reside in the surface ocean and about 37 000 Pg C in the deepest ocean (USDOE 2008). Carbon dioxide is continuously exchanged between the atmosphere and the surface ocean and is regulated by the biological pump and the solubility pump. Both processes maintain an important vertical gradient of $CO_2$ in the water column, with the highest level in the deeper layer and lowest amount nearer the surface (IPCC 2013). These biological and chemical processes are also susceptible to climate change. A major uptake of anthropogenic $CO_2$ may impact water chemical properties, global circulation, temperature, salinity, biota and the natural C cycle (Gruber et al. 2004). Gas hydrates buried in frozen ocean sediments may be very vulnerable to climate change and may release important quantities of $CH_4$ (Gruber et al. 2004). The $CH_4$ hydrate pool is estimated to contain about 10 000 Pg C under continental shelf sediments and in the Arctic permafrost (Rustad et al. 2000). Over the last centuries and under anthropogenic influences, oceans have become a larger net $CO_2$ sink than the terrestrial ecosystems (Gruber et al. 2009).

Warming in the Arctic may also influence energy flux and the proportion of sensible and latent heat flux returned to the atmosphere. Ninety percent of the energy is absorbed in summer because of the weak albedo and the high amount of solar radiation (ACIA 2004). These changes may alter the regional temperature gradient in the atmosphere and some major atmospheric circulation patterns (Serreze and Stroeve 2009), and indirectly temperature and precipitation in southern latitudes, since major circulation systems extend far beyond the borders of the Arctic (Overland et al. 2011).

Arctic warming may also have a significant impact on global climate through important changes in ocean circulation. Analyses of ice and sediment proxy data have shown that dramatic regional climate variations over the glacial and interglacial eras may have been associated with large ocean circulation perturbations and global climate change (Mauritzen 2009). The global ocean conveyor, or thermohaline circulation, is controlled by surface heat exchange and freshwater fluxes, which determines ocean water density (IPCC 2013). Arctic warming may introduce a large input of precipitation, runoff, or ice melt into the conveyor belt and affect the strength of the thermohaline circulation or even shut it down, inducing further global climate change and impacting the C cycle (Obata 2007). This occurs because a large addition of freshwater can

affect water temperature and salinity exchange between higher and lower latitudes, as well as between the surface and deeper ocean (Kuhlbrodt et al. 2009). Some scientific observations show that there is currently a slight decrease of the thermohaline circulation and that its strength will change in the future (IPCC 2013), but a complete shutdown as was observed during the Younger Dryas is not expected (Broecker 1999). Variations in thermohaline strength may also be accompanied by significant changes in ocean pathways that would affect primary production, marine resources, the C cycle and the global ocean ecosystem (Mauritzen 2009).

Arctic warming may enhance the melting of ice sheets impacting worldwide sea level (ACIA 2004; Rignot and Cazenave 2009). Over the last decades, significant changes in the cryosphere and ice sheets have been observed and documented in polar regions (Nghiem et al. 2007; Stroeve et al. 2008; IPCC 2013). Analysis of proxy data has shown substantial changes in global sea level between glacial and interglacial periods driven by the influences of continental ice sheets. These changes are closely related to atmospheric $CO_2$ concentrations, but the interaction with the partial pressure of $CO_2$ ($pCO_2$) remains uncertain (Tripati et al. 2009). Thermal expansion is also an important process that contributes to rising sea levels (Church et al. 2011). Isostatic rebound is another factor important in determining sea level, because of the rise of land masses previously impacted by the weight of ice sheets (Peltier et al. 2002). Sea level may also impact global C balance as it controls the ratio of landmass and ocean exposed to the atmosphere with greatest impacts on low-lying coastal regions (IPCC 2013).

Historically, the Arctic Ocean has not been a significant $CO_2$ sink because of the limited atmospheric exchange associated with sea-ice cover and because of the region's limited biological productivity. Arctic warming will reverse that trend, because of sea-ice reduction and higher primary production, potentially leading to higher C sequestration (Bates 2009). A net increase of $CO_2$ released from the Arctic Ocean to the atmosphere might also be triggered by large freshwater inputs carrying increasing amounts of dissolved organic C originating from enhanced terrestrial losses of C (Bates and Mathis 2009).

Arctic warming may also lead to the release of $CH_4$ from frozen gas hydrates (ACIA 2004). Gas hydrates are solid forms of $CH_4$ and are present beneath and within the sub-sea permafrost

(Archer 2007). Large amounts of $CH_4$ hydrates are currently stored in continental and Arctic shelf deposits (Shakhova and Semiletov 2009) and permafrost (IPCC 2013). According to some estimates, the Arctic may contain about 1600 Pg C of $CH_4$ hydrate in the Arctic Ocean shelf and the subsea permafrost (Isaksen et al. 2011). $CH_4$ hydrate dissociates when water temperature increases or pressure decreases due to sea-level drop and $CH_4$ is then added to the global C cycle by diffusion into the water column or by ebullition (Kennett et al. 2000). Methane hydrate could become unstable with pressure changes, resulting in a major and abrupt bursts of $CH_4$ (Shakhova and Semiletov 2009).

### *1.7. Canadian Arctic physiography*

The Arctic landmass makes up about 5% of the total global land surface (11 million km²), while the Arctic Ocean covers about 3% of the Earth's total surface area (14 million km²). The continental shelf around the Artic Ocean's deep central basin corresponds to slightly more than half of the ocean's area. Arctic and subarctic topographies vary considerably within the territory as a function of the area's geological past. The landforms surrounding the Arctic Ocean are of three major types: rugged uplands with many scoured rock surfaces and spectacular fjords; flat-bedded plains and plateaus largely covered by deep glacial, alluvial and marine deposits; and folded mountains ranging from the high peaks of the Canadian Rockies to the older, rounded slopes of the Russian Ural Mountains (ACIA 2004).

The geological structure, relief attributes of land, the distribution of continuous permafrost, and the position of the tree line are the criteria used for physiographic regionalization of the Arctic and subarctic region (Brookes et al. 2011). The tree line is the northern limit of arboral growth, where tree growth and distribution are constrained (Payette et al 2001). The boundary between the Arctic and subarctic is approximately delimited by the northern edge of the tree line (Figure 1.1). The tree line also approximates the southern boundary of the zone of continuous permafrost (Brookes et al. 2011).

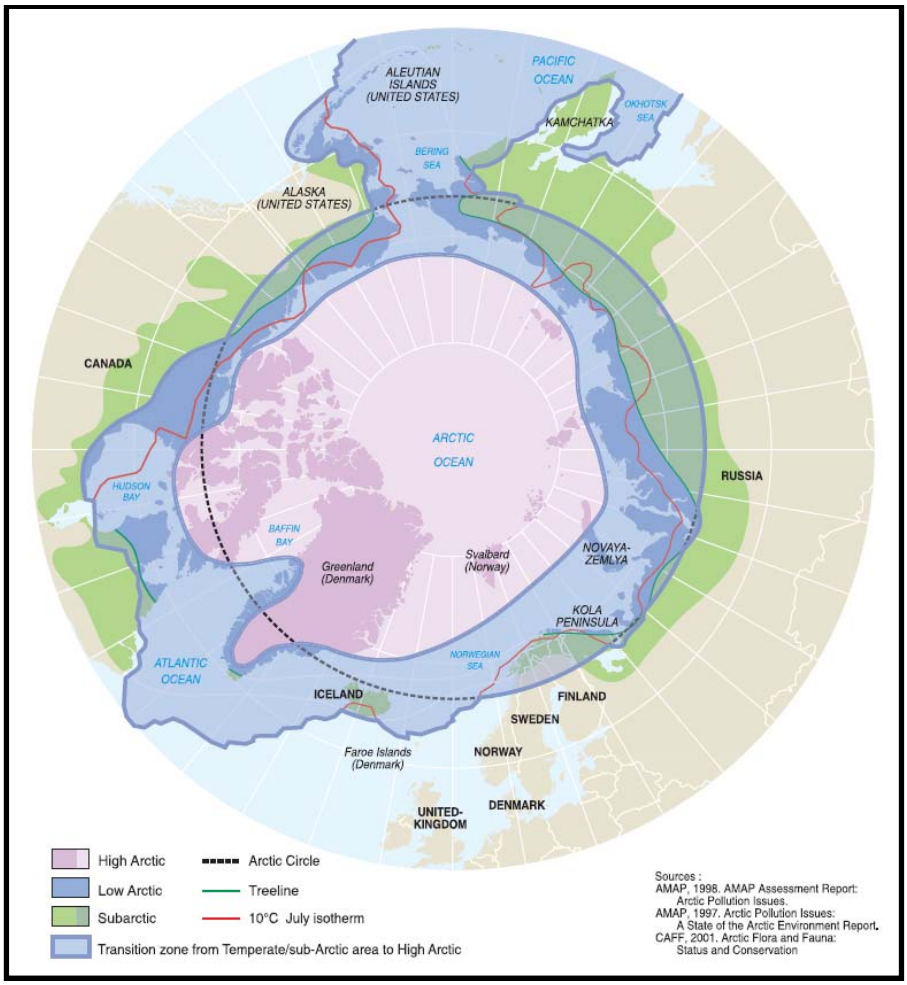


**Figure 2.1 Boundaries of subarctic, Low Arctic and High Arctic, including treeline and transition zone from temperate to high Arctic (from ACIA, 2004).**

About 26 % of Canada's land is located north of treeline while about 15-20 % is located within the subartic (Brookes et al. 2011). Canada includes 1.25 million km² or 63% of the circumpolar High Arctic region, the most of any country, and 1.30 million km² or 38% of the circumpolar Low Arctic, second only to Russia (Walker et al. 2005). High and Low Arctic regions are two major bioclimatic zones where the High Arctic is charaterized by the absence of sunlight during winter. An alternative but similar regional distinction is described using the southern Arctic, which corresponds to the northern mainland of Canada, while the northern Arctic covers almost all the Canadian Archipelago.

Physiographic regions delineate regions by geologic structure and histories and plant distribution (NRCan 2013). Canada's High and Low Arctic are separated into one minor and five major physiographic regions (Figure 1.2). These include the Arctic Coastal Plains and Arctic Lowlands, the Innuitian Region of the High Arctic, and parts of the Canadian Shield in Northern Ontario and Manitoba, Nunavut, Nunavik and Nunatsiavut, as well as part of the Cordilleran and the Interior Plains.

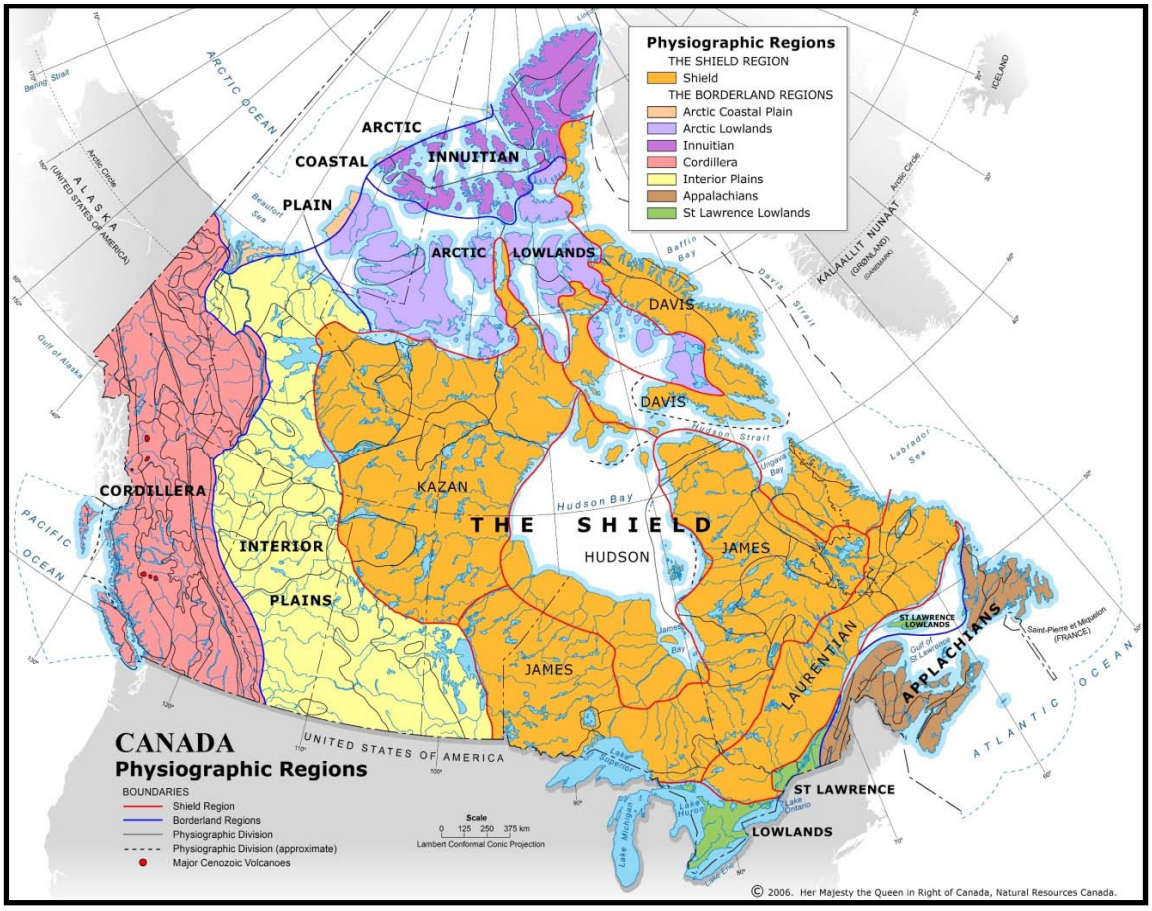


**Figure 2.2 Physiographic regions of Canada (from NRCan 2013).**

The northern Arctic and the Innuitian Region are characterized by zones of mountains—the Arctic Cordillera—interspersed with plateaus, uplands and lowlands. The Arctic Lowlands are located between the Canadian Shield and the Innuitian Region (NRCan 2013). The western Arctic Lowlands are composed mainly of lowland plains with glacial moraines, while the eastern region contains mostly plateaus and rocky hills (Prowse et al. 2009a). North of Baffin Island,

Bylot Island is representative of the northern eastern Arctic Lowlands, with high plateaus, glaciers and glacial valleys. The northern part of the Interior Plains physiographic region is part of the Arctic and is composed of taiga and tundra along low-lying plateaus and extensive wetlands (Prowse et al. 2009a). The high-latitude Taiga Cordillera is characterized by landforms produced by volcanic processes (NRCan 2013). These landforms include a mix of high peaks with narrow valleys, plateaus and plains, as well as large ice fields (Prowse et al. 2009a). The Canadian Shield dominates the eastern and central portions of the Arctic, the Taiga Shield, a part of the southern Arctic and the eastern part of Baffin Island. The shield contains a mix of lakes, ponds, swamps and rivers in expanses with a high proportion of bare rock (Prowse et al. 2009a). The specific landscape of the Canadian Shield is distinct, carved by long periods of erosion and glaciation processes, and consists of a core of old, massive Precambrian crystalline rocks (NRCan 2013). Nunavik's Taiga Shield is highly representative of the Arctic Canadian Shield but also provides a gradient of vegetation between the boreal forest and taiga. The Hudson Bay region forms the main depression of the Canadian Shield. The Hudson Bay Lowland presents a variety of wetlands and swampy plain with subdued glacial features (NRCan 2013).

Permafrost is a distinctive feature of the Arctic environment. The surface energy balance, which is regulated by climatic factors, hydrology, albedo, topography, geomorphology, surface wetness, snowpack conditions, vegetation and surface cover, controls permafrost distribution, thickness and temperature (Etzelmuller and Frauenfelder 2009; NRCan 2013). The geological history of the Quaternary, with succeeding episodes of glaciation and deglaciation, may also partly explain the distribution of permafrost (Heginbottom et al. 1997). Permafrost distribution in the Northern Hemisphere is separated into four groups: continuous, discontinuous, sporadic and isolated (ACIA 2004). Permafrost covers the entire area in the continuous zone and may be several hundred metres thick (Prowse et al. 2009c). In the discontinuous zone, permafrost covers 50 to 90% of the land surface and is only a few metres thick. In the sporadic zone, permafrost covers 10 to 50% of the landscape (ACIA 2004). Sporadic permafrost occurs only in peatland complexes (Bauer and Vitt 2011) and at high altitudes (Lewkowicz et al. 2011), and accounts for less than 10% of the total area. The impact of ice formation on the ground results in palsas or lithalsas (Calmels et al. 2008) and ice-rich periglacial mound formations that occurs especially along the east coast of the Hudson Bay in Nunavik (Fortier et al. 2008). The depth of the

seasonal active layer also influences hydrology and limits surface and subsurface water circulation and acts on the formation and distribution of wetlands and peatlands in lowlands (Prowse et al. 2009c).

### *1.8. Canadian Arctic vegetation communities, aquatic ecosystems and carbon stocks*

The Arctic is often thought of as arid and inhospitable where cold and snow prevail in a wild and treeless environment. However, there is great diversity in ecosystem characteristics across the subarctic and Arctic regions. From south to north, the biomes or major vegetation communities are lichen woodland (sparse taiga), forest tundra (or northern taiga), Artic tundra and Arctic polar desert (AC 2001). Boreal forest (southern taiga) is south of the subarctic region. The boundary between the subarctic region (forest tundra) and Arctic tundra, , the tree line, is a small latitudinal transition zone of 30 to 50 km, and extends around the Earth for more than 13 400 km (Callaghan et al. 2002). Plant diversity in the Arctic is low and follows a climate gradient, with the more developed abundant community—the boreal forest—at the southern boundaries and the poorest—polar deserts—at the highest latitudes. The Arctic contains about 3% of the world's plant species, and primitive plant species including lichens (11%) and bryophytes (6.6%) are relatively abundant compared to shrubs and other vascular plants (ACIA 2004).

The distribution of plant communities in the Arctic is governed mostly by climatic factors, temperature and precipitation, substrate chemistry, nutrient availability and geomorphologic conditions such as permafrost occurrence, active layer depth, hydrology and topographic location (Gould et al. 2003). The impact of climatic factors, temperature and moisture availability, on plant communities in the northern environment is clear and direct; climate drives the limit of the bioclimatic zones that control plant species, diversity and the amount of vegetation cover (Walker 2000). Temperature affects the dynamics of the entire tundra ecosystem (Henry and Molau 1997). The length of the snow-free season and the number of degree-days higher than 0 – 5 °C act on the active layer depth, permafrost occurence and plant biomass (Walker et al. 2010). Substrate chemistry also acts on species composition as observed in the Canadian Shield's acid soils and in the limestone and marine sediments of the Archipelago, for example (Gould et al. 2002).

Plant communities in the Arctic have been mapped as four major zones based on the controlling factors outlined above. The dry ecosystem zone represents 36.1% of the whole Arctic, the mesic zone accounts for 57.7%, the wet zone constitutes 4.1%, and the riparian zone represents 2.1% (Gould et al. 2003). A large part of the dry ecosystem consists of barren, semi-desert or polar desert vegetation, and accounts for the most abundant type of vegetation in the Canadian Arctic (Walker et al. 2005). Dry zone ecosystems are located in upland areas on steep topography, high plateaus, mountains and other landforms with low soil moisture, exposed to wind and with limited snow cover (Bliss 2000). The tundra types in this zone include polar semi-desert and desert vegetation and lichen (Gould et al. 2003). Mesic ecosystems are typically found in a moderate and well-drained habitat, mainly in rolling plains or low hills. This zone includes a variety of shrub-graminoid communities (Gould et al. 2003). The zone also includes tall shrub tundra close to stream banks, river terraces and lakeshores, mostly within the southern boundary. Heading toward the pole, low-shrub tundra is observed on slopes and uplands, while further north, dwarf shrub tundra is observed on rolling terrain with intermediate drainage (Bliss 2000). The wet ecosystem is characterized by poor drainage and is present in some specific permafrost areas and in bedrock-dominated landscapes. A large portion of wet vegetation is present in wetland, lowland and coastal plains, and is mainly composed of a variety of graminoids on mossy tundra (Walker et al. 2005). The riparian zone is a mix of wet and mesic vegetation and floodplains. The vegetation includes many graminoids complexes (Gould et al. 2003).

Within the subarctic region, the northern part of the boreal forest presents great biodiversity. This habitat is mainly dominated by coniferous trees, spruces, firs and pines (*Picea* spp., *Abies* spp., *Pinus* spp.), and some deciduous species, birchs and poplars (*Betula* spp. and *Populus* spp.) (Messaoud et al. 2007). Wetland communities with a carpet of Sphagnum moss species are also present within the area (Richardson 2000), which includes the vast areas of peatland of the Hudson Bay and James Bay lowlands (Pelletier et al. 2007). At the northern limit of the subarctic zone and north of the boreal forest, northern taiga is mainly composed of lichen woodland (or sparse taiga) and forest tundra (or forest taiga) (Elliott-Fisk 2000). Lichen woodlands have 10-40 % tree cover (mainly black spruce) with extensive coverage of lichens (western *Stereocaulon paschal* and eastern *Cladonia stellaris*) (Payette et al. 2000) and are typical of the Canadian Shield in open areas and wind-exposed landscapes (Elliot-Fisk 2000). The forest tundra is a

transition zone between the boreal forest and the Arctic tundra (Payette et al. 2001).The forest tundra is mainly composed of schrub, patchy and scarce trees and the most abundant species are black spruce (*Picea mariana*) and white spruce (*Picea glauca*). Forest tundra is mainly present in wind-protected areas, in landscape depressions and in small valleys. The transition zone between forest tundra and Arctic tundra ecozones follows an irregular vegetation distribution pattern that varies with physiography, namely surface atmospheric circulation, microclimatic conditions, topography, geologic history, soil disturbance and fire history (Auger and Payette 2010).

Freshwater ecosystems in the Arctic and subarctic regions cover a large part of the territory with high variability in size, form and structure (Reist et al. 2006). Their characteristics depend on latitude, geography, marine processes and often the size of the watershed, which sometimes extends beyond the physical boundaries of the Arctic region (Serreze et al. 2006). Freshwater ecosystems are also directly impacted by the regional climate and surface weather conditions, which influence biogeochemical cycles, ecology and biology (Prowse et al. 2006). Climate may affect wet deposition, evapotranspiration and the water table level, as well as the timing of ice formation, snow melt and springtime runoff, all of which significantly impact the hydrology of Arctic regions. Permafrost and the depth of thaw also have a major influence on the flow path and nature of the water flowing into freshwater systems (Carey 2003).

Arctic freshwater ecosystems consist of flowing water and standing water. Wetlands are dynamic terrestrial ecosystems where the water table is close to the surface (Richardson 2000) and are also discussed here. Large river ecosystems in the Arctic act as a conveyor belt for water, energy, nutrients, sediments, organic matter and biota, as well as contaminants (ACIA 2004). Rain precipitation, snow melt, thawing permafrost and groundwater discharge are main sources of water input to the river system during the summer season (ACIA 2004; Serreze et al. 2006). The Hudson Bay watershed, ~ 3.9 million km², is the largest in Canada and also contributes to a large input of freshwater into the Arctic Ocean. The Hudson Bay watershed includes Manitoba, northern Ontario and Quebec, a large part of Saskatchewan, southern Alberta, southwestern Nunavut and the southern part of Baffin Island. The Hudson Bay watershed and the Arctic Ocean watershed, ~ 3.6 million km², drain about 75% of the water that falls in Canada.

Lentic ecosystems such as standing water, lakes, ponds and wetlands are also abundant in Arctic and subarctic ecosystems (Prowse et al. 2006). Standing water varies in size, importance and distribution across the territory and includes large water bodies, as well as shallow ponds that freeze completely to the bottom during the cold season (ACIA 2004). The largest freshwater lake in the Canadian Arctic Archipelago is Nettilling Lake, 5542 km², followed by Amadjuaq Lake, 3115 km²; both are located on Baffin Island. Other standing water in the Canadian Arctic is mainly composed of shallow ponds in the tundra less than 2 m deep, small lakes, and thermokarst lakes and ponds formed by thawing permafrost and subsidence of the surface (Prowse et al. 2009d). The size and abundance of lakes is much higher in the Canadian subarctic. The largest lake in Canada, Great Bear Lake (31 080 km²), is located in the Northwest Territories. It is followed by Great Slave Lake (28 930 km²). The main sources of large lakes in the Eastern Canadian subarctic are hydroelectric artificial reservoirs such as Smallwood Reservoir (6527 km²) in Nunatsiavut and Caniaspiscau Reservoir (4318 km²) in Nunavik (NRCan 2013).

Wetland ecosystems such as peatland, bogs, fens, swamps and marshes are abundant in northern regions and are mainly associated with rivers, coastal deltas and lowlands (Prowse et al. 2006). The continuous interaction of hydrology, climate and permafrost may create particular wetland structures such as collapsed scar bogs, lowland polygon bogs, peat mound bogs, polygonal peat plateau bogs, collapsed scar fens, lowland polygon fens, palsa fens and snowpatch fens (Warner and Rubec 1997). Generally, northern peatlands are occupied by 10 or so dominant plant species but may contain 100 to 200 species of other vascular plants (Richardson 2000). The total wetland area is larger in the southern Arctic than at high latitudes. Overall, the wetland area is about 3.5 million km² or 11% of the whole Arctic landscape (ACIA 2004). About 5% of the Canadian Arctic is made up of wetlands, most within the Northwest Territories (Prowse et al. 2009d) while wetlands cover 30% of the Canadian subarctic (NRCan 2013). Peatlands are wetlands with at least 30-40 cm of peat, or partially decomposed organic matter, and include both bogs and fens. Canadian peatlands represent about 1.1 million km² of the landscape or 12% of the whole Canadian territory. The main peatland areas are in boreal (64%) and the subarctic (33%) regions (Tarnocai 2006). Peatlands in Canada are found throughout the country but are concentrated in the Mackenzie Delta and in the Hudson Bay and James Bay lowlands (Richardson 2000).

The C stocks present in permafrost, peatlands and wetlands are much larger than the amount of C present and available in the atmosphere (Davisdon and Janssens 2006). Quantifying the C stock in the Arctic and subarctic continues to be an important area of research (Hugelius et al. 2014). Due to the large quantities of C stored in permafrost-affected soils, the Arctic has the potential to play an important role in global C budgets. The C pool within the top first meter (0-1 m) of Arctic permafrost is estimated at 28% of the global total organic C, or 472 ± 27 Pg C. When considering the full profile (to 3 m or deeper), 60% of the global organic soil C is found within Arctic permafrost, 1035 ± 150 Pg C in the 0-3m layer and only 12% in the remaining deeper zone, 213 ± 52 Pg in the Yedoma region (Hugelius et al. 2014).

Carbon distribution within the Arctic depends on various factors, such as glacial history, geomorphology, physiographic characteristics and climate. Generally, the soil C content of the Canadian Arctic is relatively low because of low biomass inputs. Soil organic C in Canada is most abundant in peatlands because of the deep peat deposits that accumulate over centuries at very low rates of 0.02 to 0.03 kg $m^{-2}$ $year^{-1}$ due to a slight imbalance between $CO_2$ sequestration and losses through decomposition (Ju and Chen 2005).

### *1.9. Study site descriptions – a latitudinal gradient in the Eastern Canadian Arctic*

This section outlines the general climatic characteristics (Table 2.1), physiography and vegetation of the four study sites examined in this research. The four sites (Kuujjuarapik, Umiujaq, Bylot Island and Pond Inlet) include ecosystems typical of a latitudinal gradient in the eastern Arctic within Nunavik and Nunavut.

**Table 2-1 General climatic characteristics and of the Eastern Canadian Arctic study sites.**

| *Sites* | *Region (see Figure 2.1)* | *Latitude* | *Longitude* | *ASL* (m) | *Annual average temperature (July, January monthly values in brackets )* (°C) | *Climate normal annual precipitation (total rain and snow in brackets) (mm)* |
|---|---|---|---|---|---|---|
| Kuujjuarapik [1] | Subarctic | 55°17' N | 77°46' W | 21 | -4.4 (10.6, -23.4) | 648.5 (414.8, 241) |
| Umiujaq [2] | Low Arctic | 56°33' N | 76°32' W | 71 | -5.6 (9.0, -24) | 530.0 (330, 200) |
| Bylot Island [3] | High Arctic | 73°08' N | 80°00' W | 20 | -14.5 (6.2, -34.7) | 229.3 (94.3, 135) |
| Pond Inlet [1] | High Arctic | 72°41' N | 77°59' W | 55 | -15.1 (6.0, -32.4) | 190.8 (85.4, 144) |

(Sources: [1] EC 2013, [2] Larrivée 2007, [3] CEN 2013b)

### *1.9.1. Kuujjuarapik*

The Kuujjuarapik (Whapmagoostui) research site is located near a small village on the east coast of Hudson Bay at the mouth of the Great Whale River (Nunavik, Quebec) (Figure 2.3). This region is located a few hundred kilometres below the tree line. The climate (Table 2.1) is subarctic, although it has some Arctic components. Hudson Bay has a major climatic impact on the region, sometimes resulting in extreme weather conditions for this latitude. Ice cover on Hudson Bay during winter minimizes heat and moisture exchange between the ocean surface and atmosphere. The Bay thus acquires the properties of a continental surface, and the weather turns cold and clear. In the absence of ice cover, the climate is more maritime and involves heavy rainfall and frequent fog along the coast in spring, summer and autumn (Ricard 1998). Based on the Canadian climate normal for 1971–2000, the snow-free season extends from June to September.

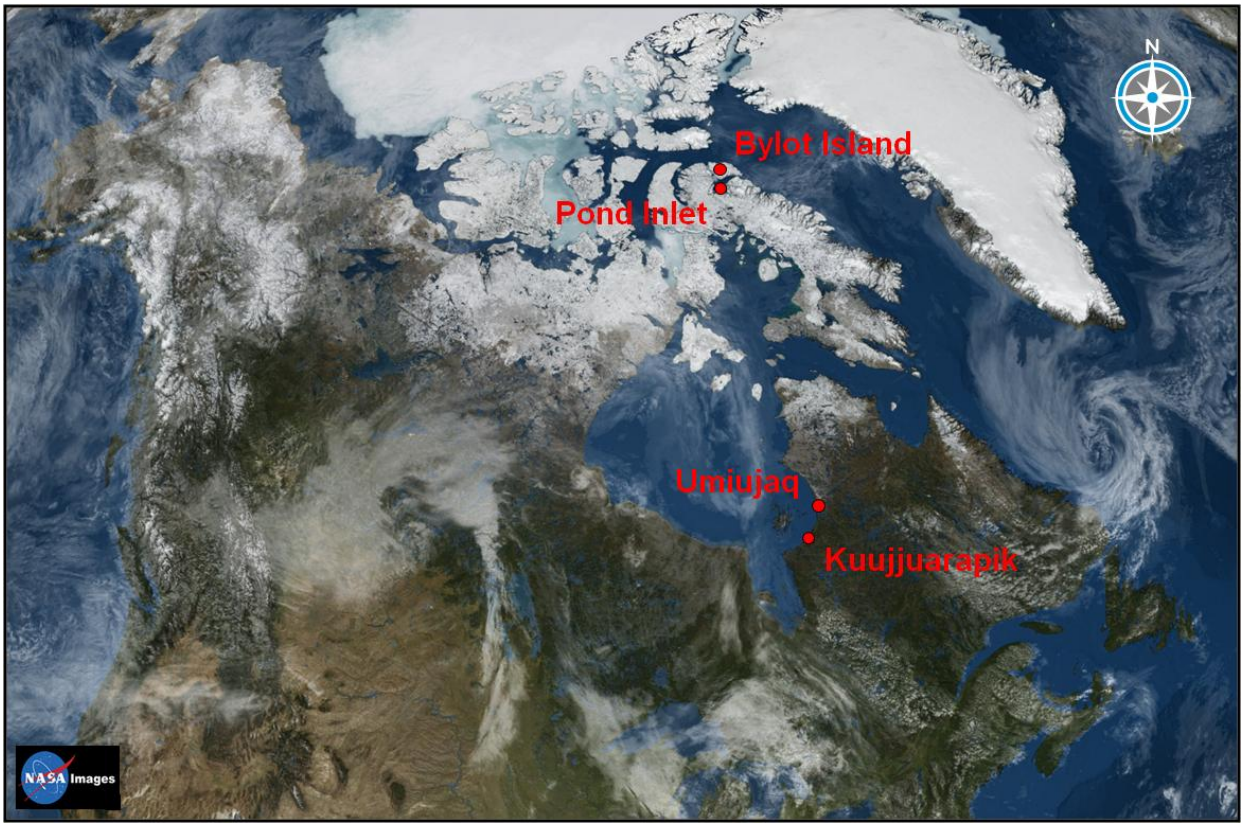


**Figure 2.3 The study areas within the eastern Arctic in Nunavik and Nunavut (modified from NOAA).**

The Kuujjuarapik area has great aquatic and terrestrial biodiversity and is identified as a transition area between lichen woodland, forest tundra and subarctic tundra, depending on the altitude, wind exposure and other climatic and geomorphological factors. Globally, conifer forests are present in sheltered and wind protected areas, shrub-dominated cover occurs in transition zones, grass-dominated cover occurs along the coast, lichen-heath covers rocky outcrops and lichen-spruce woodlands are present on the sandy shore (Bhiry et al 2011). In the research area, the land is rather flat with a carpet of moss, lichens, forbs, crowberry (*Empetrum nigrum*) and small shrubs, mainly dwarf birch (*Betula glandulosa*) and green alder (*Alnus crispa*), as well as taller trees including black spruce (*Picea mariana*), sallow (*Salix* spp.) and pine (*Pinus* spp.) in the wind-protected areas. The area surrounding the site rests on granite-gneiss rocks of the Precambrian Shield. The main site lies on Quaternary deposits of

glacial tills, marine clays, and littoral sands, topped with a small amount of organic matter (Arlen-Pouliot and Bhiry 2005). The soil characteristics are sandy loam to loamy sand. The amount of organic material is greatest in wind-protected areas and small depressions. In Canada's soil organic C database, the area of Kuujjuarapik has 35.8 kg $m^{-2}$ total C (0-1m or to bedrock) and 4 kg $m^{-2}$ surface C (0-30cm) (Tarnocai and Lacelle 1996). Measurements in Kuujjuarapik show an average of 1.76% organic C by dry weight in the surface soils of tundra-classified sites, 3.66% C in forest tundra sites and 43.52% C in thermokarst ponds. The thermokarst site is located 8 km southeast of Kuujjuarapik in a permafrost peatland and contains a mix of sedge fen dotted with palsas, 1 to 5 m in elevation, with 50 to 60 cm active layer. The main plant species are graminoids plants (*Carex* spp.), cottongrass (*Eriophorum* spp.), alpine bulrush (*Trichophorum* spp.), cloudberry (*Rubus* spp.), marsh cinquefoil (*Comarum palustris*), brown mosses and *Sphagnum* spp. (more details in Arlen-Pouliot and Bhiry 2005).

### *1.9.2. Umiujaq*

The research area is located near the Inuit community of Umiujaq on the east cost of Hudson Bay, in Nunavik, Quebec. Study sites are located at the south end of the village on the shore of Hudson Bay and in a valley called Vallée des Trois, at the northern end of Lac Guillaume-Delisle. The sites are located in discontinuous permafrost (Fortier et al. 2008) on Tyrrell Sea sediments (Allard and Seguin 1987) of till, glaciofluvial gravels, and silts (Ménard et al. 1998). The main site of Umiujaq is installed on coastal dunes and has sandy soil. The complementary sites in the valley are permafrost mounds and have silty clay soils. Permafrost mounds in the valley are oval or sometimes circular in shape, about 50 m in diameter and 3 to 4 m high. The active layer is about 1.6 m, and the base of the permafrost is 22.5 m (Buteau et al. 2005). In Canada's soil organic C database, the Umiujaq area has 0.53 kg $m^{-2}$ total C (0-1 m or to bedrock) and 0.51 kg $m^{-2}$ surface C (0-30cm) (Tarnocai and Lacelle 1996). There was 0.18% organic C by dry weight in the surface soils at the main site on the shore of Hudson Bay, 10.12% C at the top of the valley, 33.21% C on permafrost mounds and 1.69% C at the bottom of the valley.

Umiujaq is located a few kilometres south of the tree line. The area presents a contact between a distinctive geologic structure, the Archean gneissis shield, and the overlying sedimentary and

volcanic Proterozoic sequences (Fortier et al. 2008). In the surrounding environment vegetation is scarce although present in valleys and protected areas. The vegetation on the sandy dunes is poor and mainly composed of graminoids. Plant communities in the valley are more developed, with a mixture of lichens, moss and Krummholz vegetation made up of black spruce (*Picea mariana*) and various shrubs (*Betula glandulosa* and *Alnus crispa*) (Ménard et al. 1998). The climate is characterized by a relatively cool and short summer followed by long, dry and very cold winter. The topography of the area, with the proximity of Hudson Bay and the valley, causes frequent fog and low cloud conditions when the water is open. The climate (Table 2.1) is mainly maritime in the ice-free season and more continental when Hudson Bay is frozen (Larrivée 2007). Two thirds of the rainfall occurs mainly between July and November. Approximately half of the snow precipitation falls between October and December during the ice-free season (Lévesque et al. 1988). The snow-free season extends from June to September, but snow cover is weak in May and October.

### *1.9.3. Bylot Island*

Bylot Island is located just north of Baffin Island, Nunavut, within Eclipse and Lancaster Sound. Bylot Island is part of the Sirmilik National Park and is mainly covered by high mountain peaks and glaciers, but vast plains are present in the south and west margins. The study area is located in a large glacial valley with tundra polygons, thaw lakes and ponds. This specific ecosystem results from an upward growth of ice-wedges in the composite sediments (Ellis and Rochefort 2006). The area is underlain by continuous permafrost, probably more than 400 m thick, and the active layer is only 37 to 49 cm (Fortier et al. 2006). The island is composed of sedimentary rock, mainly limestone, dolomite, sandstone and shale (Devlin and Finkelstein 2011). The soils in the bottom of the valley are fine-grained wind deposits and organic sediments (CEN 2014). In Canada's soil organic C database, this area of Bylot Island has 19.1 kg $m^{-2}$ total C (0-1m or to bedrock) and 5.52 kg $m^{-2}$ surface C (0-30cm) (Tarnocai and Lacelle 1996). Soil texture is loamy sand. The glacial valleys include extensive well-drained uplands and polygon rims (90%) and wetland/polygon centers (10%) ecosystems (CEN 2014). In valleys, soil moisture is an important factor regulating plant diversity. In wetland and tundra polygons, plant communities are mainly composed of sedges (*Carex aquatilis*, *Eriophorum scheuchzeri* and *Eriophorum angustifolium*),

grasses (*Dupontia fisheri* and *Pleuropogon sabineai*) and a few forbs (herbaceous plants). In polygon rims and uplands, a large variety of moss is present, and the most abundant plants are shrubs (*Salix* spp. and *Vaccinium uliginosum*), forbs (*Cassiope tetragona* and *Oxytropis maydelliana*) and grasses (*Arctogrostis latifolia*, *Alopecurus alpinus*, *Poa glauca* and *Luzula confusa*) (Gauthier et al. 1996).

The climate (Table 2.1) in Bylot Island is representative of High Arctic weather, with extreme long and cold winters and very cool and short summers. At this latitude, full darkness in winter is typical, and there is 24 hours of daylight at the summer equinox. Within the Arctic Circle, the annual mean solar radiation is 100 $W/m^2$, and the incoming radiation is received mainly between late spring and early fall (Linacre and Geerts 1998). The snow-free season is between mid-June and the end of August (CEN 2014). This region receives weak annual precipitation and is considered as semi-desert or polar desert.

### *1.9.4. Pond Inlet*

The hamlet of Pond Inlet is a small community located on the northern shores of Baffin Island. This Arctic community faces Eclipse Sound and Bylot Island. The study area is located on the outskirts of the municipality just behind the Environment Canada weather station. The overall climate in Pond Inlet is very similar to that of Bylot Island, as expected given their proximity (Table 2.1). Based on the Canadian climate normal for 1971–2000, the snow-free season extends from mid-June to the end of August. The growing season is therefore very short and is helped by the length of the summer day. Most of the rain precipitation occurs in July and August and snow from September through November. This region receives weak annual precipitation and is considered as semi-desert or polar desert.

The Pond Inlet area is located in continuous permafrost, with only about 80 cm active layer. Soil temperatures at the surface of the active layer have high amplitude, and zero temperature fluctuation is observed at 17.6 m (Ednie and Smith 2010). Bedrock geology is mainly composed of Precambrian rock, granites and gneisses (Andrews et al. 2002). Moraines are present in the area, and glacial till rarely exceeds 5 m (Ednie and Smith 2010). In Canada's soil organic C

database, Pond Inlet has 0.63 kg $m^{-2}$ total C (0-1m or to bedrock) and 0.24 kg $m^{-2}$ surface C (0-30cm) (Tarnocai and Lacelle 1996). Soil texture is sandy loam. At the main site there was 21.19% C organic C by dry weight at the surface. However, other soil sampling in the region indicates a variation of 0.07 to 31.76% C. Organic matter tends to accumulate in small depressions and wind-protected areas. Mainly forbs, grasses, lichens and shrubs are found in this drier tundra plateau, and the surface is slightly hummocky.

## *1.10. The potential impacts of climate change and interannual weather variations in carbon exchange processes in Arctic ecosystems*

Although research programs examining $CO_2$ and $CH_4$ exchange processes between the atmosphere and the subarctic and Arctic ecosystems described above over short time periods of days to years cannot directly assess the impacts of climatic change, studies such as these help develop knowledge about the underlying mechanisms that drive spatial and temporal variations in these fluxes and provide insight into potential responses to climatic change.

### *1.10.1. Aquatic ecosystems*

As a whole, Arctic wetlands uptake $CO_2$ from the atmosphere during the growing season and are a source of $CO_2$ in fall when plants senesce and during the cold season and spring melt. A portion of the C lost within those periods can be renewed via plant sequestration and litter inputs to the soils (Whiting and Chanton 2001). Wetlands can also be an important source of $CH_4$ throughout year as function of water level and the degree of anoxia. Lakes and ponds are typically $CO_2$ and $CH_4$ sources (Kling et al. 1992). However, Arctic ponds, with substantial lined benthic microbial mats, may be highly productive and be a sink for $CO_2$ (Laurion et al. 2010). Thus, freshwater ecosystems can be a C source and/or a sink depending on the time of year and can have a significant impact on the atmosphere (Friborg et al. 2003).

An important impact of Arctic warming and the increase in the length of the ice-free season is an increase in the mean annual water temperature which may influence the chemical, mineral and nutrient status of aquatic systems. Thermal shifts in surface freshwater affect biological activity

including algae biomass and primary production and the development times of biota throughout the aquatic food chain (Hinzman et al. 2005; Kittel et al. 2011). Higher temperature also increases the assimilation and uptake of $CO_2$ by phytoplankton and periphyton (Wetzel 2001). Further, a longer ice-free season will also influence lake stratification and the size of epilimnion, metalimnion and hypolimnion in deeper lakes, as well as the mixing depth. A longer stratified season may lead to oxygen depletion in the lower layer and result in a build-up of reduced gases such as $CH_4$ and $H_2S$ and their release to the atmosphere (Rouse et al. 1997; Niemi et al. 2002). A longer ice-free season may also increase the period with sufficient underwater light and light penetration, positively affecting primary production and the length of the growing season, which influence $CO_2$ uptake from the atmosphere (Huttunen et al. 2003). However, a longer ice-free season may also increase the amount of UV-B radiation reaching aquatic ecosystems and may negatively impact the productivity, development and genetics of primary producers and reduce $CO_2$ uptake and affect global biogeochemical cycles (Hader et al. 2007).

One of the important and easily observable impacts of climate change in Arctic freshwater ecosystems will be the variation and changes in phytoplankton biomass (Vincent et al. 2009) and in the structure of aquatic plant communities (Olthof and Pouliot 2010). A marked northward migration of many species is currently observed in subarctic and Arctic regions, affecting both freshwater and terrestrial plant communities (Prowse et al. 2009d). This shift in species and the significant change in spatial distribution may impact the C cycle, nutrient transport and GHG efflux in aquatic ecosystems. The introduction of new species and the subsequent increase in plant biomass may also impact the nature and distribution of detritus and organic carbon. The amount and quality of organic matter present in the new species is different than that found in Arctic native species, and it will substantially alter aquatic ecosystems. Primary production also contributes to $CH_4$ fluxes in wetlands, regulating the amount of organic matter transferred from the water column to the sediment interface and thus influencing methanogen activity (Huttunen et al. 2003).

The biogeochemistry of freshwater ecosystems is also largely influenced by the surrounding environment. For example, smaller lakes are most influenced by the surrounding terrestrial environment and by shoreline plant communities and processes such as erosion (Walter et al.

2007) that enhance $CH_4$ oxidation, production and emission (Ström et al. 2003). Autochthonous production of aquatic organic matter in the freshwater ecosystem is normally low, therefore significant changes of the amount of allochthonous materials from the surrounding environment due to increasing active layer and permafrost thaw may irreversibly impact the entire biogeochemistry of aquatic ecosystems, since the main input of organic matter occurs from allochthonous input (Stottlemyer et al. 2001). Allochthonous C and nutrients are transported through catchments via streams, rivers, surface runoff and groundwater (Huttunen et al. 2003). Shallow waters and small aquatic systems are more sensitive to external C inputs than larger aquatic systems (Torgersen and Branco 2007). Although it is difficult to predict the magnitude of climate change and vegetation changes on C input to the aquatic system (Dittmar and Kattner 2003), it is clear that the oxygen level in aquatic ecosystems will be impacted by significant changes in autochthonous C input. A large input of easily degradable fresh organic matter promotes oxygen consumption through the decomposition of organic matter in the water column and sediment and may promote $CH_4$ production and emission (Huttunen et al. 2003).

Snow depth, the timing of snow melt and ice break-up has a direct impact on river flow, sediment loading, turbidity, habitat and biota, as well as affecting runoff (Kittel et al. 2011). Arctic warming may also significantly affect hydrology and the water budget, altering lake water storage and water availability by having an impact on snow duration, occurrence and depth (Kittel et al. 2011). Changes in snow depth will also impact directly the aquatic ecosystem by impacting snow's insulating properties during the cold season. Snow controls the amount of ice that forms on aquatic surfaces. Ice and snow cover influence aquatic ecosystems by controlling the incoming solar radiation, the amount of biological activity underwater and the transport of gases. Ice cover may prevent gas exchange for several months and may cause oxygen depletion and $CH_4$ formation, which is mainly released in springtime at ice melt (Rouse et al. 1997). Furthermore, a large number of Arctic wetlands and small freshwater systems are characterized by shallow water; with an increase in winter precipitation and warmer temperatures, these ponds may no longer freeze completely to the bottom, and the limnological characteristics of these ponds, such as biological, chemical and physical parameters, may be significantly changed (Rouse et al. 1997).

Significant changes in ice and snow cover may impact the water balance, which is tightly linked to the rate of evaporation and transpiration as well as to the amount of precipitation. A positive balance, i.e., higher precipitation than evapotranspiration, results in higher lake levels, soil moisture, surface runoff, river flow and groundwater stock (Rouse et al. 1997). This may also influence the size and distribution of Arctic wetlands. In wetlands, $CH_4$ emissions increase considerably, up to 60%, in warmer and wetter climates (Bubier et al. 2005). Alternatively, warmer and drier conditions could switch wetlands from a net sink to a net source of C (Rouse et al. 1997), since most of the interannual gas exchange variations in peatlands are related to climatic and hydrological conditions (Öquist and Svensson 2002). However, given the wide variety of Arctic wetlands, a drier climate may reduce $CO_2$ uptake in some areas while increasing it in others (Bubier et al. 2003).

Probably by far the greatest impact of climate change on freshwater Arctic ecosystems is the influence of degrading permafrost (Khvorostyanov et al. 2008). Permafrost plays an important role in the hydrological cycle by acting as a barrier and limiting water infiltration, surface runoff and groundwater storage. A large number of wetlands and small lakes exist in the Arctic because impermeable permafrost prevents and limits percolation and drainage of the active layer to the groundwater system or to surface runoff above the impermeable frost table (Rouse et al. 1997, O'Connor et al. 2010). In the last few decades, research has shown a significant warming, 0.5 to 2 °C, of the near-surface permafrost in Alaska and northern Russia (Kattsov et al. 2010). Permafrost degradation may promote wetland drainage while warmer air temperatures also promote drying in some locations (Kwon et al. 2006; Schuur et al. 2008; Avis et al. 2011). Wetland coverage could be substantially reduced or wetlands could disappear altogether with changes in geomorphology and land subsidence that promote lateral drainage of water bodies and wetlands (Wrona et al. 2004; Rodionow et al. 2006), which should limit future $CH_4$ efflux in the Arctic (Avis et al. 2011). In other regions, thaw of ice-rich permafrost may lead to the development of wetlands and thaw lakes through thermokarst activity (Walter et al. 2007; Kittel et al. 2011) and promote $CH_4$ production and emission to the atmosphere (Mazeas et al. 2009). Another important impact of permafrost thaw is enhanced erosion that can lead to increased water turbidity, export suspended matter, and sediment loads (Rouse et al. 1997).

Increasing wind speed and turbulence over lakes and wetlands may promote gas transfer and the emission of GHGs to the atmosphere. Numerous studies have clearly demonstrated the impact of wind and meteorological conditions on gas transfer (Poissant et al. 2000; Else et al. 2008). A decrease in atmospheric pressure coupled with an increase in near-surface turbulence can promote $CH_4$ ebullition and emission (Sachs et al. 2008). A large amount of $CH_4$ released by bubbling can thus contribute significantly to the global C cycle, exceeding the contribution of $CH_4$ oxidation in sediment and the water column (Huttunen et al. 2003).

### *1.10.2. Terrestrial Arctic ecosystems*

In most terrestrial ecosystems, $CO_2$ is the main component of the C budget (relative to $CH_4$, dissolved inorganic and organic C). A warmer and wetter climate may either promote the uptake of $CO_2$ through photosynthesis or the loss of $CO_2$ through autotrophic and heterotrophic respiration, distributed among soil microbes, roots and plants (Sagerfors et al. 2008). Some of the main factors regulating $CO_2$ flux in the environment are biotic factors, such as the structure of plant communities, or abiotic factors, such as climate and weather, hydrology and permafrost occurrence (McNamara et al. 2008).

Temperature is an important factor driving and affecting the control of biochemical reactions (Veteli et al. 2007). Temperature regulates respiration processes in soil and plants as well as photosynthesis (Davidson and Janssens 2006). As discussed above, temperature also impacts the duration, depth and temperature of the soil active layer, as well as the water table, and thus affects heterotrophic respiration in terrestrial ecosystems (Grant et al. 2011). An increase in plant productivity would also increase the amount of $CO_2$ emitted into the atmosphere (Schlesinger and Andrews 2000; King et al. 2006) since autotrophic respiration and rhizospheric respiration are the main processes regulating $CO_2$ production in upland soil and tundra (Davidson and Janssens 2006; Fox et al. 2008). Longer growing seasons with greater plant biomass production result in greater $CO_2$ uptake (Corradi et al. 2005). Gross primary production and uptake of $CO_2$ may also be promoted by increasing mineralization and nutrient uptake (Grant et al. 2011).

Slight variations in soil water content may also impact C uptake, heterotrophic respiration and net ecosystem production (Ju et al. 2006). Heterotrophic respiration and root respiration are controlled by soil moisture (Davidson and Janssens 2006). In dry and non-saturated upland soils, microbial activity, plant assimilation and respiration processes increase rapidly with soil moisture gains. The impact of water addition on soil $CO_2$ efflux may be observed over small distances and is highly dependent on microtopography, soil organic carbon content and climatic factors (Elberling et al. 2004). The long-term effect of an increase in soil water is a change in plant community structure, soil C stocks, and the composition of microbial communities (Risch and Frank 2007). The impact of warming and changes in precipitation is large and will certainly impact the regional C budget (Risch and Frank 2007).

In terrestrial ecosystems, vegetation acts directly on microclimate and regulates surface air and soil temperature (Adams 2007) via water and energy fluxes (Eugster et al. 2000). This is explained in part by an increase in the leaf area index through the growth of shrubs and larger species, which reduces surface albedo and increases heat transfer. Increasing the leaf area index may also increase photosynthesis and the $CO_2$ uptake capacity of terrestrial ecosystems (Shaver et al. 2007). In non-vascular plants, gas exchange is less efficient and is performed simply by diffusion. In vascular plants, gases pass through stomata in the cuticle and epidermis, which are normally open during the day when the rate of photosynthesis is highest (Kaplan and New 2006). Vegetation communities are highly dependent on climatic zone, latitude and topography, and warming will impact each plant species and community in a different way depending on its specific physiological characteristics (Kittel et al. 2011). Impacts on species, population levels, physiological characteristics and plant distribution also depend on past climate (Cannone et al. 2006). Similarly, observations show that important changes in vegetation communities are currently underway in northern regions (Kaplan and New 2006). These changes may also result in significant changes in soil organic matter, nutrients and microfauna, since they are interconnected within each plant community (Elberling et al. 2004). In Arctic and subarctic regions, the extent of lichen, moss and other bryophytes tends to decrease in favour of larger species such as vascular plants, graminoids and shrubs under warmer conditions (Henry and Elmendorf 2008). One potential result is the northern migration of the tree line as has been observed during past warm periods in the Arctic (Nichols 1976). The impact of vegetation

change at high latitudes is complex, and a complete understanding is crucial in order to measure and analyze the overall feedback between climate and atmospheric GHG concentrations (Bunn et al. 2005). Subarctic and Arctic vegetation is vitally important to animals and humans, who depend on plant resources for their food and their living environment; each species will have to adapt to climate change and Arctic warming. Climate change has major impacts both on ecosystems and the social economy (Kaplan and New 2006).

In the last decade's Arctic warming lead to significant reduction of the snow-season extent, and consequently 10 % snow cover declined, because of a shorter accumulation period despite an increase of precipitation as snow. Models estimate an additional loss of between 10 and 20% by the end of the 21st century (Kattsov and Kallen 2004). Locally snowfall amounts may also be limited downstream of pollution sources because of the impact of aerosols on cloud physics (Barnett et al. 2005). A decrease in snowpack and its insulating properties may increase winter damage to Arctic plants where typically the snowpack protects from winter injury (Moore 2008; Bokhorst et al. 2010). Shorter snow-seasons, reduction of snow cover, advance of spring melt and a shift in the timing of peak river surface runoff can lead to significant impacts on the hydrological cycle and nutrient transport (Barnett et al. 2005). The extent, height and duration of snow cover also influences subsurface temperature due to snow's insulating properties (Elberling 2007) with the potential to impact belowground C cycling in winter (Brooks et al. 2011). In contrast, increasing the abundance of shrubs may lead to snow accumulation in protected areas, thereby reducing wind impacts and increasing soil temperature, microbial activity and heterotrophic respiration (Henry and Elmendorf 2008).

Permafrost thaw can expose large amounts of sequestered organic matter to microbial decomposition and contribute to a positive feedback to the atmosphere. In terrestrial ecosystems, the speciation, structure and bioavailability of C are important factors regulating and controlling $CO_2$ and $CH_4$ efflux and atmospheric feedback (Hinzman et al. 1997). Warming also affects the depth and structure of the soil active layer depth, impacting soil water content, below-ground vegetation root structures and heterotrophic organisms (Wickland et al. 2006). Plant productivity can also be promoted by soil warming as enhanced decomposition rates promote nutrient

availability such that the increase in plant productivity may offset losses of soil organic C (Schuur et al. 2008; Schneider von Deimling et al. 2011).

Current research over the last few decades has attempted to establish with the greatest possible accuracy GHGs exchange trends in the Arctic subject to a changing climate. Process models suggest a mean NEE of 110 Tg C $yr^{-1}$ for the terrestrial Arctic, indicating that Arctic tundra has been a net C sink over the last two decades (McGuire et al. 2012). Primary production and the increase of C uptake by photosynthetic activity largely counterbalanced the increase of heterotrophic respiration caused by warming. However, NEE measurements across the Arctic tundra are scarce and site specific resulting in large uncertainties such that it is difficult to determine if the Arctic is a sink or a source from scaling exercises with field measurements. Current estimates range from a small source 80 Tg C $yr^{-1}$ to a large sink 291 Tg C $yr^{-1}$ (McGuire et al. 2012). In the future, NEE model scenarios estimate cumulative C emissions from thawing permafrost of 120 ± 85 Tg C by 2100 (Schaefer et al. 2014).

Between 2007 and 2010, global $CH_4$ emissions increased by 16-20 Tg C $yr^{-1}$ but were not found to relate to changes in the Arctic. Instead, emissions are sourced as being largely from biomass burning and wetlands mostly related to in the tropics (9-14 Tg C $yr^{-1}$) and mid-latitudes of northern hemisphere (6-8 Tg C $yr^{-1}$) (Bergamaschi et al. 2013). Nevertheless, a regional process-based model suggest that warming has increased $CH_4$ emissions in the last century, which is estimated to be a source of $CH_4$ of 19 Tg C $yr^{-1}$ (with estimates ranging from 8 to 29 Tg C $yr^{-1}$) (McGuire et al. 2012).

### *1.11. Conclusion*

The Arctic and subarctic is a wide and diverse region with a multitude of interacting ecosystems where C exchange processes operate with great sensitivity to the prevailing weather conditions during the short warm season before slowing dramatically during long cold winters. Although much is known about general C flux mechanisms and the important biotic and abiotic factors and processes controlling them, as described above, few measurements in subarctic and Arctic regions limit our understanding of the magnitude of these fluxes and how they vary and interact

in space and time now and in the future. The unprecedented change that is presently occurring and evolving rapidly in the climate sensitive polar regions may lead to significant, unprecedent and irreversible changes to the earth's climate system and C cycle.

## *Chapter 3: Spatial variability and landscape-scale estimates of $CO_2$ and $CH_4$ emissions in the Eastern Canadian subarctic*


## *ABSTRACT*

The carbon cycle of subarctic ecosystems is expected to be particularly sensitive to changing temperature and hydrologic regimes. These may affect the distribution of permafrost, wetlands and plant communities, as well as promote emissions of GHGs (such as $CO_2$ and $CH_4$) to the atmosphere. During the summers of 2006 and 2007, $CO_2$ and $CH_4$ emissions were measured in the Eastern Canadian subarctic in various terrestrial ecosystems, ranging from forest tundra to tundra, and aquatic ecosystems from wetlands to lakes using opaque chambers. This study emphasizes the impacts of substrate, land cover class and environmental factors on GHGs emissions. Landscape $CO_2$ respiration was highly variable among all land cover classes and soil substrates, ranging from near zero to 234.7 mg $CO_2$ $m^2$ $h^{-1}$ with a slight but not significant increase with increasing plant cover category. Landscape $CH_4$ fluxes were also highly variable with the highest emission rates observed in wetlands and collapsed palsa ponds, ranging from near zero to 17.3 mg $m^2$ $h^{-1}$. In aquatic ecosystems, $CO_2$ emissions were significantly correlated with redox potential, conductivity, major ions and TOC, and suggest a strong link with both microbial activity and allochthonous materials from the surrounding environment. Based on these flux measurements a regional (50 km) landscape estimate of $CO_2$ and $CH_4$ emissions were 0.9 g $CO_2$ $ha^{-1}$ $h^{-1}$ and 1.3 g $CH_4$ $ha^{-1}$ $h^{-1}$ respectively.


### *2.1. Introduction*

Direct and remotely sensed observations have shown that surface temperature has risen globally in the past number of decades, with important regional variations (Overpeck et al. 1997; Galbraith and Larouche 2011). The most pessimistic scenarios predict an increase of 0.7–2.0 °C by mid century and 1.0–3.7 °C by the end of 2100 (Kirtman et al. 2013; Collins et al. 2013), with rates of warming expected to be greatest at high northern latitudes (Rodionow et al. 2006). The Arctic and subarctic regions were one of the first environments to show the effects of climate change including significant impacts on ecosystems and communities (Hinzman et al. 2005;

Prowse et al. 2006; Schindler and Smol 2006). Warming is expected to have the greatest impact on subarctic and treeline ecosystems along the 0 °C mean annual isotherm (Christensen et al. 2004; Stottlemyer et al. 2001). In the Canadian Eastern subarctic taiga shield ecozone or forest tundra (Wiken 1986), there has been a significant temperature increase of close to 2 °C since the 1960s (Tremblay and Furgal 2008). In this area, where mean annual temperature is only a few degrees below 0 °C, even a small temperature change could significantly affect soil thermal and moisture regimes, and consequently affect ecosystem functions such as C cycling.

It remains uncertain how C pools in northern regions will respond to climate change. Landscape $CO_2$ respiration may be enhanced as warming soil, permafrost degradation, and lowering water tables enhance aerobic decomposition (Smith et al. 2004). Warming may also influence vegetation productivity and inputs to the soil that may also increase microbial activity as a result of extended growing seasons and greater photosynthetic activity, and, over longer time scales, changes to more productive plant communities depending on moisture and nutrient availability (Grant et al. 2011; Elberling et al. 2004; Kaplan and New 2006). In many northern ecosystems, $CO_2$ and $CH_4$ fluxes are strongly linked. Surface temperature and hydrology impact $CH_4$ emissions through influences on the relative rates of $CH_4$ production and oxidation, storage, and transport (Christensen et al. 2004). Wetlands and waterlogged soils are recognized as an important source of $CH_4$ in subarctic environments (Sjogersten and Wookey 2002). Thus warming that enhances permafrost degradation and leads to wetland expansion and formation, particularly in ice-rich soils, may enhance anaerobic decomposition and $CH_4$ emissions (Corradi et al. 2005).

Canada's forest tundra ecozone, located on either side of Hudson Bay, has a subarctic continental climate with a diverse mix of uplands, wetlands and innumerable water bodies and transition zones between open forests and Arctic tundra (NRCan 2013). Models predict a significant reduction of the sea-ice season on Hudson Bay with the greatest impact on climate and ecosystems along the eastern coast and James Bay (Joly et al. 2011). Since the 1990s, various studies have examined the impact of reservoirs and the production of hydroelectricity on GHGs emissions in northern boreal ecosystems surrounding James Bay (Duchemin et al. 1995; Demarty et al. 2009). Many studies have examined the C dynamics of the extensive peatlands of

the Hudson Bay and James Bay lowlands (Kuhlmann et al. 1998; Rouse et al. 2002; Pelletier et al. 2007; McEnroe et al. 2009; Humphreys et al. 2014). Carbon sequestration and peat accumulation in the Hudson Bay Lowland started during the mid-Holocene, due to rapid glacial isostatic adjustment and cooler and drier climate (Packalen et al 2014). As a result, there has been considerable C buildup in peat soils. Climate warming can seriously affect the biogeochemical cycles of these ecosystems thus potentially releasing large amounts of accumulated C and contributing significantly to climate change (Roulet et al. 2007). Thawing permafrost and C cycling in palsa mounds may also release large amounts of GHGs to the atmosphere (Laurion et al. 2010). However, C inventories and gas exchange studies in the subarctic have focused mainly on "hot spot" environments where the magnitudes of $CO_2$ and $CH_4$ fluxes were expected to be large and non-representative of the region. Little is known about the magnitude of $CO_2$ and $CH_4$ emissions from the full range of lakes, ponds, shallow water and surrounding terrestrial ecosystems.

The aim of this study was to quantify summer $CO_2$ and $CH_4$ emissions for the full range of aquatic and terrestrial ecosystems in Canada's Eastern subarctic and to examine the importance of limnology, vegetation cover and underlying substrate on spatial variations in C emissions. These fluxes were then scaled by cover type to provide a first estimate of this subarctic region's landscape-scale summer emissions of $CO_2$ and $CH_4$. Quantifying current atmospheric C emissions is critical for constraining current estimates of C feedbacks to the atmosphere in this region and providing insight into how this and other regions may change with further warming.

## *2.2. Materials and methods*

### *2.2.1. Site description*

The study area is located near the village of Kuujjuarapik/Whapmagoostui on the east coast of Hudson Bay at the mouth of the Great Whale River in the Nunavik area of northern Quebec, Canada (55°17'N and 77°46'W) (Figure 3.1). This region is located a few hundred km below the treeline in the subarctic zone and in sporadic permafrost. Hudson Bay has a major climatic impact on the region, sometimes resulting in extreme weather conditions for this latitude. In the

cold season, the Hudson Bay ice cover mimics conditions of a continental surface, and the weather is cold and clear. The climate is subject to marine influences and includes heavy rainfall and frequent fog along the coast in spring, summer and autumn (Ricard 1998). Based on the Canadian climate normals from 1971-2000 (EC 2013), the snow-free season extends from June to September, but snow cover is shallow in May and October, with an average depth of 4.7 and 3.4 cm, respectively. On average, Kuujjuarapik receives 414.8 mm of rain and 241.3 mm of snow annually. The 30-year climate normal annual temperature is -4.4 °C, with a daily average maximum of 11.4 °C in August and a minimum of -23.4 °C in January. The average daily maximum temperatures in July and August are 15.5 °C and 15.7 °C, respectively. The daily average air temperature, relative humidity and total precipitation for the three sampling months (June-August), and the climate normals are summarized in Table 3.1 with relevant method details described in Section 3.2.2.

The study region is known as forest tundra and represents a transition between boreal forest and tundra ecozones (Bhiry et al. 2011). The main research area, near Kuujjuarapik, is located on Quaternary deposits of glacial tills, marine clays and, mainly, littoral sands, topped with a small amount of organic matter, while the surrounding area is located on granite-gneiss rocks of the Precambrian Shield (Arlen-Pouliot and Bhiry 2005). The soil texture is mostly sand, both in open areas and non-vascular plant sites, while the soil texture in the areas colonized by vascular plants is mostly sandy loam to loamy sand. The amount of soil organic matter is larger in wind-protected areas, small depressions, and in areas of dense vegetation. In this area, soil organic C has been mapped as 35.8 kg $m^{-2}$ with 4 kg $m^{-2}$ in the top 30 cm of soil (Tarnocai and Lacelle 1996). In-situ measurements of soil organic C from the 0-10 cm depth show significant variability of soil organic C among sampling sites (Table 3.2) with relevant method details described in Section 3.2.2.

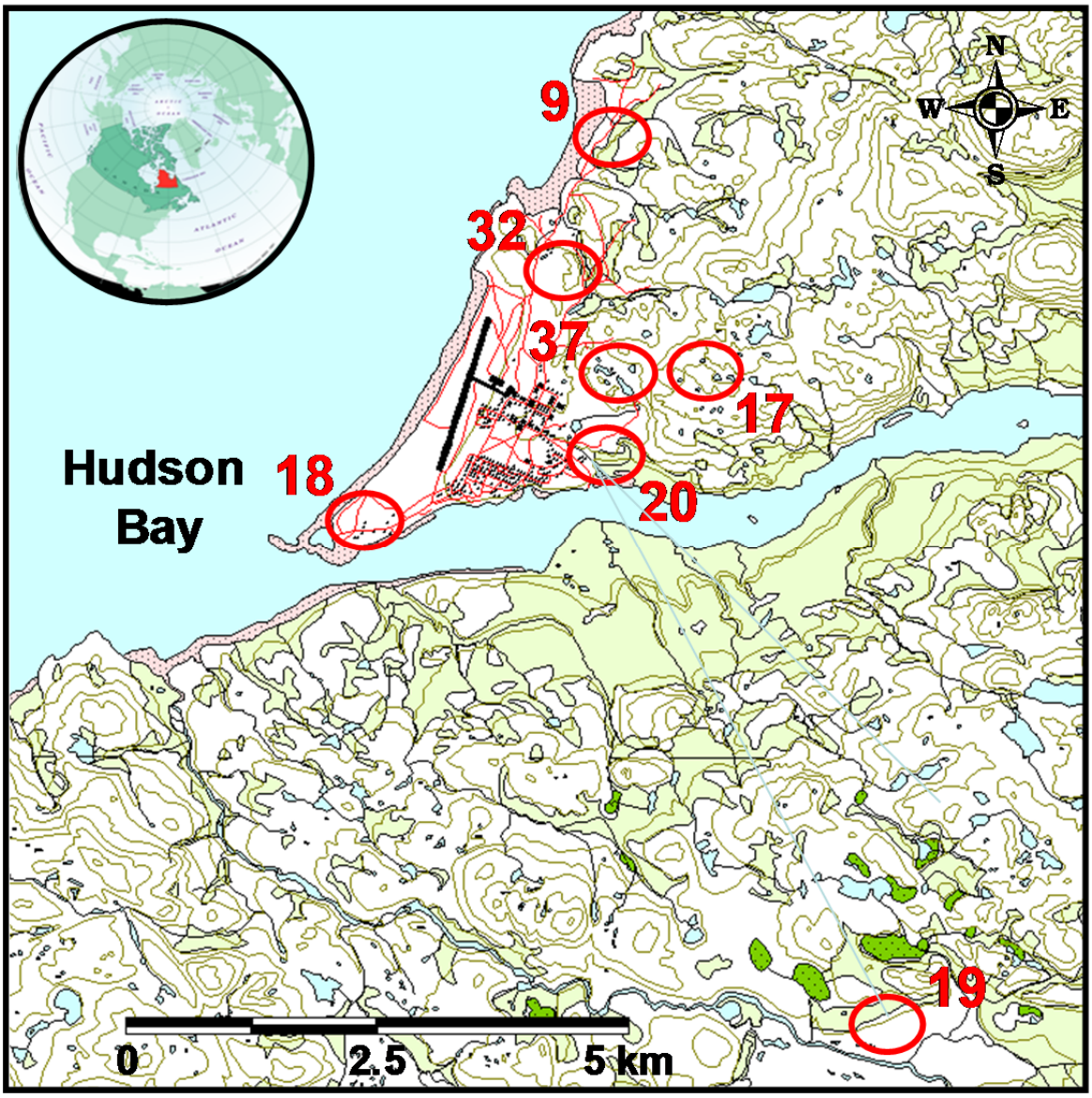


**Figure 3.1** **Eastern Canadian Subarctic study area, near Kuujjuarapik (Nunavik, Canada) and the various land cover classes where measurements were made (9: Temperate or subpolar needle-leaved evergreen low-density lichen (rock) understory; 17: Grassland; 18: Herb-shrub-bare cover; 19: Wetlands; 20: Sparse needle-leaved evergreen herb-shrub cover; 32: Lichen-spruce bog; 37: Water bodies) based on NRCan land cover map of Canada (Global map insert from Makivik Corporation).**

**Table 3-1 Weather observations during 2006 and 2007 field sampling months of June through August including average temperature, relative humidity and total amount of precipitation compared to Kuujjuarapik climate normal (1971-2000). The standard deviation of the mean is given for the climate normals.**

| | Units | Weather observations | | | Climate normal 1971-2000 | |
|---|---|---|---|---|---|---|
| | | July 2006 | July 2007 | August 2007 | July | August |
| **Air temperature average** | **(°C)** | 12.1 | 10.4 | 12.0 | 10.6 ± 1.4 | 11.4 ± 1.6 |
| **Relative humidity average** | **(%)** | 78.7 | 86.6 | 84.6 | 72.8 ± 3.4 | 72.4 ± 4.2 |
| **Precipitation** | **(mm)** | 73.0 | 135.2 | 100.8 | 79.4 ± 35.9 | 91.5 ± 42.4 |

In this paper, all the terrestrial sampling sites were classified into five main land-cover classes as defined by NRCan land cover map of Canada (NRCan 2008). The land cover map represents a baseline map of the major biome and land cover in Canada. The land cover database was produced from a 0.25km spatial resolution MODIS imagery (Moderate Resolution Imaging Spectroradiometer), and showed ~70% accuracy with reference data and good agreement with independent references (NRCan 2008). Within a 10-km radius of Kuujjuarapik (Hudson Bay excluded), which is a perimeter covering the entire study area and is representative of the region, 27.9% of the territory is sparse needle-leaved evergreen shrub-herb moss cover (category 20), 19.7% is lichen-spruce bog (category 32), 18.6% is grassland (category 17), 11.8% of the area is temperate or sub-polar needle-leaved evergreen open-tree canopy of low density with a lichen (rock) understory (category 9), and 2.3% is herb-shrub-bare cover (category 18) (Figure 3.2). Those five land cover classes correspond to more than 80% of the area (Table 3.4).

**Table 3-2** **Surface soil (0-10 cm) and terrestrial substrate characteristics within the land cover classes including gravimetric water content (GWC), percent soil and plant carbon (C) and nitrogen (N) by mass and number of flux measurements (n) for each cover class.**

| | | 9: Temperate or subpolar needle-leaved evergreen low-density lichen (rock) understory | 17: Grassland | 18: Herb-shrub-bare cover | 20: Sparse needle-leaved evergreen herb-shrub cover | 32: Lichen-spruce bog |
|---|---|---|---|---|---|---|
| **Soil texture** | | sandy loam | loamy sand | sandy loam / sand | loamy sand | loamy sand |
| **Bulk density** | **(g/cm³)** | 0.74 ± 0.50 | 0.24 ± 0.07 | 1.17 ± 0.36 | 0.43 ± 0.56 | 0.52 ± 0.40 |
| **GWC** | **(%)** | 0.73 ± 0.82 | 32.33 ± 11.24 | 1.33 ± 1.83 | 7.97 ± 8.46 | 7.30 ± 5.65 |
| **pH** | **(units)** | 5.25 ± 0.35 | 5.60 ± 0.42 | 5.41 ± 0.48 | 5.40 ± 0.42 | 5.50 ± 0.00 |
| **Soil C** | **(%)** | - | 36.58 ± 5.19 | 1.30 ± 0.77 | 0.39 | 2.09 |
| **Soil N** | **(%)** | - | 1.53 ± 0.46 | 0.08 ± 0.04 | 0.03 | 0.34 |
| **C:N - Soil** | **(ratio)** | - | 23.9 | 16.3 | 13.0 | 6.1 |
| **Plants C** | **(%)** | 39.54 ± 3.32 | 46.32 ± 3.33 | 44.21 ± 6.61 | 44.07 ± 0.90 | 44.08 |
| **Plants N** | **(%)** | 0.68 ± 0.63 | 0.76 ± 0.21 | 1.10 ± 0.30 | 0.73 ± 066 | 0.27 |
| **C:N - Plants** | **(ratio)** | 58.1 | 60.9 | 40.2 | 60.4 | 163.3 |
| **n** | **(units)** | 2 | 5 | 17 | 5 | 2 |

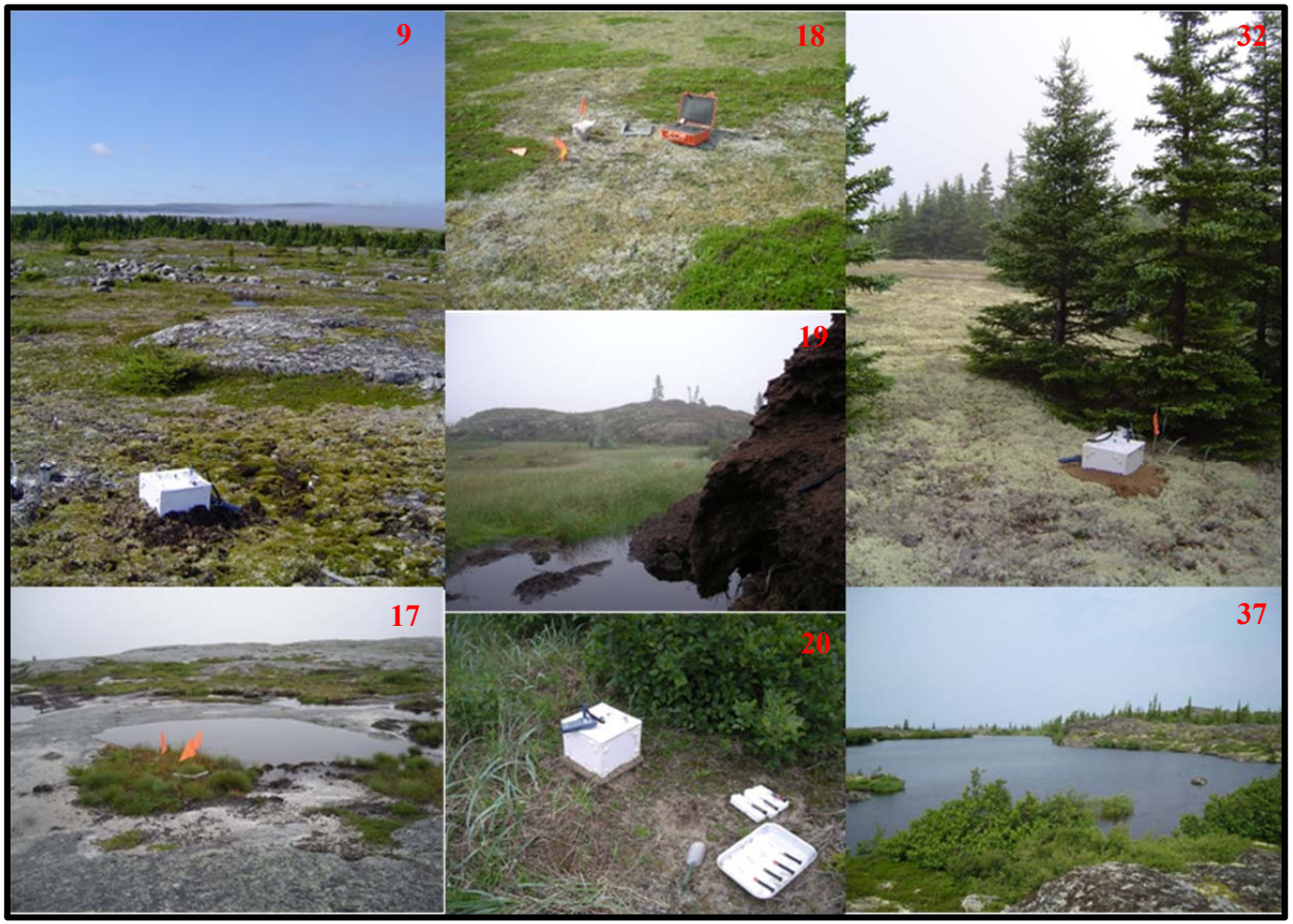


**Figure 3.2** **Examples of the various land cover classes where measurements were made near Kuujjuarapik (Nunavik, Canada) based on the NRCan land cover descriptions and map of Canada 2005. 9: Temperate or subpolar needle-leaved evergreen low-density lichen (rock) understory; 17: Grassland; 18: Herb-shrub-bare cover; 19: Wetlands; 20: Sparse needle-leaved evergreen herb-shrub cover; 32: Lichen-spruce bog; 37: Water bodies.**

Approximately 5% of the remaining land cover comprises water bodies (NRCan 2008). In this study, these water bodies are further classified based on the Canadian wetland classification system (Warner and Rubec 1997) into three water body groups (category 37): lake, pond and shallow water; and two wetland groups (category 19): marsh and collapsed permafrost palsa (Figure 3.2). Note that the lichen-bog areas here are grouped with the terrestrial cover types. The physical and chemical parameters of these water bodies and wetland cover types are summarized in Table 3.3. Most of the sites are located on the north side of the Great Whale River near Kuujjuarapik (Figure 3.1). The palsa site is located ~ 7 km southeast of Kuujjuarapik in a sedge fen dotted with palsas 1 to 5 m in elevation with an active layer that is between 50 and 60 cm deep, where the main plant species are sedges (*Carex* spp.), cottongrass (*Eriophorum* spp.), alpine bulrush (*Trichophorum* spp.), cloudberry (*Rubus chamaemorus*), marsh cinquefoil (*Potentilla palustris*), brown mosses and *Sphagnum* spp. (further details are provided by Arlen-Pouliot and Bhiry 2005).

**Table 3-3 Physical and chemical parameters of aquatic substrate within the land cover classes including temperature, total dissolved solid (TDS), total dissolved gas (TDG), oxygen content as percent saturation ($O_2$ sat) and dissolved concentration ($O_2$ conc) and total organic carbon (TOC).**

| | | Wetlands | | Water bodies | | |
|---|---|---|---|---|---|---|
| | | Marsh | Palsa | Lake | Pond | Shallow water |
| **Temperature** | **(°C)** | 13.2 ± 1.1 | 17.1 ± 4.3 | 16.8 ± 3.8 | 14.6 ± 4.2 | 13.9 ± 2.4 |
| **pH** | **(units)** | 6.5 ± 0.1 | 5.3 ± 0.6 | 6.7 ± 0.2 | 6.6 ± 0.1 | 5.9 ± 0.3 |
| **Conductivity** | **(µs/cm)** | 54.4 ± 10.7 | 32.9 ± 7.5 | 41.5 ± 15.8 | 42.7 ± 4.9 | 7.8 ± 0.4 |
| **Redox** | **(mv)** | 433.0 ± 4.2 | 425.8 ± 130.6 | 474.7 ± 63.8 | 506.0 ± 2.8 | 501.0 ± 5.7 |
| **TDS** | **(g/L)** | 0.03 ± 0.01 | 0.02 ± 0.01 | 0.02 ± 0.00 | 0.03 ± 0.00 | 0.00 ± 0.00 |
| **TDG** | **(mm Hg)** | 754.0 ± 15.6 | 733.3 ± 6.3 | 734.7 ± 10.5 | 750.5 ± 13.4 | 750.5 ± 0.7 |
| ***$O_2$ sat*** | **(%)** | 73.8 ± 8.9 | 58.4 ± 16.7 | 88.1 ± 4.8 | 72.2 ± 5.8 | 93.8 ± 0.5 |
| ***$O_2$ conc*** | **(mg/L)** | 7.8 ± 1.1 | 5.7 ± 2.1 | 8.6 ± 1.1 | 7.4 ± 1.3 | 9.7 ± 0.5 |
| **Color** | **(Pt/Co)** | 138.0 ± 43.8 | 424.4 ± 108.4 | 126.6 ± 25.9 | 144.3 ± 28.6 | 97.3 ± 1.1 |
| **TOC** | **(mgC/L)** | 6.0 ± 0.3 | 16.1 ± 17.1 | 4.2 ± 5.4 | 3.9 ± 0.7 | 0.8 ± 0.2 |
| **Chlorophyll** | **(µg/L)** | 2.7 ± 1.0 | 13.7 ± 6.6 | 2.5 ± 0.8 | 0.4 ± 0.0 | 3.1 ± 2.1 |
| **Water depth** | **(m)** | 0.2 ± 0.0 | 0.6 ± 0.4 | 0.6 ± 0.2 | 0.8 ± 0.0 | 0.8 ± 0.0 |
| **n** | **(units)** | 2 | 4 | 3 | 2 | 2 |

### *2.2.2. Instrumentation and field experiments*

Emissions of $CO_2$ and $CH_4$ were measured using a static flux chamber (SFC) based on the design described by Savage and Davidson (2003). The flux chamber is composed of Plexiglas sheets (30 cm x 30 cm x 30 cm) covered by an opaque Teflon liner (Bytac®) with a volume of 0.027 m³ and a sampling area of 0.09 m². An injection port with a Teflon septum is located at the top for collecting gas samples. A stainless steel vent tube is also installed to avoid the impact of transient over-pressure. A built-in sensor probe and handheld meter with data logging ability (Omega®, SE 310) were used to measure the temperature and relative humidity inside the SFC,

and temperature outside the chamber, using a K-type thermocouple. In terrestrial ecosystems, the chamber was placed over an aluminum soil collar (30 cm x 30 cm x 12.5 cm) buried 10 cm into the soil and with a 2.5-cm overlap to the soil surface. A seal between the collar and chamber resulted from the snug fit between the collar and Teflon-lined chamber. In addition, soil was added to the exterior of the collar to improve the stability of the chamber and reduce wind turbulence. A life-ring buoy (~ 75 cm) was used over the aquatic substrates to maintain the SFC at the air/water interface and mitigate the wave's effects. The lower part of the chamber was set slightly (2.5 cm) below the water surface to ensure a perfect seal. The internal volume of the SFC remains the same in both cases.

After the chamber was set on the collar or buoy, an initial 10-ml gas sample was taken using a 10-ml glass syringe (Hamilton®, Gastight #1010) coupled with an inert Teflon gas sampling SYR valve (Hamilton®, Gastight #86580) and a precision-glide needle (BD®, 20G 1½). Samples were taken every 10 minutes for 1 hour (N = 7). In 2006, the gas samples were transferred immediately after collection into a nitrogen ($N_2$)-flushed and -evacuated 10-ml serum glass vial with a Vacutainer® septum, and were analyzed (within 1-2 months due to field logistic limits) by a dual-detector gas chromatography RGA5 - Trace analytical® (Constant et al. 2005). In 2007, the same overall sampling protocol was applied, but the samples were analyzed within 12 hours with the RGA5, which had been moved to laboratory facilities. Quality control samples show no variation between 2006 and 2007 methodology. Gas analysis was performed through direct injection of 10 ml of the sample into the injection port of the analyzer, and an automated sample loop transferred 1 ml of the injected volume to the chromatographic columns (Poissant et al. 2007). The RGA5 was calibrated daily with a standard gas mixture, 1884.0 ppbv $CH_4$ and 380.3 ppmv $CO_2$ (Scott Marin®), certified by the Climate Monitoring and Diagnostics Laboratory of the National Oceanic and Atmospheric Administration (NOAA). No particular baseline drift was observed day-to-day, and the detection limit (3σ) was lower than 0.18 ppm $CH_4$ and 7.13 ppm $CO_2$. Concentrations of $CO_2$ and $CH_4$ were plotted to extract the linear regression with time to compute flux rates (Savage and Davidson 2003).

Flux measurements were made during the growing season during two periods: July 11 to 28, 2006 and July 18 to August 16, 2007. A single flux measurement was carried out each day

between 10:30 and 11:30 am EDT. Overall, 31 flux measurements over soil (trees not included) and water were made on as many sites. These were distributed among the land cover classes as follows: Category 9, temperate or subpolar needle-leaved evergreen low density, lichen (rock) understory (N = 2); Category 17, grassland (N = 5); Category 18, herb-shrub-bare cover (N = 17); Category 20, sparse needle-leaved evergreen, herb-shrub cover (N = 5); Category 32, lichen-spruce bog (N = 2); Category 19, wetlands (N = 6); and Category 37, water bodies (N = 7) (Figure 3.2). Within the previous land cover categories, flux measurements were performed on areas dominated by i) vascular plants (*Carex sp*. and *Ericaceae sp*.) in categories 17, 18 and 20; and on areas dominated by ii) non-vascular plants (*Mosses sp.* and *Lichens sp.)* in the whole land cover category (9, 17, 18, 20 and 32). Also, in land cover category 18, a third area of iii) bare soil (sand) was sampled. Thereafter, a regional C budget (radius of 50 km) was estimated based on mean flux measurements in each of the represented cover classes. Cover class 9) temperate or subpolar needle-leaved evergreen low density, lichen (rock) understory, 17) grassland, 18) herb-shrub-bare cover, 19) wetlands, 20) sparse needle-leaved evergreen herb-shrub cover, 32) lichen-spruce bog and 37) water bodies correspond to 67% of area. Standard deviation of the regional C budget is based on flux variability within each class.

Weather conditions during flux measurements were measured at the main research site in forest tundra using an extended Bowen ratio system (Campbell Scientific®), including air temperature, relative humidity, soil temperature, soil heat flux, soil water content, solar radiation, atmospheric pressure, and wind speed and direction. A portable (Omega®) sensor was also used to measure temperature and relative humidity at the chamber flux measurement sites. Daily average temperature, relative humidity and total precipitation measured at the Kuujjuarapik / Whapmagoostui airport were only used for gap filling and climate normals (EC 2013). Chamber flux measurement sites were located within 10 km of these various weather stations.

Soil and plants were collected from each chamber flux location and stored until analysis at ~ 4 °C. Surface soils from 0-10 cm, were collected for further laboratory soil characterization (Table 3.2). After measurements, lichen, moss and non-vascular plants at the sampling spot were clipped at the soil surface. Soils were analyzed for soil texture, pH and gravimetric water content (GWC). Soil bulk density was roughly estimated from bulk soil samples slightly disturbed.

Plants were identified to species (Blondeau et al. 2011). Sub-samples of soils and plants were analyzed for C and N content. Soil samples (~ 1 g) were acidified with 2 ml of HCl Seastar® (1M) in porcelain crucibles, and dried at 60 °C for 18 hours in a bench-top laboratory furnace to remove inorganic C and carbonates prior to the organic isotope analysis (Ryba and Burgess 2002).

In the aquatic ecosystems, a Hydrolab multi-probe DS5 (Hatch®), equipped with a wide range of water quality sensors and luminescent dissolved oxygen technology was used to measure the physical properties of water. Water samples were also collected for further water quality analyses.

### *2.2.3. Quality control and statistical analyses*

All the analyzers and instrumentation used during this campaign were previously calibrated with certified standards (National Institute of Standards and Technology [NIST] and NOAA) to ensure high accuracy of measurements and maximum quality assurance. Each analytical method used was scientifically recognized and certified. Gas fluxes were calculated in Microsoft Excel 2007 and all the statistical analyses were computed using SAS® 9.3 and/or Systat®, SigmaPlot 12.0.

## ***2.3. Results and discussion***

In the Eastern Canadian subarctic, landscape $CO_2$ respiration varied widely among and within land covers types with fluxes ranging from -59.8 to 234.7 mg $CO_2$ $m^{-2}$ $h^{-1}$ (Figure 3.3a). There was a significant difference among land cover classes (Kruskal-Wallis $Chi^2 = 13.6$, $p = 0.03$) but given the small number of replicates and large spatial variability within cover classes, only 37) water bodies and 20) sparse needle-leaved evergreen, herb-shrub cover classes differed significantly (Tukey-Kramer test, $p < 0.05$). However, mean $CO_2$ emissions were generally larger over terrestrial land cover classes than over 19) wetlands with negative fluxes (indicating uptake of $CO_2$) over the remaining 37) water bodies. These terrestrial $CO_2$ flux measurements are on the same order of magnitude as in previous studies in the northern part of the Canadian

boreal forest and forest tundra (Rayment and Jarvis 2000) and much larger than measurements at higher latitude in Alaska and the Canadian tundra (Oberbauer et al. 2007; Dagg and Lafleur 2011). Aquatic $CO_2$ fluxes are also in the same range as a recent study on boreal lakes in northern Québec (Rasilo et al. 2015).

There was also a significant difference in $CH_4$ emissions among land cover classes (Kruskal-Wallis $Chi^2 = 18.7$, $p = 0.005$), but given the small number of replicates and large spatial variability within cover classes, only the Category 18, herb-shrub-bare cover and Category 19, wetlands classes differed significantly (Tukey-Kramer test, $p < 0.05$). Similarly, there is equally high $CH_4$ flux variability among land cover types with $CH_4$ fluxes ranging from -0.4 to 17.3 mg $m^{-2}$ $h^{-1}$ (Figure 3.3b). The collapsed palsa pond sites (included in the 19) wetlands cover class) is where $CH_4$ emissions were greatest. These $CH_4$ fluxes are within the range observed at other wetlands (Pelletier et al. 2007). The lower $CH_4$ emissions observed at all the other terrestrial and aquatic sites in this study are similar to those in the Canadian boreal forest and natural lakes (Ullah et al. 2009; Rasilo et al. 2015).

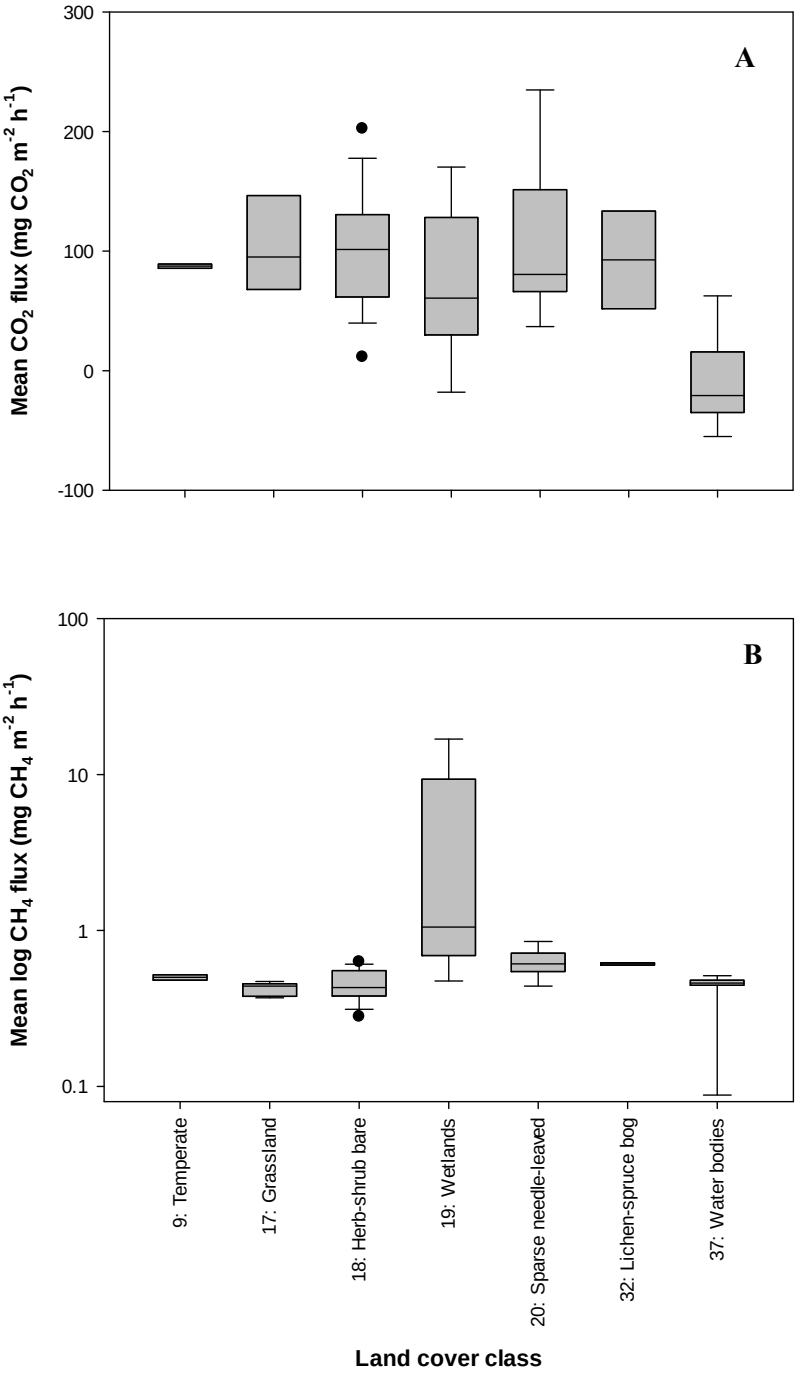


**Figure 3.3** **$CO_2$ (A) and $CH_4$ (B) fluxes measured within various land and aquatic cover classes near Kuujjuarapik (Nunavik, Canada). Box plot mid-lines illustrate the median fluxes, extent of the box illustrates the 25$^{th}$ and 75$^{th}$ percentiles, errors bar indicate the 10$^{th}$ and 90$^{th}$ percentiles and dots show outlying points**

### *3.3.1 $CO_2$ and $CH_4$ emissions in terrestrial ecosystems*

Plant community, vegetation cover and distribution are mainly controlled by factors such as topography, landscape and climate (Brooks et al. 2011), which are also important factors regulating $CO_2$ fluxes in terrestrial ecosystems. In our study, SFC measurements have been carried out over three different substrates (bare soil clear of plants, surface dominated by non-vascular plants, and surface dominated by vascular plants) and five distinct forest tundra land cover classes, 9) temperate or subpolar needle-leaved evergreen low density lichen [rock] understory; 17) grassland; 18) herb-shrub-bare cover; 20) sparse needle-leaved evergreen herb-shrub cover; and 32) lichen-spruce bog).

In terrestrial ecosystems, $CO_2$ respiration did not differ significantly among substrate types (Kruskal-Wallis $Chi^2 = 1.2$, $p = 0.75$) despite a small increase in emissions with increasing plant cover (Figure 3.4a). The $CO_2$ respiration rates range from 83.6 to 128.0 mg $m^{-2}$ $h^{-1}$ between bare soil, lichen, moss and vascular plants. Biomass (not measured) and physiologic characteristics of plant species may explain this variability since no significant correlation was found with soil C content (not shown). As noted in the Low Arctic regions (Dagg and Lafleur 2010) and the High Arctic (Laurila et al. 2001; Walker et al. 2012), more biomass tends to be associated with greater LAI. Leaf area index is an important variable controlling gas exchange in northern latitudes beacause leaves fix $CO_2$ by photosynthesis and release $CO_2$ by respiration (Shaver et al. 2007). Photosynthesis rates are greater in vascular plants (per unit LAI) than in non-vascular plants (Bansal et al. 2012). Although photosynthesis ceases in the darkened chamber, plant respiration from both above and below ground parts continues (Lankreijer et al. 2009). In addition, greater plant productivity should enhance rhizospheric respiration rates due to greater presence of substrates (Hartley et al. 2012).

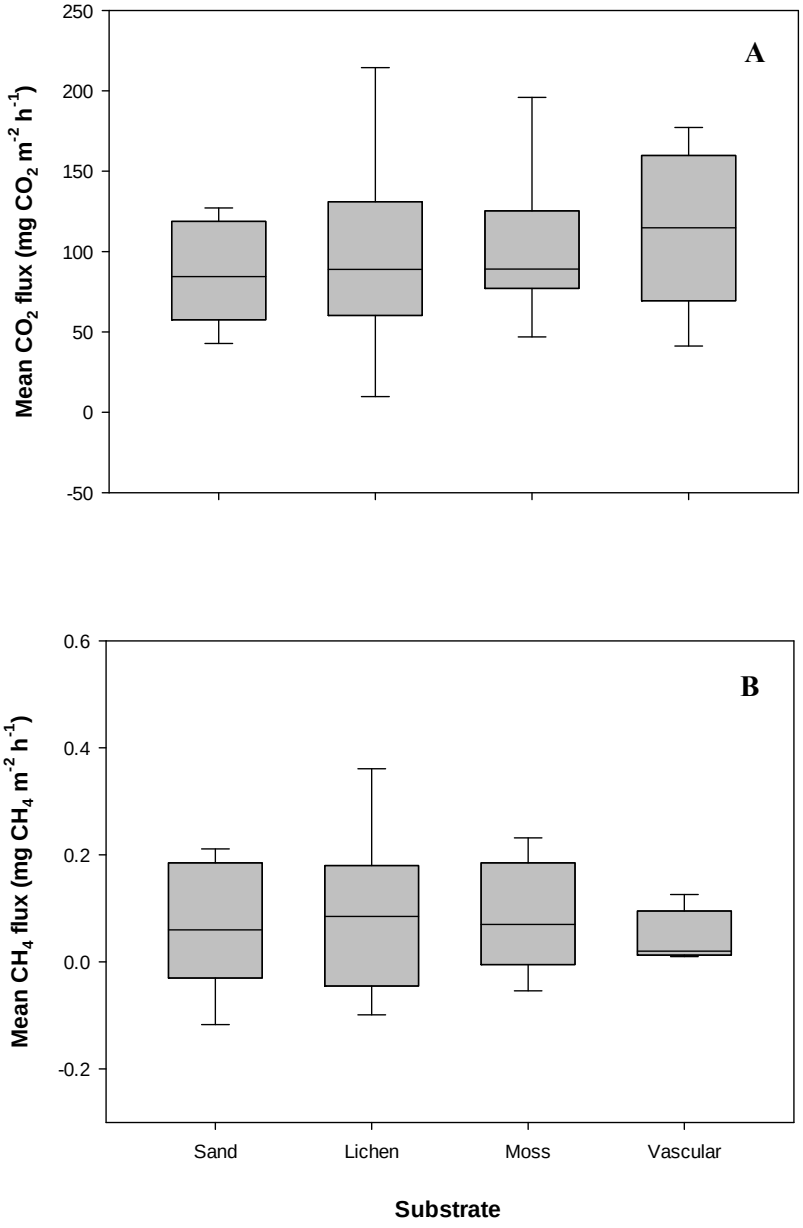


**Figure 3.4** **$CO_2$ (A) and $CH_4$ (B) fluxes measured in various surface types (bare soil, lichen, moss and vascular plants) in terrestrial ecosystems. Box plot mid-lines illustrate the median fluxes, extent of the box illustrates the 25$^{th}$ and 75$^{th}$ percentiles and errors bar indicate the 10$^{th}$ and 90$^{th}$ percentiles.**

Lafleur et al. (2012) have shown increasing summer $CO_2$ uptake during the day and losses at night using micrometeorological techniques when moving from more vegetated lower latitudes to sparsely vegetated high latitudes in the Canadian Arctic. The hypothesis that $CO_2$ respiration might increase when moving from sparsely vegetated tundra cover classes (mainly lichen and mosses) to boreal forest classes (more graminoids and vascular plants) was not clearly supported in this study under a similar climatic regime. This shows, in part, the limit of small-scale measurement techniques to obtain a comprehensive picture of C exchanges in Northern latitudes. It is likely that far more replicates would be needed to identify the impacts of small-scale vegetation cover, biomass and structure, and below ground microbial activity on $CO_2$ emissions.

In our study, terrestrial $CH_4$ emissions were also not significantly different among substrate types (Kruskal-Wallis $Chi^2 = 0.3$, $p = 0.95$). When only considering the terrestrial cover types (not wetlands and palsa formations), average $CH_4$ exchange was small at 0.07 mg $CH_4$ $m^{-2}$ $h^{-1}$ but significantly different than zero (Wilcoxon signed rank test, $p = 0.004$). Methane is produced by methanogens in soil under anoxic conditions. It was perhaps surprising that net emissions rather than uptake of $CH_4$ was observed at the terrestrial ecosystem sites (Figure3.4b). Only 24% of the terrestrial sites had $CH_4$ uptake. Gravimetric water content does not significantly differ for sites with $CH_4$ uptake vs. sites with emissions. But gravimetric water content significantly differs among substrate (Kruskal-Wallis $Chi^2 = 8.1$, $p = 0.04$) with greatest water content in substrates with higher $CH_4$ emissions. Soil moisture significantly controls $CH_4$ release in non-water–saturated and upland Arctic tundra (Natali et al. 2015).

Our measurements did not show a positive correlation between soil temperature and $CO_2$ respiration with all measurement sites combined. This suggests the other variables influencing $CO_2$ fluxes among the different sites were of greater importance despite temperature being well known to control chemical and physical reactions in natural environments. Increasing temperature generally increases kinetic energy, root respiration and microbial activities (Mikan et al. 2002). Root respiration and microbial decomposition are the sources of $CO_2$ production in soils (Davidson and Janssens 2006; Fox et al. 2008). In contrast, $CO_2$ uptake in the water bodies (under opaque chamber measurement conditions) is a result of a concentration gradient where $CO_2$ concentrations are lower in the water than in the air. Net $CO_2$ uptake in water bodies was

generally observed during rainy days and/or following rainy conditions. These conditions may have been associated with cooler, cloudier conditions that had reduced $CO_2$ production in the water. In mesic, dry and non-saturated upland soils, small changes in soil moisture can affect microbial activity (ie. heterotrophic respiration), root respiration, and plant assimilation (Illeris et al. 2004; Davidson and Janssens 2006; Ju et al. 2006). However, in our study, increasing soil water content (as measured at the nearby Bowen ratio flux station) did not impact $CO_2$ respiration, but did promote $CH_4$ production. A very strong link between the regional weather temporal trends, based on continuous VWC and in-situ $CH_4$ flux measurements was observed (Spearman rank correlation $r = 0.59$, $p < 0.001$). Wetting of the soil during precipitation events may have lowered $O_2$ within the surface soils enough to promote $CH_4$ production and limit $CH_4$ oxidation. Methanogens are omnipresent in upland aerated soils and are stimulated by wet, anoxic conditions (Angel et al. 2011). Overall, weather conditions during flux measurements in August 2007 were wetter than July 2006 and 2007 (Table 3.1).

*2.3.2.* $CH_4$ and $CO_2$ emissions in aquatic systems

Trophic status and land cover classification are important factors controlling $CH_4$ emissions in aquatic ecosystems. Freshwater ecosystems in northern latitudes vary in size, form and structure (Reist et al. 2006; Serreze et al. 2006). In this study, flux measurements have been carried out in two land cover classes (wetlands and water bodies) and five aquatic systems (pond, shallow water, lake, marsh, and collapsed palsa pond).

At a landscape level, the $CH_4$ emissions in 19) wetlands were much higher (4.62 mg $CH_4$ $m^{-2}$ $h^{-1}$) than in other 37) water bodies (-0.02 mg $CH_4$ $m^{-2}$ $h^{-1}$) (Figure 3.3b). Our lowest $CH_4$ emission measurements are similar to those in lakes and reservoirs in northern Québec where fluxes ranged from 0.01 to 0.1 mg $m^{-2}$ $h^{-1}$ (Bastien et al. 2007), in peatlands in the La Grande River watershed (James Bay), 0.31 mg $m^{-2}$ $h^{-1}$ (Pelletier et al. 2007), and in boreal lakes across northern Quebec, 0.7 mg $m^{-2}$ $h^{-1}$ (Rasilo et al. 2015). However, in the collapse palsa ponds, the $CH_4$ production was approximately 2-50 times higher. Therefore, in the Eastern Canadian subarctic, $CH_4$ emissions and their contribution to the regional C budget are underestimated if these features are not accounted for. The large influence of environmental factors and their physical and chemical parameters (Table 3.3) can explain this difference. As expected, $O_2$

concentration and saturation were lower ($p < 0.05$) in the palsa ponds (wetlands) (6.4 mg $l^{-1}$ and 63.5%, respectively) than in water bodies (8.6 mg $l^{-1}$ and 85.2%, respectively). Trophic status was also different between those two ecosystems: water bodies mostly ranged from oligotrophic to mesotrophic, and wetlands were mainly eutrophic. The apparent colour of water, total phosphorus and chlorophyll were significantly higher ($p < 0.05$) in wetlands than other water bodies: 328.9 vs. 123.3 Pt $Co^{-1}$, 0.03 vs. 0.01 mg P $l^{-1}$, and 10.0 vs. 2.0 mg Chla $l^{-1}$, respectively. Biogeochemical processes occurring in the water column are interconnected with the surrounding landscape and this is particularly important in shallow lakes and small ponds (Torgersen and Branco 2007; Rasilo et al. 2015). The amount of allochthonous organic matter and nutrients newly introduced into aquatic ecosystems may increase primary production and microbial activity (Rouse et al. 1997). Our results also show higher $CO_2$ respiration in both palsa ponds and marshes, 19) wetlands, than over other 37) water bodies, (Figure 3.5a). In the 37) water body land cover class, fluxes of both $CH_4$ and $CO_2$ were small with the potential for uptake or loss. Rasilo et al. (2015) found much greater variability in these fluxes among boreal lakes with average mean $CO_2$ emissions of 68.3 mg $CO_2$ $m^{-2}$ $h^{-1}$ (-75 to 621 mg $CO_2$ $m^{-2}$ $h^{-1}$).

Water/air interface exchange of $CO_2$ was significantly correlated with TOC and $O_2$ (Figures 3.6a and 3.6b). Increasing TOC and decreasing $O_2$ was associated with greater $CO_2$ emissions, while decreasing TOC and increasing $O_2$ was associated with greater $CO_2$ uptake in aquatic systems. Emissions of $CO_2$ and $CH_4$ were also significantly correlated in our study aquatic systems (Speaman rank, $r = 0.48$, $p < 0.1$). Maximum uptake was observed at $O_2$ super-saturation and in the deeper ponds, and $O_2$ was strongly correlated with wetlands and water bodies depth (Spearman rank, $r = -0.73$, $p < 0.01$). In water bodies with a status of net heterotrophy, $CO_2$ saturation can be enhanced by a significant input of allochthonous C (Huttunen et al. 2003). In our study, wetlands and water bodies were relatively small and appear to be subject to terrestrial input of allochthonous organic matter and minerals. This hypothesis is supported by significant correlation of $CO_2$ emissions and TOC as noted above and also with conductivity and major ions, i.e., Ca (Spearman rank, $r = 0.67$, $p < 0.05$), Mg (Spearman rank, $r = 0.69$, $r < 0.05$) and Na (Spearman rank, $r = 0.71$, $p < 0.01$) (Figures 3.6c and 3.6c). However, emissions of $CO_2$ were not correlated with apparent colour (Spearman rank, $r = 0.46$, $p = 0.12$) and were also not correlated with chlorophyll (Spearman rank, $r = 0.17$, $p = 0.59$), two other water quality variables

that often reflect dissolved organic matter content in the water (Pace and Cole 2002) and photosynthetic potential of the water (Michelutti et al. 2005), respectively. However, for all aquatic ecosystems combined, $CO_2$ emissions increased with solar radiation (Spearman rank, $r = 0.62$, $p < 0.05$) likely reflecting the importance of temperature on biogeochemical processes (Spearman rank, $r = 0.41$, $p = 0.18$ for $CO_2$ exchange and temperature).

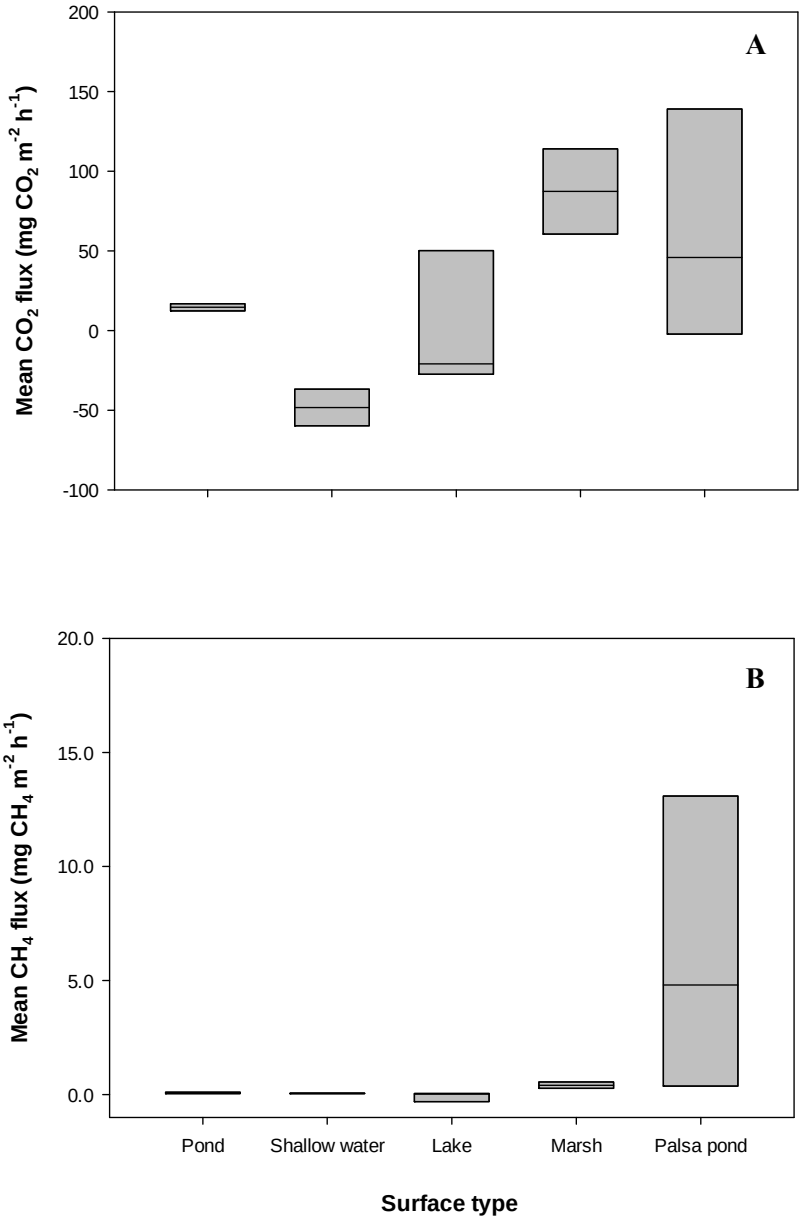


**Figure 3.5** **$CO_2$ (A) and $CH_4$ (B) fluxes measured in various aquatic ecosystem (marsh, thermokarst collapsed palsa pond, lake, pond and shallow water). Box plot mid-lines illustrate the median fluxes and extent of the box illustrates the 25$^{th}$ and 75$^{th}$ percentiles.**

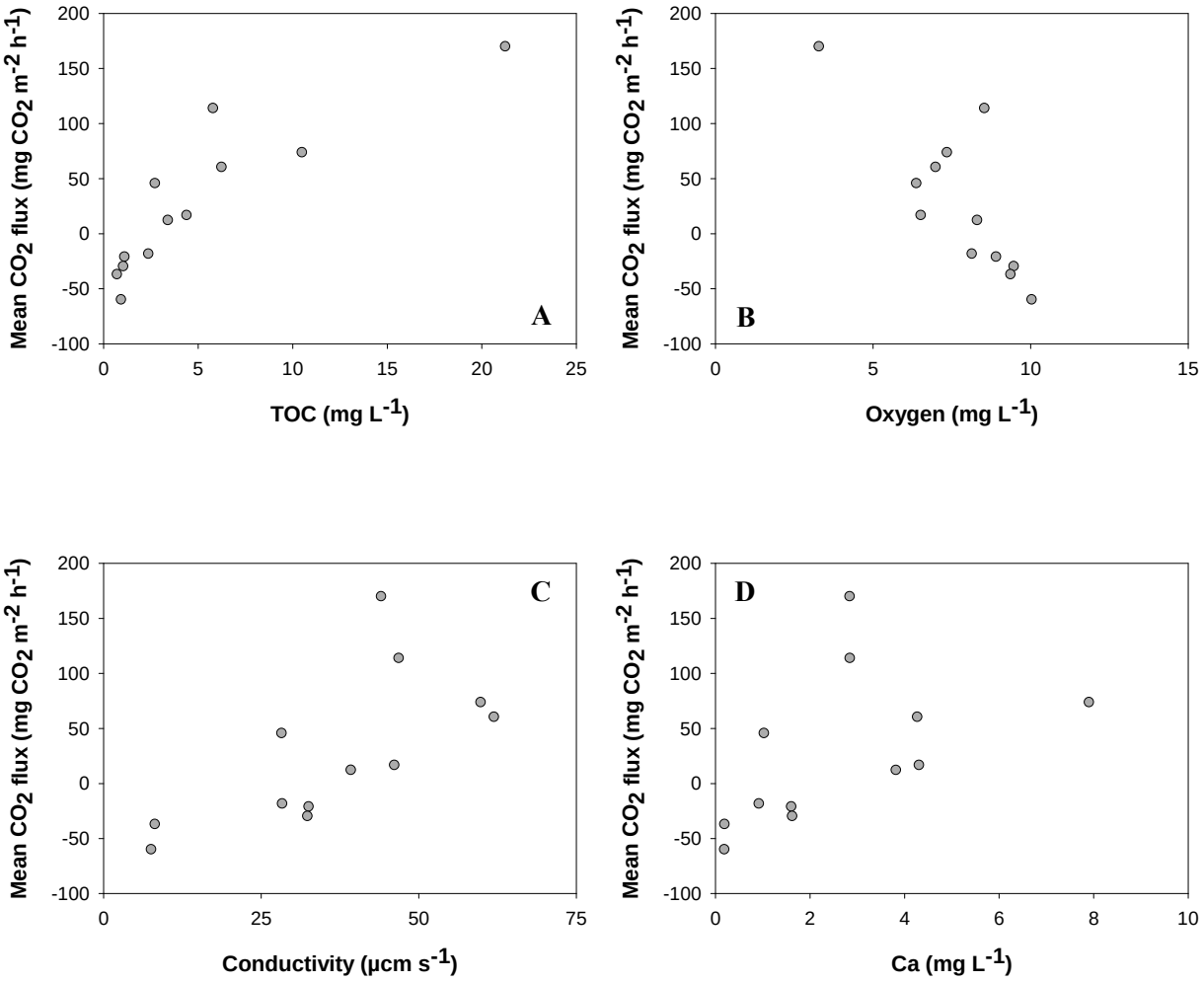


**Figure 3.6 Relationships between $CO_2$ exchange in aquatic systems and environmental factors including total organic carbon (A), oxygen concentration (B), conductivity (C) and calcium ion (D).**

Wetlands and other water bodies play an important role in determining $CH_4$ emissions in the subarctic (Figure 3.3b). Lentic ecosystems, such as standing water, lakes, ponds and wetlands, are abundant in the subarctic and Arctic environment (Prowse et al. 2006) but the limnology and nutrient status of aquatic systems are widely variable (Wrona et al. 2004). At subarctic sites, $CH_4$ emissions in collapsed palsa ponds were much higher than other aquatic systems (Figure 3.5b). High variability in the 4 measurements over two consecutive years in palsa ponds was related to water chemistry (Table 3.3) and morpho-geological features. Highest $CH_4$ emissions were

measured in ponds formed through thermokarst processing during the 2006 growing season or created less than one year before measurement. Thus, large amounts of organic matter and ions present in perennially frozen peat and mineral material were released by thawing into the recently formed collapsed palsa ponds. Thaw ponds are generally heterotrophic and characterized by large inputs of total suspended solids and nutrients (Breton et al. 2009). Therefore, the impact of thermokarst activities and the formation of new collapsed palsa ponds can contribute significantly to $CH_4$ emissions in the subarctic (Shirokova et al. 2013). However, permafrost thaw may also promote drainage of thaw lakes and could reduce $CH_4$ emissions (van Huissteden et al 2011).

Methane emissions in subarctic 19) wetlands and other 37) water bodies slightly increase with water temperature (Spearman rank, $r = 0.50$, $p = 0.09$) and were significantly correlated with $O_2$ ($r = -0.74$, $p < 0.01$) and TOC (Spearman rank, $r = 0.73$, $p < 0.01$) (Figure 3.7a, b & d). Methane emissions increased directly with higher temperature and TOC and decreased significantly with lower $O_2$. Microbial decomposition of organic C in aquatic systems produces $CH_4$ in anoxia by methanogens and $CO_2$ in aerobic conditions (Sachs et al. 2008) primarily in sediments (Walter et al. 2008), but also in the bottom water column (Likens 2010). Methane may also be consumed by methanotrophs in the water column (Kankaala et al. 2006). In this study, $CH_4$ emissions largely increased with decreasing redox potential (Spearman rank, $r = -0.64$, $p < 0.05$) (Figure 3.7c). Redox potential reflects the thermodynamics of the systems with more negative redox potentials as oxygen and other alternative electron acceptors are depleted. Although no negative redox potentials were observed, lower positive values reflect lower $O_2$ concentrations and potentially less methanotroph activity in the water column (Jones and Grey 2011). In this study, highest $CH_4$ emissions were measured at the lowest $O_2$ level, i.e., approximately 3.3 mg $l^{-1}$ and 37% saturation. Larger emissions were also measured in shallow ponds, and $CH_4$ fluxes were strongly negatively correlated with water depth (Spearman rank, $r = -0.51$, $p = 0.08$, not shown), wich may be linked with surface hydrology. Changing surface-weather conditions may also affect gas exchange, since $CH_4$ emissions at the air/water interface were slightly correlated with atmospheric pressure (Spearman rank, $r = -0.49$, $p = 0.10$, not shown). Wind velocity is a significant factor controlling gas exchange between water and the atmosphere (Poissant et al.

2000; Else et al. 2008), and a decrease of atmospheric pressure and increase of near-surface turbulence can promote $CO_2$ and $CH_4$ ebullition and emission (Sachs et al. 2008).

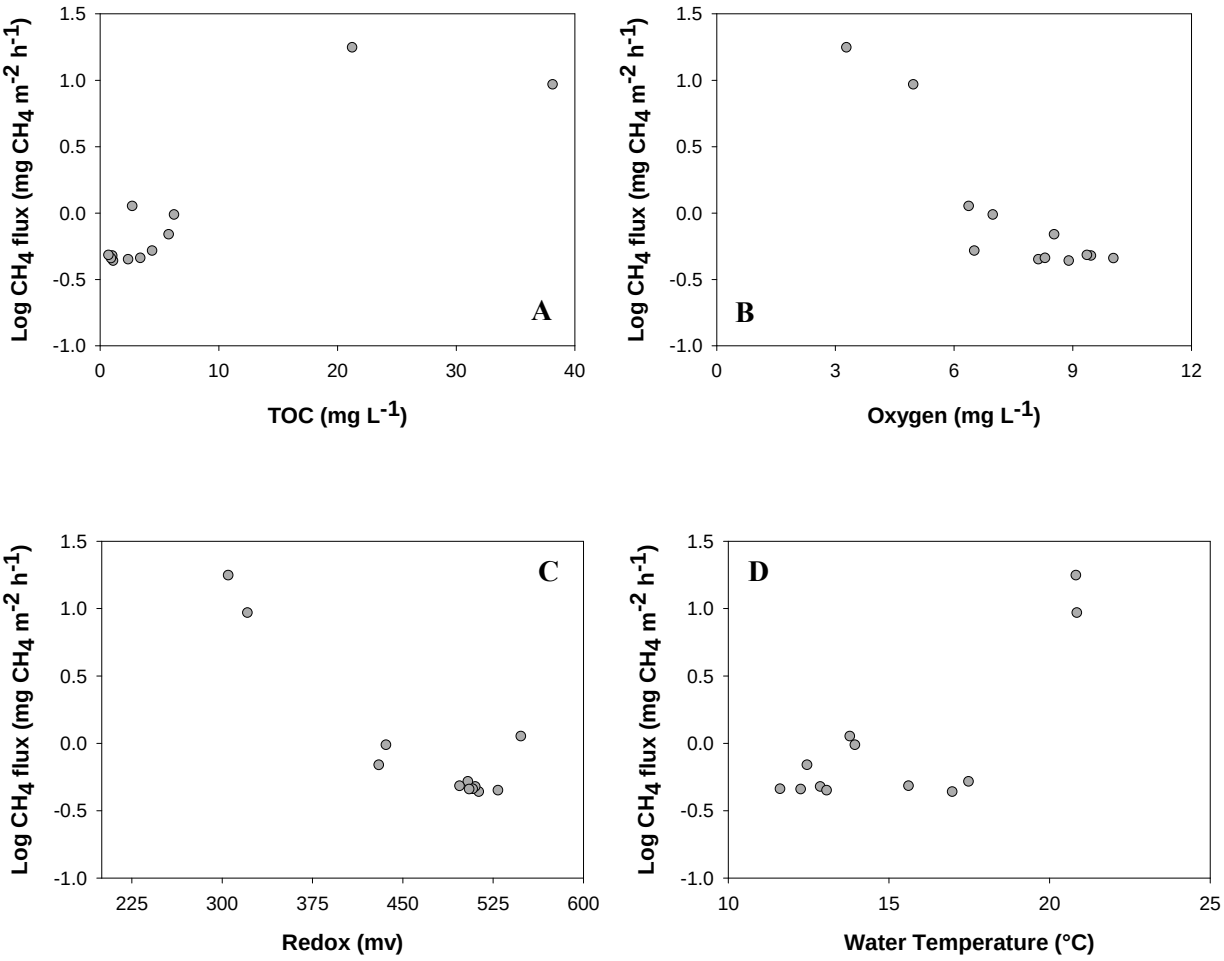


**Figure 3.7 Relationship between $CH_4$ emissions in aquatic systems and environmental factors including total organic carbon (TOC) (A), oxygen concentration (B), redox potential (C) and water temperature (D).**

*2.3.3. Estimation of landscape $CO_2$ and $CH_4$ budget at a subarctic site*

The results of this study are used to estimate $CO_2$ and $CH_4$ emissions from soil and water in the subarctic region. Our results, based on the land cover map of Canada 2005 (NRCan 2008), are summarized within seven land cover classes that correspond to more than 85% of the

surrounding aquatic and terrestrial ecosystems and that are highly representative of forest tundra (Table 3.4). Those classes correspond to approximately 30% of the entire land cover in Nunavik (the open forest tundra), while the remaining dominant zone is tundra.

Within 50 km of Kuujjuarapik (not including Hudson Bay), the landscape-scale $CO_2$ emission is estimated to be 197.3 ± 90.44 ton $h^{-1}$ (or 0.62 kg $ha^{-1}$ $h^{-1}$) mainly driven by the 9) temperate or subpolar needle-leaved evergreen low-density lichen (rock) understory, 20) sparse needle-leaved evergreen herb-shrub cover, and 32) lichen-spruce bog (Figure 3.8). The landscape-scale $CH_4$ emission is estimated to be 0.28 ± 0.17 ton $h^{-1}$, mainly driven by 20) sparse needle-leaved evergreen herb-shrub cover and 32) lichen-spruce bog (Table 3.4). Although $CH_4$ emissions were very small in terrestrial cover classes, their extensive distribution resulted in a higher contribution to the regional C budget than the large $CH_4$ emissions from 19) wetlands and 37) water bodies covering only a combined 3.39% of the area. Thus, efforts to improve on the estimation of the magnitude of terrestrial $CH_4$ uptake/emissions will be important to an overall picture of GHG emissions in the subarctic zone.

**Table 3-4 Regional $CO_2$ and $CH_4$ fluxes and their standard deviation and the estimated C budget within 50 km of Kuujjuarapik in the Eastern Canadian subarctic. The relative areal proportion of each land cover class within this region is also given.**

| Land cover classes | Land cover descriptions | $CO_2$ fluxes (mg $m^{-2}$ $h^{-1}$) | $CH_4$ fluxes (mg $m^{-2}$ $h^{-1}$) | r / 50 km (3192 $km^2$) (%) | $CO_2$ budget (tons $h^{-1}$) | $CH_4$ budget (kg $h^{-1}$) |
|---|---|---|---|---|---|---|
| 1 | Temperate or subpolar needle-leaved evergreen closed tree canopy | | | 1.08 | | |
| 2 | Cold deciduous closed tree canopy | | | 0.02 | | |
| 3 | Mixed needle-leaved evergreen – cold deciduous closed tree canopy | | | 0 | | |
| 4 | Mixed needle-leaved evergreen – cold deciduous closed young tree canopy | | | 0 | | |
| 5 | Mixed cold deciduous – needle-leaved evergreen closed tree canopy | | | 0 | | |
| 6 | Temperate or subpolar needle-leaved evergreen medium density, moss-shrub understory | | | 0.32 | | |
| 7 | Temperate or subpolar needle-leaved evergreen medium density, lichen-shrub understory | | | 7.95 | | |
| 8 | Temperate or subpolar needle-leaved evergreen low density, shrub-moss understory | | | 2.01 | | |
| 9 | Temperate or subpolar needle-leaved evergreen low density, lichen (rock) understory | 87.35 ± 2.54 | 0.08 ± 0.03 | 24.03 | 66.99 ± 1.95 | 62.78 ± 22.65 |
| 10 | Temperate or subpolar needle-leaved evergreen low density, poorly drained | | | 0.53 | | |
| 11 | Cold deciduous broad-leaved, low to medium density | | | 0.01 | | |
| 12 | Cold deciduous broad-leaved, medium density, young regenerating | | | 1.58 | | |
| 13 | Mixed needle-leaved evergreen – cold deciduous, low to medium density | | | 9.64 | | |
| 14 | Mixed cold deciduous - needle-leaved evergreen, low to medium density | | | 0 | | |
| 15 | Low regenerating young mixed cover | | | 6.70 | | |
| 16 | High-low shrub dominated | | | 1.87 | | |
| 17 | Grassland | 105.79 ± 53.25 | 0.001 ± 0.05 | 4.28 | 14.46 ± 7.28 | 0.11 ± 6.30 |
| 18 | Herb-shrub-bare cover | 101.34 ± 54.72 | 0.04 ± 0.11 | 3.00 | 9.70 ± 5.24 | 3.78 ± 10.50 |
| 19 | Wetlands | 74.51 ± 71.26 | 4.62 ± 7.07 | 0.04 | 0.08 ± 0.08 | 5.20 ± 7.96 |
| 20 | Sparse needle-leaved evergreen, herb-shrub cover | 110.31 ± 76.03 | 0.21 ± 0.15 | 19.90 | 70.06 ± 48.29 | 132.42 ± 95.33 |
| 21 | Polar grassland, herb-shrub | | | 0 | | |
| 22 | Shrub-herb-lichen-bare | | | 0 | | |
| 23 | Herb-shrub poorly drained | | | 0 | | |
| 24 | Lichen-shrub-herb-bare soil | | | 0 | | |
| 25 | Low vegetation cover | | | 0.07 | | |
| 26 | Cropland-woodland | | | 0 | | |
| 27 | High biomass cropland | | | 0 | | |
| 28 | Medium biomass cropland | | | 0 | | |
| 29 | Low biomass cropland | | | 0 | | |
| 30 | Lichen barren | | | 0 | | |
| 31 | Lichen-sedge-moss-low shrub wetland | | | 0 | | |
| 32 | Lichen-spruce bog | 92.64 ± 57.72 | 0.19 ± 0.02 | 12.40 | 36.67 ± 22.85 | 75.04 ± 8.04 |
| 33 | Rock outcrops | | | 0 | | |
| 34 | Recent burns | | | 0.03 | | |
| 35 | Old burns | | | 1.20 | | |
| 36 | Urban and Built-up | | | 0 | | |
| 37 | Water bodies | -6.26 ± 44.46 | -0.02 ± 0.18 | 3.35 | -0.67 ± 4.76 | -1.62 ± 19.49 |
| 38 | Mixes of water and land | | | 0 | | |
| 39 | Snow / ice | | | 0 | | |

These regional estimates represent exchanges of $CO_2$ and $CH_4$ from terrestrial and aquatic ecosystems in dark conditions. These are dominated by respiration process but may also include uptake in some conditions. For $CO_2$, the most comparable estimate would be derivations of ecosystem respiration (combined auto- and heterotrophic respiration) from models using opaque flux chamber measurements as validation data. For $CO_2$, emission rates of 0.5 to 2.1 kg $CO_2$ $ha^{-1}$ $h^{-1}$ were measured in moist-sedge Arctic tundra and 0.3 to 1.6 kg $CO_2$ $ha^{-1}$ $h^{-1}$ in wet-sedge Arctic tundra (Vourlitis et al. 2000). Our regional landscape estimate of 0.62 kg ha-1 h-1 is on the low end of these prior observations. In addition, none of the cover classes' $CO_2$ emissions exceeded 1.1 kg $CO_2$ $ha^{-1}$ $h^{-1}$ (Table 3-4). For $CH_4$, the most comparable estimate would be process-based model estimates of the $CH_4$ budget. Emissions rates of 0.004 g $CH_4$ $ha^{-1}$ $h^{-1}$ in Arctic tundra (including alpine and subarctic tundra) (Aronson et al. 2013) and 9.1 g $CH_4$ $ha^{-1}$ $h^{-1}$ in Arctic wetlands (Ito and Inatomi 2012) bracket our combined regional landscape estimate of 5.05 g $CH_4$ $ha^{-1}$ $h^{-1}$. Our highest $CH_4$ emission rates of 46.2 g $CH_4$ $ha^{-1}$ $h^{-1}$ in wetlands, which is directly related to high $CH_4$ emission rates in recently formed palsa ponds was 5 times higher than the Ito and Inatomi (2012) study.

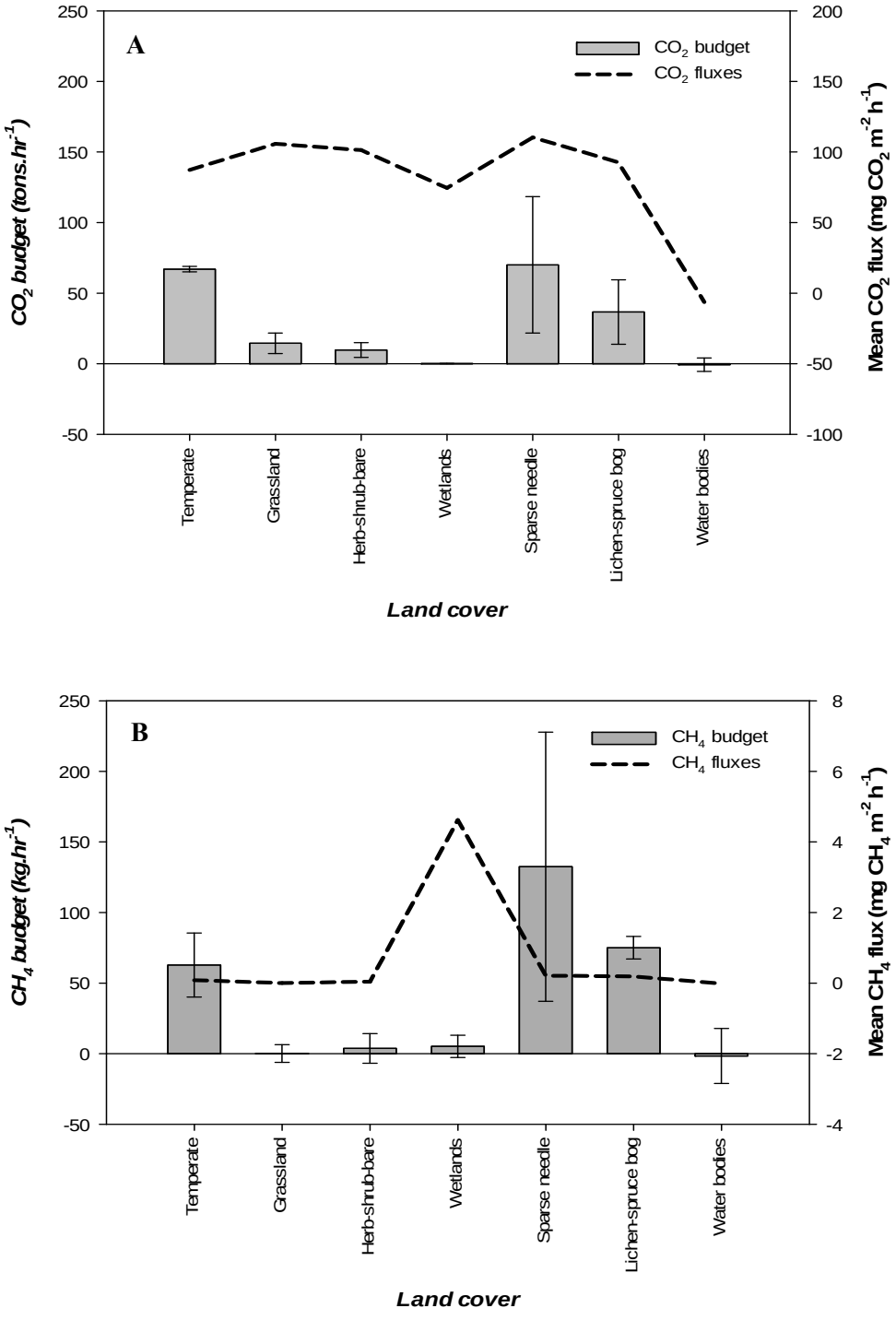


**Figure 3.8 Landscape $CO_2$ (A) and $CH_4$ (B) fluxes and regional budget in the vicinity of Kuujjuarapik (radius of 50 km), and the influence of land covers in subarctic aquatic and terrestrial ecosystem.**

### *2.4. Conclusion*

At a landscape-scale, $CO_2$ fluxes in subarctic terrestrial ecosystems vary depending on weather conditions, substrates and land cover classes. Landscape $CO_2$ respiration slightly increases with plant biomass, i.e., it increases from bare soil to non-vascular plants (moss and lichen), and from non-vascular to vascular plants (shrubs and trees). Our results also indicated some variations in $CO_2$ emissions with cover class but there was often as much variation within a class as among classes. Warming the tundra will affect plant and soil microbial communities but the impacts of vegetation change on $CO_2$ emissions may be as variable as currently observed among cover classes with ongoing sensitivity to temperature and moisture controls.

In aquatic ecosystems, highest $CH_4$ emissions were observed in 19) wetlands, mainly thermokarst collapsed palsa ponds and the lowest emissions (or uptake rates) were observed in the remaining 37) water bodies. Our results confirm the role of anoxia and water temperature on microbial $CH_4$ production and the impact of TOC on the $CH_4$ emissions. $CO_2$ fluxes in aquatic systems seem largely affected by allochthonous materials and the surrounding environment and strongly suggest a close link between aquatic and terrestrial ecosystems. In this sensitive transition zone the impact of climate change on gas exchange might be amplified by changes in plant communities and transfer of allochthonous materials into aquatic ecosystems.

A warmer and wetter climate that may significantly affect the hydrological regime, permafrost distribution and the water table level, and thereby increase $CH_4$ emissions in sub-Arctic wetlands, will not likely result in a large change to the total regional C budget near Kuujuarapik. Because the response of the major cover classes to climate change should remain more important than more responsive but spatially limited 'hotspots' for $CO_2$ and $CH_4$ emissions in this area of the Eastern subarctic. However, it is hard to predict if the importance of 'hotspot' will change with significant cover classes change (ie. expansion of thermokarst). In the regional $CH_4$ budget, wetlands and marshes, in spite of their high $CH_4$ emission rate, only make up a small portion of the region relative to upland areas dominated by non-vascular plants and thus do not have as large an impact as in other areas where thermokarst is abundant and/or wetlands make up a larger portion of the region.

## *Chapter 4: Annual and seasonal variations in ecosystem-scale $CO_2$ exchange over forest tundra in Eastern Canada*


### *ABSTRACT*

Between 2008 and 2010, ecosystem-scale measurements of the net ecosystem exchange (NEE) of $CO_2$ were made over shrub vegetation in forest tundra in the Eastern Canadian subarctic. This region is among those most severely impacted by climate warming in the Canadian North. Annual mean temperatures throughout this study were warmer than normal while annual precipitation was near normal. This study clearly shows that NEE—both annually and during the growing season—has considerable inter-annual and intra-annual variability, which can be related to climate anomalies and significant variations in temperature and precipitation. During the cold season, the site was a net source of $CO_2$ from 0.1 to 0.7 g C $m^{-2}$ $day^{-1}$ (monthly averages). However, these $CO_2$ emissions were either impacted by snowpack depth or extent. Net $CO_2$ uptake, -2.6 to -0.1 g C $m^{-2}$ $day^{-1}$ (monthly averages), was measured during the growing season and temporal variations could be related to temperature and precipitation. This results in an annual $CO_2$ budget from a small net source of $CO_2$, 28.5 g C $m^{-2}$ $yr^{-1}$, to a strong net source of $CO_2$, 119.9 C $m^{-2}$ $yr^{-1}$, during the 3 years. Cumulative annual NEE was slightly correlated to the length of the snow-free season and strongly to the number of degree days, with greater net uptake of $CO_2$ with a longer growing season and more growing degree days. This short data set, the first NEE measurements in the Eastern Canadian subarctic region and covering large year-to-year variability in weather, suggests that the $CO_2$ sink strength of this forest tundra site has the potential to increase with climatic warming with the caveat that many other weather factors and vegetation dynamics could reverse this trend.


### *3.1. Introduction*

A large amount of C is presently stocked in circumpolar permafrost with recent estimates of 217 ± 12 Pg C (0-0.03m soil depth) and 472 ± 27 Pg C (0-1 m soil depth) (Hugelius et al. 2014). Rapid warming and disruption of the hydrological regimes in tundra regions may result in a significant release of C accumulated during the last millennium and can contribute to a positive feedback on the global C cycle and climate change (Tarnocai 2006). In contrast, plant

communities may become more productive with the potential to affect a negative feedback (Grant et al. 2011). Net $CO_2$ uptake may increase considerably as a result of earlier snow melt and longer growing seasons, greater photosynthetic activity, and may over longer time scales, lead to succession to more productive plant communities (Grant et al. 2011; Elberling et al. 2004; Kaplan and New 2006).

In the Eastern Canadian Arctic and in northern Quebec, global climate models predict a mean increase of 4–5 °C in winter and 2–3 °C in summer before the end of the century (Cournoyer et al. 2007; Logan et al. 2011). Precipitation should also increase by 5–10% in summer and 10–25% in winter within the century (Cournoyer et al. 2007). These important climate changes have the potential to impact plant communities and the C mass balance of tundra ecosystems (Tremblay and Furgal 2008).

In the last decade, Nunavik and the Great Whale River region has been significantly affected by climate change. Weather observations in the Eastern Canadian subarctic (Inukjuak, Kuujjuaq and Kuujjuarapik) and in northern Quebec (Shefferville) show a warming trend of 2.9 °C during the last century (Tremblay and Furgal 2008). Warming of the region is unprecedented within climate records and within local elder oral history. Changes in vegetation cover and northern migration of plant species, for example, have been observed by the Inuit community of Nunavik (Furgal et al. 2002). This has been supported by longtime weather observations and scientific research. The expansion of shrub cover and plant community changes in the Eastern Canadian subarctic and Low Arctic, particularly below and near the tree line, has been clearly demonstrated and correlated to contemporary climate change (Tremblay et al. 2012; Laliberté and Payette 2008).

Another of the major impacts of the regional warming is on the extent of sea ice. Direct observations show clearly that Hudson Bay presents the fastest loss of sea ice of any region in the Canadian Arctic (Bhiry et al. 2011). This has resulted in a major change in weather conditions throughout the year. Increase in the length of snow-free season and changes in the nature of the maritime climate of the region (due to changes in sea-ice extent and duration) will impact plant communities. Grass-dominated cover, lichen-heath and lichen-spruce woodlands are mostly observed in open areas, whereas shrub and dwarf cover are seen on slopes and

transition zones, and conifer forests in habitat that is sheltered from extreme weather conditions (Payette and Gauthier 1972). Over the last few decades, subarctic forests have expanded with clear impacts on shrub and tree growth including greater heights, stem diameters, and larger tree-rings (Caccianiga et al. 2008).

Warming can also influence periglacial processes and accentuate the degradation of discontinuous or scattered permafrost (Beaulieu and Allard 2003). For example, permafrost degradation can cause slumping and land subsidence impacting both man made infrastructure and the natural landscape. For example, subsidence can impact surface hydrology resulting in ecosystem shifts from forested bogs to nonforested poor fens (Vitt et al. 2000; Fortier et al. 2011). Through these influences on weather conditions, soil thermal regime, moisture conditions and plant communities, changes in the whole C cycle are expected. Consequently, contemporary $CO_2$ exchange between the surface and the atmosphere in this transition zone (forest tundra to tundra) may be particularly sensitive to climate change, making it difficult to predict its impact on the C cycle. It may also be very responsive to inter-annual variations in weather, such as temperature, precipitation and snow cover changes, as well as the length of winter and the growing season.

Multi-year studies of NEE in tundra regions show the potential for significant inter-annual variations in NEE within the same ecosystem (Euskirchen et al. 2012; Parmentier et al. 2011) and the potential for a site to switch from a net source to a net sink of $CO_2$ (Kwon et al. 2006). However, multi-year studies of annual NEE in the Arctic tundra are still rather rare compared to NEE studies at more southerly latitudes.

One hypothesis is that the inter-annual variability in NEE for a transitional zone such as the Eastern Canadian subarctic will be substantial given the large variety of plant communities and microclimates within an area where the average annual temperature is just below 0 ºC. The large climate anomaly observed in this region over the past few decades and its influences on hydrology, permafrost and plant communities may have resulted in communities that can quickly capitalize on warmer conditions and rapidly cycle C through the ecosystem. To test this hypothesis, eddy covariance measurements of NEE in an Eastern Canadian subarctic ecosystem

were made to examine the magnitude of the variations in annual NEE and the explanatory role of precipitation and temperature on annual and seasonal variability in NEE. Quantifying current atmospheric $CO_2$ exchanges is critical for constraining current estimates of $CO_2$ feedbacks to the atmosphere in this region and provides insight into how these and other regions may change with further warming.

## *3.2. Materials and methods*

### *3.2.1. Site description*

From 2008 through 2010, NEE was measured over shrub vegetation in forest tundra on the east coast of Hudson Bay at the mouth of the Great Whale River, slightly outside and east of the small community of Kuujjuarapik (pop. ~ 1500) in the Nunavik area of northern Quebec, Canada (55° 17' N and 77° 46' W) (Figure 4.1a). The region is located north of the boreal forest and a few hundred kilometres below the tree line in the zone of sporadic permafrost. The region is characterized by a transition forest between boreal forest and tundra and is part of the taiga shield or forest tundra ecozone (Bhiry et al. 2011). The eddy covariance micrometeorological tower was installed north of the Great Whale River on a small plateau close to the Centre for Northern Studies (Figure 4.1b & c). The site is rather flat and homogeneous with a carpet of moss, lichens, forbs, crowberry (*Empetrum nigrum*) and small shrubs (~ 0.75 m), mainly dwarf birch (*Betula glandulosa)* and green alder (*Alnus crispa)* and, to a lesser extent, black spruce (*Picea mariana)*, sallow (*Salix* spp.) and pine (*Pinus* spp.). The site is located on Quaternary deposits of glacial tills, marine clays and littoral sands topped with a small amount of organic matter surrounded by the granite-gneiss rocks of the Precambrian Shield (Arlen-Pouliot and Bhiry 2005). Near surface soils at the measurement site were sandy loam to loamy sand with an average organic C content of 3.7% C by mass in the upper 10 cm and no permafrost. In the Canadian soil organic C database, the area of Kuujjuarapik has 4 kg C $m^{-2}$ within the top 30 cm (Tarnocai and Lacelle 1996).

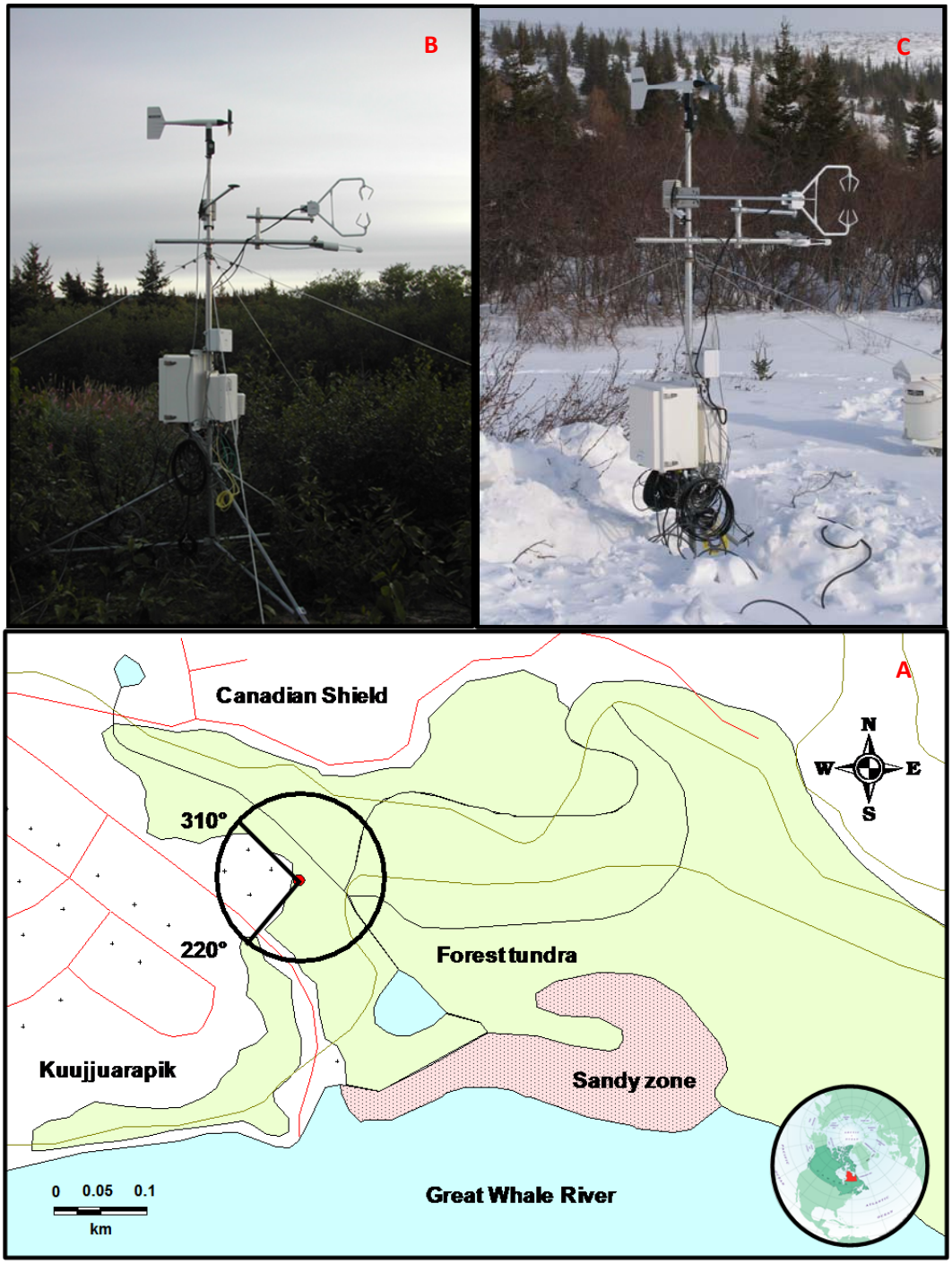


**Figure 4.1** **Study area in the Eastern Canadian subarctic (Kuujjuarapik, Nunavik, Canada), including flux footprint (~ 0.09 km) and area examined (310° to 220°) excluding the community area to the west (A), the flux tower in summer (B), and in winter (C) in forest tundra ecozone (global map insert from Makivik Corporation).**

Hudson Bay has a major climatic impact on the region, sometimes resulting in extreme weather conditions for this latitude. In the cold season, Hudson Bay ice cover mimics the conditions of a continental surface, and the weather is cold and clear. The climate is subject to marine influences and involves heavy rainfall and frequent fog along the coast in spring, summer and fall (Ricard 1998). Based on Canadian climate normals from 1971 to 2000 (EC 2013), the snow-free season extends from June to September, but snow cover is shallow in May and October, with an average depth of 4.7 and 3.4 cm, respectively. On average, Kuujjuarapik receives 414.8 mm of rain and 241.3 mm of snow annually. The rainiest months are August and September (91.5 and 99 mm), while the snowiest months are November and December (56.1 and 42.4 cm). The 30-year climate normal mean annual temperature is -4.4 °C; the warmest month is August with a daily average of 11.4 °C; and the coldest month is January, with a daily average of -23.4 °C. The maximum average daily temperatures in Kuujjuarapik are measured in July and August (15.5 and 15.7 °C, respectively), while the minimum average daily temperatures are observed in January and February (-27.9 and -28.6 °C, respectively). The mean prevailing wind direction is east. Weather observations for 2008, 2009, 2010 and climate normals are summarized in Table 4.1.

**Table 4-1 Annual weather conditions at Kuujjuarapik in 2008, 2009 and 2010 and compared with Environment Canada's climate normals (1971–2000).**

| | | Weather observations | | | Climate normal |
|---|---|---|---|---|---|
| **Parameter** | **Units** | ***2008*** | ***2009*** | ***2010*** | ***1971–2000*** |
| Temperature | (°C) | -2.8 | -2.9 | 0.2 | -4.4 ± 1.4 |
| RH | (%) | 78.4 | 77.6 | 77.3 | 77.5 |
| Growing degree day | (> 0 °C) | 1753.3 | 1456.0 | 1731.5 | 1309.8 |
| Growing degree day | (> 5 °C) | 929.2 | 737.2 | 888.0 | 608.0 |
| Snow-free season length | (days) | 190 | 145 | 225 | 167.8 |
| Snow season length | (days) | 176 | 220 | 140 | 197.5 |
| Wind speed | (m/s) | 3.6 | 4.6 | 4.5 | 4.7 |
| Wind direction | (°) | SE | SE | SE | E |
| Pressure | (kpa) | 101.1 | 101.2 | 101.1 | 101.1 |
| Rainfall | (mm) | 433.8 | 415.6 | 421.4 | 414.8 |
| Snowfall | (mm) | 198.3 | 316.6 | 190.6 | 241.3 |
| Precipitation | (mm) | 616.2 | 717.1 | 640.3 | 648.5 |

### *3.2.2. Instruments and measurements*

A tripod tower was erected in 2008 during the IPY and equipped with standard meteorological sensors. Temperature and humidity were measured at 0.5 and 2 m (HMP45C212, Vaisala®), wind speed and direction at 2.6 m (5106-10, RM Young®), net solar radiation at 2 m (NR Lite, Kipp & Zonen®) and atmospheric pressure at 0.5 m (PTB10B, Vaisala®). In addition, photosynthetically active radiation (PAR) was measured within a few meters at the CEN weather station (LI-190, LI-COR®). Precipitation data were retrieved from Kuujjuarapik weather stations, located within 1 km of the flux tower. Soil heat flux plates (HFT3, Campbell Scientific®) and type E thermocouple averaging soil temperature probes (TCAV, Campbell Scientific®) were

installed at 8 cm and 2–6 cm, respectively. Volumetric soil moisture content for the surface 0–10 cm layer was measured with a water content reflectometer (CS616, Campbell Scientific®) installed at 45° angle to integrate with the soil surface's active layer (for more installation details and sensor technical information, see the Open Path Eddy Covariance System Operation Manual, Campbell Scientific 2006). For the measurements of turbulent energy and $CO_2$ fluxes, a 3D sonic anemometer-thermometer (CSAT3, Campbell Scientific®) and $CO_2$/$H_2O$ open-path infrared gas analyzer (IRGA) (LI-7500, LI-COR®) were installed 2 m above the surface. The open-path IRGA analyzer was oriented horizontally to reduce rain and snow impacts, 30 cm below the centre of sampling volume and 10 cm to the north side of the sonic. The 90% flux footprint was estimated to be 91.6 m (Kljun et al. 2004). The area of interest, a relatively flat shrub tundra, was located northward, eastward and southward, extending approximately 200 m from the tower. Fluxes associated with wind directions between 220° and 310° were rejected due to large vegetation cover variations in that sector and the presence of small buildings (Figure 4.1a). This sector covers equally mast turbulence (300°), because micrometeorological tower and devices also directly impact flux measurements. All flux instrument signals were recorded on a data logger (CR23X, Campbell Scientific®) at a scan rate of 0.1 s and stored as 5 min averages, including variance and covariance calculations for flux measurements. Weather variables were monitored at a scan rate of 5 s and stored as 5 min averages. The tower was powered directly by 110 VAC and directly connected to a telephone line to facilitate data retrieval and quality control, as well as to provide continuous annual measurements.

### *3.2.3. Quality checking, data correction and gap filling*

Fluxes were calculated from the covariance of high frequency vertical velocity and the entity of interest, sonic temperature for sensible heat flux, water vapour density for latent heat flux, and $CO_2$ density for $CO_2$ flux. The $CO_2$ fluxes were corrected for the effects of air density fluctuations using the WPL procedure (Webb et al. 1980). The NEE was the sum of the $CO_2$ flux and the rate of change in the $CO_2$ stored below the height of the eddy covariance instrumentation. High-pass filtering losses (Moncrieff et al. 1997) and low-pass filtering losses related to the instrument design and field set-up (Horst 1997) were not applied. The Monin-Obukhov length scale was then used in quality control and data preparation to determine the

importance of buoyancy and vertical wind speed profile on flux measurements (Monin and Obukhov 1954). Additionally, use of the open-path gas analyzer during the cold season has limitations mainly related to the heat produced by the sensor (Burba et al. 2008; Amiro 2010). In this study, cold season $CO_2$ uptake was rarely observed and given that the IRGA was oriented horizontally, it would be inappropriate to apply correction factors established for vertical sensors (Burba et al. 2008). Consequently, no heating correction was applied to the NEE measurements.

The extended flux data set compiled through 2008 to 2010 was quality checked with a number of criteria. First, 5 min fluxes were averaged for 30 min intervals. Half hour measurements were discarded when the standard deviation of the six 5 min fluxes exceeded 5 at any time or 1.5 in non-growing season months (Jan – May, Nov – Dec) when little photosynthesis is expected and only respiration should dominate. NEE measurements from the sector 220° to 310° were removed to ensure that only the surface of interest was represented and NEE measurements were not affected by the turbulence related to the tower structure (300°). The rate of change in $CO_2$ storage was calculated and added to Fc to determine NEE on a 30 min basis. Any non-growing season $CO_2$ emissions larger than 9 μmol $m^{-2}$ $s^{-1}$ were also removed being deemed unreasonably large. During the nighttime (PAR < 20 μmol $m^{-2}$ $s^{-1}$) and during cold periods (as defined as the period when the 3-day running mean of air temperature < 0 °C) NEE were filtered for calm conditions using a friction velocity threshold of 0.1 m $s^{-1}$. NEE were also removed during the nighttime and cold season when NEE < -0.5 μmol $m^2$ $s^{-1}$, as any $CO_2$ uptake larger than this estimate of random error was considered erroneous. Instrument and power failures led to a loss of data for 17 days beginning July 17, 2009, 58 days beginning June 19, 2010 and 80 days between October 12 and December 31, 2010. Outside of these times, approximately 58.7% of NEE measurements were rejected in this flux study using quality control criteria with most of them, 44.1 %, occurring during winter months and at night, while 14.7% occurred in the day during the growing season. Falge et al. (2001) showed that equipment failure and data rejection reduced the average annual data coverage of NEE measurements to about 50%, a fraction typical of continuous eddy covariance measurements. The meteorological dataset was quality controlled manually, based on Environment Canada's QA/QC protocol.

Filling these data gaps is crucial to gain a better understanding of the ecosystem's interactions with the atmosphere and to estimate defensible annual cumulative NEE (Falge et al 2001). Weather data were directly filled when possible using duplicate sensors or those collocated on nearby weather stations to develop linear relationships with the main weather variables that are used to adjust the secondary readings to ensure continuity and similarity of measurements. Hour long gaps in NEE were filled by linear interpolation. Longer gaps were filled by non-linear regressions between NEE measurements and environmental variables (Barr et al. 2004; Moffat et al. 2007). First, the GEP was estimated by a rectangular hyperbolic relationship with photosynthetic active radiation (PAR), the maximum photosynthetic uptake ($A_{max}$) and the effective quantum yield ($\alpha$) as shown as the first term in Eqn (1):

$$NEE = -\frac{\alpha \times PAR \times A\max}{\alpha \times PAR + A\max} + R_{10} \times Q_{10}^{(T-T_{ref})/10} \qquad (1)$$

The second term of Eqn (1) represents the exponential relationship or $Q_{10}$ function between ER and temperature where $R_{10}$ is ER at a reference soil temperature of 10 °C ($T_{ref}$). Nighttime and winter NEE data were gap-filled with a $Q_{10}$ relationship (second term of equation 1) adjusted for seasonal variation using a 200 data point moving window moved in increments of 40 data points following the method described by Lafleur and Humphreys (2008). To gap-fill the missing winter period in 2010, the average NEE of the two previous years, 2008 and 2009, was used. GEP (NEP + ER) for available NEE (-NEP) data were then calculated in order to develop a growing season (June 15 – Aug 15) light response curve adjusted to seasonal variation as described for ER above. As a result of the large growing season data gaps in 2009 and 2010, this method needing seasonal adjustments were not appropriate and a slightly modified version of equation 1 was parameterized using the 2008 non-gap-filled dataset for the period June 19 to Aug 16, 2008. The parameters for the first term of equation 1 were 0.0168 mol $mol^{-1}$ ($\alpha$) and 25.3 μmol $m^{-2}$ $s^{-1}$ ($A_{max}$) while the second terms was fit simply as the slope of a linear temperature response resulting in a temperature offset of 0.21 μmol $m^{-2}$ $s^{-1}$ $degC^{-1}$. Any resulting $CO_2$ emissions larger than 12 μmol $m^{-2}$ $s^{-1}$ were taken as being unreasonably large and removed. Daily, seasonal and annual NEE are expressed here in g of C rather than in g $CO_2$ with negative values indicating a net uptake $CO_2$ by the ecosystem.

### *3.2.4. Quality control and statistical analysis*

All the meteorological sensors were previously calibrated with certified standards and methods to ensure high accuracy of measurements. The $CO_2/H_2O$ open-path analyzers were initially calibrated with a certified $CO_2$ standard (NIST & NOAA) and portable dew point generator (LI-610, LI-COR®). Thereafter, on-site tower inspections were made approximately every 6 months, while chemicals were replaced and the IRGA was calibrated approximately every 12 months. Zero drifts were low, about 0.1 %, and calibration drift about 2.5 % annually. All measurements were rigorously submitted to a strong QA/QC protocol (see Section 2.3 above). Data handling was carried out in Microsoft Office, Excel 2007, and all quality checking, gap filling, and statistical analyses were computed using SAS®, version 9.2 for Windows and Systat®, SigmaPlot 12.0, while spectral correction was estimated with MATLAB® for Mac.

## ***3.3. Results***

### *3.3.1. Meteorology*

Mean annual air temperatures in 2008 and 2009 were similar (-2.8 and -2.9 °C, respectively), and were higher than the 30-year climate -4.4 °C normal (1971–2000) (Table 4.1). This increase of ~1.5 °C is representative of the actual warming observed over the past decade in Nunavik and the Eastern Canadian subarctic region (Logan et al. 2011). The mean annual temperature of 0.2 °C in 2010 was much higher than the climate normal, mainly due to a warmer-than-normal winter and spring (Figure 4.2a). This coincided with a moderate El Niño southern oscillation (ENSO) in 2009, which continued until the first quarter of 2010 (Figure 4.3b). Inter-annual surface temperature variations in the Northern Hemisphere and mid-latitudes have been linked to large atmospheric processes such as ENSO (Adler et al. 2008). The warm conditions in winter in 2009–2010 were also corroborated by a strong negative Arctic Oscillation (AO) index in December 2009 and January and February 2010 (Figure 4.3a).

Total precipitation in 2008 and 2010 was very similar (616.2 and 640.3 mm respectively) and was representative of the climate normal at 648.5 mm (Table 4.1). Precipitation in 2009 was

higher at 717.1 mm, due to heavier snowfall in earlier months. The precipitation anomaly observed at Kuujjuarapik also correlated to ENSO. ENSO is known to greatly enhance precipitation in the Northern Hemisphere, particularly in summer and fall (Ropelewski and Halpert 1987). This is largely consistent with the 2009 precipitation trend although the greater precipitation arrived in spring (Figure 4.2c). Snow depth and winter precipitation impacts surface soil temperature and the length of the growing season. In 2008, snow cover ended on about DOY 134 resulting in approximately 199 snow-free days. In 2009, the snow-free season was shorter (143 days), while it was much longer in 2010 (222 days) (Figure 4.2d). Accordingly, the depth of the snowpack was deepest in 2009 during the snow-covered period at 45.8 cm and shallowest in 2010 at 34.8 cm (Figure 4.2d). Soils remained cooler longer during the later snowmelt in 2009 when compared to the other two years (Figure 4.2b). Rainfall in this region controls soil water content during the warmer months and there was little difference among years with average July and August VWC of 0.019 and 0.022 $m^3$ $m^{-3}$ respectively, for all years combined (Figure 4.2e). The maximum VWC monthly average occurred in May 2009 at 0.036 $m^3$ $m^{-3}$ directly after snow melt.

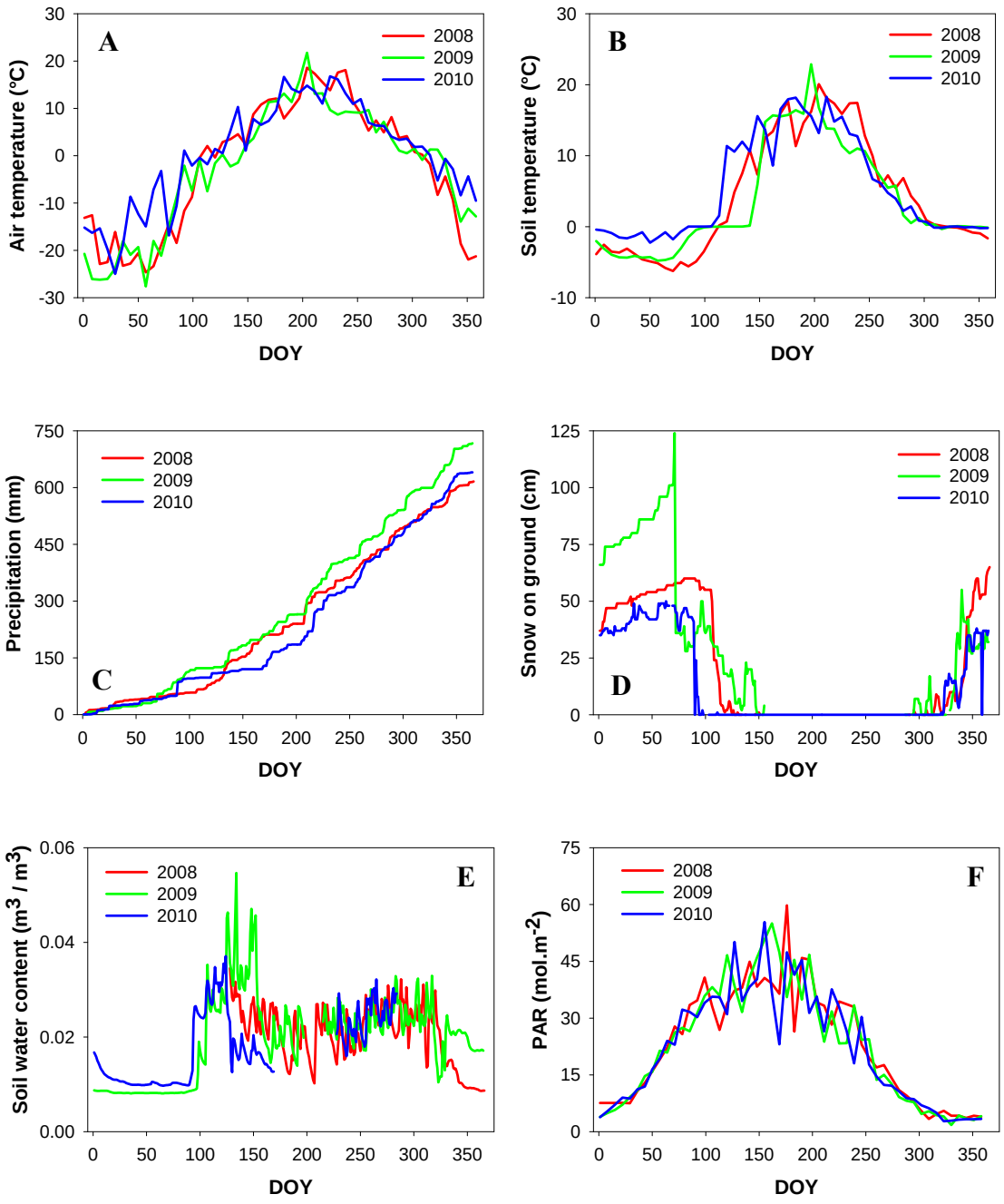


**Figure 4.2** **Trends of (A) air temperature (7 day mean); (B) soil temperature (C) sum of precipitation; (D) snow depth on ground; (E) soil water content; and (F) photosynthetic active radiation as function of day of year (DOY) measured at Kuujjuarapik (Nunavik, Canada) from 2008 to 2010.**

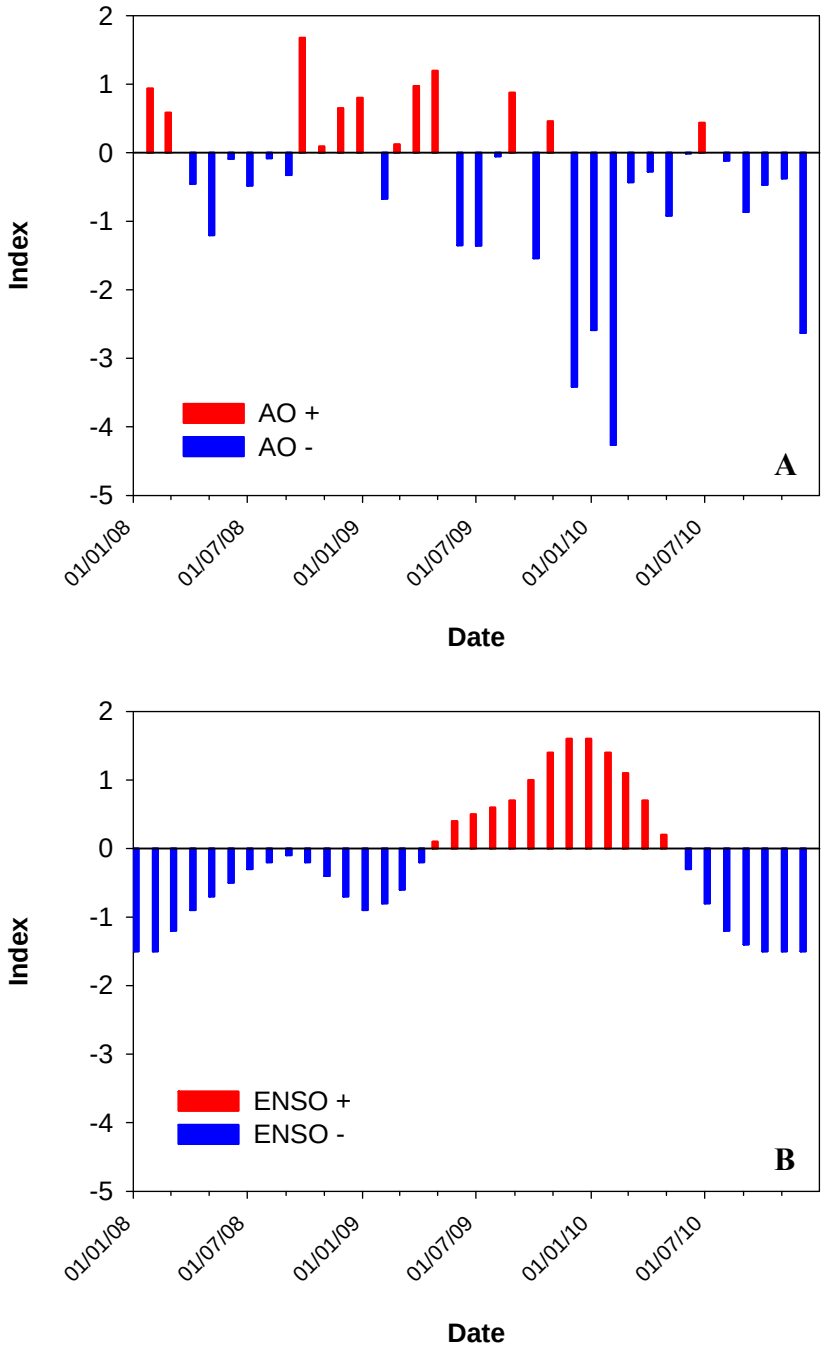


**Figure 4.3** **Monthly mean index of the most prominent teleconnection over the Northern Hemisphere and the Arctic: (A) Arctic Oscillation (AO), and 3-month running mean index of (B) El Niño Southern Oscillation (ENSO) (NOAA 2012).**

*3.3.2. Seasonal and annual NEE trends*

Months with an average net uptake of $CO_2$ occurred only in June, July or August but with large variability among years from a net loss of 0.4 g C $m^{-2}$ $day^{-1}$ in June 2009 to a net uptake of -2.6 g C $m^{-2}$ $day^{-1}$ in July 2008 (Figure 4.4). The maximum daily uptake of $CO_2$ in 2008, 2009 and 2010 were always observed in July (-6.6, -3.5, and -4.9 g C $m^{-2}$ $day^{-1}$, respectively).

Net emissions of $CO_2$ were consistently measured during the remaining months of the year ranging from 0.1 to 1.2 g C $m^{-2}$ $day^{-1}$ with little difference in average monthly losses among years between September and March (Figure 4.4) despite substantial differences in fall and winter air temperatures and snow pack depths (Figure 4.2a & 4.2d).

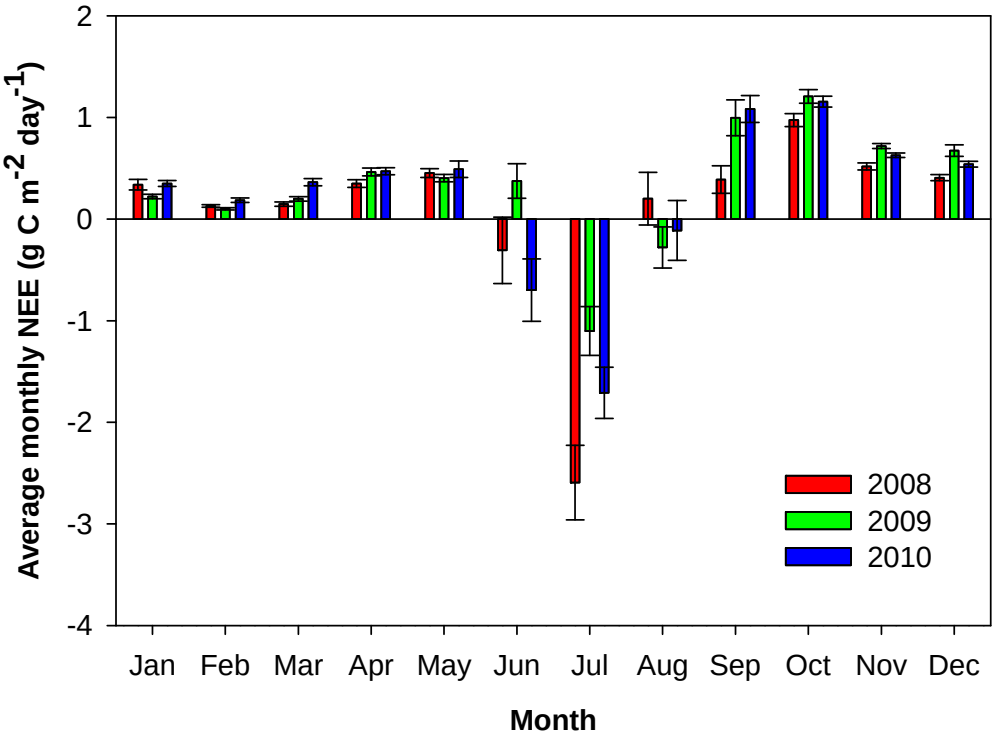


**Figure 4.4 Monthly average NEE trends with standard errors measured over shrub vegetation in forest tundra ecozone in 2008, 2009 and 2010.**

### *3.3.3. Cumulative NEE budget*

The cumulative annual NEE in forest tundra was clearly impacted by weather conditions especially beginning of spring until early fall (Figure 4.5). Cumulative NEE trends were very similar in the cold season until spring and then again through late fall into winter (as noted by the slope of the cumulative NEE time series). In 2008 and 2009, the majority of snowmelt occurred by DOY 115 in 2008 and DOY 127 in 2009, although a late spring snowfall in 2009 extended the snow-covered period another 2 weeks with a shallow snow cover with final full melt on ~DOY 150, Figure 4.2d). Consequently the date when daily NEE had a net uptake rather than net loss of $CO_2$ was earlier in 2008 (DOY 169) than in 2009 (DOY 176) but resulted in similar net losses of $CO_2$ up until that point in time (56. 9 g C $m^{-2}$ in 2008 and 56.0 g C $m^{-2}$ in 2009) (Figure 4.5). Snowmelt in 2010 took place a number of weeks earlier on DOY 94, but did not result in an earlier start to the period of net $CO_2$ uptake nor did it decrease the net losses of $CO_2$ before the uptake period (63.3 g C.$m^{-2}$).

As expected, the length of period where net uptake of $CO_2$ was observed (a negative trend in the cumulative NEE record, Figure 4.5) correlated with the total net $CO_2$ uptake. The highest $CO_2$ uptake 103.5 (2008) and 97.5 g C $m^{-2}$ (2010) occurred during the longest "growing seasons", 71 and 57 days respectively. In 2009, only 49.6 g C $m^{-2}$ was sequestered over 54 days. This short uptake season reflected the short snow-free season of 140 days (Table 1). However, the longer snow-free season (225 days) in 2010 did not result in more uptake than in 2008 (190 days). It is important to also note the large uncertainty surrounding the 2010 growing season results and the 2009 results (to a lesser extent) given the 58 and 17 day data gaps, respectively. The number of degree days also seemed to impact the amount of net $CO_2$ uptake during the growing season and more closely related to the growing season net $CO_2$ uptake over the three years. Cumulative GDDs can be used as an integrative indicator of plant growth and photosynthetic activity throughout the growing season (Martel et al. 2005). This indicator also includes the impact of timing and the length of the growing season. The number of GDDs above 0 (Figure 4.6) and 5 °C at Kuujjuarapik was highest in 2008 and lowest in 2009, but all 3 years had more GDDs than the 30-year climate normal, while also being representative of the Canadian subarctic zone with 750 to 1000 GDDs as defined by Hebert (2002). 2008 had the highest number of degree days

(929.2) and greatest growing season net $CO_2$ uptake, followed by 2010 (888.0 GDD) with the next highest net $CO_2$ uptake while the lowest uptake was in 2009 with the lowest numbers of degree days (737.2 GDD) (Table 4.1).

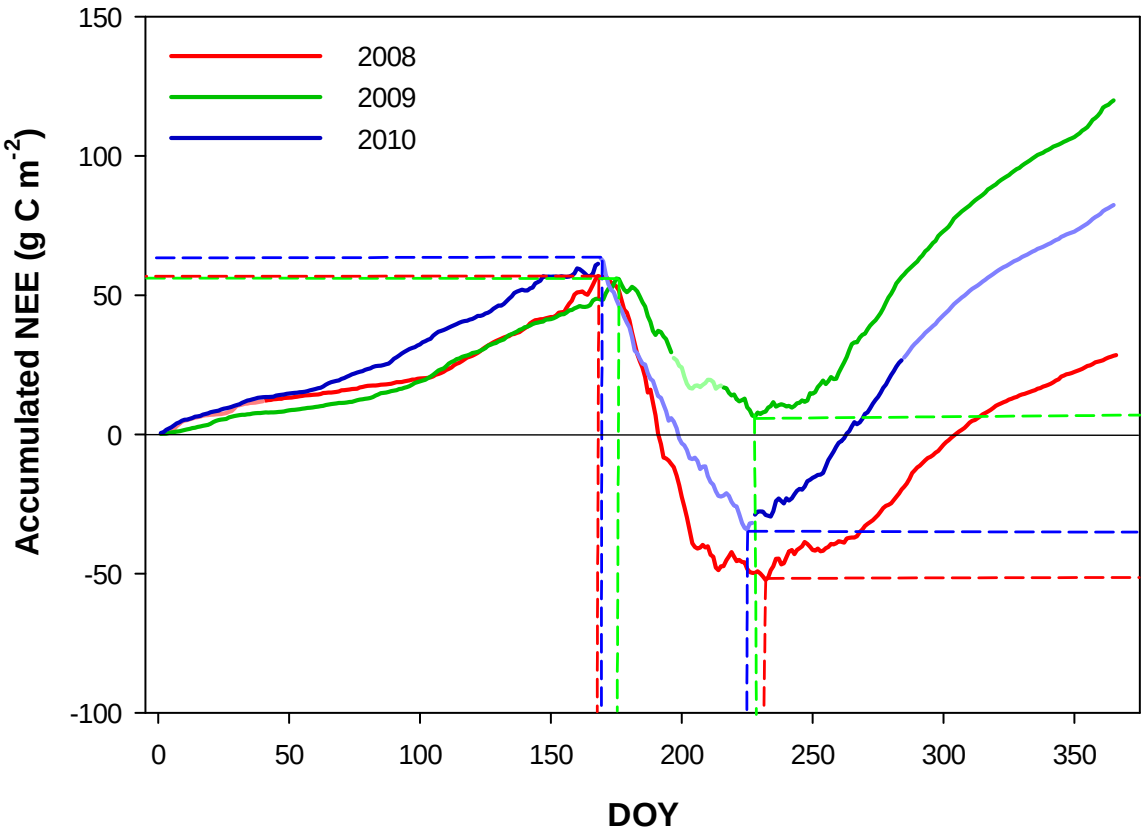


**Figure 4.5** **Annual cumulative Net Ecosystem Exchange (NEE) measured in the Eastern Canadian subarctic (Kuujjuarapik, Nunavik) over shrub vegetation in forest tundra ecozone in 2008, 2009 and 2010. Shadowed lines indicate long gaps in the measurement record. Dashed lines indicate cumulative NEE maximum and minima during the year.**

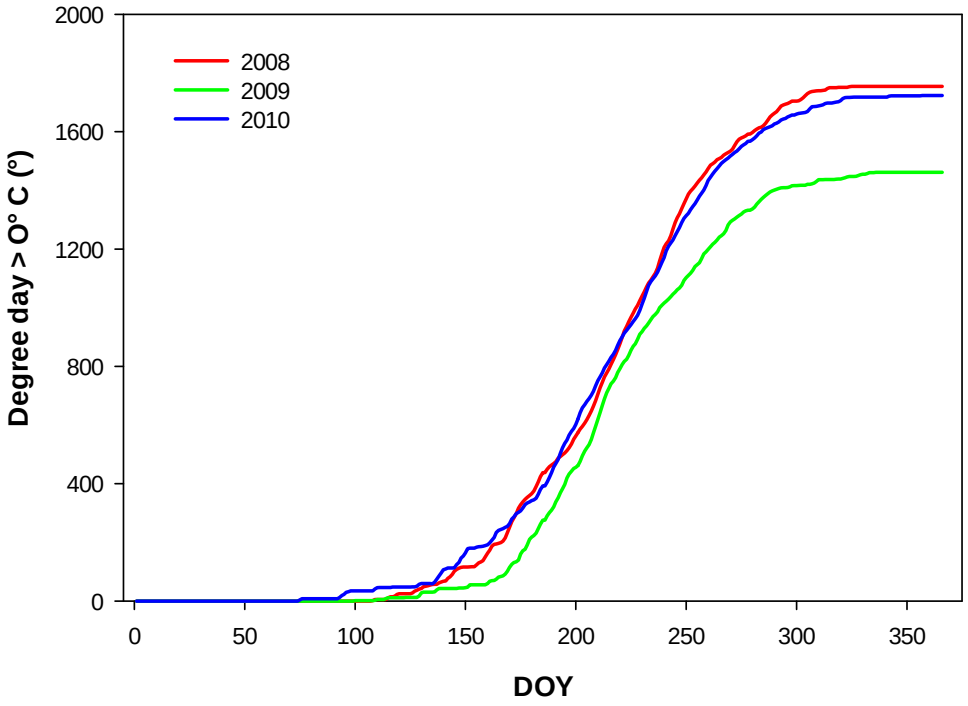


**Figure 4.6 Accumulated growing degree days above 0 ºC for Kuujjuarapik, Nunavik, 2008 to 2010.**

After a full year of measurements, 2008 had the smallest $CO_2$ emissions (28.5 g C $m^{-2}$ $yr^{-1}$), followed by 2010 (82.3 g C $m^{-2}$ $yr^{-1}$) and 2009 (119.9 g C $m^{-2}$ $yr^{-1}$) (Figure 4.5). Over the three years, annual NEE tended to decrease (less net $CO_2$ loss) with increasing GDDs (Figure 4.7b) while there wasn't a clear pattern for annual NEE and the length of the snow-free season (Figure 4.7a). The warmest year was 2010 while 2008 and 2009 were both about 3 °C cooler (Table 4-1). As discussed above, there was a large difference in annual NEE between 2008 (small $CO_2$ source) and 2009 (strong $CO_2$ source) despite the similarity in average annual air temperature.

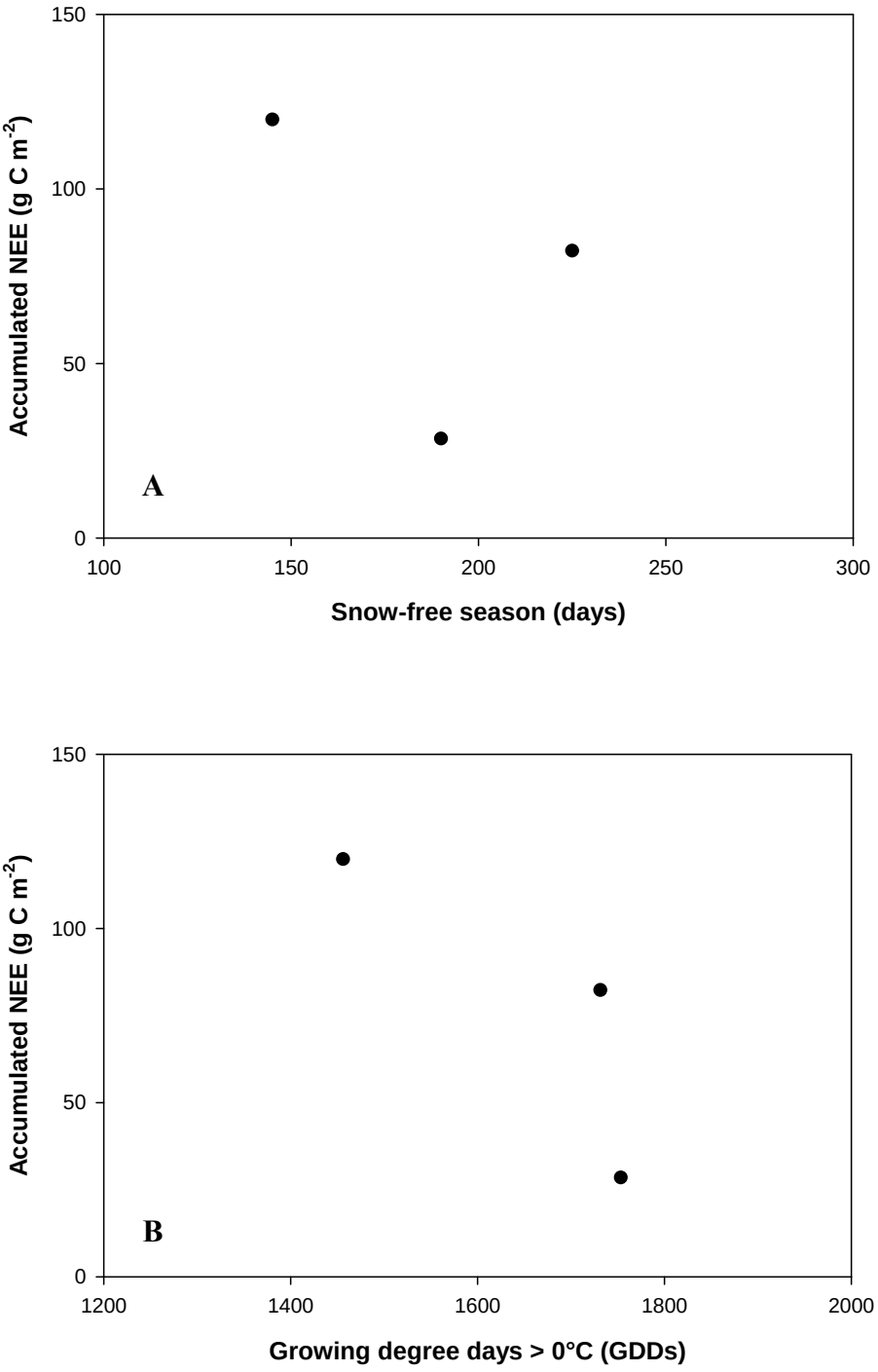


**Figure 4.7** **Total annual NEE and A) the length of the snow-free season and B) the number of growing degree days (GDDs) above 0 °C over shrub vegetation in forest tundra between 2008 and 2010.**

### *3.3.4. Hydrological regime, precipitation and water balance*

Precipitation regimes in winter and summer in this region are very different—continental or maritime influences—due to the proximity of Hudson Bay. Rain influences soil water content. Monthly mean VWC slightly increased with precipitation ($r^2 = 0.06$, $n = 29$, $p = 0.18$) throughout the year but particularly in fall (September - November) ($r^2 = 0.86$, $n = 7$, $p < 0.01$). Throughout the years, no significant relationship was found between monthly precipitation and monthly NEE ($r^2 = 0.01$, $p = 0.95$). Based on general plant growth trends, three specific periods can be examined for the influence of precipitation. During dormancy between December to April, monthly average NEE was 0.1 to 0.7 g C $m^{-2}$ $day^{-1}$ and significantly increased with precipitation (snowfall) ($r^2 = 0.60$, $n = 14$, $p < 0.001$) (Figure 4.8) but was not significantly correlated to snowpack depth ($r^2 = 0.07$, $n = 14$, $p = 0.38$). Monthly snowfall during this period was greater during warmer periods ($r^2 = 0.18$, $n = 14$, $p = 0.14$) and as a result, monthly average NEE also increased with increasing monthly air temperature ($r^2 = 0.43$, $n = 14$, $p = 0.01$).

During the period of senescence through fall (September through November), plant metabolism slows, the deciduous leaves are shed and ER is more significant than GEP. At this time of year, Kuujjuarapik was not totally frozen and received a mix of rain and light snow. During this season, the NEE (0.4 to 1.2 g C $m^{-2}$ $day^{-1}$) significantly increased with precipitation (47.4 to 106.3 mm) with more precipitiation promoting ER ($r^2 = 0.60$, $n = 9$, $p = 0.01$) (Figure 4.8). As above, monthly rainfall during this period was greater during warmer periods ($r^2 = 0.19$, $n = 9$, $p = 0.24$) and as a result, monthly average NEE also increased with increasing monthly air temperature ($r^2 = 0.10$, $n = 9$, $p = 0.40$).

The final period is the growing season when photosynthetic activity and net $CO_2$ uptake occurs. Monthly average NEE (-2.6 to 0.5 g C $m^{-2}$ $day^{-1}$) was not significantly correlated to precipitation (10.8 to 105.5 mm ($r^2 = 0.13$, $n = 13$, $p = 0.23$)) (Figure 4.8) and that suggests that other physical variables, such as temperature as discuss with GDDs above, were the main drivers of NEE during the growing season.

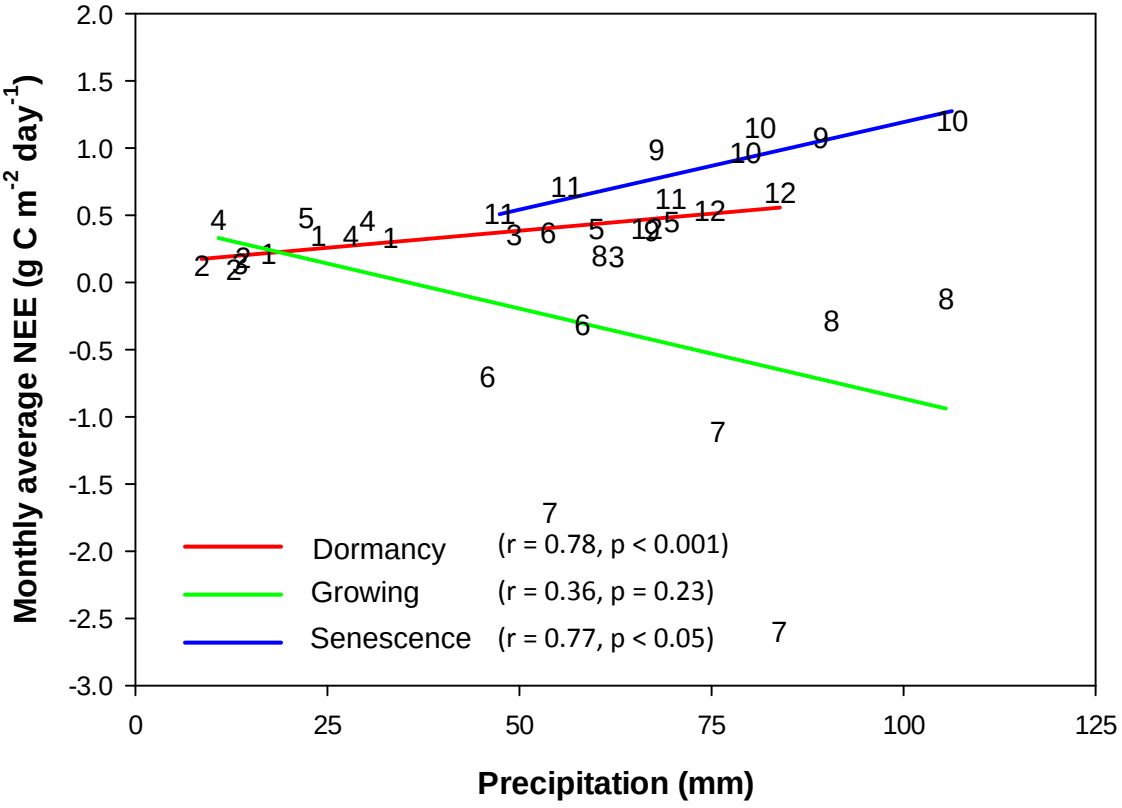


**Figure 4.8 Seasonal impacts of precipitation on monthly average NEE view through three distinct trends based on climate and plant physiology, dormancy (NEE measurements over snowpack), growing (NEE over plant and high photosynthetic activity) and senescence (NEE over plant and low photosynthetic process), symbol numbers correspond to the respective month (1-Jan, 2-Feb, 3-Mar, 4-Apr, 5-May, 6-Jun, 7-Jul, 8-Aug, 9-Sep, 10-Oct, 11-Nov & 12-Dec).**

### *3.4. Discussion*

Year-round measurements of NEE in subarctic climates, those with mean annual temperatures near 0°C, are relatively rare in the literature and include studies in Finland, Sweden, Siberia, and Alaska (for details, see studies Ge et al. 2011; Christensen et al. 2012; Merbold et al. 2009; Parmentier et al. 2011; Euskirchen et al. 2012 in Table 4.2). To place the Kuujuarapik results in

context, the interannual variability of NEE over a broad range of climates cooler and warmer than the subarctic is given in Table 4.2. Interannual variability of annual NEE is typically higher in boreal forest sites, from 13 to 2298 % of the mean measured flux, than in subarctic and Arctic regions where the range in NEE is 44 to 505 % of the mean measured flux. In boreal forests, the year-to-year range in growing season NEE ranges from 7 to 17 % of the mean measured flux, while in seasonal subarctic and Arctic studies, variability is smaller in absolute terms but again, up to 7 to 367% of the mean measured flux (Table 4.2). For example, the range in interannual NEE variability (ΔNEE) for wet sedge tundra and heath tundra (40 to 80 g C $m^{-2}$) (Euskirchen et al. 2012) and boreal black spruce forests (-19 to -142 g C $m^{-2}$) (Arain et al. 2002; Dunn et al. 2007) but these are lower than for temperate deciduous forest (ΔNEE = 376 g C $m^{-2}$) (Wu et al. 2012) and boreal deciduous aspen forest (ΔNEE = 313 g C $m^{-2}$) (Barr et al. 2004). Compared to these studies, annual NEE at Kuujuarapik has a range of 91 g C $m^{-2}$ $year^{-1}$ or 119% of the mean net annual NEE of 77 g C $m^{-2}$ $yr^{-1}$ for the three year study, similar to ecosystems ranging from Arctic tundra to boreal evergreen forest. This is in large part due to the high $CO_2$ loss in 2009 associated with colder and wetter weather, and which appears to be the highest loss of $CO_2$ ever measured in subarctic or Arctic regions (Table 4.4). For example, net cumulative NEE in 2009, 120 g C $m^{-2}$, is higher than previous studies in Arctic tundra (82 g C $m^{-2}$) (Euskirchen et al. 2012) and boreal black spruce forests (84 g C $m^{-2}$) (Dunn et al. 2007).

Since many NEE studies in Arctic tundra are mainly limited to the growing season (May to August), cumulative NEE for the same period at Kuujjuarapik indicates the site is a strong sink for $CO_2$ in warmer years, varying from -71.3 g C $m^{-2}$ (2008) to -63.0 g C $m^{-2}$ (2010) while it is a slight sink for $CO_2$ in the colder and wetter year, -19.0 g C $m^{-2}$ (2009). These seasonal NEE are in the same range of values obtained in Arctic and subarctic tundra demonstrating smaller seasonal sinks for $CO_2$ when compared to boreal forests (Table 4.2). Longer snow-free season and greater GDDs coincided with greater $CO_2$ uptake as was also observed in a boreal evergreen forest (Dunn et al. 2007).

**Table 4-2 Summary of seasonal and inter-annual variability of NEE, as measured using the eddy covariance technique, at northern latitude sites spanning 44° to 74° N from boreal deciduous and conifer forest to Arctic tundra.**

| Location | Ecosystem type | Period | NEE budget (g C $m^{-2}$) | Δ NEE (g C $m^{-2}$) | Avg Air T (°C) | Reference |
|---|---|---|---|---|---|---|
| Zackenberg, Greenland (74° N, 20° W) | High Arctic heath | Seasonal, Jun–Aug (2000–2010) | -40 to -4 | 36 | 7.1 ± 1.0 | Lund et al. 2012 Groendahl et al. 2007 |
| Barrow, Alasaka (71° N, 156° W) | Wet sedge tundra | Seasonal, Jun–Aug (1999–2003) | -70 to -46 | 24 | 2.2 ± 0.6 | Kwon et al. 2006 |
| Barrow, Alasaka (71° N, 156° W) | Moist tussock tundra | Seasonal, Jun–Aug (1999–2003) | -2 to 61 | 63 | 6.7 ± 0.7 | Kwon et al. 2006 |
| Sibarian tundra, Yakutia (70° N, 147° W) | Lowland tundra | Seasonal, Jun–Aug (2003–2010) | -95 to -69 | 26 | NA | Parmentier et al. 2011 |
| Cherskii, Yakutia (69° N, 161° W) | Arctic wet tundra | Seasonal, Jul–Oct (2002–2005) | -53 to 15 | 65 | NA | Merbold et al. 2009 |
| Brooks Range, Alaska (68° N, 149° W) | Heath tundra | Seasonal, Jun–Aug (2008–2010) | -58 to -51 | 7 | 8.0 ± 1.1 | Euskirchen et al. 2012 |
| Brooks Range, Alaska (68° N, 149° W) | Tussock tundra | Seasonal, Jun–Aug (2008–2010) | -84 to -62 | 22 | 8.0 ± 1.1 | Euskirchen et al. 2012 |
| Brooks Range, Alaska (68° N, 149° W) | Wet sedge tundra | Seasonal, Jun–Aug (2008–2010) | -95 to -59 | 26 | 8.0 ± 1.1 | Euskirchen et al. 2012 |
| Brooks Range, Alaska (68° N, 149° W) | Heath tundra | Annual (2008–2010) | 21 to 61 | 40 | -1.6 ± 0.4 | Euskirchen et al. 2012 |
| Brooks Range, Alaska (68° N, 149° W) | Wet sedge tundra | Annual (2008–2010) | 2 to 82 | 80 | -1.6 ± 0.4 | Euskirchen et al. 2012 |
| Stordalen Mire, Sweden (68° N, 87° E) | Subarctic palsa mire | Annual (2001–2008) | -95 to -20 | 75 | -0.5 ± 0.3 | Christensen et al. 2012 |

| | | | | | | |
|---|---|---|---|---|---|---|
| Stordalen Mire, Sweden (68° N, 87° E) | Subarctic palsa mire | Seasonal, May–Aug (2001–2008) | -166 to -87 | 79 | NA | Christensen et al. 2012 |
| Daring Lake, NWT, Canada (65° N, 111° W) | Low Arctic Tundra | Seasonal, May–Aug (2004–2006) | -61 to -32 | 29 | 7.8 ± 2.1 | Lafleur and Humphreys 2008 |
| Delta Junction, Alaska (64° N, 145° W) | Evergreen conifer forest, Black spruce | Seasonal, Apr–Sep (2002–2004) | -172 to -152 | 20 | 9.7 ± 1.3 | Welp et al. 2007 |
| Delta Junction, Alaska (64° N, 145° W) | Deciduous broadleaf forest, Aspen | Seasonal, Apr–Sep (2002–2004) | -227 to -162 | 71 | 9.7 ± 1.3 | Welp et al. 2007 |
| Mekrijärvi Finland (63° N, 21° E) | Boreal 50-year-old Scots pine stand | Seasonal, May–Sep (1999–2008) | -268 to -195 | 73 | NA | Ge et al. 2011 |
| Mekrijärvi, Finland (63° N, 21° E) | Boreal 50-year-old Scots pine stand | Annual (1999–2008) | -232 to -158 | 74 | NA | Ge et al. 2011 |
| NOBS, Manitoba, Canada (56° N, 98° W) | Boreal Black spruce forest | Annual (1995–2004) | -58 to 84 | 142 | -2.7 ± 1.3 | Dunn et al. 2007 |
| Soro Euroflux, Denmark (55° N, 11° E) | Temperate deciduous Beech forest | Annual (1997–2009) | -344 to 32 | 376 | 8.5 ± 0.5 | Wu et al. 2012 |
| Kuujjurapik, Canada (55° N, 77° W) | Forest tundra, Shrub vegetation | Annual (2008–2010) | 28.5 to 119.9 | 91 | -1.8 ± -1.8 | This study |
| Kuujjurapik, Canada (55° N, 77° W) | Forest tundra, Shrub vegetation | Seasonal, May-Aug (2008–2010) | -71.3 to -19.0 | 52 | -1.8 ± -1.8 | This study |
| SOA, Saskatchewan, Canada (54° N, 106° W) | Boreal deciduous, Aspen forest | Annual (1994–2003) | -367 to -54 | 313 | 1.9 ± 1.2 | Barr et al. 2004 |
| SOBS, Saskatchewan, Canada (54° N, 105° W) | Boreal conifer, Black spruce forest | Annual (1994, 1996, 1999) | -79 to -60 | 19 | 0.6 ± 1.9 | Arain et al. 2002 |
| EOBS, Québec, Canada (50° N, 74° W) | Boreal Black spruce forest | Annual (2004–2005) | -6 to 0 | 6 | 0.6 ± 1.2 | Bergeron et al. 2008 |
| Borden forest, Ontario, Canada (44° N, 80° W) | Mixed hardwood and coniferous forest | Annual (1996–2003) | -281 to -19 | 262 | 7.4 ± 1.1 | Teklemariam et al. 2009 |

Warmer temperatures may significantly impact cumulative NEE in both the short and long-term in northern ecosystems such as forest tundra. Temperature limitations to growth remains one of the dominant and limiting factor regulating photosynthetic activity (GEP), as well as autotrophic and heterotrophic respiration (ER) at this latitude. With warming, rapid spread of shrubs significantly increases the leaf area index (LAI), reduces surface albedo and increases heat transfer at the ground level, thus largely promoting photosynthetic activity of a terrestrial ecosystem (Shaver et al. 2007). The increase of phytomass, LAI and NDVI and the link with the summer warmth index is well defined in the Arctic (Raynolds et al. 2006). $CO_2$ uptake may increase considerably as a result of longer growing seasons and greater photosynthetic activity (Grant et al. 2011; Elberling et al. 2004). A longer growing season may also impact the structure and productivity of plant communities (Kaplan and New 2006).

Our results are consistent with a previous study in a subarctic palsa mire in Sweden (68° 20' N and 19° 03' W) (Christensen et al. 2012) despite substantial disparity in vegetation types. This palsa mire consists of a mix of elevated dry ombrotrophic areas with mostly mosses, lichens and dwarf shrubs, and wet minerotrophic depressions with tall graminoids. Substantial differences in the length of the snow-free season and NEE were observed from 2001 to 2008, ranging from 99 to 126 days with NEE ranging from -166 to -87 g C $m^{-2}$. This compared with 143 to 222 days (-71 to -19 g C $m^{-2}$) in our study. However, with 8 years of measurements, Christensen et al. (2012) was able to evaluate a relationship between NEE and the length of the growing season ($r^2$ = 0.48, n = 8). Ueyama et al. (2013) also found a strong link between GPP and net $CO_2$ uptake and the length of the snow-free season, even if ER also increases with longer seasons and warmer temperatures in tundra ecosystems in Alaska. However, our results do not show a clear pattern between cumulative NEE and day of snowmelt. Humphreys and Lafleur (2011) also did not find snow-melt date related to NEE in two different tundra types in the Canadian low Arctic. Delays in Arctic winter onset and snowpack depth largely influence tundra C budget by directly impacting temperature sensitive factors (microbial activity, respiration and cold season gas exchange) but are not necessary correlated to longer growing season since the start of plant growth is also directly correlated to snow depth and temperature at snow melt (Cooper 2014). A longterm $CO_2$ exchange study in high Artcic tundra heath (northeast Greenland) concluded that timming of snowmelt controls the beginning of GPP, and that interannual variability of NEE was

directly impacted by temperature sensitive variables, such as maximum thaw depth and the number of GDDs (Lund et al. 2012). Another longterm study in northeastern Siberian graminoid tundra found no evidence of an increase in NEE with longer snow-free season, since higher GPP in warmer temperature was offset by an increase in ER (Parmentier et al. 2011). These results suggest that NEE trend across the subarctic and Artic ecosystems are site-specific, and are a function of soil, vegetation and climate conditions.

Since it corresponds to the heat available for plant growth, the number of GDDs currently used in agroforestry may be a more valuable tool for linking temporal patterns of NEE with plant phenology and related plant and soil functions (Bonsal et al. 2001; Asselin et al. 2003). The number of GDDs during a year can be used as an integrated variable to examine the influence of cumulative heat on C cycling (Yasuda et al. 2012). On short time scales, a slight temperature change may impact NEE, but only within the physiologic limits of plant species. A significant input of energy does not increase C uptake at the end of summer and fall, for instance, when plant growth is almost finished while decomposition rates may be enhanced. On a longer time scale, temperature may act on plant community structure, changing dominant species and their functions including net $CO_2$ uptake. The results of this study strongly suggests that a minimum number of GDDs is needed during the growing season to ensure a significant plant C uptake and to ensure that forest tundra does not shift to a net C source. A previous study in southeastern Canada has shown that photosynthesis activity in one conifer species began only once soil temperature was above 0 °C; no photosynthesis proceeds at an air temperature of 10 °C if the soil is frozen (Goodine et al. 2008). Another study found that growing season C uptake coincided with a soil temperature equal to or exceeding 0 °C in combination with a mean air temperature above 4 °C (Krishnan et al. 2008). The number of GDDs is used in connection with the length of the snow-free season to more accurately predict the uptake of $CO_2$ during the warmer months. In this study the highest cumulative NEE estimated between May to August coincides to the highest number of GDDs for this period (growing season), with stronger uptake of $CO_2$ with larger number of GDDs above 0 and 5 °C. The length of the snow-free season was considerably higher in 2010 than in 2008, 225 and 190 days respectively. Our results suggest that the main driver controlling the annual cumulative NEE is the number of GDDs followed by the length of the

growing season and the day of snow melt. Note that the number of GDDs above 0 and 5 °C were related to the length of the snow free period ($r^2 = 0.76$, n = 3 and $r^2 = 0.63$, n = 3, respectively).

During this study, conducted from 2008 to 2010, air temperature was impacted by two major processes: large-scale climatology and atmospheric teleconnection; and regional and local meteorology. Variations of temperature directly impacted photosynthetic uptake of $CO_2$, autorotrophic and heterotrophic respiration and consequently year to year variations in accumulated NEE. The impacts of ENSO on Canada's climate and inter-annual temperature variation have been previously demonstrated, thus significantly impacting temperature and the length of growing season (Zhang et al. 2000b). The NAO and AO also influence Canada's climate and the number of GDDs available for plant growth, particularly in spring across the northeastern region (Fillol 2003). Furthermore, inter-annual changes in snow cover, height and duration in the Northern Hemisphere can be easily correlated to ENSO and NAO/AO (Bamzai 2003). Those processes directly impacted weather conditions, which influenced plant growth and photosynthetic uptake of $CO_2$, and consequently annual accumulated NEE in Kuujjuarapik. In 2010, the length of the growing season was 10 to 35% longer than 2008 and 2009. This finding strongly correlated with a warm episode associated with ENSO (from July 2009 to April 2010) (Figure 4.3b), and a highly negative AO index (December 2009 to February 2010) (Figure 4.3a). Significant warming during this period impacts snowpack in the area of study, promoting early snow-free ground, accelerating soil warming and direct energy and mass exchange between soil, plants and the atmosphere. Snowpack clearly impacts ER during the cold season and may also impact NEE in the following season (Caleigh 2012).

Climate during this period also significantly impacted ice cover on Hudson Bay, which largely influences temperature trend and precipitation regime. The area of concern, which is located on the east side of Hudson Bay in the Eastern Canadian subarctic zone, is mainly affected by two precipitation regimes. In the cold season, when ice cover limits gas exchange and evapotranspiration, the climate of the region is continental. Precipitation was significantly lower between January and April from 2008 to 2010 (about 25 mm/month) than during the warmer months, when Hudson Bay is ice-free. At this time, the maritime influence on climate is significant and precipitation increases to about 70 mm a month (2008 to 2010) with greater sea

evaporation rates and duration, thus promoting precipitation in the area. During 2009–2010 season, the Hudson Bay freeze-up arrived about 10 days later than in previous years (2007–2008 and 2008–2009), and resulted in 5 times less accumulated ice coverage than the historical median (1981–2010), while the previous season was slightly below or above the median (EC 2012).

Based on this three year study, the snow-free period corresponds to 30 to 60% of the year in subarctic ecosystems, leaving a potentially long period with a net emission of $CO_2$. In the cold season, the insulating properties of the snowpack can limit soil cooling resulting in warmer soil under deeper snowpack, and colder soil under shallower snowpack (Lawrence and Slater 2010). In this study, precipitation (including snowfall) correlated positively with $CO_2$ emissions in the dormant period. Monthly mean NEE slightly increased with snowpack ($r^2 = 0.27$, $p = 0.06$, $n = 14$) and resulted in higher emissions of $CO_2$ with deeper snowpacks. Contrary to expectations, during the study period, deeper snowpack was associated with colder soil temperatures. Two possible hypotheses that can explain this include: there may have been substantial cooling of the soil surface before the onset of snow cover and/or the relatively small amount of snow on the ground during winter in this area has little buffering effect on soil temperatures.

In this study, the snow free season was divided in two periods, i.e. growing season and scenescence. During the growing season, no relationship was found between NEE and precipitation ($r^2 = 0.13$, $p = 0.23$, $n = 13$). This confirms that other factors such as temperature and solar radiation, both acting on GEP, were the main drivers controlling NEE during this period. Heavy precipitation events significantly increase soil water content, thus have the potential to promote plant photosynthesis and C uptake in some environments (Parton et al. 2012). This process occurs within a few days of the event, when optimal conditions for plant photosynthesis are reached. In particular, if a rain event occurs after a significant period of soil dryness, it has much greater impact than a rain event occurring when soil moisture is higher and not a limiting factor to plant growth. However, frequent rain events may have a negative effect on plant growth due to associated cloudiness limiting PAR and reducing air temperatures. It is well known that increasing solar radiation greatly enhances photosynthesis and plant activity in terrestrial ecosystems (Caldwell et al. 2007). However, PAR did not greatly change from one

year to another. Therefore the results of this study do not distinguish if this absence of correlation was related to simultaneous decrease of ER and GEP, resulting in non significant variation of NEE. In contrast, during the scenescence season, NEE was significantly related to precipitation trends ($r^2 = 0.60$, $p = 0.01$, $n = 9$) with an increase in NEE with increasing precipitation. During this period, plant metabolism slows, the deciduous leaves are shed and ER is more significant than GEP. Large precipitation events in fall significantly impact soil water content and promote ER although this is difficult to disentangle from the effects of warmer air temperatures that coincide with greater rainfall in the fall months.

### *3.5. Conclusion*

After three years of continuous $CO_2$ exchange measurements over shrub vegetation in forest tundra, a better understanding of the dynamics of $CO_2$ in a transition zone between temperate and Arctic regions is achieved. Warming and increasing the length of the snow-free season may increase the C uptake during summer months, which has a direct impact on the annual accumulated NEE budget. If longer growing seasons are also warmer (with higher GDD), photosynthetic $CO_2$ uptake (GEP) may potentially exceed net $CO_2$ losses (ER) and act as a negative feedback to climate change in forest tundra. However, nutrient availability and soil moisture can play an important role in moderating this response. This study shows that exceptionally wet and cold weather results in a substantial source of $CO_2$ to the atmosphere in forest tundra. Overall, the length of the snow-free season and GDDs controls the interannual NEE variations.

The impacts of year-to-year variability in precipitation are not as clear. Increasing snow precipitation in the cold seasons directly impacts soil temperatures and ER, but also increases soil water content at snowmelt and impacts the length of the growing season. In summer, no direct relationship was found between montly mean NEE and precipitation. However, the wetter and colder year (2009) showed significantly lower $CO_2$ uptake during the growing season than the drier and warmer years (2008 and 2010). Large precipitation events in fall significantly impact soil water content and promote ER although this is difficult to disentangle from the effects of warmer air temperatures that coincide with greater rainfall in the fall months.

Quantifying $CO_2$ exchanges in a changing environment is crucial, given the large influence of temperature and precipitation on the annual NEE balance. This appears to be particularly critical in the transition zone where future trends are difficult to predict.

## *Chapter 5: General trends of $CO_2$ exchange between ecosystems and the atmosphere along a latitudinal gradient from 55° to the 72° north in the Eastern Canadian Arctic*


### *ABSTRACT*

During the International Polar Year, a study in the Eastern Canadian Arctic and subarctic was carried out to improve our knowledge on the spatial and temporal variations in atmospheric carbon exchange. Between 2006 and 2009, summer net ecosystem exchange of $CO_2$ (NEE) was quantified using eddy covariance and Bowen ratio techniques at four sites along a latitudinal gradient spanning 55° to 72° north. Maximum net $CO_2$ uptake at noon during the month of July was significantly higher in forest tundra at Kuujjuarapik, -8.7 ± 0.8 μmol $m^{-2}$ $s^{-1}$ (± SE, average over 3 years), than in tundra ecosystems at Kuujjuarapik, -4.2 ± 2.0 μmol $m^{-2}$ $s^{-1}$ (± SE, average over 2 years), Pond Inlet, -0.9 μmol $m^{-2}$ $s^{-1}$, and Umiujaq, -0.4 μmol $m^{-2}$ $s^{-1}$. This is also directly reflected in the accumulated NEE at each location during the month of July. Uptake of $CO_2$ was greatest in the forest at Kuujjuarapik ranging from -102.4 to -56.3 g $CO_2$-C $m^{-2}$ (between 2007 and 2009), while the nearby tundra NEE varied from -33.4 to -6.2 g $CO_2$-C $m^{-2}$ in 2007 and 2006, respectively. The tundra sites further north, Pond Inlet (2008) and Umiujaq (2009), were a small net sink of $CO_2$, -6.2 and -1.7 g $CO_2$-C $m^{-2}$ respectively. In this study, July NEE and GEP were not directly correlated to latitude nor average July or annual air temperature but instead were strongly correlated to the length of growing season and to soil organic C stocks at each site, as determined from the soil organic carbon database of Canada (SOCDC), which varied from 0.24 to 9.61 kg $m^{-2}$ among these sites. These results suggest that soil organic C stocks may well represent both past and current C sequestration of subarctic and Arctic terrestrial ecosystems.


### *Introduction*

Global warming is occurring worldwide linked primarily to increasing concentrations of greenhouse gases in the atmosphere as a result of the industrial era and recent human activity (AMAP 2010; IPCC 2013). However, the impacts of warming on aquatic and terrestrial ecosystems may vary greatly around the world. With climate warming occurring at nearly twice the rate as elsewhere on the planet, impacts on Arctic and subarctic regions' permafrost, vegetation, hydrology, C cycle, wildlife and local communities are expected and have been

documented (ACIA 2004; Prowse et al. 2006). Warming is expected to have some of the greatest impacts on subarctic and treeline ecosystems along the 0 °C mean annual isotherm (Christensen et al. 2004; Stottlemyer et al. 2001).

Warming trends in the Arctic also vary regionally as function of geomorphology, topography, land-sea relationships and large-scale atmospheric processes (Bliss 2000, Zhang et al. 2000b). Over the last 50 years, significant warming has been measured in the western Canadian Arctic (1.5 to 2.0 °C) while slight cooling (-1.0 to -1.5 °C) has been recorded in eastern regions. This specific regional trend is mainly related to large-scale hemispheric background phenomena, such as ocean and atmospheric circulation, the El Niño Southern Oscillation (ENSO) and the North Atlantic Oscillation (NAO) (Zhang et al. 2000b). In the Eastern Canadian subarctic, more precisely in the taiga shield ecozone or forest tundra (Wiken 1986), there has been a significant temperature increase of close to 2 °C since the 1960s, despite considerable interannual variability (Tremblay and Furgal 2008). In recent years, the mean annual temperature during the 4 year period from 2006 to 2009, -2.6 °C, was 1.4 °C warmer than the 1981-2010 climate normal, -4.0 °C (EC 2013).

One potential consequence of warming is the impact on the C cycle through terrestrial ecosystems. Carbon distribution within the Arctic depends on various factors including glacial history, geomorphology, physiographic characteristics and climate. The geomorphology and past climate has dictated the different physiographic regions and terrestrial ecozones across the Canadian Arctic (NRCan 2013). The delineation and boundaries of each of these regions is also a result of longitudinal and latitudinal temperature variations (Prowse et al. 2009a). This has directly influenced the colonization and development of above ground vegetation, as well as below ground biomass and organic C content and sequestration in the soil. Plant diversity and abundance in the Arctic is low and decreases mainly along a latitudinal gradient from the boreal forest at the southern boundaries to the polar deserts at the highest latitudes (Bliss 2000). Broadly, the soil C content is lowest at high latitudes in the Canadian Arctic and increases at lower latitudes with large C stores in northern peatlands and boreal forests (Tarnocai and Lacelle 1996).

Plant biomass and soil C content largely influence the loss of $CO_2$ from ecosystems defined as ecosystem respiration (ER) (Rodionow et al. 2006). These losses of $CO_2$ are contrasted by the photosynthetic uptake of $CO_2$, which results in the net ecosystem exchange (NEE) of $CO_2$ (Shaver et al. 2007; Euskirchen et al. 2012). Studies in Arctic and subarctic regions suggest a latitudinal gradient in NEE (eg. Lafleur et al. 2012). Seasonal uptake of $CO_2$ (-NEE) measured during the growing season is much larger in the boreal forest, -268 to -156 g C $m^{-2}$ (63° N, 21° E) (Ge et al. 2011) and decreases considerably moving northward to -61 to -32 g C $m^{-2}$ in Low Arctic tundra (65°N & 111°W) (Lafleur and Humphreys 2008), -58 to -51 g C $m^{-2}$ in heath tundra (68°N & 149°W) (Euskirchen et al. 2012) and -40 to -4 g C $m^{-2}$ in High Arctic heath (74°N & 20°W) (Lund et al. 2012). These patterns may reflect the latitudinal gradients in plant abundance, soil C stocks and the sensitivity of photosynthesis and decomposition to temperature (Davidson and Janssens 2006). However, scientific studies on C fluxes in northern regions are limited and dispersed throughout the Arctic along both latitudinal and longitudinal gradients, confounding the interpretation of the influence of latitudinal gradients in soil C content and vegetation on ER and NEE.

The aim of this study was to quantify summer (July) NEE fluxes along a latitudinal gradient spanning 55° to 72° north in the Eastern Canadian Arctic and subarctic and identify factors that influence both temporal and spatial variations in NEE. In the Arctic, NEE in July represents much of the growing season NEE (Lafleur et al. 2012, Humphreys and Lafleur 2011) and is expected to vary considerably through the region given widely varying climate and ecosystem characteristics. We test the hypothesis that the net $CO_2$ uptake in summer will correlate well with soil C content as an indicator of past (and current) productivity. As the first dataset of this kind in this region, it provides a snapshot of the spatial variation in NEE and a baseline from which to interpret the impact of future climate warming in this region.

## *3.7. Materials and methods*

### *3.7.1. Site description*

This study was carried out near Kuujjuarapik, Umiujaq, and Pond Inlet (Figure 5.1). Kuujjuarapik is nestled in sand dunes on the east coast of the Hudson Bay at the mouth of the Great Whale River and a small community (pop. ~1500) in the Nunavik area of Northern Quebec, Canada (55° 17' N and 77° 46' W). The region is characterized by a transition forest between boreal forest and tundra, and is part of the taiga shield or forest tundra ecozone (Bhiry et al. 2011). The geology of the area is Quaternary deposits of glacial tills, marine clays, but mainly littoral sands, topped with a small amount of organic matter while the surrounding area is granite-gneiss rocks of the Precambrian Shield (Arlen-Pouliot and Bhiry 2005). NEE and C exchanges were measured at two different sites at the southern location. The first site (KUF) for NEE measurements is located close to the Centre for Northern Studies (University Laval), on a small plateau to the east of the village and north of the Great Whale River in forest shrub tundra (Figure 5.2). The site is rather flat and homogeneous with a carpet of moss, lichens, forbs, crowberry (*Empetrum nigrum*) and small shrubs (~ 0.75 m), mainly as *Betula glandulosa* and *Alnus crispa*, and to a lesser extent, *Picea mariana*, *Salix* spp., and *Pinus* spp. Soil is loamy sand with a weak apparent F horizon, overlain by a thin organic L horizon. Grab samples (N = 2) of the first upper 10 cm of soil were collected, sorted to remove gravel, roots and vegetation, dried and homogenised for subsequent determination of C and N content by the G.G. Hatch Stable Isotope Laboratory, University of Ottawa and found to contain less than 2% organic C on average (Table 5.2). Soil surface C estimates to 30 cm and to 1 m or to bedrock (< 1 m) from the soil organic carbon database of Canada (SOCDC) (Tarnocai and Lacelle 1996) for this and the other study locations are also given in Table 5.2. The SOCDC map was compiled from an existing soil survey database and high quality LANDSAT imagery, and validated by in-situ soil survey (Tarnocai and Lacelle 1996). The carbon estimates to 30 cm from SOCDC for KUF was 2.2 %. The second site at Kuujjuarapik (KUT) is located close to the shore of Hudson Bay, on a small plain to the west of the village in heath tundra (Figure 5.1). The site is also flat and homogeneous but with a carpet of moss, lichens, graminoids, *Carex* spp., forbs, sea pea (*Lathyrus japonicus)* and crowberry (*Empetrum nigrum)* on top of littoral sand (Figure 5.2). Soil

has a sandy loam to sand texture with a weak FH organic horizon. Grab sample' (N=2) soil C measurements (1.3 %) and the top 30 cm soil C estimate from SOCDC (0.3 %) is lower at KUT than at KUF (Table 5.2). The climate at Kuujjuarapik is subarctic and based on 1971 – 2000 climate normals, the mean annual temperature is -4.4 °C, and the maximum daily average temperature occurs in July and August, 10.6 and 11.4 °C (Table 5.1). The average precipitation is 648.5 mm with about 37 % falling as snow and average precipitation in July is 79.4 mm (EC 2013).

The Umiujaq site (UMT) is located about 150 km north of Kuujjuarapik and a few kilometers below the tree line (Figure 5.1). Umiujaq is a small Inuit community (pop. ~450) located on the east cost of the Hudson Bay and at the northern tip of the Richmond Gulf (Lac Guillaume-Delisle) in the Nunavik area of Northern Québec (56° 33' N and 76° 32'W). The area presents a contact between distinctive geologic structures, the Archean shield and the overlying sedimentary and volcanic Proterozoic sequences (Fortier et al. 2008). The landscape is a mix of bare summits and scarce vegetation in protected areas. NEE measurements were made at the south end of the community, directly on a coastal dune in a very windy area, where organic matter accumulation is limited (Figure 5.2). The soil is only composed of sand without evidence of an upper organic horizon. Consequently, measurements of soil C (collection methods described above for KUF) and the surface C estimates from SOCDC were very low at 0.27 and 0.04 %, respectively (Table 5.2). Vegetation on the sandy dune is mainly graminoids. The climate is subarctic and the mean annual temperature is -5.6 °C (1971-2000), and maximum daily average temperature in August is 9.0 °C (Table 5.1). Mean annual precipitation is about 550 mm and about 36 % falls as snow (EC 2013). The climate is subject to marine influences and the topography of the area and the orientation of the valley cause frequent fog and low cloud conditions (Ricard 1998).


**Figure 5.1** **Study area in the Eastern Canadian subarctic and Arctic and research sites: Kuujjuarapik and Umiujaq (Nunavik, Canada), Pond inlet (Nunavut, Canada) (Google map, 2013).**

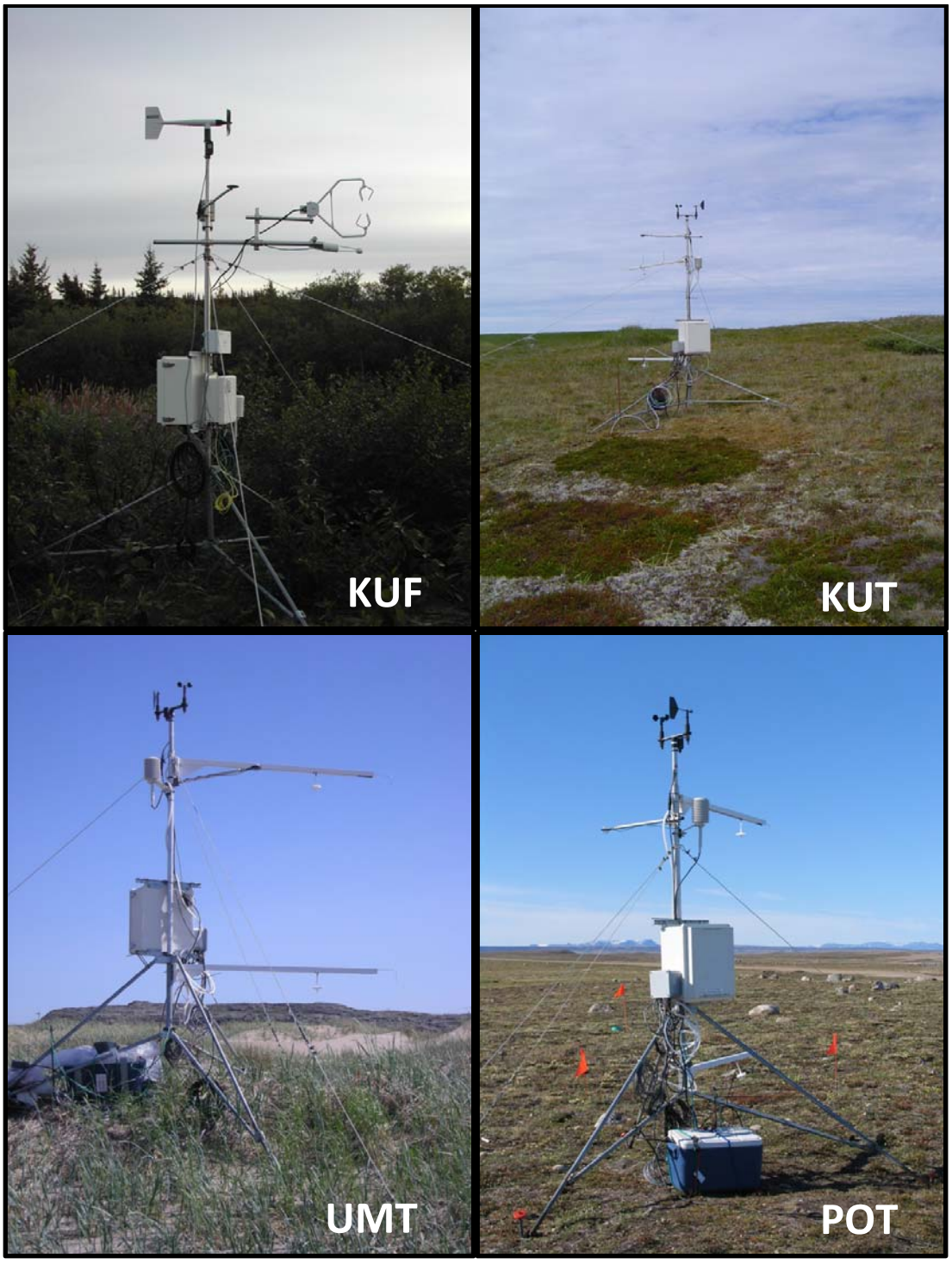


**Figure 5.2** **Flux measurement instrumentation at a) Kuujjuarapik forest tundra (KUF), b) Kuujjuarapik tundra (KUT), c) Umiujaq tundra (UMT), and d) Pond Inlet tundra (POT) in the Eastern Canadian Arctic along a gradient spanning 55° to 72° north.**

**Table 5-1** **Site characteristics, including annual temperature and precipitation trends as well as weather observations during sampling month (July) at Kuujjuarapik, Umiujaq, Pond Inlet along a latitudinal gradient in the Eastern Canada Arctic.**

| *Sites* | *Biome and coordinates* | *ASL (m)* | *Climate normal Period/Year* | *Mean annual temp (°C)* | *Mean July temp (°C)* | *Min July temp (°C)* | *Max July temp (°C)* | *Total annual precip (mm)* | *Total July precip (mm)* |
|---|---|---|---|---|---|---|---|---|---|
| Kuujjuarapik [1] | Subarctic | 21 | 1971-2000* | -4.4 ± 1.4 | 10.6 ± 1.4 | -2.2 | 33.3 | 648.5 | 79.4 |
| | (55°17' N, 77° 46' W) | | 1981-2010 | -4.0 ± 4.5 | 11.1 ± 1.7 | -2.2 | 37.0 | 660.8 | 75.8 |
| | | | 2006 | -1.0 | 11.8 | 2.1 | 28.2 | 596.0 | 73.0 |
| | | | 2007 | -3.6 | 10.4 | 1.8 | 28.3 | 708.8 | 135.2 |
| | | | 2008 | -2.8 | 12.2 | 1.9 | 27.4 | 616.2 | 83.8 |
| | | | 2009 | -2.9 | 14.8 | 1.1 | 29.9 | 717.1 | 71.4 |
| Umiujaq [2] | Low Arctic | 71 | 1971-2000 | -5.6 | -- | -- | -- | -- | -- |
| | (56°33' N, 76° 32' W) | | 2009 | -3.1 | 15.6 | 2.8 | 28.4 | -- | -- |
| Pond Inlet [1] | High Arctic | 55 | 1971-2000 | -15.1 ± 5.1 | 6.0 ± 1.3 | -6.1 | 22.0 | 190.8 | 31.1 |
| | (72°41' N, 77° 59' W) | | 1981-2010 | -14.6 ± 4.9 | 6.6 ± 1.3 | -6.1 | 22.0 | 189.0 | 32.0 |
| | | | 2008 | -13.7 | 7.3 | 0.1 | 18.1 | 223.5 | 70.4 |

*Climate normals based on 1981-2010 records are given where available. Otherwise, only climate normals based on 1971-2000 records are given for Umiujaq. (Sources: [1] Environment Canada, 2013; [2] CEN, 2013a;[3] CEN, 2013b);

**Table 5-2 Surface soil (0-10 cm) characteristics along a latitudinal gradient in the Eastern Canada Arctic, from south to north, Kuujjuarapik, Umiujaq, Pond Inlet.**

| Sites<br>Ecosystems<br>Acronyms | | Kuujjuarapik<br>Tundra<br>KUT | Kuujjuarapik<br>Forest tundra<br>KUF | Umiujaq<br>Tundra<br>UMT | Pond Inlet<br>Tundra<br>POT |
|---|---|---|---|---|---|
| Mineral soil texture | | Sandy loam / Sand | Loamy sand | Sand | Sandy loam |
| pH | (unit) | 5.4 ± 0.5 | 5.4 ± 0.4 | 5.7 ± 0.6 | 6.4 ± 0.5 |
| Total C (to 1 m)* | (kg $m^{-2}$) | 35.80 | 12.98 | 0.53 | 0.63 |
| Surface C (top 30 cm)* | (kg $m^{-2}$) | 4.00 | 9.61 | 0.51 | 0.24 |
| Surface C (top 30 cm)* | (%) | 0.34 | 2.23 | 0.04 | 0.03 |
| C - Soil | (%) | 1.30 ± 0.77 | 1.96 ± 2.27 | 0.27 ± 0.25 | 1.45 |
| N - Soil | (%) | 0.08 ± 0.04 | 0.07 ± 0.08 | 0.09 ± 0.06 | 0.12 |
| C:N - Soil | (ratio) | 16.3 | 28.0 | 3.0 | 12.1 |

*Estimate from the SOCDC. (Tarnocai and Lacelle, 1996); Total C is a measure of the average amount of C within soil landscape polygon. For mineral soils, in most cases, the total carbon content was calculated for a depth of 1 m but for mineral soils with lithic contact (shallow soils over bedrock), it is calculated for the depth to contact and for organic soils the total C content was calculated for the total depth of the peat deposit.

The northernmost site is located in the hamlet of Pond Inlet (POT) at the north end of the Baffin Island facing Eclipse Sound and Bylot Island (Figure 5.1). Pond Inlet is a small Inuit community (pop. ~1500) in Nunavut, Canada (72° 41' N and 77° 59' W). NEE measurements were made on the outskirts of the municipality and close to the Environment Canada weather station (Figure 5.2). The bedrock geology is Precambrian rock, granites and gneiss. Accumulations of glacial debris (moraine) are frequent and present in the area and glacial till rarely exceeds 5 m (Andrews et al. 2002; Ednie and Smith 2010). Soil texture is sandy loam with a thin organic layer and lots of gravel. Sparse vegetation cover and low soil moisture in semi-desert tundra are not favorable for organic matter accumulation and decomposition. Consequently, measurements of soil C (collection methods described above for KUF) and the surface C estimates from SOCDC were very low, respectively 0.24 and 0.03 % (Table 5.2), with a mix of fine gravel and organic soils (mainly F horizon). Continuous permafrost is present in the area with an active layer of about 80 cm. The vegetation consists mainly of lichens, moss, evergreen shrubs, *Dryas* spp. and *Cassiope* spp., deciduous shrubs, *Salix* spp., graminoids, *Carex* spp. and *Luzula* spp, herbs and small vegetation leguminous such as *Oxytropis* spp. were found in this semi-desert tundra plateau. The mean annual temperature is -15.1 °C (1971-2000), and the maximum daily average temperature occurs in July and August, 6.0 and 4.2 °C, respectively (Table 5.1). The average precipitation is 190.8 mm with about 75 % falling as snow, and average precipitation in July is 30.5 mm.

### *3.7.2. Instruments and measurements*

July NEE was either measured by the eddy covariance (EC) technique (KUF, 2008 and 2009) or the Bowen ratio flux gradient technique (KUT, 2006 & 2007; KUF, 2007; POT, 2008; UMT, 2009). The EC micrometeorological tower consisted of a 3D sonic anemometer-thermometer (CSAT3, Campbell Scientific Inc (CSI), Logan, Utah, USA) and $CO_2$/$H_2O$ open-path infrared gas analyzer (IRGA) (LI-7500, LI-COR Ltd. (LI-COR), Lincoln, Nebraska, USA) installed 2 m above the surface. The signals were recorded on a data logger (CR23X, CSI, Logan, Utah, USA) at a scan rate of 0.1 s and stored as 5 min averages for flux measurements. The Bowen ratio micrometeorological tower consisted of a two-level intake device (CSI) for the measurement of temperature (fine wire thermocouple, type E), and $H_2O$ and $CO_2$ above the surface (0.5 and 2.0

m) with a closed-path IRGA (LI-6262, LI-COR, Lincoln, Nebraska, USA). The Bowen ratio (ratio of sensible to latent heat fluxes) was estimated from those measurements and used to derive the flux of $CO_2$, assuming similarity of eddy diffusivities for heat and $CO_2$ (Lafleur et al. 2012). The signals were recorded on a data logger (CR23X, CSI, Logan, Utah, USA) at a scan rate of 0.1 s and stored as 20 min averages for flux measurements. Average temperature and humidity (HMP45C212, Vaisala Ltd., Vantaa, Finland), wind speed (5106-10, RM Young Ltd., Traverse City, Michigan, USA), net radiation (NR Lite, Kipp & Zonen Ltd., Delft, Netherlands) and atmospheric pressure (PTB10B, Vaisala Ltd., Vantaa, Finland) were measured with the fluxes at each location. Photosynthetically active radiation (PAR) (LI-190, LI-COR, Lincoln, Nebraska, USA) was measured on-site at a permanent weather station (CEN) and was available from the CEN database (Nordicana D). Soil measurements included soil heat flux (HFT3, CSI, Logan, Utah, USA), soil temperature integrated between 0 and 5 cm (TCAV, CSI, Logan, Utah, USA) and volumetric water content (CS616, CSI, Logan, Utah, USA) at each of the flux towers. The signals were recorded on the data logger at a scan rate of 5 s and stored as 5 min averages. More installation and sensor details are given in the Open Path Eddy Covariance System Operation Manual (Campbell Scientific 2006) and Bowen Ratio Operation Manual (Campbell Scientific 1998). Precipitation records were from the nearest Environment Canada weather station.

### *3.7.3. Quality checking, data correction and gap filling*

The data sets were quality checked with a number of criteria. For the eddy covariance data at KUF, 5 min fluxes were first averaged for 30 min intervals. Half hours where the standard deviation of the six 5 min fluxes exceeded 5 during summer months were discarded. Measurements from the sector 220° to 310° were removed to ensure that only the surface of interest was represented and flux measurements were not affected by the turbulence related to the tower structure (300°). Any non-growing season $CO_2$ emissions larger than 9 μmol $m^{-2}$ $s^{-1}$ were also removed being deemed unreasonably large. During the nighttime (PAR < 20 μmol $m^{-2}$ $s^{-1}$) and during cold periods (as defined as the period when the 3-day running mean of air temperature < 0 °C), fluxes were filtered for calm conditions using a friction velocity threshold of 0.1 m $s^{-1}$. Fluxes were also removed during the nighttime and cold season when $CO_2$ uptake

was greater than 0.5 μmol $m^{-2}$ $s^{-1}$, as any $CO_2$ uptake larger than this estimate of random error was considered erroneous. For Bowen ratio flux measurements at KUF, KUT, UMT and POT, 20 min fluxes were first averaged to 1 hour intervals. Signal errors and $CO_2$ measurements from the dead sector were removed to ensure that only the surface of interest was represented and flux measurements were not affected by the turbulence related to the tower structure. Flux measurements were then classified into day-time and night-time periods (PAR < 20 μmol $m^{-2}$ $s^{-1}$) and outliers were excluded when they exceeded 3 standard deviations of the monthly mean value. Flux data were also removed during night-time when NEE < -0.25 μmol $m^2$ $s^{-1}$ (indicating unrealistic uptake of $CO_2$ in the dark).

In addition to these criteria, data loss resulted from problems related to instrument failure, calibration and maintenance in a remote area were removed. Gaps in the weather data were directly filled when possible using duplicate sensors. If not available, readings collected at nearby weather stations were used to develop linear relationships with the main weather variables such that gaps were filled with these adjusted secondary readings, to ensure continuity and similarity of measurements. Short gaps in NEE of 1 hour were directly filled by linear interpolation. Longer gaps were filled by non-linear regressions between NEE measurements and environmental variables (Barr et al. 2004; Moffat et al. 2007). Nighttime NEE represents ecosystem respiration (ER) and an exponential relationship with 5 cm soil temperature was developed for the month of July to determine $Q_{10}$, the rate of increase in ER with a 10 degree increase in temperature, and $R_{10}$, ER at a reference soil temperature of 10 °C ($T_{ref}$) (see second term of Eqn (1) below). Gross ecosystem production (GEP) was then derived from the difference of daytime NEE and modeled ER. A rectangular hyperbolic relationship with photosynthetic active radiation (*PAR*) was derived for all available GEP to determine the maximum photosynthetic uptake ($A_{max}$) and the effective quantum yield ($\alpha$) as shown as the first term in Eqn (1):

$$NEE = -\frac{\alpha \times PAR \times A\max}{\alpha \times PAR + A\max} + R_{10} \times Q_{10}^{(T-T_{ref})/10} \quad (1)$$

Gaps in nighttime NEE were filled using Eqn (1) (with PAR = 0) and daytime NEE were gap-filled using Eqn (1). Table 5.3 summarizes period of measurement, measurement techniques and model parameters for all sites. Negative NEE and GEP indicate uptake of $CO_2$ by the surface while positive fluxes indicate C losses to the atmosphere.

**Table 5-3 NEE measurement period and model parameters ($R_{10}$ and $Q_{10}$) used for gap filling.**

| Sites and Years | Period | Measurement technique | $R_{10}$ | $Q_{10}$ | N 1 hour* average |
|---|---|---|---|---|---|
| **KUT 2006** | July 8-30 | Bowen ratio | 3.21 | 1.75 | 268 |
| **KUT 2007** | July17-31 | Bowen ratio | 2.76 | 1.64 | 328 |
| **UMT 2009** | July 6-22 | Bowen ratio | 1.70 | 1.76 | 355 |
| **POT 2008** | July 1-20 | Bowen ratio | 1.97 | 1.32 | 452 |
| **KUF 2007** | July 16-31 | Bowen ratio | 1.35 | 1.31 | 351 |
| **KUF 2008** | July 1-31 | Eddy Covariance | 1.75 | 2.42 | 344 |
| **KUF 2009** | July 1-31 | Eddy Covariance | 1.64 | 1.99 | 178 |

*Bowen ratio fluxes computed on 20 min interval while eddy covariance derived fluxes computed on 30 min interval.

### *3.7.4. Quality control and statistical analysis*

All the meteorological sensors were previously calibrated with certified standards and methods to ensure high accuracy of measurements. The Bowen ratio flux gradient system and the EC $CO_2/H_2O$ open path analyzers were initially calibrated in the Environment Canada laboratory facilities in Montreal with certified $CO_2$ standard (NIST & NOAA) and a dew point generator (LI-610, LI-COR, Lincoln, Nebraska, USA ). On-site tower inspections were made for the open path EC system approximately every 6 months, while chemicals were replaced and the IRGA was calibrated approximately every 12 months. Zero drifts were low, about 0.1 %, and calibration drift was about 2.5 % annually. All measurements were rigorously submitted to a strong QA/QC protocol. Data handling was carried out in Microsoft office, Excel 2007, and all

quality checking, gap fillings, and statistical analyses were computed using SAS version 9.2 for windows (SAS Institute Inc., Cary, North Carolina, USA) and Systat (Systat Software Inc., San Jose, California, USA).

## *3.8. Results*

### *3.8.1. Weather*

Long-term (1981-2010) mean annual temperatures along the latitudinal gradient spanning 55° to the 72° north (Figure 5.1) ranged from -4.0 to -14.6 °C, from Kuujjuarapik to Pond Inlet, (EC 2013) (Table 5.1). During the 5 year study period, the mean annual temperature at Kuujjuarapik varied from -3.6 °C (2007) to -1.0 °C (2006) with temperatures varying from cooler than normal to warmer than normal (Table 5.1). Mean air temperature of -2.6 °C for this 4 year period was about 1.5 degrees warmer than the recent 30-year climate normal. Long-term (1981-2010) mean July temperature ranged from 6.6 °C to 11.1 °C for the Arctic to subarctic sites. During the study period, July temperatures at Kuujjuarapik varied from 10.4 °C (2007) to 14.8 °C (2009) (Table 5.1). Mean July temperature of 12.3 °C for this 4 year period was slightly warmer than the recent 30-year climate normal, 11.1 °C. Compared to Kuujjuarapik, mean annual temperature (1971-2000) at Umiujaq, about 150 km north east of Kuujjuarapik, is about 1 degree colder. In July 2009, average air temperature at Umiujaq was about 1 degree warmer than Kuujjuarapik (Table 5.1).

Precipitation decreases as latitude increases in this region (Logan et al. 2011). Long-term (1981-2010) climate normals were only available for Kuujjuarapik and Pond Inlet where mean annual precipitation was about 3.5 times larger in Kuujjuarapik (Table 5.1). This was also reflected in long-term mean July precipitation at the two sites with 75.8 and 32.0 mm, respectively. During the study period, precipitation at Kuujjuarapik was similar to the long-term normal except in 2007 with nearly 2 times the July rainfall. July rainfall at Pond inlet in 2008 was more than twice the normal. Umiujaq, located 150 km north of Kuujjuarapik, receives slightly more precipitation than Kuujjuarapik because of the marine influence and the topography of the region (Ménard et al. 1998). A large part of the evaporated moisture from Hudson Bay remains confined to

Umiujaq and in the valley because the surrounding hills limit wind dispersion and trap air moisture.

### *3.8.2. Soil carbon content*

Soil organic C content along the Eastern Canadian Arctic and subarctic varies greatly. According to the SOCDC, the soil C content throughout this region ranges from 0 to 357 kg $m^{-2}$ (total C, top 100 cm of soil profile or to bedrock) and 0 to 30 kg $m^{-2}$ (surface C, top 30 cm of soil profile) (Tarnocai and Lacelle 1996). In this study, soil C to 30 cm was greatest at the subarctic sites with as much as 9.61 kg $m^{-2}$ at KUF and least at the Arctic POT site with 0.24 kg $m^{-2}$. In-situ measurements of organic C from the 0 – 10 cm layer were significantly correlated to the top 30 cm estimates from the SOCDC ($r^2 = 0.51$, $p < 0.05$) (Table 5.2).

### *3.8.3. Net ecosystem exchange*

Daily NEE had large day-to-day and site-to-site variability throughout the month of July ranging from large daily $CO_2$ uptake of -7.1 g C $m^{-2}$ $day^{-1}$ (KUF 2008) to moderate $CO_2$ losses of 3.1 g C $m^{-2}$ $day^{-1}$ (KUT 2007) (Figure 5.3). Daily variability in NEE was greatest at KUF with the average difference in maximum and minimum daily NEE at 7.0 ± 0.8 g C $m^{-2}$ $day^{-1}$ (for 2007 through 2009). This difference was only 1.3 (POT), 4.2 (UMT), and 5.4 ± 1.8 g C $m^{-2}$ $day^{-1}$ (KUT) at the tundra sites. Non–parametric Spearman's correlation was used to compare daily NEE with weather variables (Table 5.5). Daily variations in NEE at KUF were consistently correlated with daily PAR over the three study seasons (2007 to 2009). Other variables that were significantly correlated with daily NEE include daily precipitation (2008 & 2009), air temperature (2007 & 2008), and VWC (2007) (Table 5.4). For the tundra sites (KUT, UMT, and POT), air temperature consistently correlated with daily NEE, while daily soil temperature, VWC, precipitation and PAR were also significant in some years at some sites (Table 5.5).

Average diel trends of gap-filled NEE in July show maximum uptake of $CO_2$ around noon, ranging from -0.5 (UMT 2009) to -10.4 μmol $m^{-2}$ $s^{-1}$ (KUF 2008) and show strong spatial variability (Figure 5.4a). Diel patterns illustrate stronger uptake of $CO_2$ in forest tundra (KUF) than in tundra sites (KUT, UMT and POT). In 2007, simultaneous NEE measurements at

neighboring sites (KUF and KUT) with similar weather conditions clearly show a stronger uptake of $CO_2$ in forest tundra than tundra. Average total July NEE increased (ie. decreasing net $CO_2$ uptake) with increasing latitude and vegetation changes, -79.9 ± 13.3 (KUF, 3 years), -21.5 ± 21.6 (KUT, 2 years), -6.2 (POT, 1 year) and -1.7 g C $m^{-2}$ (UMT, 1 year) (Figure 5.6, Table 5.6).

Average diel patterns in July GEP show the same trend as NEE, but with a better spatial definition between sites, more specifically in tundra. July GEP in tundra sites clearly increase (decreasing photosynthetic uptake of $CO_2$) with latitude from KUT, UMT to POT. Total July GEP was -188.8 ± 10.0 (KUF), -150.9 ± 2.9 (KUT), -80.7 (UMT) and -72.7 g C $m^{-2}$ (POT) (Table 5.6). These differences in GEP did not reflect differences in incoming PAR (Figure 5.5a) and instead are expected to reflect the differences in photosynthetic capacity among sites.

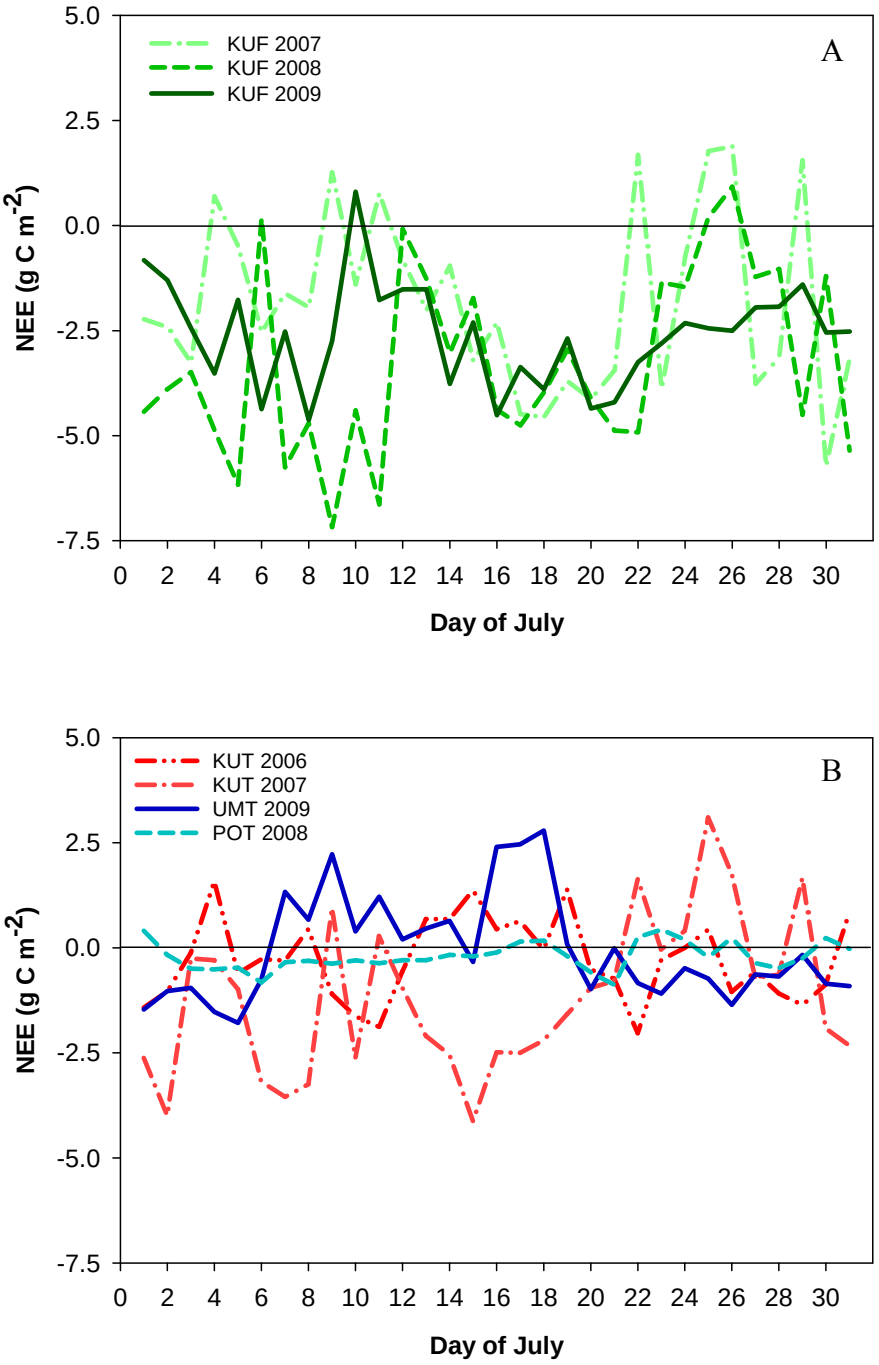


**Figure 5.3** **Gap-filled daily mean of July NEE at Kuujjuarapik forest tundra (KUF), Kuujjuarapik tundra (KUT), Umiujaq tundra (UMT) and Pond Inlet tundra (POT) ecosystems. Averages include only 1 season of data at UMT and POT, 2 seasons at KUT, and 3 seasons at KUF. Note the difference in the axis limits for the KUF site (top panel - A) and tundra sites (bottom panel - B).**

**Table 5-4** **Spearman correlation of daily net ecosystem exchange of $CO_2$ (NEE) with weather and microclimate factors: air and soil temperature, volumetric water content - VWC, precipitation and photosynthetically active radiation - PAR at Kuujjuarapik forest tundra (KUF) during 3 seasons.**

| Sites | | Air T | Soil T | VWC | Precipitation | PAR |
|---|---|---|---|---|---|---|
| **KUF 2007** | **NEE** | ***0.58 [<0.001]*** | 0.29 [0.11] | ***-0.57 [0.02]*** | 0.32 [0.08] | ***-0.42 [0.02]*** |
| | **Air T** | | ***0.85 [<0.001]*** | ***-0.72 [<0.01]*** | -0.03 [0.88] | -0.01 [0.98] |
| | **Soil T** | | | ***-0.66 [<0.01]*** | ***-0.39 [0.03]*** | 0.35 [0.06] |
| | **VWC** | | | | -0.13 [0.62] | 0.34 [0.20] |
| | **Precipitation** | | | | | ***-0.80 [<0.001]*** |
| **KUF 2008** | **NEE** | ***0.53 [<0.01]*** | ***0.39 [<0.05]*** | 0.05 [0.78] | ***0.67 [<0.001]*** | ***-0.52 [<0.01]*** |
| | **Air T** | | ***0.94 [<0.001]*** | -0.12 [0.53] | 0.12 [0.53] | 0.08 [0.68] |
| | **Soil T** | | | -0.30 [0.10] | -0.11 [0.56] | 0.25 [0.17] |
| | **VWC** | | | | ***0.42 [0.02]*** | -0.24 [0.19] |
| | **Precipitation** | | | | | ***-0.80 [<0.001]*** |
| **KUF 2009** | **NEE** | 0.05 [0.77] | -0.09 [0.64] | 0.29 [0.11] | ***0.59 [<0.001]*** | ***-0.47 [<0.001]*** |
| | **Air T** | | ***0.95 [<0.001]*** | ***-0.71 [<0.001]*** | -0.20 [0.29] | 0.29 [0.11] |
| | **Soil T** | | | ***-0.78 [<0.001]*** | -0.22 [0.24] | 0.33 [0.07] |
| | **VWC** | | | | ***0.50 [<0.05]*** | ***-0.70 [<0.01]*** |
| | **Precipitation** | | | | | ***-0.64 [<0.001]*** |

**Table 5-5** **Spearman correlation of daily net ecosystem exchange of $CO_2$ (NEE) with weather and microclimate factors: air and soil temperature, volumetric water content – VWC, precipitation and photosynthetically active radiation - PAR at 3 sites: Kuujjuarapik tundra (KUT), Umiujaq tundra (UMT) and Pond Inlet tundra (POT) ecosystems. Correlations include 2 seasons of data at KUT and only 1 season at UMT and POT.**

| Sites | | Air T | Soil T | VWC | Precipitation | PAR |
|---|---|---|---|---|---|---|
| **KUT 2006** | **NEE** | ***0.56 [<0.001]*** | 0.17 [0.35] | ***0.45 [0.03]*** | 0.18 [0.33] | -0.25 [0.18] |
| | **Air T** | | 0.26 [0.16] | 0.29 [0.18] | 0.09 [0.65] | 0.02 [0.93] |
| | **Soil T** | | | 0.09 [0.69] | -0.25 [0.18] | 0.35 [0.06] |
| | **VWC** | | | | 0.23 [0.29] | -0.16 [0.46] |
| | **Precipitation** | | | | | ***-0.60 [<0.001]*** |
| **KUT 2007** | **NEE** | ***0.72 [<0.001]*** | ***0.59 [<0.001]*** | -0.10 [0.71] | 0.19 [0.30] | -0.29 [0.12] |
| | **Air T** | | ***0.81 [<0.001]*** | -0.21 [0.45] | -0.01 [0.97] | -0.01 [0.95] |
| | **Soil T** | | | -0.16 [0.56] | ***-0.39 [0.03]*** | ***0.36 [0.05]*** |
| | **VWC** | | | | ***0.57 [0.03]*** | -0.39 [0.14] |
| | **Precipitation** | | | | | ***-0.80 [<0.001]*** |
| **UMT 2009** | **NEE** | ***0.82 [<0.001]*** | ***0.78 [<0.001]*** | ***-0.59 [<0.01]*** | - | -0.06 [0.73] |
| | **Air T** | | ***0.93 [<0.001]*** | ***-0.68 [<0.001]*** | - | 0.13 [0.49] |
| | **Soil T** | | | **-0.65** ***[<0.001]*** | - | 0.22 [0.23] |
| | **VWC** | | | | - | 0.15 [0.45] |
| | **Precipitation** | | | | | - |
| **POT 2008** | **NEE** | ***0.47 [<0.01]*** | 0.11 [0.57] | -0.23 [0.35] | ***0.66 [<0.001]*** | ***-0.59 [<0.001]*** |
| | **Air T** | | ***0.64 [<0.001]*** | -0.44 [0.06] | 0.28 [0.12] | -0.17 [0.36] |
| | **Soil T** | | | ***-0.89 [<0.001]*** | 0.02 [0.92] | 0.13 [0.48] |
| | **VWC** | | | | 0.07 [0.78] | -0.21 [0.39] |
| | **Precipitation** | | | | | ***-0.83 [<0.001]*** |

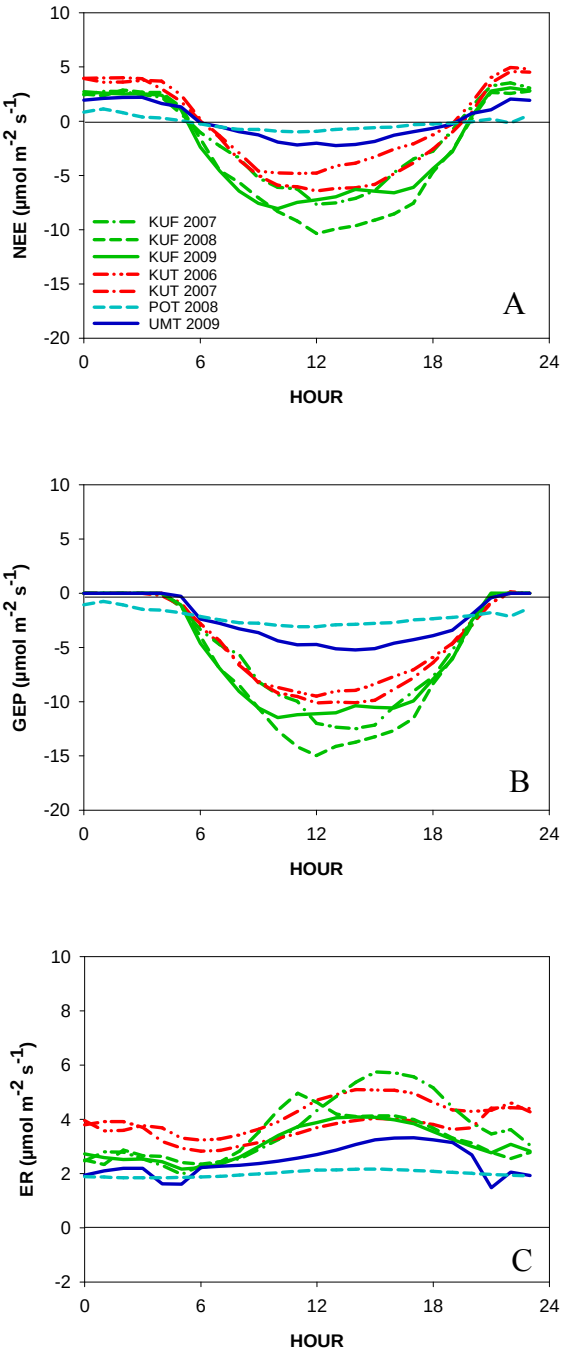


**Figure 5.4** **Average diel trends in July of gap-filled (A) net ecosystem exchange - NEE, (B) gross ecosystem production – GEP, and (C) ecosystem respiration – ER at Kuujjuarapik forest tundra (KUF), Kuujjuarapik tundra (KUT), Umiujaq tundra (UMT) and Pond Inlet tundra (POT) ecosystems. Averages include 1 season of data at UMT and POT, 2 seasons at KUT, and 3 seasons at KUF.**

**Table 5-6** **Summary table of total NEE, GEP, ER, average air and soil temperature, total PAR and total rainfall in July and the length of the growing season at 4 sites: Kuujjuarapik forest tundra (KUF), Kuujjuarapik tundra (KUT), Umiujaq tundra (UMT) and Pond Inlet tundra (POT) ecosystems. Results are based on only 1 season of data at UMT and POT, 2 seasons at KUT, and 3 seasons at KUF.**

| Sites | Cumulative NEE ($g\ C\ m^{-2}$) | Cumulative GEP ($g\ C\ m^{-2}$) | Cumulative ER ($g\ C\ m^{-2}$) | Average T air (°C) | Average T soil (°C) | Total PAR ($mmol\ m^{-2}$) | Rainfall (mm) | Length of growing season (days) |
|---|---|---|---|---|---|---|---|---|
| **KUT 2006** | -6.2 | -142.8 | 134.1 | 11.8 | 13.3 | 125.1 | 73 | 172 |
| **KUT 2007** | -33.4 | -151.3 | 117.9 | 10.6 | 13.4 | 83.7 | 135.2 | 175 |
| **UMT 2009** | -1.7 | -80.7 | 79.0 | 14.8 | 17.5 | 103.8 | - | 143 |
| **POT 2008** | -6.0 | -70.2 | 64.2 | 7.3 | 10.2 | 106.4 | 70.4 | 106 |
| **KUF 2007** | -56.3 | -176.9 | 121.3 | 10.5 | 13.8 | 83.7 | 135.2 | 175 |
| **KUF 2008** | -102.4 | -208.7 | 106.3 | 12.4 | 15.7 | 103.2 | 83.8 | 199 |
| **KUF 2009** | -80.9 | -181.0 | 100.1 | 15.3 | 17.8 | 103.8 | 75.8 | 143 |

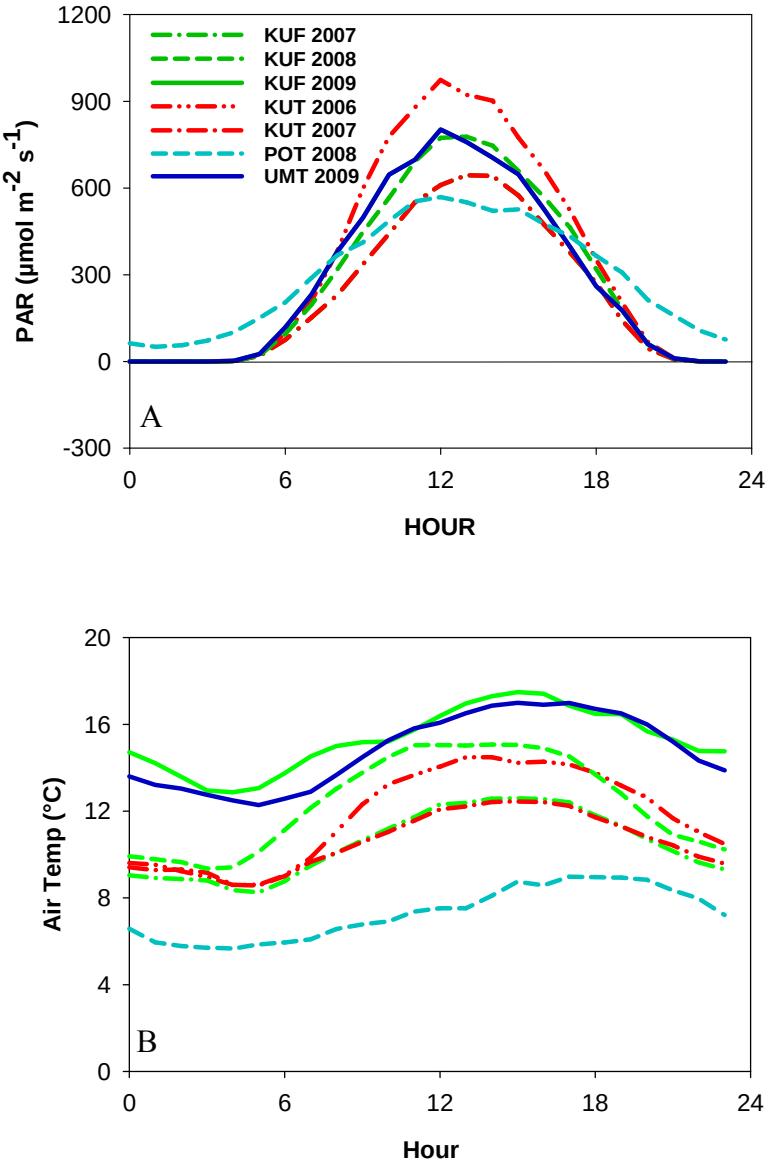


**Figure 5.5** **July hourly average trends in July of (A) photosynthetically active radiation - PAR and (B) air temperature at Kuujjuarapik forest tundra (KUF), Kuujjuarapik tundra (KUT), Umiujaq tundra (UMT) and Pond Inlet tundra (POT) ecosystems. Averages include only 1 season of data at UMT and POT, 2 seasons at KUT, and 3 seasons at KUF.**

At night (21 h – 4 h), the exchange of $CO_2$ does not reflect a latitudinal gradient. Greatest mean $CO_2$ emissions were from KUT 2006 & 2007 (4.0 & 3.9 μmol $m^{-2}$ $s^{-1}$), followed by KUF 2007, 2009, and 2008 (2.9, 2.7 & 2.6 μmol $m^{-2}$ $s^{-1}$), POT (2.0 μmol $m^{-2}$ $s^{-1}$), and lastly UMT 2009 (1.9 μmol $m^{-2}$ $s^{-1}$) (Figures 5.4a & 5.4c). Greatest $CO_2$ emissions occurred in the afternoon approximately when air temperature peaked (Figure 5.5b) as expected given the estimation of daytime ER using an exponential relationship with temperature. Mid-afternoon ER was lowest at KUF (2007) and POT and largest at KUF in 2010 (Figure 5.5b). Total July ER was significantly correlated to average July air and soil temperature (Table 5.6) with decreasing total ER as latitude (and temperature) decreases: 128.0 ± 11.0 (KUT), 109.3 ± 6.3 (KUF), 79.0 (UMT) and 66.5 g C $m^{-2}$ (POT) (Table 5.6).

Variations in mean July NEE, GEP, and ER were not well explained by variations in latitude ($r^2$ from 0.2 to 0.5). Instead, variations in surface soil organic C (top 30 cm SOCDC) explained 96 %, 95 %, and 48 % of the variability between sites in mean July NEE, GEP, and ER, respectively (Figure 5.6). While, in situ measurement of soil organic C (top 10 cm) explained 56 %, 44 % and 13 % of the variability between sites in monthly mean NEE, GEP and ER. No significant trends were found between total organic C to 1 m from the SOCDC and NEE ($r^2 = 0.05$), and GEP ($r^2 = 0.37$) but with ER ($r^2 = 0.83$). Regional weather variables such as annual or July temperature and total annual precipitation or total July precipitation did not have significant relationships with the mean July $CO_2$ exchange values from these four sites. However, the average length of snow-free season explained 85 % and 83 % of the spatial variability in average July ER and GEP, and 50 % of the variability in NEE (Table 5.6).

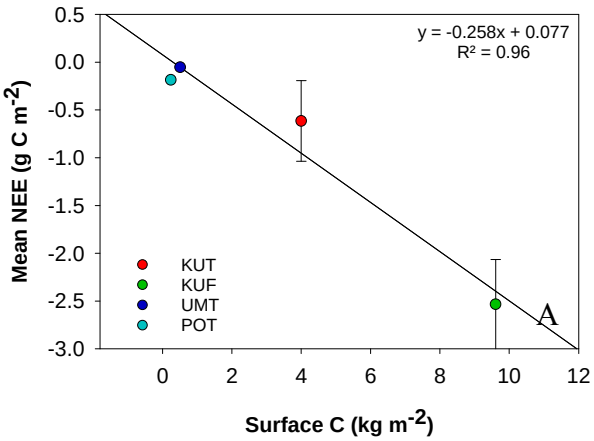


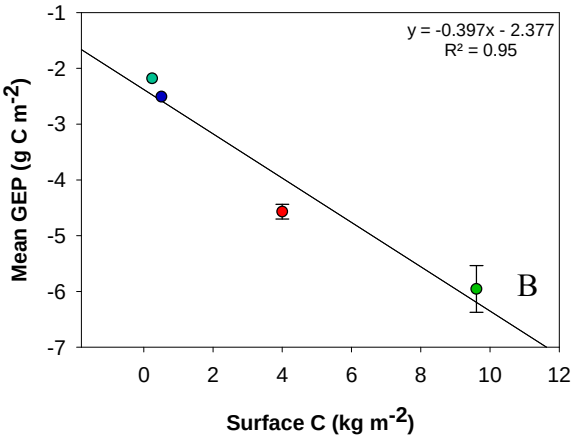


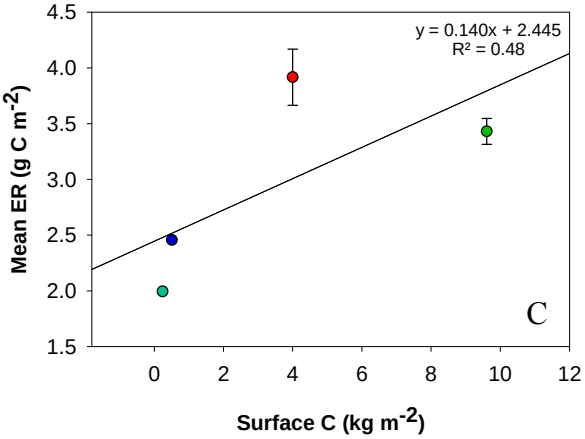


**Figure 5.6** **The relationship between average daily July NEE (A), GEP (B), and ER (C) and 0-30 cm soil organic carbon content from the SOCDC (Tarnocai and Lacelle, 1996) in the Eastern Canadian subarctic and Arctic.**

For the two sites with multiple years of flux measurements (KUF and KUT), year to year variability in diel trends for NEE was greatest at KUF. Peak daytime net $CO_2$ uptake rates ranged from -19.3 (2007) to -16.9 μmol $m^{-2}$ $s^{-1}$ (2009) at KUF (Figure 5.4a). Greatest net July $CO_2$ uptake was in 2008 due to relatively low ER and relatively high photosynthesis (Table 5.6). 2007 saw the lowest net July $CO_2$ uptake due to the relatively high ER and low photosynthesis (Table 5.6). This was the coldest and rainiest July (low cumulative PAR) of the three years. July GEP explained a greater proportion of the variation in NEE (95 %) than did ER (48 %). Mean annual temperature, total annual precipitation, July rain, and the length of the growing season explained 47%, 96%, 19%, and 56% of the year-to-year July GEP variability at KUF, with greater photosynthesis in July during warmer years with longer growing seasons and less precipitation (Table 5.1 & Table 5.6). Similarly, mean annual temperature, total annual precipitation, July rain and the length of the growing season explained 87%, 65%,62% and 20 %, respectively of the year-to-year variability in total July NEE at KUF, with greater net $CO_2$ uptake in July during years with less annual rainfall and longer growing seasons. For July ER at KUF, mean annual temperature, July precipitation and the length of the growing season explained 84%, 99%, and 13% of year-to-year variability with greater $CO_2$ release in warmer and drier conditions. With only two years of measurements at KUT, there were insufficient data to confirm trends although net uptake of $CO_2$ was greatest in the year with cloudier, cooler and rainier conditions (2007) due to lower ER while GEP was similar in 2006 and 2007 (Table 5.6).

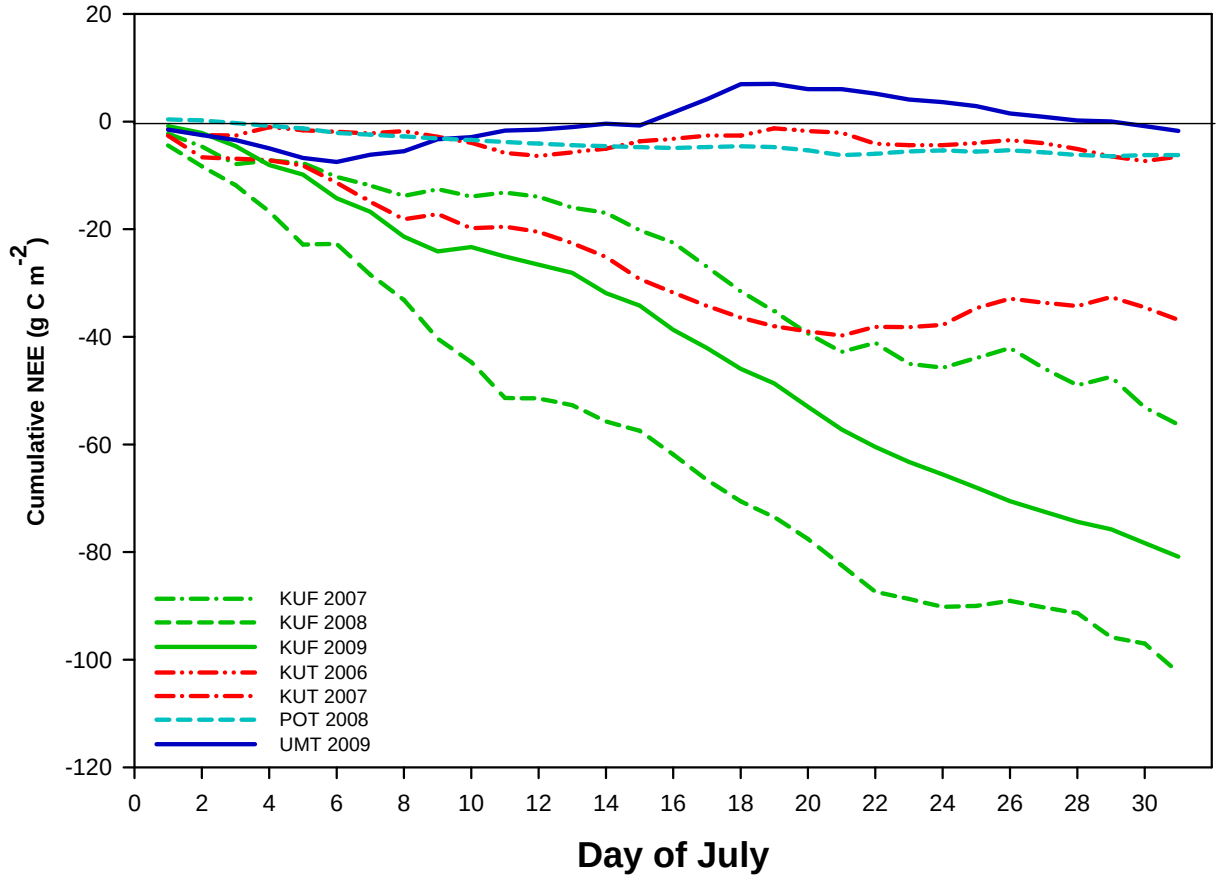


**Figure 5.7** **Cumulative July NEE at Kuujjuarapik forest tundra (KUF), Kuujjuarapik tundra (KUT), Umiujaq tundra (UMT) and Pond Inlet tundra (POT) ecosystems. Averages include only 1 season of data at UMT and POT, 2 seasons at KUT, and 4 seasons at KUF.**

## *3.9. Discussion*

### *5.4.1 Daily NEE and weather conditions*

Over a period of 4 consecutive years, 2006 to 2009, NEE was measured in July at four sites from forest tundra to polar semi-desert along a latitudinal gradient spanning 55° to 72° north in order to examine the spatial and temporal variability in peak summer $CO_2$ exchange.

Over forest tundra, the major environmental factors controlling variability in daily NEE in July were PAR (2007 to 2009), followed by air temperature (2007 & 2008), precipitation (2008 & 2009), WVC (2007 & 2009), and soil temperature (2009) (Table 5.4). In contrast, daily variations in NEE at the tundra sites were much lower and the major factors controlling those fluctuations in July were air temperature (KUT 2006 & 2007, UMT 2009 & POT 2008), followed by soil temperature (KUT 2007 & UMT 2009), VWC (KUT 2006 & UMT 2009), precipitation and PAR (POT 2008) (Table 5.5). These differences may have related to the relative importance of GEP vs. ER in controlling daily variations in NEE. For example, although not strictly independent of each other, daily NEE correlated significantly (data not shown) with GEP at KUF 2008-2009 and at POT 2008, two sites where PAR was an important driver. In the warmer year, KUT 2006 GEP was correlated with NEE but not in the cooler wetter year when neither daily GEP nor ER significantly correlated with NEE. In contrast, ER significantly correlated with NEE at UMT 2009 explaining the importance of soil and air temperature on respiration processes on NEE at this site. Others have also highlighted the relative importance of GEP (Welker et al. 2004; Steltzer et al. 2008; Lara et al. 2012; Welp et al. 2007) and ER (Law et al. 2002; Henry et al. 2012) on NEE where GEP dominates in ecosystems with more vegetation and higher LAI such as dwarf-shrub herb tundra (Steltzer et al. 2008; Lara et al. 2012) and deciduous broadleaf and evergreen conifer forest (Welp et al. 2007), while ER dominates in drier ecosystems such as dry tundra (Lara et al. 2012) and herbaceous tundra (Henry et al. 2012). For KUF, where GEP drives variations in NEE, it was expected that PAR would play a key role as it is well known to control plant photosynthetic activity through the day and is often explored using light response curves (Lafleur et al. 2012). The strong correlation between daily variations in NEE with precipitation in 2008 and 2009 were likely an indirect impact of cloudy days reducing

PAR and photosynthetic uptake of $CO_2$ as was also seen in a mixed deciduous forest (Oliphant et al. 2011).

Although no quantitative measurements of vegetation abundance or leaf area index (LAI) were done in this study, the tundra sites had clearly less leaf area and vegetation cover than the forest tundra at KUF (Figure 5.2). At the forest tundra site, temperature was significantly correlated to NEE in only two of the three years, the coldest two summers (July 2007 and 2008, with mean temperature of 10.5 and 12.4 °C, respectively). Despite the well-known temperature dependence of ER (Davidson and Janssens 2006), it was not significantly correlated to NEE in 2007 at KUF. Instead the temperature dependence may have manifested most strongly in GEP as a result of these cooler temperatures limiting photosynthesis relative to other years with mean July temperature all above 12 °C. GEP has also been observed to be sensitive to temperature in a broadleaf forest and an open spruce forest in boreal ecosystems (Alaska, USA) (Ueyama et al. 2013).

With less vegetation biomass, GEP was not the main driver of day-to-day variations in NEE at three of four tundra sites and in fact, there was typically less net uptake of $CO_2$ during warmer vs. cooler days. The suggestion here is that ER is equally or more important in the $CO_2$ balance on a daily basis. This is in keeping with Oberbauer et al. (2007) who suggested that respiration generally determined the $CO_2$ balance in dry heath Arctic tundra. Despite the significant correlation between NEE and GEP at POT where PAR was a significant driver of daily variations, net $CO_2$ uptake significantly decreased with increasing temperature as did all the other tundra sites in this study (Table 5.5). Lafleur et al. (2012) also found less daily net $CO_2$ uptake with warmer days in Low Arctic low shrub / tussock, sedge-dwarf shrub, as well as in semi-desert (the same POT dataset) but other High Arctic sites, such as polar oasis, gave mixed results with either no trend or increasing uptake with warmer conditions. Welker et al. (2004) also found mixed results where warming stimulated GEP more than ER resulting in greater net $CO_2$ uptake in mesic tundra while in wet tundra, warming reduced net C uptake. Similarly, Oberbauer et al. (2007) found a variety of responses of net C uptake to experimental warming although in general, warming enhanced GEP while ER increases depended on the wetness of the

tundra with higher water contents limiting the potential for greater ER. These results in wet tundra confirm the importance of hydrological regime on C cycling in Arctic tundra.

The influence of precipitation on daily variations in NEE at tundra and forest tundra sites was important. In semi-desert tundra (POT) NEE turned directly from a net sink to a net source of $CO_2$ with large precipitation events leading to a significant positive correlation between NEE and precipitation (Table 5.5). Similarly, NEE also increased (less net $CO_2$ uptake) on rainy days in the forest tundra (KUF), both of which may also be directly related to lower PAR and less photosynthetic uptake of $CO_2$ during wet weather. However, both ecosystems are on well-drained mesic soil and increased soil water may support microbial activity and rapidly enhance ER as was found by Christiansen et al. (2012) in High Arctic heath soil. Between rain events, there was some indication that the additional moisture helped promote GEP at POT. For example at POT in semi-desert tundra, a large precipitation event ( 23.4 mm from July 15 to July 19) after 14 days of dryness resulted in greater net $CO_2$ uptake on July 20 and 21 (Figure 5.3). These trends are in keeping with the various direct and indirect impacts precipitation can have on NEE in Arctic tundra. For example, ER is sensitive to precipitation in soil water-limited ecosystems such as in desert grassland (Thomey et al. 2011) and at the same time, photosynthetic activity may be promoted with remoistening (dew, fog & rain) in dry ecosystems such as desert (Zhang et al. 2011) and grassland steppe (Hao et al. 2010), with the potential to impact NEE. A multi-level warming and wetting in-situ study in upland Arctic soil showed the potential interactions between warming and wetting. Low-level warming promoted the uptake of $CO_2$,while high-level warming resulted in a net loss of $CO_2$, but with the input of water, the system at this later high-level of warming remained a net sink of $CO_2$ (Sharp et al. 2013). Clearly soil moisture distribution across the Arctic tundra is a dominant factor controlling $CO_2$ flux (Dagg and Lafleur 2011).

### *5.4.2 Interannual NEE variability*

The Kuujjuarapik sites (KUF and KUT) set the baseline of this extended study and through the years showed large interannual variability in NEE (Figure 5.3) that could be related to significant change of regional weather conditions and large atmospheric processes such as ENSO and AO

(Chapter 4). From 2007 to 2009, mean July NEE at KUF switched from a small sink of $CO_2$ in 2007 and 2009, -1.82 and -2.61 g C $m^{-2}$ $d^{-1}$, respectively, to a larger sink of $CO_2$ in 2008, -3.30 g C $m^{-2}$ $d^{-1}$. This represented a daily average July NEE of -2.60 ± 0.43 g C $m^{-2}$ $d^{-1}$ for this three years study. This is consistent wither previous studies in mesic tundra above the treeline ( ~ -1.0 g C $m^{-2}$ $d^{-1}$, Lafleur and Humphreys 2008; -2.2 C $m^{-2}$ $d^{-1}$, Euskirchen et al. 2012) and in both northern and southern boreal mature black spruce in Canada in either June (~ -1.3 to -2 g C $m^{-2}$ $d^{-1}$ ) or July (~ -0.3 g C $m^{-2}$ $d^{-1}$ ) when high rates of respiration nearly offset photosynthesis during the peak growing period (Fig 5.3. in Bergeron et al. 2007).

Total July NEE in forest tundra was correlated with the total annual precipitation and the length of the growing season (Table 5.1; Table 5.6), with larger uptake of $CO_2$ in the years with less precipitation and longer growing season. It appeared that the weather conditions observed during July moderated the impact of growing season length on NEE. The two years with least July net $CO_2$ uptake at KUF were 2007 and 2009 but the reasons differed. Exceptionally cold and wet conditions in 2007 worked with a relatively short growing season to limit $CO_2$ uptake in that summer. In contrast, July temperatures in 2009 were above the climate normal and conditions were moderately dry but the growing season was only 143 days compared to 175 to 222 days in the other years, resulting in the lowest cumulative July NEE. Deep snow in winter 2008-2009 and cold temperatures in springtime delayed the beginning of the growing season and the initiation of plant development and leaf growth (Chapter 4).

The highest net uptake of $CO_2$ occurred in 2008 (Figure 5.6), with temperature and precipitation trends in the range of normal and a relatively long growing season (Table 5.6). Warmer temperature promotes both photosynthetic activity and the uptake of $CO_2$ as well as respiration of plants and microbes and the emission of $CO_2$ (Sage and Kubien 2007; Smith and Dukes 2012). In the short term, NEE trends are likely not reflecting changes in the composition of the plant community as these processes occur over longer time periods (Christensen et al. 2012), but rather on year to year variations in the length of the growing season, plant physiological processes and photosynthetic activity (Elberling et al. 2004; Grant et al. 2011). Length of the growing season, a crucial period for plant development and photosynthetic activity, is directly impacted by the moment of snowmelt in springtime (Keller et al. 2005). Timing of snowmelt

thus has significant impact on phenology and growth of subarctic plants, particularly on species that develop rapidly after snowmelt, while the number of degree days has significant impact on subarctic plants with late spring development (Wipf 2010). Plant growth, ecosystem respiration and photosynthetic uptake in polar regions have been hypothesized to increase with longer and warmer growing seasons (Myneni et al. 1997). However, a number of studies in tundra above the treeline have not found a correlation between NEE and growing season length (Humphreys and Lafleur, 2011; Parmentier et al. 2011). This suggests that moderating factors during the growing season and other variables, such as the number of growing degree days, winter bud protection and changes in leaf area are important factors influencing summer NEE (Humphreys and Lafleur 2011). In forest tundra, earlier seasons may promote greater net $CO_2$ uptake in July due the advantage of greater leaf production possible for the shrub community, primarily *Betula glandulosa* and *Alnus crispa.* Our results confirm a link between the length of growing season and July NEE but also highlight the importance of within-growing season weather that can moderate the advantage of an earlier and longer growing season.

At KUT, two consecutive years of measurements over subarctic tundra with similar growing season length also point out the importance of temperature and precipitation on NEE. Warmer temperatures (KUT 2006) promoted ER resulting in lower cumulative NEE, offsetting the increase in GEP. In 2007, colder and wetter conditions limited ER, resulting in greater cumulative uptake of $CO_2$ for July. Thus the results at KUF and KUT support both statements in that growing season length does impact NEE but may be moderated or accentuated by additional growing season weather characteristics.

### *5.4.3 Spatial variation in NEE*

Overall, net $CO_2$ uptake did not reflect a latitudinal gradient. Laurila et al. (2001) also did not find a latitudinal NEE gradient in various European sites (fen, mountain birch, heathland, snowbed willow and polar semi-desert) and instead concluded that the main factor regulating summer NEE was LAI. Street et al. (2007) also clearly demonstrated that 80 % of the variation in Low Arctic tundra (tussock, wet sedge, heath vegetation and shrub) can be explained by GEP and canopy LAI. Lafleur et al. (2012) also did not observed a strong latitudinal NEE gradient

between southern location (~58° N) and northern location (~81° N) in the Canadian Arctic, but found large step change between Low and High Arctic ecosystems with significant variability within each general region related to ecosystem characteristics. Spatial trend of NEE was mainly controlled by variation in GEP (photosynthesis) rather than ER (respiration) in this study. Mcfadden et al. (2003) also found that spatial regional trends of NEE in various sites (barrens, dry tundra, forest tundra, shrub tundra, moist tundra and wet tundra) in the Brooks Range Alaska were largely controlled by GEP, rather than by ER. In contrast, others have demonstrated a latitudinal NEE gradient from south to north when examining greater range in biomes. Yuan et al. (2009) clearly observed a trend in annual NEE in broadleaf forests and evergreen nedleleaf forests from 39 northern hemisphere sites ranging from ~29°N to ~64°N. Spatial variations were mainly controlled by variation in GEP (evergreen nedleleaf forests) and ER (broadleaf forests).

In this study however, the close proximity of KUF, KUT, and UMT and the contrasting NEE between these sites highlights the variability that occurs due to other important factors within the subarctic and Arctic tundra. These factors include biogeographic factors, longitudinal trends, plant distribution and biomass, soil organic matter content, and terrestrial ecoregions which are largely influenced by regional climate. In the vicinity of Kuujjuarapik (~ 25 km), at the same latitude and within the same ecoregion, surface soil organic carbon ranged from 0.74 to 9.61 kg $m^{-2}$ (Tarnocai and Lacelle 1996). The significant relationship between soil organic C and NEE largely suggests that NEE spatial variations are more strongly linked to microbial activity, rhizosphere processes, soil components and plant communities, rather than solely a south to north temperature gradient. In other studies, the C balance of tundra ecosystem is also strongly correlated with soil biota, organic C, and plant biomass (De Deyn et al. 2008; Sistla et al. 2013) in addition to the abiotic characteristics of temperature and moisture availability that greatly impact all biogeochemical processes. For example, De Deyn et al. (2008) found that plant traits largely influence soil C input (high primary productivity from GEP or slow decomposition) and nutrient availability, as well as C output from below ground biomass activity (ER). Although this study examines only July NEE rather than the full growing season, others have shown that peak growing season fluxes largely determine the growing season $CO_2$ budget (Humphreys and Lafleur, 2011). Thus, we suggest that surface soil organic C may act as a variable that integrates

the biotic and abiotic characteristics that determine spatial variations in net summer (and growing season) $CO_2$ among these Eastern Canadian Arctic sites.

### *3.10. Conclusion*

After a four year study along a latitudinal gradient spanning 55° to 72° north in the Eastern Canadian subarctic and Arctic, factors regulating and/or reflecting spatial and temporal variations in summer $CO_2$ exchange in this region were identified. This study represents the first estimates of summer $CO_2$ exchange in the Eastern Canadian subarctic and Arctic and sets a baseline for future examination of how $CO_2$ exchanges in this region may change with further warming. Two and three measurement seasons in subarctic and forest tundra suggest that longer growing seasons may not necessarily increase mid-summer $CO_2$ uptake. Instead, PAR, temperature and soil moisture are important factors influencing $CO_2$ uptake during the growing season. PAR was generally more important at forest tundra vs. subarctic and Arctic tundra where GEP drives day-to-day variations in NEE while above the tree line, warmer temperatures generally increased ER and drove temporal variations in NEE. This study also suggests an important link between summer NEE and surface organic C rather than a simple latitudinal gradient, with higher net $CO_2$ uptake, GEP and ER in ecosystems with greater soil organic C. Soil organic C stocks appear to integrate factors that influence current $CO_2$ exchanges between tundra and the atmosphere such as plant and microbial activity, specific microclimate factors and broad climate factors. However, it is not clear if the stronger relationship between soil organic C and NEE sugest that net C storage is still ongoing or that net C is a stronger link to present vegetation instead of past communities. The soil organic C database of Canada may be useful to estimate the $CO_2$ budgets of ecosystems across the Canadian Arctic and subarctic, but further work is crucial to validate this finding among Arctic tundra and peatlands.

## *Chapter 6: Conclusions*

This research examines the exchange of $CO_2$ and $CH_4$ in the Eastern Canadian subarctic and Arctic regions. Landscape $CO_2$ and $CH_4$ exchange were quantified along a gradient spanning 55° to the 72° north over a 5 years period from 2006 to 2010 including the International Polar Year. This research included three main studies, which attempt to link $CO_2$ and $CH_4$ exchanges to substrate, plant community, and weather characteristics in both terrestrial and aquatic ecosystems.

It was expected that more biomass would tend to be associated with greater photosynthtetic activity and respiration rates. Among land cover classes at the same latitude (55° N), dark chamber measurements of $CO_2$ were significantly greater in the sparse needle leaved class. However, when separated by substrate type, there was no significant difference in emissions despite a slight increase when moving from sparsely vegetated tundra cover classes (mainly lichen and mosses) to boreal forest classes (more graminoids and vascular plants) with greater plant biomass. Flux tower results obtained along a latitudinal gradient from 55° to 72° N reflected the expected trend with lower ER over semi-desert tundra (mostly mosses, lichens and herbs) and subarctic coastal dune (graminoids) than subarctic tundra (mostly mosses, lichens and forbs) and subarctic forest tundra (shrubs). In contrast and in agreement with the chamber study, total July ER was very similar for subarctic tundra and subarctic forest tundra despite the latter having greater biomass overall. It is also possible that the limitations associated with the chamber study (discrete measurements in time with relatively low sample sizes) limited the appearance of expected biomass/substrate trends on ER while the additional impact of climate differences along the latitudinal gradient amplified the trend in the flux tower study.

In aquatic ecosystems, dark chamber measurements of $CO_2$ and $CH_4$ exchange show significant differences among substrates with higher $CO_2$ respiration and $CH_4$ emission over wetlands (particularly over collapse palsa ponds) than other water bodies (shallow water, ponds, and lakes). Higher $CO_2$ respiration was associated with higher TOC and conductivity, while higher $CH_4$ emission was linked to higher TOC, lower redox and $O_2$. Trophic level then plays an

important role in the gas echange process with higher emissions in eutrophic substrates than in oligotrophic to mesotrophic systems.

The discrete chamber measurements did not show a positive correlation between soil temperature and $CO_2$ respiration, despite a well-known temperature dependence of ER. This suggests that other variables influencing $CO_2$ fluxes among the different terrestrial substrates were of greater importance. In aquatic systems, $CO_2$ emissions increased with solar radiation likely reflecting the importance of temperature on productivity and other biogeochemical processes while $CH_4$ emissions increased directly with higher water temperature. The flux tower results in terrestrial systems exhibited a strong link with air temperature. A $Q_{10}$ relationship was established at all the sites predicting greatest $CO_2$ emissions in the afternoon when air temperature peaked. Also, warmer days tended to correlate with smaller daily net $CO_2$ uptake (or greater net $CO_2$ losses) because of higher ER, but overall warmer growing seasons reduced the net losses of $CO_2$ on an annual basis because of higher GEP. Temperature had a greater impact on NEE in subarctic and Arctic tundra because of a greater influence of ER on NEE when compared to subarctic forest tundra where PAR and photosynthetic activity drove day-to-day variations in NEE. The three years of NEE data from the subarctic forest tundra provided further insight into the importance of temperature and precipitation on intra- and inter-annual variability in NEE and potential importance of the major atmospheric teleconnections, such as ENSO and NAO/AO. The impacts of ENSO, NAO and AO on Canada's weather including inter-annual temperature variation, snowpack height and the number of growing degree days have been previously recognized (Zhang et al. 2000b). The number of GDDs has been used in agriculture and forestery for decades for analysis of vegetation community trends since it is directly impacted by day of snow melt, the length of the snow-free season and day-to-day weather conditions (McMaster and Wilhelm 1997). As shown in this study, it is a potentially valuable metric for predicting annual NEE as greater GDD was associated with decreasing annual accumulated NEE (resulting in more $CO_2$ uptake) in the subarctic forest tundra. Again, the implication is that warmer conditions enhanced photosynthetic uptake of $CO_2$ more than respiration and resulted in a negative feedback to climate warming. Further study will be needed to understand if this response is common among subarctic and Arctic ecosystems including open tundra with less vegetation and

lower photostynthetic uptake of $CO_2$. In addition, possible nutrient limitations and changes in soil moisture may play a role in eventually moderating this response here and elsewhere.

Precipitation may have both direct and indirect impacts on $CO_2$ and $CH_4$ gas exchange in subarctic and Arctic tundra. Precipitation has the potential to impact summer $CO_2$ uptake in water limited situations by stimulating plant growth and/or soil respiration. There was a significant positive correlation between daily NEE and rainfall in July at a number of the flux tower sites which supported the hypothesis of rainfall enhancing respiration. At the same time, daily NEE was negatively correlated to PAR and given the correlation between daily PAR and precipitation, days with more rainfall also tended to have less PAR which lead to less photosynthetic uptake of $CO_2$ on cloudy days at a number of the sites. This pattern occurred at both the forest tundra in the subarctic and the semi-desert tundra in the High Arctic. In the High Arctic, the site changed from being a net sink to a net source of $CO_2$ with large precipitation events. However, at the subarctic forest tundra site, no specific trend was found between NEE and precipitation on an annual basis nor during the growing season on a monthly basis. However, there were significant positive relationships between monthly precipitation and NEE during periods of dormancy and senescence in forest tundra. Higher precipitation in cold seasons directly impacts snow depth and duration which may reduce soil cooling and enhance ER.

$CH_4$ emissions from terrestrial ecosystems were also strongly linked to regional weather and the moisture regime. In mesic, dry and non-saturated upland soils, wetting of the soil during precipitation events may have lowered $O_2$ within the surface soils enough to promote $CH_4$ production and limit $CH_4$ oxidation. During this study, no specific trend was found between precipitation and $CH_4$ emission in wetlands and other water bodies, but net $CO_2$ uptake was generally observed in water bodies during rainy days and/or following rainy conditions. These conditions may have been associated with cooler, cloudier conditions that had reduced $CO_2$ production in the water.

The soil organic C content of near-surface soil may be a good indicator of ecosystem NEE. In this study, July uptake of $CO_2$ varied among ecosystems but generally increasing with higher surface soil organic C content. Soil organic C stocks appear to integrate factors that influence

current $CO_2$ exchanges between tundra and the atmosphere such as plant and microbial activity, specific microclimate factors and broad climate factors. However, it is not clear if the stronger relationship between soil organic C and GEP relative to ER suggests that net C storage is still ongoing or is strongly linked to present vegetation instead of past communities. Nevertheless, the soil organic C database of Canada may be a useful tool, with basic meteorological parameters such as air temperature and photosynthetic active radiation, to estimate NEE across the subarctic and Arctic region but further work is crucial to validate this finding across Arctic tundra and peatlands. In aquatic systems ranging from wetlands to water bodies, $CO_2$ fluxes were also impacted by the input of organic materials from the surrounding environment. Higher emissions of $CO_2$ occurred with higher levels of TOC in the water column. $CH_4$ emissions in aquatic system were also stimulated when the concentration of TOC was higher. Despite the presence of 'hotspots' such as these where $CH_4$ emissions are much greater than elsewhere, this study sugested that the response of the major cover classes to climate change should remain more important than more responsive but spatially limited hotspots for $CO_2$ and $CH_4$ emissions in this area of the Eastern subarctic. However, if the proportion of cover classes changes sufficiently (ie.due to expansion of thermokarst), the importance of hotspots may increase.

This research on $CO_2$ and $CH_4$ exchanges in various natural waters and terrestrial landscapes has contributed to knowledge on C exchange in the Eastern Canadian subarctic and Arctic regions. Carbon fluxes in these regions are highly variable in space and time but these observations help establish a baseline for future examinations of how these carbon exchanges may change with further warming. Despite the major findings of this research, future work on the C exchange in subarctic and Arctic region in a changing environment are essential to improve our knowledge on the fate of C in northern regions.

***References***


[ACIA] Arctic Climate Impact Assessment. 2004. Impacts of a warming Arctic: Arctic Climate Impact Assessment. Cambridge (UK). New York (NY): Cambridge University Press. 140pp.

Adams J. 2007. Microclimates and vegetation. In Vegetation–climate interaction: How plants make the global environment. Berlin (DE): Springer Praxis Books. 79-99.

Adler RF. Gu G. Wang J-J. Huffman GJ. Curtis S. Bolvin. D. 2008. Relationship between global precipitation and surface temperature on interannual and longer timescales (1979-2006). J Geophys Res 113 (D22104): 1-15.

Allard M. Séguin MK. 1987. Le pergélisol au Québec nordique: bilan et perspectives. Geogr Phys Quartern 41(1): 141-152.

Alley RB. 2000. The Younger Dryas cold interval as viewed from central Greenland. Quaternary Sci Rev 19: 213-226.

[AMAP] Arctic Monitoring and Assessment Programme. 2006. AMAP assessment 2006: Acidifying pollutants, Arctic haze, and acidification in the Arctic. [Symon C. Wilson S. (eds.)]. Oslo (NO): Arctic Monitoring. 112 pp.

[AMAP] Arctic Monitoring and Assessment Programme. 2010. AMAP assessment 2009: POPs in the Arctic. Sci Tot Environ special issue 408: 2851-3051.

Amiro B. 2010. Estimating annual carbon dioxide eddy fluxes using open-path analysers for cold forest sites. Agr Forest Meteorol 150: 1366-1372.

Andrews JT. Holdsworth G. Jacobs JD. Williams RS. Ferrigno JG. 2002. Satellite image atlas of glaciers of Baffin Island. United States Geological Survey. 1386DJD1.

Angel R. Claus P. Conrad R. 2011. Methanogenic archea are globally ubiquitous in aerated soils and become active under wet anoxic conditions. ISME J. DOI: 10.1038.

Arain MA. Black TA. Barr AG. Jarvis PG. Massheder JM. Verseghy DL. Nesic Z. 2002. Effects of seasonal and interannual climate variability on net ecosystem productivity of boreal deciduous and conifer forests. Can J For Res 32: 878-891.

Archer D. 2007. Methane hydrates stability and anthropogenic climate change. Biogeosciences 4: 521-544.

[AC] Arctic Council. 2001. Conservation of Arctic Flora and Fauna (CAFF) Working Group. Map No.33 - Major biomes (vegetation zones) of the Arctic. [URL] http:// library.arcticportal.org/ id/eprint/1364.

Arlen-Pouliot Y. Bhiry N. 2005. Palaeoecology of a palsa and a filled thermokarst pond in a permafrost peatland, subarctic Québec, Canada. Holocene 15(3): 408-419.

Aronson EL. Allison SD. Helliker BR. 2013. Environmental impacts on the diversity of methane-cycling microbes and their resultant function. Front Microbiol 4: 1-15.

Asselin H. Payette S. Fortin M-J. Vallée S. 2003. The northern limit of Pinus banksiana Lamb. In Canada: Explaining the difference between the eastern and western distributions. J Biogeogr 30 (11): 1709-1718.

Auger S. Payette S. 2010. Four millennia of woodland structure and dynamics at the Arctic treeline of eastern Canada. Ecology 91(5): 1367-1379.

Aurela M. Laurila T. Tuovinen JP. 2004. The timing of snow melt controls the annual $CO_2$ balance in a subarctic fen. Geophys Res Lett 31 (L16119): 1-4.

Avis CA. Weaver AJ. Meissner KJ. 2011. Reduction in areal extent of high-latitude wetlands in response to permafrost thaw. Nat Geosci 4: 444-448.

Bamzai AS. 2003. Relationship between snow cover variability and Arctic oscillation index on a hierarchy of time scales. Int J Climatol 23: 131-142.

Bansal S. Nilsson MC. Wardle DA. 2012. Response of photosynthetic carbon gain to ecosystem retrogression of vascular plants and mosses in the boreal forest. Oecologia 169: 661-672.

Barnett TP. Adam JC. Lettenmaier DP. 2005. Potential impacts of a warming climate on water availability in snow-dominated regions. Nature 438(17): 303-309.

Barr AG. Black TA. Hogg EH. Kljun N. Morgenstern K. Nesic Z. 2004. Inter-annual variability in leaf area index of boreal aspen-hazel forest in relation to net ecosystem production. Agr Forest Meteor 126: 237-255.

Bastien J. Blais A-M. Tremblay A. 2007. Étude des flux de gaz à effet de serre des milieux aquatiques. Suivi 2006, Région de la côte nord, Report prepared by Environnement illimité Inc. For the direction barrages et Environnement d'hydro-Québec Production. 43 pp.

Bates NR. Mathis JT. 2009. The Arctic Ocean marine carbon cycle: evaluation of air-sea $CO_2$ exchanges, ocean acidification impacts and potential feedbacks. Biogeosciences 6: 2433-2459.

Bates NR. 2009. Marine carbon cycle feedbacks. In: Arctic climate feedbacks: Global implications. [Sommerkorn M. Hassol SJ. (eds.)]. Washington (DC). WWF International Arctic Program. 54-68.

Bauer IE. Vitt DH. 2011. Peatland dynamics in a complex landscape: Development of a fen-bog complex in a sporadic discontinuous permafrost zone of northern Alberta, Canada. Boreas 40(4): 714-726.

Beaulieu N. Allard M. 2003. The impact of climate change on an emerging coastline affected by discontinuous permafrost: Manitounuk Strait, northern Quebec. Can J Earth Sci 40: 1393-1404.

Bendel M. Berner R. Freeman KH. Field C. Galloway J. Hedges J. Hedin LO. Mackenzie F. Mora C. Schimel J. Schlesinger W. Stallard R. Sundquist E. Torn M. Wofsy SC. 2000. The changing carbon cycle: A terrestrial focus. Report of the workshop on the terrestrial carbon cycle. The National Sciences Foundation, Division of Earth Sciences. 15 pp.

Bengtsson L. Semenov VA. Johannessen OM. 2004. The early twentieth century warming in the Arctic – A possible mechanism. J Climate 17: 4045-4057.

Bergamaschi P. Houweling S. Segers A. Krol M. Frankenberg C. Scheepmaker RA. Dlugokencky E. Wofsy SC. Kort EA. Sweeney C. Schuck T. Brenninkmeijer C. Chen H. Beck V. Gerbig C. 2013. Atmospheric $CH_4$ in the first decade of the 21$^{st}$ century: Inverse modeling analysis using SCIAMACHY satellite retrievals and NOAA surface measurements. J Geophys Res Atmos 118: 7350-7369.

Bergeron O. Margolis HA. Black A. Coursolle C. Dunn AL. Barr AG. Wofsy SC. 2007. Comparison of carbon dioxide fluxes over three boreal spruce forests in Canada. Glob Change Biol 13: 89-107.

Bergeron O. Margolis HA. Coursolle C. Giasson MA. 2008. How does forest harvest influence carbon dioxide fluxes of black spruce ecosystems in eastern North America? Agr For Meteor 148: 537-548.

Bhiry N. Delwaide A. Allard M. Bégin Y. Filion L. Lavoie M. Nozais C. Payette. S. Pienitz R. Saulnier-Talbot E. Vincent WF. 2011. Environmental change in the Great Whale river region, Hudson Bay: five decades of multidisciplinary research by Centre d'études Nordiques (CEN). Ecoscience 18 (3): 182-203.

Bliss LC. 2000. Arctic tundra and polar desert biome. In: North American terrestrial vegetation, 2nd edition. [Barbour MG. Billings WD. (eds.)]. Cambridge (UK): Cambridge University Press. 1-40.

Blondeau M. Cuerrier A. Roy C. 2011. Atlas des plantes des villages du Nunavik. Éditions MultiMondes. 610 pp.

Blunden J. Arndt DS. Baringer MO. 2011. State of the climate in 2010. Special supplement to the Bull Am Meteorol Soc 92(6): 266 pp.

Blunier T. Brook EJ. 2001. Timing of millennial-scale climate change in Antarctica and Greenland during the last glacial period. Science 291: 109-112.

Bokhorst S. Bjerke JW. Davey MP. Taulavuori K. Taulavuori E. Laine K. Callaghan TV. Phoenix GK. 2010. Impacts of extreme winter warming events on plant physiology in a sub-Arctic heath community. Physiol Plantarum 140(2): 128-140.

Bonsal BR. Zhang X. Vincent LA. Hogg WD. 2001. Characteristics of daily and extreme temperature over Canada. J Climate 14 (9): 1959-1976.

Bousquet P. Ciais P. Miller JB. Dlugokencky EJ. Hauglustaine DA. Prigent C. Van der Werf GR. Peylin P. Brunke EG. Carouge C. Langenfelds RL. Lathiere J. Papa F. Ramonet M. Schmidt M. Steele LP. Tyler SC. White J. 2006. Contribution of anthropogenic and natural sources to atmospheric methane variability. Nature 443: 439-443.

Breton J. Vallieres C. Laurion I. 2009. Limnological properties of permafrost thaw ponds in northeastern Canada. Can J Fish Aquat Sci 66 (10): 1635-1648.

Broecker WS. 1999. What if the conveyor were to shut down? Reflections on a possible outcome of the great global experiment. GSA Today 9(1): 1-7.

Brohan P. Kennedy JJ. Harris I. Tett SFB. Jones PD. 2006. Uncertainty estimates in regional and global observed temperature changes: a new dataset from 1850. J Geophys Res 111 (D12106): 1-21.

Bromwich DH. Fogt RL. Hodges KI. Walsh JE. 2007. A tropospheric assessment of the ERA-40, NCEP, and JRA-25 global reanalyses in the polar regions. J Geophys Res 112(D10111): 1-21.

Brookes IA. French H. Slaymaker O. Ryder JM. Acton DF. 2011. Physiographic region. In: The Canadian encyclopedia. [URL] http://www.thecanadianencyclopedia.com.

Brooks PD. Grogan P. Templer PH. Groffman P. Oquist MG. Schimel J. 2011. Carbon and nitrogen cycling in snow-covered environments, Geography Compass 5/9: 682-699.

Bubier J. Crill P. Mosedale A. Frolking S. Linder E. 2003. Peatland responses to varying interannual moisture conditions as measured by automatic $CO_2$ chambers. Global Biogeochem Cy 17(2): 35.1-35.15.

Bubier J. Moore T. Savage K. Crill P. 2005. A comparison of methane flux in a boreal landscape between a dry and a wet year. Global Biogeochem Cy 19(GB1023): 1-11.

Bunn AG. Goetz SJ. Fiske GJ. 2005. Observed and predicted responses of plant growth to climate across Canada. Geophys Res Lett 32 (L16710): 1-4.

Burba GG. McDermitt DK. Grelle A. Anderson DJ. Xu L. 2008. Addressing the influence of instruments surface heat exchange on the measurements of $CO_2$ flux from open-path gas analyzers. Glob Change Biol 14: 1854-1876.

Buteau S. Fortier R. Allard M. 2005. Rate-controlled cone penetration tests in permafrost. Rev Can Geotech 42(1): 184-197.

Caccianiga M. Payette S. Filion L. 2008. Biotic disturbance in expanding subarctic forests along the eastern coast of Hudson Bay. New Phytol 178: 823–834.

Caldwell MM. Bornman JF. Ballaré CL. Flint SD. Kulandaivelu G. 2007. Terrestrial ecosystems, increased solar radiation, and interaction with other climate change factors. Photochem Photobiolo S 6 (3): 252-266.

Caleigh C. 2012. Carbon dioxide efflux response with experimental warming across a soil moisture gradient in a subarctic environment. Thesis bachelor of science. Department of geography. University of Winnipeg. 61 pp.

Callaghan TV. Werkman BR. Crawford RMM. 2002. The tundra-taiga interface and its dynamics: concepts and applications. Ambio Special Report 12: 6–14.

Calmels F. Allard M. Delisle G. 2008. Development and decay of a lithalsa in Northern Québec: a geomorphological history. Geomorphology 97(3-4): 287-299.

Campbell Scientific. 1998. O23/CO2 Bowen ratio system with $CO_2$ flux. Utah. USA. 51pp.

Campbell Scientific. 2006. Open path Eddy covariance system operator's manual, CSAT3, LI-7500, and KH20. Utah. USA. 58 pp.

Canadell JG. Raupach MR. 2008. Managing forests for climate change mitigation. Science 320: 1456-1457.

Canadell JG. Raupach MR. 2009. Land carbon cycle feedbacks. In: Arctic climate feedbacks: global implications. [Sommerkorn M. Hassol SJ. (eds.)]. Washington (DC). WWF International Arctic Program. 69-80.

Cannone N. Ellis Evans JC. Strachan R. Guglielmin M. 2006. Interactions between climate, vegetation and the active layer in soil at two maritime Antarctic sites. Antarct Sci 18(3): 323-333.

Carey Sk. 2003. Dissolved organic carbon fluxes in a discontinuous permafrost subarctic alpine catchment. Permafrost Periglac 14(2): 161-171.

[CEN] Centre d'études Nordiques. 2014 Ecological studies and environmental monitoring at Bylot Island, Sirmilik National Park. [URL] http://www.cen.ulaval.ca/bylot.

[CEN] Centre d'études Nordiques. 2013a. Environmental data from the Umijuaq region in Nunavik, Quebec, Canada. v.1.0 (1997-2012). Nordicana D9. doi: 10.5885/45120SL-067305A53E914AF0.

[CEN] Centre d'études Nordiques. 2013b. Environmental data from Bylot Island in Nunavut, Canada. v.1.2 (1992-2012). Nordicana D2. doi: 10.5885/45039SL-EE76C1BDAADC4890.

Chapin III. McGuire AD. Randerson J. Pielke Sr R. Baldocchi D. Hobbie SE. Roulet N. Eugster W. Kasischke E. Rastetter EB. Zimov SA. Running SW. 2000. Arctic and boreal ecosystems of western North America as components of the climate system. Glob Change Biol 6(1): 211-223.

Chisholm SW. 2000. Oceanography: stirring times in the southern Ocean. Nature. 407: 685-687.

Christensen TR. Johansson T. Akerman HJ. Mastepanov M. Malmer N. Friborg T. Crill P. Svensson BH. 2004. Thawing sub-arctic permafrost: effects on vegetation and methane emissions. Geophys Res Lett 31(4): 1-4.

Christensen TR. Jackowicz-Korczynski M. Aurela M. Crill P. Heliasz M. Mastepanov M. Friborg T. 2012. Monitoring the multi-year carbon balance of a subarctic palsa mire with micrometeorological techniques. Ambio 41 (3): 207-277.

Christiansen CT. Svendsen SH. Schmidt NM. Michelsen A. 2012. High Arctic heath soil respiration and biogeochemical dynamics during summer and autumn freeze-in – effects of long-term enhanced water and nutrient supply. Glob Change Biol 18 (10): 3224-3236.

Church JA. Gregory JM. White NJ. Platten SM. Mitrovica JX. 2011. Understanding and projecting level change. Oceanography 24(2): 130-143.

Cohen J. Screen JA. Furtado JC. Barlow M. Whittleston D. Coumou D. Francis J. Dethloff K. Entekhabi D. Overland J. Jones J. 2014. Recent Arctic amplification and extreme mid-latitude weather. Nat Geosci 7: 627-637.

Collins M. Knutti R. Arblaster J. Dufresne JL. Fichefet T. Friedlingstein P. Gao X. Gutowski WJ. Johns T. Krinner G. Shongwe M. Tebaldi C. Weaver AJ. Wehner M. 2013. Long-term Climate Change: Projections, Commitments and Irreversibility. Chapter 12. In: Climate Change 2013: The Physical Science Basis. Contribution of Working Group I to the Fifth Assessment Report of the Intergovernmental Panel on Climate Change [Stocker TF. Qin D. Plattner GK. Tignor M. Allen SK. Boschung J. Nauels A. Xia Y. Bex V. Midgley PM. (eds.)]. Cambridge University Press, Cambridge (UK), New York (USA). 1029-1136.

Comas X. Slater L. Reeve A. 2008. Seasonal geophysical monitoring of biogenic gases in a northern peatland: implications for temporal and spatial variability in free phase gas production rates. J Geophys Res 113(G1): 1-12.

Constant P. Poissant L. Villemur R. 2005. Impact de la variation du niveau d'eau d'un marais du lac Saint-Pierre (Québec, Canada) sur les concentrations et les flux d'hydrogène, monoxyde de carbone, méthane et dioxyde de carbone. Rev Sci Eau 18: 521-539.

Cooper EJ. 2014. Warmer shorter winters disrupt Arctic terrestrial; ecosystems, Annu Rev Ecol Evol Syst 45: 271-295.

Corradi C. Kolle O. Walter K. Zimov SA. Schulze ED. 2005. Carbon dioxide and methane exchange of a north-east Siberian tussock tundra. Glob Change Biol 11: 1910-1925.

Cortese G. Abelmann A. Gersonde R. 2007. The last five glacial-interglacial transitions: a high-resolution 450,000-year record from the subantarctic Atlantic. Paleoceanography 22(4): 1-14.

Cournoyer L. Yagouti A. Bégin Y. Vescovi L. Boulet G. 2007. Analyse spatio-temporelle des températures pour un meilleur suivi du climat dans le nord du Québec. Centre d'études Nordiques (CEN). 97 pp.

Crowley J. 2000. Causes of climate change over the past 1000 years. Science 289: 270-277.

Dagg J. Lafleur PM. 2011. Vegetation community, foliar nitrogen, and temperature effects on tundra $CO_2$ exchange across a soil moisture gradient. Arct Antarct Alp Res 43(2): 189-197.

Davidson EA. Janssens IA. 2006. Temperature sensitivity of soil carbon decomposition and feedbacks to climate change. Nature 440(9): 165-173.

De Deyn GB. Cornelissen HC. Bardgett RD. 2008. Plant functional traits and soil carbon sequestration in contrasting biomes. Ecol Lett 11: 1-16.

Degens ET. Wong HK. Kempe S. 1981. Factors controlling global climate of the past and the future. In: Some perspectives of the major biogeochemical cycles Chichester (UK). [Likens GE. (ed.)]. New York (NY). Wiley on behalf of the Scientific Committee on Problems of the Environment. 3-24.

Demarty M. Bastien J. Tremblay A. 2009. Carbon dioxide and methane annual emissions from two boreal reservoirs and nearby lakes in Quebec, Canada. Biogeosci Discuss 6: 2939-2963.

Devlin JE. Finkelstein SA. 2011. Local physiographic controls on the responses of Arctic lakes to climate warming in Sirmilik National Park, Nunavut, Canada. J Paleolimnol 45: 23-29.

Dittmar T. Kattner G. 2003. The biogeochemistry of the river and shelf ecosystem of the Arctic Ocean: a review. Mar Chem 83: 103-120.

Dormann CF. Woodin SJ. 2002. Climate change in the Arctic: using plant functional types in a meta-analysis of field experiments. Funct Ecol 16: 4-17.

Duchemin E. Lucotte M. Canuel R. Chamberland A. 1995. Production of the greenhouse gases $CH_4$ and $CO_2$ by hydroelectric reservoirs of the boreal region. Global Biogeochem Cy 9 (4): 529-540.

Dunn AL. Barford CC. Wofsy SC. Goulden ML. Daube BC. 2007. A long-term record of carbon exchange in a boreal black spruce forest: means, responses to interannual variability, and decadal trends, Glob Change Biol 13: 577-590.

[EC] Environment Canada. 2012. Canadian ice service. [URL] http://www.ec.gc.ca/ glaces-ice.

[EC] Environment Canada. 2013. National climate data and information archive. [URL] http://www.climate.weatheroffice.gc.ca.

Ednie M. Smith SL. 2010. Establishment of community-based permafrost monitoring sites, Baffin Region, Nunavut. GEO 2010. 63rd Canadian Geotechnical Conference and 6th Canadian Permafrost Conference. Calgary (AB). 1205-1211.

Elberling B. Jakobsen BH. Berg P. Sondergaard J. Sigsgaard C. 2004. Influence of vegetation, temperature, and water content on soil carbon distribution and mineralization in four High Arctic soils. Arct Antarct Alp Res 36(4): 528-538.

Elberling B. 2007. Annual soil $CO_2$ effluxes in the High Arctic: the role of snow thickness and vegetation type. Soil Biol Biochem 39: 646-654.

Elliot-Fisk DL. 2000. The taiga and boreal forest. In: North American Terrestrial Vegetation. 2nd edition. [Barbour MG. Billings WD. (eds.)]. Cambridge University Press. Cambridge (UK). 1-40.

Ellis CJ. Rochefort L. 2006. Long-term sensitivity of a High Arctic wetland to Holocene climate change. J Ecol 94: 441-454.

Else BGT. Papakyriakou TN. Granskog MA. Yackel JJ. 2008. Observations of sea surface $fCO_2$ distributions and estimated air-sea $CO_2$ fluxes in the Hudson Bay region (Canada) during the open water season. J Geophys Res 113(C8): 1-12.

Epstein HE. Walker MD. Chappin III FS. Starfield Am. 2000. A transient, nutrient-based model of arctic plant community response to climatic warming. Ecol Appl 10(3): 824-841.

Etzelmuller B. Frauenfelder R. 2009. Factors controlling the distribution of mountain permafrost in the Northern Hemisphere and their influence on sediment transfer. Arct Antarct Alp Res 41(1): 48-58.

Eugster W. Rouse W. Pielke Sr RA. McFadden JP. Baldocchi D. Kittel D. Chapin III TGF. Liston FS. Vidale GE. Vaganov PL. Chambers ES. 2000. Land-atmosphere energy exchange in Arctic tundra and boreal forest: available data and feedbacks to climate. Glob Change Biol 6(1): 84–115.

Euskirchen ES. Bret-Harte MS. Scott CJ. Edgar C. Shaver GR. 2012. Seasonal patterns of carbon dioxide and water fluxes in three representative tundra ecosystems in northern Alaska. Ecosphere 3 (1): 1-19.

Falge E. Baldocchi D. Olson R. Anthoni P. Aubinet M. Bernhofer C. Burba G. Ceulemans R. Clement R. Dolman H. Granier A. Gross P. Grunwald T. Hollinger D. Jensen N-O. Katul G. Keronen P. Kowalski A. Lai CT. Law BE. Meyers T. Moncrieff J. Moors E. Munger JW. Pilegaard K. Rannik U. Rebmann C. Suyker A. Tenhunen J. Tu K. Verma S. Vesala T. Wilson K. Wofsy S. 2001. Gap filling strategies for defensible annual sums of net ecosystem exchange. Agr Forest Meteorol 107: 43-69.

Falkowski P. Scholes RJ. Boyle E. Canadell J. Canfield D. Elser J. Gruber N. Hibbard K. Hogberg P. Linder S. Mackenzie FT. Moore III B. Pedersen T. Rosental Y. Seitzinger S. Smetacek V. Steffen W. 2000. The global carbon cycle: A test of our knowledge of earth as a system. Science. 290 (5490): 291-296.

Fillol E. 2003. Application de la télédétection à l'analyse de la variabilité climatique des régions boréales et subarctiques du Canada et à la validation du modèle régional canadien du climat. Thèse de doctorat. Département de géographie et télédétection. Université de Sherbrooke. Québec. Canada. 183 pp.

Fisher H. Schmitt J. Luthi D. Stocker TF. Tschumi T. Parekh P. Joos F. Kohler P. Volker C. Gersonde R. Barbante C. Le Floch M. Raynaud D. Wolff E. 2010. The role of southern ocean processes in orbital and millennial $CO_2$ variations – a synthesis. Quaternary Sci Rev 29(1-2): 193-205.

Fluckiger J. Monnin E. Stauffer B. Schwander J. Stocker TF. 2002. High-resolution Holocene $N_2O$ ice core record and its relationship with $CH_4$ and $CO_2$. Glob Biogeochem Cy 16(1): 1-8.

Forland EJ. Hanssen-Bauer I. 2000. Increased precipitation in the Norwegian Arctic: true or false? Clim Chang 46: 485-509.

Forster P. Artaxo P. Berntsen T. Betts R. Fahey DW. Haywood J. Lean J. Lowe DC. Myhre G. Nganga J. Prinn R. Raga G. Schulz M. Van Dorland R. 2013. Changes in Atmospheric Constituents and in radiative Forcing. Chapter 2. In: Climate Change 2007: The Physical Science Basis. Contribution of Working Group I to the Fourth Assessment Report of the

Intergovernmental Panel on Climate Change [Solomon S. Qin D. Manning M. Chen Z. Marquis M. Averyt KB. Tignor M. and Miller HL. (eds.)]. Cambridge University Press, Cambridge (UK). New York (USA). 129-234.

Fortier D. Allard M. Pivot F. 2006. A late-Holocene record of loess deposition in ice-wedge polygons reflecting wind activity and ground moisture conditions. Bylot Island. eastern Canadian Arctic. Holocene 16(5): 635-646.

Fortier R. LeBlanc A-M. Allard M. Buteau S. Calmels F. 2008. Internal structure and conditions of permafrost mounds at Umiujaq in Nunavik, Canada, inferred from field investigation and electrical resistivity tomography. Can J Earth Sci 45: 367-387.

Fortier R. LeBlanc A-M. Yu W. 2011. Impacts of permafrost degradation on a road embankment at Umiujaq in Nunavik (Quebec), Canada. Can Geotech J 48: 720-740.

Fowler D. Pilegaard K. Sutton MA. Ambus P. Raivonen M. Duyzer J. Simpson D. Fagerli H. Fuzzi S. Schjoerring JK. Granier C. Neftel A. Isaksenm ISA. Laj P. Maione M. Monks PS. Burkhardt J. Daemmgen U. Neirynck J. Personne E. Wichink-Kruit R. Butterbach-Bahl K. Flechard C. Tuovinen JP. Coyle M. Gerosa G. Loubet B. Altimir N. Gruenhage L. Ammannl C. Cieslik S. Paoletti E. Mikkelsen TN. Ro-Poulsen H. Cellier P. Cape JN. Horvath L. Loreto F. Niinemets U. Palmer PI. Rinne J. Misztal P. Nemitz E. Nilsson D. Pryor S. Gallagher MW. Vesala T. Skiba U. bruggemann N. Zechmeister-Boltenstern S. Williams J. O'Dowdap C. Facchini MC. de Leeuw G. Flossman A. Chaumerliac N. Erisman JW. 2009. Atmospheric composition change: ecosystems–atmosphere interactions. Atmos Environ 43: 5193-5267.

Fox AM. Huntley B. Lloyd CR. Williams M. Baxter R. 2008. Net ecosystem exchange over heterogeneous arctic tundra: scaling between chamber and eddy covariance measurements. Glob Biogeochem Cy 22(2): 1-15.

Friborg T. Soegaard H. Christensen TR. Lloyd CR. Panikov NS. 2003. Siberian wetlands: where a sink is a source. Geophys Res Lett 30(21): 5.1-5.4.

Furgal C. Martin D. Gosselin P. 2002. Climate Change and Health in Nunavik and Labrador: Lessons from Inuit Knowledge. In: The Earth is Faster Now: Indigenous Observations of Arctic Environmental Change. [Krupnik I. Jolly D. (eds.)]. Arctic Research Consortium of the United States. Arctic Studies Centre. Smithsonian Institution. Washington DC. 266-300.

Galbraith PS. Larouche P. 2011. Sea-Surface temperature in Hudson Bay and Hudson Strait in relation to air temperature and ice cover breakup, 1985-2009. J Marine Syst 87(1): 66-78.

Gauthier G. Rochefort L. Reed A. 1996. The exploitation of wetland ecosystems by herbivores on Bylot Island. Geosci Can 23(4): 253-259.

[GCP] Global Carbon Project. 2014. Global Carbon Project database. [URL] http://www.globalcarbonproject.org/.

Ge ZM. Kellomaki S. Zhou X. Wang KY. Peltola H. 2011. Evaluation of carbon exchange in a boreal coniferous stand over a 10-year period: An integrated analysis based on ecosystem model simulations and eddy covariance measurements. Agr For Meteorol 151: 191-203.

Gerlach T. 2011. Volcanic versus anthropogenic carbon dioxide. EOS 92(24): 201-202.

Ghatak D. Frei A. Gong G. Stroeve J. Robinson D. 2010. On the emergence of an Arctic amplification signal in terrestrial Arctic snow extent. J Geophys Res 115(D24): 1-8.

Goodine GK. Lavigne MB. Krasowski MJ. 2008. Springtime resumption of photosynthesis in balsam fir (Abies balsamea). Tree Physiol 28 (7): 1069-1076.

Gould WA. Raynolds M. Walker DA. 2003. Vegetation, plant biomass, and net primary productivity patterns in the Canadian Arctic. J Geophys Res 108(D2): 1-14.

Gould WA. Zoltai ES. Raynolds M. Walker DA. Maier H. 2002. Canadian Arctic vegetation mapping. Int J Remote Sens 23(21): 4597-4609.

Grant RF. Humphreys ER. Lafleur PM. Dimitrov DD. 2011. Ecological controls on net ecosystem productivity of a mesic arctic tundra under current and future climates. J Geophys Res 116(G1): 1-17.

Graversen RG. Mauritsen T. Tjernstrom M. Kallen E. Svensson G. 2008. Vertical structure of recent Arctic warming. Nature 451: 53-56.

Groendahl L. Friborg T. Soegaard H. 2007. Temperature and snow-melt controls on interannual variability in carbon exchange in the High Arctic. Theor Appl Climatol 88: 111-125.

Gruber N. Friedlingstein P. Field CB. Valentini R. Heimann M. Richey JE. Romero-Lankao P. Schulze ED. Chen CTA. 2004. The vulnerability of the carbon cycle in the 21st century: an assessment of carbon-climate-human interactions. In: The global carbon cycle: integrating humans, climate, and the natural world. [Field CB. Raupach MR. (eds.)]. Washington DC. Island Press. 45-76.

Gruber N. Gloor M. Mikaloff Fletcher SE. Doney SC. Dutkiewicz S. Follows MJ. Gerber M. Jacobson AR. Joos F. Lindsay K. Menemenlis D. Mouchet A. Muller SA. Sarmiento JL. Takahashi T. 2009. Oceanic sources, sinks, and transport of atmospheric $CO_2$. Glob Biogeochem Cy 23(1): 1-21.

Hader DP. Kumar HD. Smith RC. Worrest RC. 2007. Effects of solar UV radiation on aquatic ecosystems and interactions with climate change. Photochem Photobiol Sci 6: 267-285.

Hansen J. Ruedy R. Sato M. Lo K. 2010. Global surface temperature change. Rev Geophys 48 (RG4004): 1-29.

Hao Y. Wang Y. Mei X. Cui X. 2010. The response of ecosystem $CO_2$ exchange to small precipitation pulses over a temperate steppe. Plant Ecol 209 (2): 335-347.

Hartley IP. Garnett MH. Sommerkorn M. Hopkins DW. Fletcher BJ. Sloan VL. Phoenix GK. Wookey PA. 2012. A potential loss of carbon associated with greater plant growth in the European Arctic. Nat. Clim. Chang. 2: 875-879.

Hartmann DL. Klein Tank AMG. Rusticucci M. Alexander LV. Brönnimann S. Charabi Y. Dentener FJ. Dlugokencky EJ. Easterling DR. Kaplan A. Soden BJ. Thorne PW. Wild M. Zhai PM. 2013. Observations: Atmosphere and Surface. Chapter 2. In: Climate Change 2013: The Physical Science Basis. Contribution of Working Group I to the Fifth Assessment Report of the Intergovernmental Panel on Climate Change [Stocker, TF. Qin D. Plattner GK. Tignor M. Allen SK. Boschung J. Nauels A. Xia Y. Bex V. Midgley PM. (eds.)]. Cambridge University Press, Cambridge (UK). New York (USA). 159-254.

Hebert PDN. 2002. Canada's Polar Environments. CyberNatural Software. University of Guelph. [URL] http://www.polarenvironments.ca.

Heginbottom JA. Brown J. Melnikov ES. Ferrians OJ. 1997. Circumarctic map of permafrost and ground ice conditions, revised. First published in Permafrost 2: 1132-1136.

Henry GHR. Molau U. 1997. Tundra plants and climate change: the International Tundra Experiment (ITEX). Glob Change Biol 3(1): 1-9.

Henry GHR. Elmendorf S. 2008. Trends in tundra vegetation over the past 20 years: analysis of long-term data sets from the International Tundra Experiments (ITEX). Arctic Change 2008. Québec.

Henry GHR. Harper KA. Chen W. Deslippe JR. Grant RF. Lafleur PM. Lévesque E. Siciliano SD. Simard SW. 2012. Effects of observed and experimental climate change on terrestrial ecosystems in northern Canada: results from the Canadian IPY program. Clim Chang. DOI 10.1007/s10584-012-0587-1.

Hinzman LD. Goering DJ. Li S. Kinney TC. 1997. Numeric simulation of thermokarst formation during disturbance. In: Disturbance and recovery in Arctic lands: an ecological perspective. [Crawford RMM. (ed.)]. Dordrecht (NL). Boston (MA). Kluwer Academic Pub. 199-212.

Hinzman LD. Bettez ND. Bolton WR. Chapin FS. Dyurgerov MB. Fastie CL. Griffith B. Hollister RD. Hope A. Huntington HP. Jensen AM. Jia GJ. Jorgenson T. Kane DL. Klein DR. Kofinas G. Lynch AH. Lloyd AH. McGuire AD. Nelson FE. Oechel WC. Osterkamp TE. Racine CH. Romanovsky VE. Stone RS. Stow DA. Sturm M. Tweedie GE. Vourlitis

GL. Walker MD. Walker DA. Webber PJ. Welker JM. Winker KS. Yoshikawa K. 2005. Evidence and implications of recent climate change in northern Alaska and other Arctic regions. Clim Chang 72 (3): 251-298.

Holland MM. Bitz CM. 2003. Polar amplification of climate change in coupled models. Clim Dynam 21: 221-232.

Horst TW. 1997. A simple formula for attenuation of eddy fluxes measured with first-order-response scalar sensor. Bound-Layer Meteorol 82: 219-233.

Houghton JT. Ding Y. Griggs DJ. Noguer M. van der Linden PJ. Dai X. Maskell K. Johnson CA. 2001. Climate change 2001: the scientific basis. Contribution of Working Group I to the Third Assessment Report of the Intergovernmental Panel on Climate Change (IPCC). Cambridge University Press. Cambridge (UK). 84 pp.

Hugelius G. Strauss J. Zubrzycki S. Harden JW. Schuur EAG. Ping CL. Schirrmeister L. Grosse G. Michaelson GJ. Koven CD. O'Donell JA. Elberling B. Mishra U. Camill P. Yu Z. Palmtag J. Kuhry P. 2014. Estimated stocks of circumpolar permafrost carbon with quantified uncertainty ranges and identified gaps. Biogeosciences 11: 6573-6593.

Humphreys ER. Lafleur PM. 2011. Does earlier snowmelt lead to greater $CO_2$ sequestration in two low Arctic tundra ecosystems? Geophys Res Lett 38 (L09703): 1-5.

Humphreys ER. Charron C. Brown M. Jones R. 2014. Two bogs in the Canadian Hudson bay lowlands and a temperate bog reveal similar annual net ecosystem exchange of CO2. Arct. Antarct. Alp. Res. 46(1):103-113.

Huntington H. Weller G. 2004. An introduction to the Arctic Climate Impact Assessment. In Arctic Climate Impact Assessment. [Symon C. Arris L. Heal B. (Eds.)]. Cambridge University Press. New York. USA.1-20.

Huttunen JT. Alm J. Liikanen A. Juutinen S. Larmola T. Hammar T. Silvola J. Martikainen PJ. 2003. Fluxes of methane, carbon dioxide and nitrous oxide in boreal lakes and potential anthropogenic effects on the aquatic greenhouse gas emissions. Chemosphere 52: 609-621.

Illeris L. Konig SM. Grogan P. Jonasson S. Michelsen A. Ro-Poulsen H. 2004. Growing-season carbon dioxide flux in a dry subarctic heath: responses to long-term manipulations. Arct Antarct Alp Res 36 (4): 456-463.

[IPCC] Intergovernmental Panel on Climate Change. 2013. Climate change 2013: The physical science basis. Contribution of Working Group I to the Fifth Assessment Report of the Intergovernmental Panel on Climate Change. [Stocker TF. Qin D. Plattner GK. Tignor M. Allen SK. Boschung J. Nauels A. Xia Y. Bex V. Midgley PM. (eds.)]. Cambridge University Press. Cambridge (UK). New York (USA). 1535 pp.

Isaksen ISA. Gauss M. Myhre G. Walter Anthony KM. Ruppel C. 2011. Strong atmospheric chemistry feedback to climate warming from Arctic methane emissions. Glob Biogeochem Cy 25(2): 1-11.

Ito A. Inatomi M. 2012. Use of process-based model for assessing the methane budgets of global terrestrial ecosystems and evaluation of uncertainty. Biogeosciences 9: 759-773.

Joly S. Senneville S. Cava D. Saucier FJ. 2011. Sensitivity of Hudson Bay Sea ice and ocean climate to atmospheric temperature forcing. Clim Dyn 36: 1835-1849.

Jones RI. Grey J. 2011. Biogenic methane in freshwater food webs, Freshwater Biol 56: 213-229.

Jones PD. Lister DH. Osborn TJ. Harpham C. Salmon M. Morice CP. 2012. Hemispheric and large-scale land-surface air temperature variations: An extensive revision and an update to 2010. J Geophys Res Atmos 117 (D05127).

Ju W. Chen JM. 2005. Distribution of soil carbon stocks in Canada's forests and wetlands simulated based on drainage class, topography and remotely sensed vegetation parameters. Hydrol Process 19(1): 77-94.

Ju W. Chen JM. Black TA. Barr AG. McCaughey H. Roulet NT. 2006. Hydrological effects on carbon cycles in Canada's forests and wetlands. Tellus 58B: 16-30.

Kankaala P. Huotari J. Peltomaa E. Saloranta T. Ojala A. 2006. Methanotrophic activity in relation to methane efflux and total heterotrophic bacterial production in a stratified, humic, boreal lake. Limnol Oceanogr 51(2): 1195-1204.

Kaplan JO. New M. 2006. Arctic climate change with a 2 °C global warming: timing, climate patterns and vegetation change. Clim Chang 79: 213-241.

Kattsov VM. Kallen E. 2004. Future climate change: Modelling scenarios for the Arctic. Chapter 4. In Arctic Climate Impact Assessment Seientific Report. [Symon C. Arris L. Heal B. (Eds.)]. Cambridge University Press. New York (USA). 99-150.

Kattsov V. Hibbard K. Rinke A. Romanovsky V. Verseghy D. 2010. Terrestrial permafrost carbon in the changing climate. Doc 6 CAPER CliC SSG-VI. Valdivia (CL). 14 pp.

Keller F. Goyette S. Beniston M. 2005. Sensitivity analysis of snow cover to climate change scenarios and their impact on plant habitats in alpine terrain. Clim Chang 72: 299-319.

Kennett JP. Cannariato KG. Hendy IL. Behl RJ. 2000. Carbon isotopic evidence for methane hydrate instability during quaternary interstadials. Science 288(5463): 128-133.

Khvorostyanov DV. Krinner G. Ciais P. Heimann M. Zimov SA. 2008. Vulnerability of permafrost carbon to global warming. Part I: model description and role of heat generated by organic matter decomposition. Tellus 60B: 250-264.

King AW. Gunderson CA. Post WM. Weston DJ. Wullschleger SD. 2006. Plant respiration in a warmer world. Science 312(5773): 536-537.

Kirschke S. Bousquet P. Ciais P. Saunois M. Canadell JG. Dlugokencky EJ. Bergamaschi P. Bergmann D. Blake DR. Bruhwiler L. Cameron-Smith P. Castaldi S. Chevallier F. Feng L. Fraser A. Heimann M. Hodson EL. Houweling S. Josse B. Fraser PJ. Krummel PB. Lamarque JF. Langenfelds RL. Le Quéré C. Naik V. O'Doherty S. Palmer PI. Pison I. Plummer D. Poulter B. Prinn RG. Rigby M. Ringeval B. Santini M. Schmidt M. Shindell DT. Simpson IJ. Spahni R. Steele LP. Strode SA. Sudo K. Szopa1 S. van der Werf GR. Voulgarakis A. van Weele M. Weiss RF. Williams JE. Zeng G. 2013. Three decades of global methane sources and sinks. Nat Geosci 6: 813-823.

Kirtman B. Power SB. Adedoyin JA. Boer GJ. Bojariu R. Camilloni I. Doblas-Reyes FJ. Fiore AM. Kimoto M. Meehl GA. Prather M. Sarr A. Schär C. Sutton R. van Oldenborgh GJ. Vecchi G. Wang HJ. 2013. Near-term Climate Change: Projections and Predictability. Chapter 11. In: Climate Change 2013: The Physical Science Basis. Contribution of Working Group I to the Fifth Assessment Report of the Intergovernmental Panel on Climate Change [Stocker TF. Qin D. Plattner GK. Tignor M. Allen SK. Boschung J. Nauels A. Xia Y. Bex V. Midgley PM. (eds.)]. Cambridge University Press. Cambridge (UK). New York (USA). 953-1028.

Kittel TGF. Baker BB. Higgins JV. Haney JC. 2011. Climate vulnerability of ecosystems and landscapes on Alaska's north slope. Reg Environ Change 11(1): 249-264.

Kling GW. Kipphut GW. Miller MC. 1992. The flux of $CO_2$ and $CH_4$ from lakes and rivers in Arctic Alaska. Hydrobiologia 240: 23-36.

Kljun N. Calanca P. Rotach MW. Schmid HP. 2004. A simple parameterisation for flux footprint predictions. Bound-Layer Meteorol 112: 503-523.

Krey V. Canadell JG. Nakicenovic N. Abe Y. Andruleit H. Archer D. Grubler A. Hamilton NTM. Johnson A. Kostov V. Lamarque JF. Langhorne N. Nisbet EG. O'Neil B. Riahi K. Riedel M. Wang W. Yakushev V. 2009. Gas hydrates: entrance to a methane age or climate threat? Environ Res Lett 4(3): 1-6.

Krishnan P. Black TA. Barr AG. Grant NJ. Gaumont-Guay D. Nesic Z. 2008. Factors controlling the interannual variability in the carbon balance of a southern boreal black spruce forest. J Geophys Res-Atmos 113 (9): D09109.

Kuhlbrodt T. Rahmstorf S. Zickfeld K. Vikebo FB. Sundby S. Hofmann M. Link PM. Bondeau A. Cramer W. Jaeger C. 2009. An integrated assessment of changes in the thermohaline circulation. Clim Chang 96(4): 489-537.

Kuhlmann AJ. Worthy DEJ. Trivett NBA. Levin I. 1998. Methane emission from wetland region within the Hudson Bay Lowland: An atmospheric approach. J Geophys Res 103(D13): 16009-16016.

Kwon HJ. Oechel WC. Zulueta RC. Hastings SJ. 2006. Effects of climate variability on carbon sequestration among adjacent wet sedge tundra and moist tussock tundra ecosystems. J Geophys Res 111(G3): 10.1-10.10.

Lafleur PM. Humphreys ER. 2008. Spring warming and carbon dioxide exchange over low Arctic tundra in central Canada. Glob Change Biol 14: 740-756.

Lafleur PM. Humphreys ER. St. Louis VL. Myklebust MC. Papakyriakou T. Poissant L. Barker JD. Pilote M. Swystun KA. 2012. Variation in peak growing season net ecosystem production across the Canadian Arctic. Environ Sci Technol 46: 7971-7977.

Laliberté A-C. Payette S. 2008. Primary succession of subarctic vegetation and soil on the fast-rising coast of eastern Hudson Bay, Canada. J Biogeogr 35: 1989-1999.

Lankreijer HJM. Lindroth A. Stromgren M. Kulmala L. Pumpanen J. 2009. Forest floor CO2 flux measurements with a dark-light chamber. Biogeosciences Discuss. 6: 9301-9329.

Lara MJ. Villarreal S. Johnson DR. Hollister RD. Webber PJ. Tweedie CE. 2012. Estimated change in tundra ecosystem function near Barrow, Alaska between 1972 and 2010. Enviro Res Lett 7: 015507.

Larrivée E. 2007. Tomographie électromagnétique du pergélisol près d'Umiujaq, Nunavik (Québec). Ste-Foy (QC). Université Laval. 137 pp.

Laurila T. Soegaard H. Lloyd CR. Aurela M. Tuovinen JP. Nordstroem C. 2001. Seasonal variations of net $CO_2$ exchange in European Arctic ecosystems. Theor Appl Climatol 70: 183-201.

Laurion I. Vincent WF. MacIntyre S. Retamal L. Dupont C. Francus P. Pienitz R. 2010. Variability in greenhouse gas emissions from permafrost thaw ponds. Limnol Oceanogr 55: 115-133.

Law BE. Falge E. Gu L. Baldocchi DD. Bakwin P. Berbigier P. Davis K. Dolman AJ. Falk M. Fuentes JD. Goldstein A. Granier A. Grelle A. Hollinger D. Janssens IA. Jarvis P. Jensen NO. Katul G. Mahli Y. Matteucci G. Meyers T. Monson R. Munger W. Oechel W. Olson R. Pilegaard K. Paw U KT. Thorgeirsson H. Valentini R. Verma S. Vesala T. Wilson K.

Wofsy S. 2002. Environmental controls over carbon dioxide and water vapor exchange of terrestrial vegetation. Agri For Met 113: 97-120.

Lawrence DM. Slater AG. 2010. The contribution of snow condition trends to future ground climate. Clim Dynam 34 (7): 969-981.

Lawrimore JH. Menne MJ. Gleason BE. Williams CN. Wuertz DB. Vose RS. Rennie J. 2011. An overview of the Global Historical Climatology Network monthly mean temperature data set. version 3. J Geophys Res Atmos 116 (D19121).

Lesins G. Duck TJ. Drummond JR. 2012. Surface energy balance framework for Arctic amplification of climate change. J Climate 25: 8277-8288.

Lévesque R. Allard M. Séguin MK. 1988. Le pergélisol dans les formations quaternaires de la région des rivières Nastapoca et Sheldrake, Québec nordique. Collection nordicana 51. 23 pp.

Lewkowicz AG. Etzelmuller B. Smith SL. 2011. Characteristics of discontinuous permafrost based on ground temperature measurements and electrical resistivity tomography, southern Yukon, Canada. Permafrost Periglac 22(4): 320-342.

Likens GE. 2010. Biogeochemistry of inland waters, Academic press, 744pp.

Linacre E. Geerts B. 1998. The Arctic Ocean, sea ice, icebergs, and climate. [URL] http://www-das.uwyo.edu/~geerts/cwx/notes/chap17/arctic.html.

Logan T. Charron I. Chaumont D. Houle D. 2011. Atlas de scenarios climatiques pour la forêt québécoise. Ouranos. Ministère des ressources naturelles et de la faune du Québec. 125pp.

Lund M. Christensen TR. Lindroth A. Schubert P. 2012. Trends in CO2 exchange in a high Arctic tundra heath, 2000-2010, J Geophys Res 117, G02001: 1-12.

Mahli Y. 2002. Carbon in the atmosphere and terrestrial biosphere in the 21st century. Phil Trans R Soc Lond A 360: 2925-2945.

Marotzke J. 2000. Abrupt climate change and thermohaline circulation: mechanisms and predictability. P Nat Acad Sci 97(4): 1347-1350.

Martel MC. Margolis HA. Coursolle C. Bigras FJ. Heinsch FA. Running SW. 2005. Decreasing photosynthesis at different spatial scales during the late growing season on a boreal cutover. Tree Physiol 25 (6): 689-699.

Mauritzen C. 2009. Ocean cisrculation feedbacks. In: Arctic climate feedbacks: global implications. [Sommerkorn M. Hassol SJ. (eds.)]. Washington (DC). WWF International Arctic Program. 28-38.

Maxwell B. 1987. Atmospheric and climatic change in the Canadian Arctic. Canadian Arctic Resources Committee 15(5).

Mazeas O. Von Fischer JC. Rhew RC. 2009. Impact of terrestrial carbon input on methane emissions from an Alaskan Arctic lake. Geophys Res Lett 36(18): 1-5.

McBean G. 2004. Arctic climate: Past and present. Chapter 2. In Arctic Climate Impact Assessment Scientific Report. [Symon C. Arris L. Heal B. (Eds.)]. Cambridge University Press. New York (USA). 21-60.

McEnroe NA. Roulet NT. Moore TR. Garneau M. 2009. Do pool surface area and depth control $CO_2$ and $CH_4$ fluxes from an ombrotrophic raised bog, James Bay, Canada? J Geophys Res 114 (1): 1-9.

McFadden JP. Eugster W. Chapin FS III. 2003. A regional study of the controls on water vapour and $CO_2$ exchange in Arctic tundra. Ecology 84: 2762-2776.

McGuire AD. Christensen TR. Hayes D. Heroult A. Euskirchen E. Kimball JS. Koven C. Lafleur P. Miller PA. Oechel W. Peylin P. Williams M. Yi Y. 2012. An assessment of the carbon balance of Arctic tundra: comparisons among observations' process models, and atmospheric inversions. Biogeosciences 9: 3185-3204.

McMaster GS. Wilhelm W. 1997. Growing degree-days: one equation , two interpretations. Agric For Meteorol 87: 291-300.

McNamara NP. Plant T. Oakley S. Ward S. Wood C. Ostle N. 2008. Gully hotspot contribution to landscape methane ($CH_4$) and carbon dioxide ($CO_2$) fluxes in a northern peatland. Sci Total Environ 404: 354-360.

Meehl GA. Stocker TF. Collins WD. Friedlingstein P. Gaye AT. Gregory JM. Kitoh A. Knutti R. Murphy JM. Noda A. Raper SCB. Watterson IG. Weaver AJ. Zhao ZC. 2007. Global Climate Projections. Chapter 10. In: Climate Change 2007: The Physical Science Basis. Contribution of Working Group I to the Fourth Assessment Report of the Intergovernmental Panel on Climate Change [Solomon S. Qin D. Manning M. Chen Z. Marquis M. Averyt KB. Tignor M. & Miller HL. (eds.)]. Cambridge University Press, Cambridge (UK). New York (USA). 747-845.

Ménard E. Allard M. Michaud Y. 1998. Monitoring of ground surface temperatures in various biophysical micro-environments near Umiujaq, Eastern Hudson Bay, Canada. Permafrost. Collection Nordicana 55: 723-729.

Merbold L. Kutsch WL. Corradi C. Kolle O. Rebmann C. Stoy PC. Zimov SA. Schulze ED. 2009. Artificial drainage and associated carbon fluxes ($CO_2$/$CH_4$) in tundra ecosystem. Glob Change Biol 15: 2599-2614.

Messaoud Y. Bergeron Y. Asselin H. 2007. Reproductive potential of balsam fir (Abies balsamea), white spruce (Picea glauca), and black spruce (P. mariana) at the ecotone between mixedwood and coniferous forests in the boreal zone of western Quebec. Am J Bot 94(5): 746-754.

Michelutti N. Wolfe AP. Vinebrooke RD. Rivard B. Briner JP. 2005. Recent primary production increases in Arctic lake. Geophys Res Lett 32, L19715: 1-4.

Mikan CJ. Schimel JP. Doyle AP. 2002. Temperature controls of microbial respiration in Arctic tundra soils above and below freezing. Soil Biol Biochem 34 (11): 1785-1795.

Miller GH. Brigham-Grette J. Alley RB. Anderson L. Bauch HA. Douglas MSV. Edwards ME. Elias SA. Finney BP. Fitzpatrick JJ. Funder SV. Herbert TD. Hinzman LD. Kaufman DS. MacDonald GM. Polyak L. Robock A. Serreze MC. Smol JP. Spielhagen R. White JWC. Wolfe AP. Wolff EW. 2010. Temperature and precipitation history of the Arctic. Quaternary Sci Rev 29: 1679-1715.

Moffat AM. Papale D. Reichstein M. Hollinger DY. Richardson AD. Barr AG. Beckstein C. Braswell BH. Churkina G. Desai AR. Falge E. Gove JH. Heimann M. Hui D. Jarvis AJ. Kattge J. Noormets A. Stauch VJ. 2007. Comprehensive comparison of gap-filling techniques for eddy covariance net carbon fluxes. Agr Forest Meteorol 147: 209-232.

Moncrieff JB. Massheder JM. de Bruin H. Elbers J. Friborg T. Heusinkveld B. Kabat P. Scott S. Soegaard H. Verhoeh A. 1997. A system to measure surface fluxes of momentum, sensible heat, water vapour and carbon dioxide. J Hydrol 188-189: 589-611.

Monin AS. Obukhov AM. 1954. Basic laws of turbulent mixing in the surface layer of the atmosphere. Tr Akad Nauk SSR Geophiz Inst 24 (151): 163-187.

Moore P. 2008. Tundra. Facts on File Inc. New York (USA). ISBN 0-8160-5933-0. 261 pp.

Myhre G. Shindell D. Bréon FM. Collins W. Fuglestvedt J. Huang J. Koch D. Lamarque JF. Lee D. Mendoza B. Nakajima T. Robock A. Stephens G. Takemura T. Zhang H. 2013. Anthropogenic and natural radiative forcing. Chapter 8. In climate change 2013: The physical science basis. Contribution of working group I to fifth assessment report of the Intergovernmental Panel on Climate Change. [Stocker TF. Qin D. Plattner GK. Tignor M. Allen SK. Boschung J. Nauels A. Xia Y. Bex V. Midgley PM. (Eds.)]. Cambridge University Press. Cambridge (UK). New York (USA). 659-740.

Myneni RB. Keeling CD. Tucker CJ. Asrar G. Nemani RR. 1997. Increased plant growth in the northern high latitudes from 1981 to 1991. Nature 386: 698-702.

Natali SM. Schuur EAG. Mauritz M. Scade JD. Cellis G. Crummer KG. Johnston C. Krapek J. Pergoraro E. Salmon VG. Webb EE. 2015. Permaforst thaw and soil moisture driving $CO_2$ and $CH_4$ release from upland tundra. J Geophys Res Biogeosci 120: 10.1002/2010JG002872.

New M. 2005. Arctic climate change with a 2 °C global warming, In: Evidence and implications of dangerous climate change in the Arctic. [Rosentrater L. (ed.)]. Washington (DC). WWF International Arctic Program. 7-24.

New M. Todd M. Hulme M. Jones P. 2001. Precipitation measurements and trends in the twentieth century. Int J Climatol 21: 1899-1922.

Nghiem SV. Rigor IG. Perovich DK. Clemente-Colon P. Weatherly JW. Neumann G. 2007. Rapid reduction of Arctic perennial sea ice. Geophys Res Lett 34(19): 1-6.

Nichols H. 1976. Historical aspects of the northern Canadian treeline. Arctic 29(1): 38-47.

Niemi R. Martikainen P. Silvola J. Wulff A. Turtola S. Holopainen T. 2002. Elevated UV-B radiation alters fluxes of methane and carbon dioxide in peatland microcosms. Glob Change Biol 8: 361-371.

[NOAA] National Oceanic and Atmospheric Administration. 2012. National weather service, Climate prediction center. [URL] http://www.cpc.ncep.noaa.go.

[NRCan] Natural Resources Canada. 2008. Land cover map of Canada 2005. Earth Sciences Sector Program. Ottawa ON Canada. [URL] http://atlas.nrcan.gc.ca.

[NRCan] Natural Resources Canada. 2013. The atlas of Canada, 5th edition, 1978 to 1995. [URL] http://atlas.nrcan.gc.ca.

[NSIDC] National Snow and Ice Data Centre. 2011. Arctic climatology and meteorology. [URL] http://nsidc.org.

O'Connor FM. Boucher O. Gedney N. Jones CD. Folberth GA. Coppell R. Friedlingstein P. Collins WJ. Chappellaz J. Ridley J. Johnson CE. 2010. Possible role of wetlands, permafrost, and methane hydrates in the methane cycle under future climate change: a review. Rev Geophys 48(4): 1-33.

Obata A. 2007. Climate-carbon cycle model response to freshwater discharge into the North Atlantic. J Climate 20: 5962-5976.

Oberbauer SF. Tweedie CE. Welker JM. Fahnestock JT. Henry GHR. Webber PJ. Hollister RD. Walker MD. Kuchy A. Elmore E. Starr G. 2007. Tundra $CO_2$ fluxes in response to experimental warming across latitudinal and moisture gradients. Ecol Monogr 77 (2): 221-238.

Öquist MG. Svensson BH. 2002. Vascular plants as regulators of methane emissions from a subarctic mire ecosystem. J Geophys Res-Atmos 107(21): 10-1-10-10.

Öquist MG. Laudon H. 2008. Winter soil frost conditions in boreal forests control growing season soil $CO_2$ concentration and its atmospheric exchange. Glob Change Biol 14: 2839-2847.

Oliphant AJ. Dragoni D. Deng B. Grimmond CSB. Schmid HP. Scott SL. 2011. The role of sky conditions on gross primary production in a mixed deciduous forest. Agric For Meteorol 151(7): 781-791.

Olthof L. Pouliot D. 2010. Treeline vegetation composition and change in Canada's western subarctic from AVHRR and canopy reflectance modeling. Remote Sens Environ 114(4): 805-815.

Overland J. Wang M. Walsh J. 2011. The Arctic - atmosphere, state of the climate in 2010. Special supplement to the Bull Am Meteorol Soc 92 (6): 272 pp.

Overpeck J. Hughen K. Hardy D. Bradley R. Case R. Douglas M. Finney B. Gajewski K. Jacoby G. Jennings A. Lamoureux S. Lasca A. MacDonald G. Moore J. Retelle M. Smith S. Wolfe A. Zielinsk G. 1997. Arctic environmental change of the last four centuries. Science 278(5341): 1251-1256.

Pace ML. Cole J. 2002. Synchronous variation of dissolved organic carbon and color in lakes. Limnol Oceanogr 47 (2): 333-342.

Packalen MS. Finkelstein SA. McLaughlin JW. 2014. Carbon storage and potential methane production in the Hudson Bay Lowlands since mid-Holocene peat initiation. Nature 5: 4078.

Parmentier FJW. van der Molen MK. van Huissteden J. Karsanaev SA. Kononov AV. Suzdalov DA. Maximov TC. Dolman AJ. 2011. Longer growing seasons do not increase net carbon uptake in the northeastern Siberian tundra. J Geophys Res 116 (G04013): 1-11.

Parton W. Morgan J. Smith D. Del Grosso S. Prihodko L. Lecain D. Kelly R. Lutz S. 2012. Impact of precipitation dynamics on net ecosystem productivity. Glob Change Biol 18: 915-927.

Payette S. Gauthier R. 1972. Les structures de végétation: interprétation géographique et écologique, classification et application. Nat Can 99: 1–26.

Payette S. Bhiry N. Delwaide A. Simard M. 2000. Origin of the lichen woodland at its southern range limit in eastern Canada: the catastrophic impact of insect defoliators and fire on the spruce-moss forest.Can J For Res 30: 288-305.

Payette S. Fortin MJ. Gamache I. 2001. The subarctic forest-tundra: the structure of a biome in a changing climate. BioScience 51 (9): 709-718.

Payette S. Delwaide A. Caccianiga M. Beauchemin M. 2004. Accelerated thawing of subarctic peatland permafrost over the last 50 years. Geophys Res Lett 31(18):1-4.

Pelletier L. Moore TR. Roulet NT. Garneau M. Beaulieu-Audy V. 2007. Methane fluxes from three peatlands in the La Grande Rivière watershed, James Bay lowland, Canada. J Geophys Res 112 (G01018): 1-12.

Peterson IK. Pettipas R. 2013. Trends in air temperature and seas ice in the atlantic large aquatic basin and adjoining areas. Canadian technical report of hydrography and ocean sciences 290. Fisheries and Oceans Canada. Darmouth (CA). 59pp.

Peltier WR. Shennan I. Drummond R. Horton B. 2002. On the postglacial isostatic adjustement of the British Isles and the shallow viscoelastic structure of the Earth. Geophys J Int 148: 443-475.

Petit JR. Jouzel J. Raynaud D. Barkov NI. Bharnola JM. Basile I. Bender M. Chapellaz J. Davis M. Delaygue G. Delmotte M. Kotlyakov VM. Legrand M. Lipenkov VY. Lorius C. Pépin L. Ritz C. Saltzman E. Stievenard M. 1999. Climate and atmospheric history of the past 420,000 years from the Vostok ice core, Antarctica. Nature 399: 429-436.

Pithan F. Mauritsen T. 2014. Arctic amplification dominated by temperature feedbacks in contemporary climate models. Nat Geosci 7: 181-184.

Poissant L. Amyot M. Pilote M. Lean D. 2000. Mercury water-air exchange over the upper St. Lawrence River and Lake Ontario. Environ Sci Technol 34(15): 3069-3078.

Poissant L. Constant P. Pilote M. Canario J. O'Driscoll N. Ridal J. Lean D. 2007. The ebullition of hydrogen, carbon monoxide, methane, carbon dioxide and total gaseous mercury from the Cornwall Area of Concern. Sci Total Environ 381: 256-262.

Prowse TD. Wrona FJ. Reist JD. Hobbie JE. Lévesque LMJ. Vincent WF. 2006. General features of the Arctic relevant to climate change in freshwater ecosystems. Ambio 35(7): 330-338.

Prowse TD. Furgal C. 2009b. Northern Canada in a changing climate: major findings and conclusion. Ambio 38(5): 290-292.

Prowse TD. Furgal C. Bonsal BR. Peters DL. 2009a. Climate impacts on Northern Canada: regional background. Ambio 38(5): 248-256.

Prowse TD. Furgal C. Bonsal BR. Edwards TWD. 2009b. Climatic conditions in northern Canada: past and future. Ambio 38(5): 257-265.

Prowse TD. Furgal C. Melling H. Smith SL. 2009c. Implications of climate change for northern Canada: the physical environment. Ambio 38(5): 266-271.

Prowse TD. Furgal C. Wrona FJ. Reist JD. 2009d. Implications of climate change for northern Canada: freshwater, marine, and terrestrial ecosystems. Ambio 38(5): 282-289.

Ramaswamy V. Boucher O. Haigh J. Hauglustaine D. Haywood J. Myhre G. Nakajima T. Shi GY. Solomon S. 2001. Radiative forcing of climate change. Chapter6. In: Climate Change 2001: The Scientific Basis. Contribution of Working Group I to the Third Assessment Report of the Intergovernmental Panel on Climate Change [Houghton, JT. et al. (eds.)]. Cambridge University Press, Cambridge (UK). New York (USA). 349–416.

Rasilo T. Prairie YT. Del Giorgio PA. 2015. Large-scale patterns in summer diffusive $CH_4$ fluxes across boreal lakes, and contribution to diffusive C emissions. Glob Change Biol. 21: 1124-1139.

Rayment MB. Jarvis PG. 2000. Temporal and spatial variation of soil $CO_2$ efflux in a Canadian boreal forest. Soil Biol Biochem 32: 35-45.

Rayner NA. Brohan P. Parker DE. Folland CK. Kennedy JJ. Vanicek M. Ansell TJ. Tett SFB. 2006. Improved analyses of changes and uncertainties in sea surface temperature measured in situ since the mid-nineteenth century: the HadSST2 dataset. J Climate 19: 446–469.

Raynolds MK. Walker DA. Maier HA. 2006. NDVI patterns and phytomass distribution in the circumpolar Arctic. Remote Sens Environ 102: 271-281.

Reist JD. Wrona FJ. Prowse TD. Power M. Dempson B. King JR. Beamish RJ. 2006. An overview of effects of climate change on selected Arctic freshwater and anadromous fishes. Ambio 35(7): 381-387.

Ricard B. 1998. Croissance de l'épinette blanche (Picea glauca [Moench] Voss) au front de colonisation littoral du détroit de Manitounouk, Québec nordique. Ste-Foy (QC). Université Laval. 66 pp.

Richardson CJ. 2000. Freshwater wetlands. In: North American terrestrial vegetation, 2nd edition. [Barbour MG. Billings WD. (eds.)]. Cambridge University Press. Cambridge (UK). 450-499.

Rignot E. Cazenave A. 2009. Ice sheets and sea-level rise feedbacks. In: Arctic climate feedbacks: global implications. [Sommerkorn M. Hassol SJ. (eds.)].Washington (DC). WWF International Arctic Program. 39-53.

Risch A. Frank DA. 2007. Effects of increased soil water availability on grassland ecosystem carbon dioxide fluxes. Biogeochemistry 86: 91-103.

Robock A. 2000. Volcanic eruptions and climate. Rev Geophys 38(2): 191-219.

Rodionow A. Flessa H. Kazansky O. Guggenberger G. 2006. Organic matter composition and potential trace gas production of permafrost soils in the forest tundra in northern Siberia. Geoderma 135: 49-62.

Rohde R. Muller RA. Jacobsen R. Muller E. Perlmutter S. Rosenfeld A. Wurtele J. Groom D. Wickham C. 2013. A new estimate of the average Earth surface land temperature spanning 1753 to 2011. Geoinfor Geostat: An Overview 1 (1): 1-7.

Ropelewski CF. Halpert MS. 1987. Global and regional scale precipitation patterns associated with the El Niño / Southern Oscillation. Mon Weather Rev 115: 1606-1626.

Roulet NT. Lafleur PM. Richard PJH. Moore TR. Humphreys ER. Bubier J. 2007. Contemporary balance and late Holocene carbon accumulation in a northern peatland. Glob Change Biol 13(2): 3979-411.

Rouse WR. Douglas MSV. Hecky RE. Hershey AE. Kling GW. Lesack L. Marsh P. McDonald M. Nicholson BJ. Roulet NT. Smol JP. 1997. Effect of climate change on the freshwaters of Arctic and subarctic North America. Hydrol Process 11: 873-902.

Rouse WR. Bello RL. D'Souza A. Griffis TJ. Lafleur PM. 2002. The annual carbon budget for fen and forest in a wetland at Arctic Treeline. Arctic 55 (3): 229-237.

Rustad LE. Huntington TG. Boone RD. 2000. Controls on soil respiration: implications for climate change. Biogeochemistry 48: 1-6.

Ryba SA. Burgess RM. 2002. Effects of sample preparation on the measurement of organic carbon, hydrogen, nitrogen, sulphur, and oxygen concentrations in marine sediments. Chemosphere. 48: 139-147.

Sachs T. Wille C. Boike J. Kutzbach L. 2008. Environmental controls on ecosystem-scale $CH_4$ emission from polygonal tundra in the Lena River Delta, Siberia. J Geophys Res 113(G00A03): 1-12.

Sage RF. Kubien DS. 2007. The temperature response of C3 and C4 photosynthesis. Plant Cell Environ 30 (9): 1086-1106.

Sagerfors J. Lindroth A. Grelle A. Klemedtsson L. Weslien P. Nilsson M. 2008. Annual $CO_2$ exchange between a nutrient-poor, minerotrophic, boreal mire and the atmosphere. J Geophys Res 113( G01001): 1-15.

Savage KE. Davidson EA. 2003. A comparison of manual and automated systems for soil $CO_2$ flux measurements: trade-offs between spatial and temporal resolution. J Exp Bot 54 (384): 891-899.

Schaefer K. Lantuit H. Romanovsky VE. Schuur EAG. Witt R. 2014. The impact of the permafrost carbon feedback on global climate. Environ Res Lett 9: 1-9.

Schindler DW. Smol JP. 2006. Cumulative effects of climate warming and other human activities on freshwaters of Arctic and subarctic North America. Ambio 35(4): 160-168.

Schlesinger WH. Andrews JA. 2000. Soil respiration and the global carbon cycle. Biogeochemistry 48: 7-20.

Schuur EAG. Bockeim J. Canadell JG. Euskirchen E. Field CB. Goryachkin SV. Hagemann S. Kuhry P. Lafleur PM. Lee H. Mazhitova G. Nelson FE. Rinke A. Romanovsky VE. Shiklomanov N. Tarnocai C. Venevsky S. Vogel JG. Zimov SA. 2008. Vulnerability of permafrost carbon to climate change: implications for the global carbon cycle. BioScience 58(8): 701-714.

Schuur EAG. Vogel JG. Grummer KG. Lee H. Sickman JO. Osterkamp TE. 2009. The effect of permafrost thaw on old carbon release and net carbon exchange from tundra. Nature 459: 556-559.

Schuur EAG, Abbott B. Koven CD. Riley WJ. Subin ZM. 2011. High risk of permafrost thaw. Nature 480: 32-33.

Schneider von Deimling T. Meinshausen M. Levermann A. Huber V. Frieler K. Lawrence DM. Brovkin V. 2011. Estimating the permafrost-carbon feedback on global warming. Biogeosci Discuss 8: 4727-4761.

Screen JA. Simmonds I. 2010. The central role of diminishing sea ice in recent Arctic temperature amplification. Nature 464: 1334-1337.

Sechrist FS. Fett RW. Perryman DC. 1989. Arctic climatology. In forecast handbook for the Arctic. Naval Environmental Prediction Research Facility. TR 89-12. 396 pp.

Serreze MC. Barrett AP. Slater AG. Woodgate RA. Aagaard K. Lammers RB. Steele M. Moritz R. Meredith M. Lee GM. 2006. The large-scale freshwater cycle of the Arctic. J Geophys Res 111 (C11010): 1-19.

Serreze MC. Stroeve J. 2009. Atmospheric circulation feedbacks. In: Arctic climate feedbacks: global implications. [Sommerkorn M. Hassol SJ. (eds.)]. Washington (DC). WWF International Arctic Program. 17-27.

Serreze MC. Barry RG. 2011. Processes and impacts of Arctic amplification: a research synthesis. Glob Planet Chang 77: 85-96.

Shakhova N. Semiletov I. 2009. Methane hydrate feedbacks. In: Arctic climate feedbacks: global implications. [Sommerkorn M. Hassol SJ. (eds.)]. Washington (DC). WWF International Arctic Program. 81-92.

Sharp ED. Sullivan PF. Steltzer H. Csank AZ. Welker JM. 2013. Complex carbon cycle response to multi-level warming and supplemental summer rain in the high Arctic. Glob Change Biol 19 (6): 1780-1792.

Shaver GR. Street LE. Rastetter EB. Van Wijk MT. Williams M. 2007. Functional convergence in regulation of net $CO_2$ flux in heterogeneous tundra landscapes in Alaska and Sweden. J Ecol 95(4): 802-817.

Shirokova LS. Pokrovsky OS. Kirpotin SN. Desmukh C. Pokrovsky BG. Audry S. Viers J. 2013. Biogeochemistry of organic carbon, $CO_2$, $CH_4$, and trace elements in thermokarst water bodies in discontinuous permafrost zones of Western Siberia. Biogeochemistry 113: 573-593.

Siegenthaler U. Stocker TF. Monnin E. Luthi D. Schwander J. Stauffer B. Raynaud D. Barnola JM. Fischer H. Masson-Delomte V. Jouzel J. 2005. Stable carbon cycle-climate relationship during the Late Pleistocene. Science 310(5752): 1313-1317.

Sigman DM. Boyle EA. 2000. Glacial/interglacial variations in atmospheric carbon dioxide. Nature 407: 859-869.

Sistla SA. Moore JC. Simpson RT. Gough L. Shaver GR. Schimel JP. 2013. Long-term warming restructures Arctic tundra without changing net soil carbon storage. Nature (12129): 1-5.

Sjogersten S. Wookey PA. 2002. Climatic and resource quality controls on soil respiration across a forest-tundra ecotone in Swedish Lapland. Soil Biol Biochem 34 (11): 1633-1646.

Smith LC. MacDonald GM. Velichko AA. Beilman DW. Boriskova OK. Frey KE. Kremenetski KV. Sheng Y. 2004. Siberian peatlands: a net carbon sink and global methane source since the early Holocene. Science 303: 353-356.

Smith NG. Dukes J. 2012. Plant respiration and photosynthesis in global-scale models: incorporating acclimation to temperature and $CO_2$. Glob Change Biol 19 (1): 45-63.

Steltzer H. Hufbauer RA. Welker JM. Casalis M. Sullivan PF. Chimner R. 2008. Frequent sexual reproduction and high intraspecific variation in Salix arctica: Implications for a terrestrial feedback to climate change in the High Arctic. J Geophys Res 113: G03S10.

Stocker TF. Qin D. Plattner GK. Alexander LV. Allen SK. Bindoff NL. Bréon FM. Church JA. Cubasch U. Emori S. Forster P. Friedlingstein P. Gillett N. Gregory JM. Hartmann DL. Jansen E. Kirtman B. Knutti R. Krishna Kumar K. Lemke P. Marotzke J. Masson-Delmotte V. Meehl GA. Mokhov II. Piao S. Ramaswamy V. Randall D. Rhein M. Rojas M. Sabine C. Shindell D. Talley LD. Vaughan DG. Xie S.P. 2013. Technical Summary. In: Climate Change 2013: The Physical Science Basis. Contribution of Working Group I to the Fifth Assessment Report of the Intergovernmental Panel on Climate Change [Stocker TF. Qin D. Plattner GK. Tignor M. Allen SK. Boschung J. Nauels A. Xia Y. Bex V. Midgley PM.

(eds.)]. Cambridge University Press, Cambridge, United Kingdom and New York, NY, USA. 33-115.

Stott PA. Kettleborough JA. 2002. Origins and estimates of uncertainty in predictions of twenty-first century temperature rise. Nature 418: 723-726.

Stottlemyer R. Rhoades C. Steltzer H. 2001. Soil temperature, moisture, and carbon and nitrogen mineralization at a Taiga-Tundra ecotone, Noatak National Preserve, North-western Alaska. United States Geological Survey. 1678: 127-137.

Street LE. Shaver GR. Williams M. van Wijk MT. 2007. What is the relationship between changes in canopy leaf area and changes in photosynthetic $CO_2$ flux in Arctic ecosystems? J Ecol 95: 139-150.

Stroeve J. Serreze M. Drobot S. Gearheard S. Holland M. Maslanik J. Meier W. Scambos T. 2008. Arctic sea ice extent plummets in 2007. EOS 89(2): 13-20.

Ström L. Ekberg A. Mastepanov M. Christensen TR. 2003. The effect of vascular plants on carbon turnover and methane emissions from a tundra wetland. Glob Change Biol 9: 1185-1192.

Tarnocai C. Lacelle B. 1996. Soil organic carbon of Canada database, Ottawa (ON): Eastern Cereal and Oilseed Research Centre. Agriculture and Agri–Food Canada. Research Branch (digital database).

Tarnocai C. 2006. The effect of climate change on carbon in Canadian peatlands. Glob Planet Chang 53: 222-232.

Tarnocai C. Canadell JG. Mazhitova G. Schuur EAG. Kuhry P. Zimov S. 2009. Soil organic carbon pools in the northern circumpolar permafrost region. Glob Biogeochem Cy 23 (GB2023): 1-11.

Teklemariam T. Staebler RM. Barr AG. 2009. Eight years of carbon dioxide exchange above a mixed forest at Borden, Ontario, Agric For Metorol 149: 2040-2053.

Thomey ML. Collins SL. Vargas R. Johnson JE. Brown RF. Natvig DO. Friggens MT. 2011. Effect of precipitation variability on net primary production and soil respiration in a Chihuahuan Desert grassland. Glob Change Biol 17(4): 1505-1515.

Torgersen T. Branco B. 2007. Carbon and oxygen dynamics of shallow aquatic systems: process vectors and bacterial productivity. J Geophys Res 112(G3): 1-16.

Tremblay B. Lévesques E. Boudreau S. 2012. Recent expansion of erect shrubs in the Low Arctic: evidence from eastern Nunavik. Environ Res Lett 7 (035501): 11pp.

Tremblay M. Furgal C. 2008. Les changements climatiques au Nunavik et au Nord du Québec: L'accès au territoire et aux ressources. Initiatives des écosystèmes nordiques. Environnement Canada. 167 pp.

Tripati AK. Roberts CD. Eagle RA. 2009. Coupling of $CO_2$ and ice sheet stability over major climate transitions of the last 20 million years. Science 326: 1394-1397.

Trumbore S. 2006. Carbon respired by terrestrial ecosystems – recent progress and challenges. Glob Change Biol 12: 141-153.

Turner JK. Gyakum JR. 2010. Trends in Canadian surface temperature variability in the context of climate change. Atmos Ocean 48(3): 147-162.

Ueyama M. Iwata H. Harazono Y. Euskirchen ES. Oechel WC. Zona D. 2013. Growing season and spatial variations of carbon fluxes of Arctic and boreal ecosystems in Alaska (USA). Ecol Appl 23 (8): 1798-1816.

Ullah S. Frasier R. Pelletier L. Moore TR. 2009. Greenhouse gas fluxes from boreal forest soils during the snow-free period in Québec, Canada. Can J For Res 39: 666-680.

[USDOE] United States Department of Energy. 2008. Carbon cycling and biosequestration. Report from the March 2008 Workshop. DOE/SC-108. U.S. Department of Energy Office of Science. 2-3.

[USGCRP] United States Global Change Research Program. 2009. Global Climate Change Impacts in the United States. [Karl TR. Melillo JM. Peterson TC. (eds.)]. United States Global Change Research Program. Cambridge University Press, New York (USA). 188 pp.

van Huissteden J. Berrittella C. Parmentier FJW. Mi Y. Maximov TC. Dolman AJ. 2011. Methane emission from permafrost thaw lakes limited by lake drainage. Nat Clim Chang 1: 119-123.

van Wijngaarden WA. 2014. Arctic temperature trends from the early nineteenth century to present. Theor Appl Climatol. DOI 10.1007/s00704-014-1311-z.1-14.

Venäläinen A. Tuomenvirta H. Heikinheimo M. Kellomaki S. Peltola H. Strandman H. Vaisanen H. 2001. Impact of climate change on soil-frost under snow cover in a forest landscape. Climate Res 17: 63-72.

Veteli TO. Mattson WJ. Niemalä P. Julkunen-Tiitto R. Kellomäki S. Kuokkanen K. Lavola A. 2007. Do elevated temperature and $CO_2$ generally have counteracting effects on phenolic phytochemistry of boreal trees? J Chem Ecol 33(2): 287-296.

Vincent WF. Whyte LG. Lovejoy C. Greer CW. Laurion I. Suttle CA. Corbeil J. Mueller DR. 2009. Arctic microbial ecosystems and impacts of extreme warming during the International Polar Year. Polar Sci 3(3): 171-180.

Vitt DH. Halsey LA. Zoltai SC. 2000. The changing landscape of Canada's western boreal forest: the current dynamics of permafrost. Can J For Res 30: 283-287.

Vourlitis GL. Oechel WC. Hope A. Stow D. Boynton B. Verfaillie Jr J. Zulueta R. Hastings SJ, 2000. Physiological models for scaling plot measurements of $CO_2$ flux across an Arctic tundra landscape. Ecol Appl 10 (1): 60-72.

Waldrop MP. Wickland KP. White III R. Berhe AA. Harden JW. Romanovsky VE. 2010. Molecular investigations into a globally important carbon pool: permafrost-protected carbon in Alaskan soils. Glob Change Biol 16: 2543-2554.

Walker DA. 2000. Hierarchical subdivision of arctic tundra based on vegetation response to climate, parent material, and topography. Glob Change Biol 6: 19-34.

Walker DA. Raynolds MK. Daniels FJA. Einarsson E. Elvebakk A. Gould WA. Katenin AE. Kholod SS. Markon CJ. Melnikov ES. Moskalenko NG. Talbot SS. Yurtsev BA & the other members of the CAVM team. 2005. The circumpolar arctic vegetation map. J Veg Sci 16: 267-282.

Walker DA. Bhatt US. Comiso JC. Epstein HE. Gould WA. Henry GHR. Jia GJ. Kokelj SV. Lantz TC. Mercado-Díaz JA. Pinzon JE. Raynolds MK. Shaver GR. Tucker CJ. Tweedie CE. Webber PJ. 2010. Land, state of the climate in 2009. Special supplement to the Bull Am Meteorol Soc 91(6): s115.

Walker DA. Epstein HE. Raynolds MK. Kuss P. Kopecky MA. Frost GV. Daniels FJA. Leibman MO. Moskalenko NG. Matyshak GV. 2012. Environment, vegetation and greenness (NDVI) along the North America and Eurasia Arctic transects. Environ Res Lett 7 (1): 1-17.

Walter BP. Heimann M. Matthews E. 2001. Modelling modern methane emissions from natural wetlands, 1. Model description and results. J Geophys Res 106(D24): 34189-34206.

Walter KM. Smith LC. Chapin III FS. 2007. Methane bubbling from northern lakes: present and future contributions to the global methane budget. Phil Trans R Soc 365: 1657-1676.

Walter KM. Chanton JP. Chapin III FS. Schuur EAG. Zimov SA. 2008. Methane production and bubble emissions from Arctic lakes: Isotopic implications for source pathways and ages. J Geophys Res 113, G00A08: 1-16.

Warner BG. Rubec CDA. 1997. The Canadian wetland classification system. Wetlands Research Centre, University of Waterloo. Waterloo (CA). 68 pp.

Webb EK. Pearman GI. Leuning R. 1980. Correction of flux measurements for density effects due to heat and water vapour transfer. Quart J Roy Meteorol Soc 106: 85-100.

Welker JM. Fahnestock JT. Henry GHR. O'Dea KW. Chimner RA. 2004. $CO_2$ exchange in three Canadian High Arctic ecosystems: response to long-term experimental warming. Glob Change Biol 10: 1981-1995.

Weller G. 2004. Summary and synthesis of the ACIA. Chapter 18. In: Arctic Climate Impact Assessment (ACIA) scientific report. [Symon C. Arris L. Heal B. (eds.)]. Cambridge University Press. Cambridge (UK). New York (NY). 989-1020.

Welp LR. Randerson JT. Liu HP. 2007. The sensitivity of carbon fluxes to spring warming and summer drought depends on plant functional type in boreal forest ecosystems. Agric For Meteorol 147: 172-185.

Wetzel RG. 2001. Limnology: lake and river ecosystems. Academic Press. San Diego (USA). 1006 pp.

Whiting GJ. Chanton JP. 2001. Greenhouse carbon balance of wetlands: methane emission versus carbon sequestration. Tellus 53B: 521-528.

Wickland KP. Striegl RG. Neff JC. Sachs T. 2006. Effects of permafrost melting on $CO_2$ and $CH_4$ exchange of a poorly drained black spruce lowland. J Geophys Res 111(G2): 1-13.

Wiken EB. 1986. Terrestrial Ecozones of Canada. Ecological Land Classification. Series No. 19. Environment Canada. Hull. Quebec. 26pp and map.

Wipf S. 2010. Phenology, growth, and fecundity of eight subarctic tundra species in response to Snowmelt manipulations. Plant Ecol 207: 53-66.

Wrona FJ. Prowse TD. Reist JD. 2004. Freshwater ecosystems and fisheries. Chapter 8. In Arctic Climate Impact Assessment Scientific Report [Symon C. Arris L. Heal B (eds.)]. Cambridge University Press. New York. USA. 353-452.

Wu J. van der Linden L. Lassslop G. Carvalhais N. Pilegaard K. Beier C. Ibrom A. 2012. Effects of climate variability and functional changes on the interannual variation of the carbon balance in a temperate deciduous forest. Biogeosiences. 9: 13-28.

Yasuda Y. Saito T. Hoshino D. Ono K. Ohtani Y. Mizoguchi Y. Morisawa T. 2012. Carbon balance in a cool-temperate deciduous forest in northern Japan: Seasonal and interannual variations and environmental controls of its annual balance. J For Res-Jpn 17 (3): 253-267.

Yuan W. Luo Y. Richardson AD. Oren R. Luyssaert S. Janssens IA. Ceulemans R. Zhou X. Grunwald T. Aubinet M. Berhofer C. Baldocchi DD. Chen J. Dunn AL. Deforest JL. Dragoni D. Goldstein AH. Moors E. Munger JW. Monson RK. Suyker AE. Starr G. Scott RL. Tenhunen J. Verma SB. Vesala T. Wofsy SC. 2009. Latitudinal patterns of magnitude and interannual variability in net ecosystem exchange regulated by biological and environmental variables. Glob Change Biol 15: 2905-2920.

Zhang J. Zhang YM. Downing A. Wu N. Zhang BC. 2011. Photosynthetic and cytological recovery on remoistening Syntrichia caninervis Mitt., a dessication-tolerant moss from Northwestern China. Photosynthetica 49(1): 13-20.

Zhang T. Heginbottom JA. Barry RG. Brown J. 2000a. Further statistics on the distribution of permafrost and ground ice in the Northern Hemisphere. Polar Geography 24(2): 25–131.

Zhang X. Vincent LA. Hogg WD. Niitsoo A. 2000b. Temperature and precipitation trends in Canada during the 20th century. Atmos Ocean 38(3): 395-429.